Application of Reduced Order MCS Control in the Electrohydraulic Servo Field

S. BULUT

A THESIS SUBMITTED TO THE UNIVERSITY OF BRISTOL IN ACCORDANCE WITH THE REQUIREMENTS FOR THE DEGREE OF DOCTOR OF PHILOSOPHY IN THE FACULTY OF ENGINEERING, DEPARTMENT OF MECHANICAL ENGINEERING, JULY 1997.

ABSTRACT

In this thesis a form of the Minimal Controller Synthesis (MCS) algorithm named as the reduced order MCS control is presented. The MCS control is a form of Model Reference Adaptive Control (MRAC). The thesis concentrates on the use of the reduced order MCS instead of the standard MCS control. The reduced order MCS control as well as the standard MCS control continuously adapts itself to changes in the plant parameters and the system working conditions unlike linear control strategies. The dynamics of the hydraulic systems are nonlinear and the parameters of the plant vary with time and working conditions therefore using the reduced order MCS control brings many advantages. A lot of work has been done in the application of adaptive control in hydraulic field. Adaptive control and its applications in hydraulic field will be studied in Chapter 1.

The simulation of hydraulic systems can be very helpful when choosing suitable controller gains satisfying the desired closed-loop. The importance of simulation and modelling will be emphasised in Chapter 2. In this chapter, the electrohydraulic actuator plant will be modelled and simulated in Simulink.

Model reduction is widely used in practical applications due to the fact that the full model of the plant may not be available in many cases, even if it is available the computation of the plant model and the implementation of the controller are time consuming. Ten linear model reduction methods will be presented in Chapter 3.

The stability of the reduced order MCS control will be analytically investigated in Chapter 4. The analysis will be carried out for both SISO and MIMO system. The reduced order MCS control will be assumed as the standard MCS control in which the controlled plant contains some unmodelled dynamics. This unmodelled term will be included in the disturbance term. The nature of the disturbance term is crucial, if the disturbance term is slowly varying then Popov's method will be used to guarantee the stability of the system. In the case of rapidly varying disturbance term the Lyapunov method will be used. Using the reduced order MCS control instead of the standard MCS control has many advantages: firstly the structure of the controller is simple, secondly in many cases it makes the systems more effective and efficient due to the fact that it avoids over parameterisation of the plant.

In Chapter 5, the MCS control and a Proportional Plus Derivative Feedback (P+DFB) control will be implemented on the electrohydraulic actuator plant. The performances of the reduced second order MCS control will be compared with the conventional control in the face of changes in the working condition.

The reduced order MCS control of electrohydraulic servomechanisms will be used for closed loop control of stroke and load in Chapter 6. The MCS control and a Proportional Plus Integral (P+I) Control will be implemented on the ESH material testing machine in Chapter 6. The plant has a nominal second order transfer function and the MCS control will be implemented in a reduced first order form. The performances of the MCS will be compared with the equivalent P+I under load control.

In Chapter 7, the robustness of the reduced first order MCS control in the case of the ESH material testing machine will be investigated by comparative tests. The results will be very crucial to show the robustness of the reduced order MCS in practice.

In Chapter 8, conclusions to this thesis will be presented. Finally, possible future improvements and developments will be discussed.

ACKNOWLEDGEMENTS

I would like to express my deepest gratitude to my supervisor Prof. D. P. Stoten for the all invaluable help, support, advice, guidance and friendship he provided me during this intense and rewarding period of research.

I would like to thank all my family members especially to my parents for their support, encouragement and understanding.

I also want to thank all my friends in Bristol for their help, companionship discussions and social integration they provided me during this work.

I would like to thank Mr. P. R. Brinson, Department of Aerospace Engineering, University of Bristol for the use of his Servohydraulic, rig.

I am also grateful to Prof. D. J. Smith, Department of Mechanical Engineering, University of Bristol for the use of his ESH materials testing machine, rig.

I want to thank the University of Cumhuriyet (Sivas/Turkey) for all the financial support they provided, making this work possible.

Finally, I would like to thank my colleagues Tim Parker for correcting my grammar.

AUTHOR'S DECLARATION

UNLESS OTHERWISE ACKNOWLEDGED, THE CONTEXT OF THIS THESIS IS THE ORIGINAL AND SOLE WORK OF THE AUTHOR. NO PORTION OF THE WORK IN THIS THESIS HAS BEEN SUBMITTED BY THE AUTHOR IN SUPPORT OF AN APPLICATION FOR ANY OTHER DEGREE OR QUALIFICATION, AT THIS OR ANY OTHER UNIVERSITY OR INSTITUTION OF LEARNING.

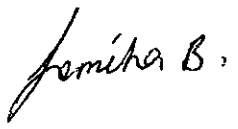

S. BULUT

CONTENTS

CHAPTER 1: REVIEW OF MODEL REFERENCE ADAPTIVE CONTROL TOGETHER WITH ITS REDUCED ORDER FORM AND ITS APPLICATIONS IN THE HYDRAULIC FIELD

CHAPTER 2: HYDRAULIC SYSTEMS MODELLING

CHAPTER 3: REVIEW OF MODEL REDUCTION METHODS

CHAPTER 4: THE ROBUSTNESS ANALYSIS OF THE REDUCED ORDER MCS CONTROL

CHAPTER 5: APPLICATION OF MCS TO AN ELECTROHYDRAULIC ACTUATOR PLANT TOGETHER WITH COMPARATIVE IMPLEMENTATION STUDIES

CHAPTER 6: IMPLEMENTATION OF MCS ON A SERVOHYDRAULIC MATERIALS TESTING MACHINE UNDER LOAD CONTROL

CHAPTER 7: COMPARATIVE ROBUSTNESS TESTS AND STRAIN MEASUREMENT UNDER MCS LOAD CONTROL

CHAPTER 8: CONCLUSIONS AND FUTURE WORK

PUBLICATION

1 - 'Application of the MCS Algorithm to the Control of an Electrohydraulic System', *Euriscon*, pp. 1861-1871, August 1994, Malaga, Spain.

Co author: **D. P. STOTEN**

LIST OF NOTATIONS

A	is the (nxn) nominal plant parameter matrix.
A_r	is the (hxh) reduced order plant parameter matrix.
A_m	(hxh) reference model matrix.
A_1, A_2	are the effective area of the first and second chambers of the actuator respectively.
A_p	is the average effective area of the actuator ($A_p = (A_1+A_2)/2$).
A_i	is the ($nixni$) i^{th} subsystem A matrix (MIMO systems).
$-a_{iik}$	is the k^{th} element of the last row of the matrix A_{ii}.
a_{ijk}	is the k^{th} element of the last row of the matrix A_{ij}.
$-am_{iik}$	is the k^{th} element of the last row of the matrix Am_{ii}.
a_i, b_i	are the unknown parameters of the plant.
ΔA	is the (nxn) matrix that contains the rapidly varying elements of A.
a_i	denotes the i^{th} element of the n^{th} (h^{th} row of the reduced order plant matrix A_r.) row of the plant A matrix (SISO Systems).
am_i	denotes the i^{th} element of the h^{th} row of the reference model A_m matrix (SISO Systems).
δa_r	is the last element of δA_r.
δA_r	is the (hx1) vector related to r and $d(x_r, t)$ (SISO reduced order plant).
B	is the (nx1) nominal plant matrix.
B_r	is the (hx1) reduced order plant matrix.
B_m	is the (hx1) reference model input matrix.
b_1	is the only non-zero element of the B (B_r in the case of the reduced order plant).
C_e	is the output error matrix.
$d(x_r, t)$	is the disturbance term due to the unmodelled dynamics, plant parameters variations and nonlinearities in the plant.
D	is the diameter of the specimen.
d_1	is the h^{th} element of the vector $d(x_r, t)$ (SISO reduced order systems).
E	is the modulus of the elasticity.
f_s	is the coefficient of viscous friction.
$\dot{f}$	is the first time derivative of a function $f(t)$.
F	is the force due to the pressure differences.
$G_p(s)$	is the nominal plant transfer function.
$G_r(s)$	is the reduced order plant transfer function.
h	is the reduced order plant state dimension.
i	is the input current.
I_n	is the (hxh) identity matrix.
J	is the moment of inertia.
k_1	is the second order MCS position gain.
k_2	is the second order MCS velocity gain.
k_r	is the second order MCS adaptive gain.
k_d	is the derivative gain.
k_p	is the proportional gain.
k_i	is the integral gain.
K	is the (kxn) MCS state feedback gain; (typically $K(0)$=0, MIMO systems).

K_r	is the (kxk) MCS forward loop gain; (typically $K_r(0)$=0, MIMO systems).
k_v	is the volumetric coefficient.
m_p	is the mass.
n	is the nominal plant state dimension.
N	is the bulk modulus of the oil.
Q_1, Q_2	are flows into the actuator chambers C_1, C_2 respectively.
Q_f	is the hydraulic volume flow ($Q_f = Q_1 = Q_2$).
Q	is an (nxn) symmetric positive definite matrix associated with the Lyapunov equation.
P_s	is the supply pressure.
P_v	is the pressure drop.
P	is an (nxn) symmetric positive definite matrix solution of Lyapunov function equation.
P_1, P_2	are pressures in the first and second chambers of the actuator.
ΔP	is the pressure difference of the first and second chambers of the actuator ($\Delta P = P_1 - P_2$).
r	denotes the reference signal.
r_s	is the restoring stiffness.
$\mathbb{R}$	denotes the set of real numbers.
$\mathbb{R}^+$	denotes the set of positive real numbers.
$\mathbb{R}^{h\text{x}h}$	denotes the set of real matrices of dimension (hxh).
$\mathbb{R}^{h\text{x}1}$	denotes the set of real matrices of dimension (hx1).
s	is Laplace variable.
x_e	denotes the state error vector.
x	is the (nx1) plant state vector.
x_r	is the (hx1) reduced order plant state vector.
x_i	is the (nix1) the state vector of the i^{th} subsystem (MIMO systems).
x_m	denotes the reference model state vector.
x_{mi}	is the (nix1) i^{th} subsystem reference model state vector (MIMO systems).
t_s	is the settling time.
t	denotes the time.
u	is the control signal.
V	is a Lyapunov function
$\dot{V}$	denotes first derivative of a Lyapunov function.
V_t	is the total half volume.
V_e	is the effective half volume.
ω	is the signal vector defined as, $\omega = \left[x^T, \quad r^T\right]^T$.
ω_n	is the natural frequency of the servovalve (rad/sec).
y	is the plant output vector.
y_p	is the nominal plant output vector.
y_r	is the reduced order plant output vector.
y_e	is the output error vector.
y_{eh}	denotes the h^{th} element of the vector y_e (SISO reduced order plant).
Γ_α	is the (kxk) matrix that contains the terms α.

Γ_β is the (kxk) matrix that contains the terms β.

θ is the angle of rotation.

ρ is the density of the fluid.

σ is the longitudinal stress.

σ_y is the yielding stress.

τ is the time constant.

ζ is the damping coefficient of the servovalve.

Φ is the (hx1)vector (SISO reduced order systems) or the (kxh+k) matrix (MIMO reduced order systems) that contains the integral gains and the plant parameters.

Ψ is the (hx1) vector (SISO reduced order systems) or the (kxn+k) matrix (MIMO reduced order systems) that contains the proportional gains and the elements of the plant B matrix.

ε is the strain.

δ is the elongation of the bar in tension.

α is the MCS integral adaption gain (scalar), $\alpha\rangle 0$.

β is the MCS proportional adaption gain (scalar), $\beta \geq 0$.

Δ is the sampling interval.

$\sigma = \beta - \alpha\Delta$

CHAPTER 1

REVIEW OF MODEL REFERENCE ADAPTIVE CONTROL TOGETHER WITH ITS REDUCED ORDER FORM AND ITS APPLICATIONS IN THE HYDRAULIC FIELD

1.1 - INTRODUCTION

In real life the unmodelled dynamics and nonlinearities always exists in the plant due to the fact that may be the dynamics of the plant is too complex or not completely understood. Additionally, parameters of the plant changes depending on the working condition and the input signal. For that reason, the effects of the unmodelled dynamics should considered for linear controllers implementation therefore, the accuracy of the system responses. If the system is containing larger unmodelled dynamics, it seems desirable to use model reference adaptive control which requires less knowledge about the plant dynamic parameters.

Reduced order adaptive control can be described as the standard adaptive controller together with some unmodelled dynamics. In this type of adaptive control the plant is represented by an approximate lower order model. Subsequently some parts of the plant are ignored and the unmodelled dynamics are included into the disturbances term. The reduced order adaptive control is capable of controlling the system in a stable manner, provided that some limitation on the reference model and input signal are considered.

Cook and Chen [1] were used such an approach and they showed that the controller is stable provided that the input signal is persistently exciting.

Hydraulic systems are inherently nonlinear and parameters of systems change during its operation depending on various reasons. In comparison with linear controller strategies using Model reference adaptive controller in hydraulic systems control brings many advantages, such as adaptivity to the changes in plant parameters and the working conditions and nonlinearities in systems. Using adaptive controller in this field increase the efficiency and accuracy of systems.

The adaptive system is exponentially stable when the input is persistently exciting then, it has a sufficiently large amplitude. Under this condition the system will remain robust when it is subject to bounded external disturbances. The adaptive system can be made robust in the presence of a class of unmodelled dynamics of the plant by suitably modifying the adaptive law.

Adaptive control has connections with other theories. First, there is a very strong connection with nonlinear system theory because adaptive systems are inherently nonlinear. Secondly, adaptive control also has links with singular perturbations and averaging theory because of the separation of the time scales in some adaptive systems. Thirdly, adaptive control has connections with stochastic control and parameter estimation. This is due to importance of parameter estimation and converge of the controller in adaptive systems. Adaptive controller can also be used in the case of system identification tests to obtain the nominal transfer function of the system. Later this model can be used to design fixed gain controller.

1.2 - ADAPTIVE CONTROL

Adaptive controllers have been used for controlling variety of systems since 1950. Many research have been done to fully understand and improve adaptive controller theory over the years [2] and [3]. Over the years it has been experienced that using adaptive controller in systems which are subject sudden changes have many advantages over linear controller. Conventional controller can produce good responses provided that the working

condition and parameters of the system are not changing much but they may not be accurate when the plant subjects to large parameter variations.

Adaptive control is not constant feedback control. In the work of Astrom [4], adaptive control was simply described as a special type of nonlinear feedback control and the states of the process were separated into two categories, which change at different rates. The states, which were varying slowly observed as parameters.

1.2.1 - State-Space Stability Proof of Adaptive Systems

In the 1960s, there were important development in the adaptive control theory. The state-space theory was introduced to describe plants by linear transfer function and Lyapunov's stability theory was also introduced to prove the convergence and stability of adaptive systems. There were also important developments and improvement in stochastic control theory [5]. The converge of model reference adaptive control was proven in [6] by using the update law, which was proposed in the 1950s.

During 1970s, adaptive regulators were implemented simply due to new developments in microelectronics. Popov's hyperstability based input-output proofs from the late 1970s appear in [7] and in the work of Landau [8]. Stability proofs in the discrete time deterministic and stochastic cases also studied at this time from Goodwin and Sin [9].

Lyapunov based state-space stability proofs for adaptive systems were showed by Narendra, Lin & Valavani in [10]. In this method, an additional feedback term was used to ensure that the fist order time derivative of the parameter error vector belongs to the stability region. It was shown that systems with relative degree greater than 2 together with high frequency unmodelled dynamics to be never exponentially stable. The paper presented a complete proof of stability in the case of multivariable continuous adaptive control systems. In [11], the stability problem was clearly defined and it was suggested that the controller could be stable provided that the output error is bounded.

Several methods have appeared in the literature discussing specific methods of adjusting parameters in the adaptive systems using Lyapunov's direct method, which use a model as a reference. In all methods, it has been suggested that the crucial point was the determination of conditions under which the entire system is asymptotically stable.

Narendra and Tripathi used Lyapunov's direct method to determine the structure of stable adaptive systems [12] in 1971. In this work, systems were described by first order differential equations. The adjustment of the gain and the time constant was considered. It was suggested that output noise and parameter variations in the plant can be compensated by introducing new adaptive parameters. The effect of measurement noise in the case of higher order system was also considered. The Lyapunov approach has been widely used in order to measure the stability of adaptive systems which are subject to bounded (unknown) time varying parameter variations.

By the beginning of 1980's several basic problems had been resolved such as identification of the adaptive controller in the case of linear time invariant plants together with some additional restrictions on inputs and disturbances [13] and [14]. It was first studied by Rohrs and co-workers that the stability of adaptive control were very sensitive in the presence of unmodelled dynamics and it has to be handled very carefully. The controller structure was simplified by neglecting the high frequency modes of the system in [15].

1.2.2 - Effects of Unmodelled Dynamics & Disturbances

In the work of Lindorff [16] the effects of disturbance and incomplete parameter adaptation on the performance of adaptive control were considered. The Lyapunov theory was used to prove the stability of the system. It was shown that parameters in the adaptive controller may not converge in the presence of disturbances and high frequency unmodelled dynamics unless the input signal is sufficient enough in mid frequency range.

In the work of Ioannau and Kokotovic [17], the original plant model-reduced order model mismatch was characterised by a scalar parameter μ, which was defined as the ratio of the modelled (dominant) and unmodelled dynamics of the plant. It was assumed that the dominant part of the plant is slow which can be matched by the reduced order model. The unmodelled dynamics are fast and they are in the high frequency range. In this adaptive law the output error played a dual role in the adjustment of the control parameter vector. The scalar constant μ appeared as a singular perturbation parameter in two-time scale representations of the plant.

The development of tools for analysis of transient behaviour of the adaptive system enabled this control strategy to be implemented on practical systems, such as reactors, robot manipulators, ship steering systems, advanced flight control systems for aircraft and spacecraft and process control. New developments in microelectronics made possible to implement the nonlinear laws to existing adaptive control. The research re-examines the robustness properties of adaptive control and whether or not adaptive controllers were at least as good as fixed gain controllers.

1.3 - ELECTROHYDRAULIC SYSTEMS

Electrohydraulic servo systems can be described as the combination of the high power of hydraulic actuation and electronic control. Electrohydraulic systems can provide very large torques together with fast dynamics, therefore, they have been used in many industrial applications, such as: heavy duty robots, materials forming machine and materials testing machine. It is difficult to obtain satisfactory results under linear controller, due to fact that the dynamic equations of systems are nonlinear and plant parameters vary greatly depending on the set point for various reasons, e.g. the nonlinear relation between the flow velocity and the pressure, the hydraulic resistance of flow through the channels, Reynolds number, the type of flows, channel geometry and friction factors.

Standard analogue control strategies are not capable of bringing out the full potential of the electrohydraulic servo systems due to nonlinear characteristics of such systems. A linear controller can only be implemented for only one operating condition. However, even at one operating point the plant characteristics will often vary during operations. For that reason, digital controllers have been applied to electrohydraulic servo systems, in particular position control systems. In this techniques, usually linearised model of the controlled plant has been used for the implementation and the controller parameters are changed easily according to variations in systems characteristics and nonlinearities Digital controllers have been using in electrohydraulic positioning systems control since 1970 [18]. Recently, adaptive controllers have been applied to powerful electrohydraulic systems easily and cheaply due to use of fast microcomputers.

The relationship between the flow and pressure is nonlinear in the servovalve and at the range of low tests frequencies its dynamics is negligible. During stress and strain tests the servovalve operates very close to its null position. In addition is such tests, supply pressure to the servovalve can assume to be constant since the flow rate variations are negligible. The unwanted feature of this type of application is the internal and external leakage of the actuator. The servovalve operation near its null position has important implications for on-line identification and controller adaptation.

In a hydraulic system the speed of the hydraulic motor can be controlled by varying either the pump displacement or the pump speed. The inverter controlled hydraulic motor system under a Self-tuning control was studied in [19]. The pump speed changed by using an inverter which adjusts the speed of an induction motor. The pump controlled system showed faster response with higher accuracy but its efficiency was lower. On the other hand the inverter controlled hydraulic systems showed higher accuracy but their response was slower and the direction of the hydraulic motor unchangeable. Nevertheless, the inverter controlled hydraulic systems have simpler structure and they cost comparatively less price.

The electrohydraulic positioning servo system shows nonlinear behaviour due to following reasons: a directional nonlinearity due to use of asymmetric actuator, the nonlinear relationship between pressure and flow in the servovalve the square root of the pressure drop across the orifice, the characteristics of the system changes during the stroke due to the volume changes and saturation of the servovalve and backlash in the actuator. The directional nonlinearity does have a significant effect on the system performances especially when the load is driven in the extend direction. This nonlinearity can be compensated for in software by scaling the valve control signal differently according to its sign. Similarly, nonlinearities due to the servovalve saturation can be avoided by limiting the control signal in software to be just within the level which saturates the valve. This will not allow to saturate the servovalve.

1.4 - APPLICATIONS OF ADAPTIVE CONTROL IN THE CASE OF ELECTROHYDRAULIC SYSTEMS

In general, Proportional or Proportional plus Derivative Feedback (P+DFB) control are used in position control of hydraulic systems. The reason of that is hydraulic positioning systems show integral action due to the nonlinear relationship between the flow from the servovalve and the position of the actuator piston. The flow is proportional to the velocity of the actuator, therefore these control strategies may produce large steady-state error in position control. Similarly, using Proportional plus Integral Control (P+I) or PID controller in order to get an zero steady-state error, will result in undesired overshoot or even oscillating transient behaviour due to the existence of a natural integrator in the plant. In general this makes, conventional controller unsuitable for the position control of hydraulic systems. Adaptive controllers are good option in this area, specially if the hydraulic actuator has single rod cylinder [20].

Direct and indirect adaptive control have been used for the practical application of adaptive control to electrohydraulic positioning systems. Model reference (direct) adaptive control coefficients are required to obtain a prescribed model following performances which are estimated from input-output data therefore, parameters not calculated from a plant model.

Self-tuning (indirect) adaptive control is based on on-line estimated model of the original system. The controller continuously adapt itself to the new estimated model. In the work of Finney, Self-tuning control was only used for the initial tuning of controller parameters [21]. For a full adaptive version the estimator should be modified to forget old data, for example by the inclusion of a fixed forgetting factor as used by Vaughan and Whiting [22]. Daley implemented a similar method to a rotary hydraulic system in 1987, which was studied in [23]. In this work, the Self-tuning control algorithm was applied to a rotary electrohydraulic test rig. It was shown that the Self-tuning control algorithm was preserved the system stability in the presence of large and sudden changes in the system characteristics. When the system controlled under a fixed gain PID controller subjected to similar changes, the controller broke down. Both controllers were shown to perform well in nominal condition despite the presence of nonlinearities, measurement noise and load disturbances. It was suggested that for a satisfactory application of indirect adaptive

controller an accurate parameter estimator together with signal filtering are necessary [24]. In this work an indirect adaptive controller was implemented to an electrohydraulic servo actuator system. Additionally, an method which was not allowing the plant parameters increase beyond the certain points used to preserve the system stability.

An implicit Self-tuning regulator (STR) control was implemented on an single rod actuator servo system in [25]. The difference between the implicit and explicit STR is there is no need to solve the Diophantine equation in the case implicit STR. In [26], another Self-tuning adaptive controller was applied to a single rod actuator positioning system based on a pole placement control. In this work the recursive least squares estimator approach and a data filter were used together with the pole placement adaptive control. This algorithm gave good responses despite the nonlinearities, unmodelled dynamics and changes in the system, even when the changes were significant and sudden. In same condition an equivalent linear controller did not produced satisfactory responses. The steady-state error was occurred partly non-symmetric characteristic of the single rod actuator electrohydraulic position system.

The performances of the implicit and standard STR were compared in [27]. It was shown that the implicit STR structure is simpler since the algorithm itself directly estimating the controller parameters. Additionally, it was demonstrated that the implicit STR yield better control performance in comparison with explicit STR, even under variations in operating conditions.

Nonlinear aspects of the material testing applications makes such applications good candidates for adaptive control. Using an adaptive controller in the material testing area has many advantages due to the fact that the controller can adapt itself to nonlinear changes in the system and specimen unlike linear controller strategies. Therefore, adaptive control can be use very effectively in tests involving higher test frequencies and tests involving nonlinear specimen deformation such as low cycle fatigue tests. In all closed-loop electrohydraulic strain and load control tests, the non-ideal nature of servovalve are significant and can be handled effectively by adaptive controller. In [28], a Self-tuning control was implemented on a electrohydraulic material testing machine and it was used in stroke, load and strain control. A pole-placement controller approach was used for controller adaptation. The self-tuning control scheme was shown to be effective in both simulation and real life operation.

A number of applications of model reference adaptive control to electrohydraulic position control systems exist (Edge and Figueredo [29] and [30]). In [31] an adaptive controller was designed and implemented on a microcomputer and successfully applied to a electrohydraulic positioning system. In this work, the model reference adaptive control was implemented based on Lyapunov's stability method and the stability of the position control system was examined in the presence of changes in load forces.

A model reference adaptive controller was implemented to a servohydraulic piston motor in which the Bessel prototype transfer function was chosen as the reference model in [32]. The adaptive controller was performed better than the PID and model following optimal controller when the plant subjected to changes in pressure, loads and input signal. This was due to the fact that the adaptive controller adapted itself changes in the dynamic parameters of the system.

Both the direct (Model Reference Adaptive Controller) and indirect (Self-tuning controller) have been used in the case of electrohydraulic system control. In many cases the adaptive control methods were applied to the systems in a reduced order form and satisfactory results were obtained. However, the Self-tuning controller requires on-line plant parameter identification. Therefore, the implementation of the Self-tuning controllers are time consuming. The structure of the direct adaptive controller, (e.g. the MCS control) is simple, therefore easy to implement.

1.5 - ADAPTIVE CONTROL WITH UNMODELLED DYNAMICS

In the presence of unmodelled dynamics adaptive controller preserve the system stability provided that the input signal is Persistently Exciting (PE). In general, the effects of unmodelled dynamics (reduced order adaptive controller) are assumed acting as disturbances therefore, it is included into the disturbances term in state-space representation of the plant. Under this condition the controller possess convergence properties which allow certain amount of disturbances can be tolerated [1]. The converge between the nominal and the reduced order plant is not global and depends on many variables.

The concept of stability of adaptive control is that it should be preserved in the presence of actual disturbances present in the system. The main difference between adaptive control and linear control system is that stability does not depend only on the plant and control system but also on the reference input in the case of adaptive control. The reference input should be persistently exciting in the case of the nominal adaptive system (suppose there is no disturbances and unmodelled dynamics) to preserve the stability.

Exponentially stable adaptive system are stable in the presence of disturbances due to the unmodelled dynamics, plant parameters variations and nonlinearities in the plant. Exponential stability condition will bring a stability margin which will preserve the stability of the adaptive system in the presence of disturbances provided that the input signal is persistently exciting [33]. In the case of uniformly asymptotically stable system the stability margin will be an equilibrium surface instead of a single equilibrium point and if the system becomes unstable then, the equilibrium surface became a locally unstable point [10].

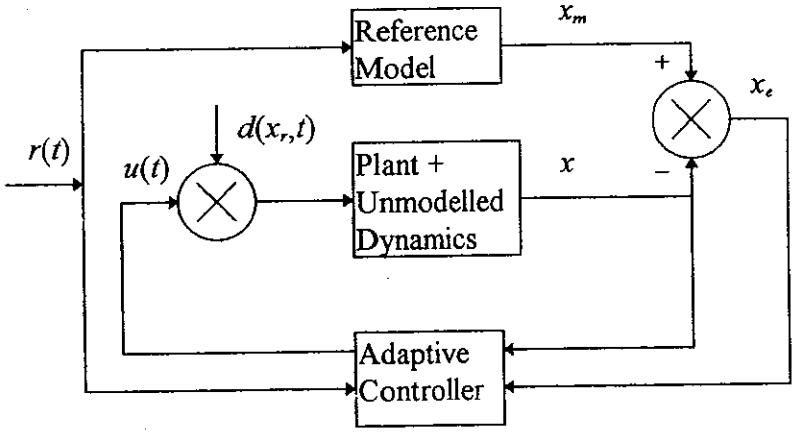

Fig. 1.1: Adaptive controller with disturbances due to unmodelled dynamics and plant parameter variations.

In Fig. 1.1, x_m is the reference model output, x_r is the reduced order plant output, r is the reference signal, u is the input signal to the plant, $d(x_r,t)$ is the disturbance term due to the unmodelled dynamics, parameter variations and nonlinearities in the plant and x_e is the output error signal.

Ideally, if the system is disturbances free then, the steady-state error goes to zero when time goes to infinity. The stability of adaptive systems can be preserved in the presence of internal (unmodelled dynamics) and external disturbances provided that maximum magnitude of the disturbance is known [34].

Two essential instability mechanisms occur due to unmodelled dynamics in adaptive control. The first one is when the adaptive controller gains are very big. This will lead to very fast adaptation and finally the instability will take place due to excitation in the high frequency range of the plant. The second instability take place when the input signal is exciting the high order unmodelled parts of the systems [35]. This kind of instability happens rather slowly even for the suitable set small values of the adaptive gains.

1.6 - REDUCED ORDER MODEL REFERENCE ADAPTIVE CONTROL

The standard adaptive controller may not be give satisfactory responses in the presence of unmodelled dynamics due to ignorance of the high order states of the plant. The stability can be preserved under this condition provided that some limitations are set on the input and reference signal. Some new adaptive laws were proposed to cope with this problem. General characteristics of this methods are that they required very little information about the plant parameters therefore, they can easily preserve the system stability in the presence of unmodelled dynamics. Park used similar method in [6]. He set a suitable set adaptive loop gain to converge the nominal and reduced order system. The adaptive system with this new adaptive law shown in Fig. 1.2. Consider a time-invariant plant in state-space form

$$\dot{x}(t) = Ax(t) + Bu(t) \tag{1.1}$$

where $A \in \mathbf{R}^{nxn}$ and $B \in \mathbf{R}^{nxl}$ and $x = \left[x_1 \;,\; x_2 \;,\; \ldots \;,\; x_n\right]^T$ $x \in \mathbf{R}^{nxl}$. The variables $x(t)$ and $u(t)$ denote the plant state vector and the control input respectively. The stable reference model is given by

$$\dot{x}_m(t) = A_m x_m(t) + B_m r(t) \tag{1.2}$$

where $x = \{x_i\}$, $x_m = \{x_{mi}\}$ are n-dimensional state vectors of the reduced order plant and reference model respectively, $r(t)$ is the m-dimensional reference signal and $u(t)$ is the

plant input signal of m-dimensional. A, B contain unknown coefficients of the plant. The output error is written as

$$x_e = x_m - x$$

$$\dot{x}_e = A_m x_e(t) + f \tag{1.3}$$

where $f = (A_m - A)x(t) + B_m r(t) - Bu(t)$, then the control objective is to manipulate f in some way so that $\lim_{t\to\infty} x_e(t) = 0$. Therefore, Lyapunov's theorem is introduced to (1.3):

$$V = x_e^T P x_e + h(\Phi + \Psi) \tag{1.4}$$

where Φ, Ψ are matrices of parameter vectors $\Phi_i (i = 1,\ldots,n)$, $\Psi_i (i = 1,\ldots,m)$ to be defined. Then, equation (1.4) becomes:

$$\dot{V} = -x_e^T Q x_e + 2x_e^T P f + \dot{h} \tag{1.5}$$

where

$$-Q = A_m^T P + P A_m \tag{1.6}$$

By Lyapunov's theorem, with any $Q > 0$, it follows that $P > 0$ is a unique solution to Equation (1.6), A_m is a stable matrix, as assumed.

Derivatives of model-plant error are sometimes required e.g., M.I.T. rule [36], but may be avoided in gain adjustment schemes if the system transfer function is 'positive real' by using Kalman's lemma. Parks's use of Kalman's lemma (1963), subsequently extended by Monopoli and co-workers in [37]. It was shown that the adaptive law $\dot{K}_m = \lambda^{-1} x_e r$, will preserve stability provided that the closed-loop transfer function is strictly positive real. If the plant transfer function is positive real then, the set $\dot{V} = 0$ must be examined to ensure asymptotic stability of x_e. In feedback schemes plant parameters are adjusted continuously, so that in the simplified case treated here, $x_e \to 0$. Equation (1.4) can be written as

$$V = x_e^T P x_e + \sum_{i=1}^{n} \Phi_i^T \Phi_i + \sum_{i=1}^{m} \Psi_i^T \Psi_i \tag{1.7}$$

where Φ_i, Ψ_i are parameter vectors to be defined in terms of the elements of the matrices $A_m - A$ and $B_m - B$ which express the parameter error between the model and the plant.

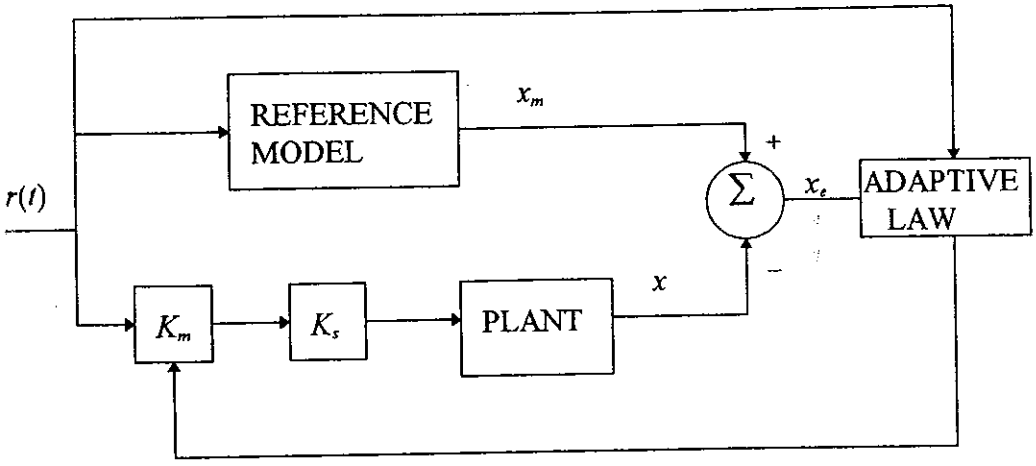

Fig. 1.2: Reduction of order configuration with adaptive gain (Taken from [6])

In this diagram K_m is the adaptive loop gain which adjusts $K_m K_s$ to mach the model gain K. Hence, the steady-state error will ideally will become zero when times goes to infinity. Following Equation (1.5) becomes

$$\dot{V} = -x_e^T Q x_e + 2\left(x_e^T P f + \sum_{i=1}^{n} \dot{\Phi}_i^T \Phi_i + \sum_{i=1}^{m} \Psi_i^T \Psi_i \right) \tag{1.8}$$

Let E define the whole state-space with $\xi \in E$ where ξ is defined by $\xi^T = \left[x_e^T, \Phi_1^T, \ldots, \Phi_n^T, \Psi_1^T, \ldots, \Psi_m^T \right]$. Let $E_1 \subset E$, where E_1 is the n-dimensional subspace with $x_e \in E_1$. In Equation (1.7) V is positive definite in E. The basic idea in feedback synthesis is to specify $\left(\dot{\Phi}_i, \dot{\Psi}_i \right)$ in (1.8) so that

$$x_e^T P f + \sum_{i=1}^{n} \dot{\Phi}_i^T \Phi_i + \sum_{i=1}^{m} \dot{\Psi}_i^T \Psi_i \equiv 0 \tag{1.9}$$

and consequently

$$\dot{V} = -x_e^T Q x_e \tag{1.10}$$

Since $\dot{V}$ is only negative *semidefinite* in E, but negative definite in E_1, it may be concluded according to the Lyapunov's theorem, that the equilibrium at $x_e = 0$ is asymptotically stable and equilibrium at $\xi = 0$ is stable. It follows that $x_e \to 0$ and the parameter error vectors are bounded. It will be shown in certain cases that $\xi \to 0$ if the frequency content of the input signal is persistently exciting.

An extended criteria which made non-positive real transfer functions to positive real by multiplying by a polynomial in s with roots of negative real parts was used in [36].

By doing so, the resulting adaptive law required n-m-2 derivatives of the output error where n is the number of plant poles and m is the number of plant zeros. It was pointed out that the indirect adaptive controller may fail when it is subject to some unmodelled dynamics even with full state measurement available and the state variables of the model and the nominal plant may not converge.

1.6.1 - Direct Adaptation

Direct adaption (Model reference adaptive control) assumes that plant parameters are adjustable and updates the controller parameters directly. In the case of *indirect* adaptation (Self tuning regulator), the adjustment takes place external to the plant. The self turning regulator first identifies the plant parameters recursively and then uses these estimates to update the controller parameters through some fixed transformation. In this case, $u = r$ and Φ, Ψ are in turn defined by $\phi = A_m - A$, $\psi = B_m - B$ with columns Φ_i, Ψ_i respectively. Then, Equation (1.3) becomes

$$\dot{x}_e = A_m x_e + f \tag{1.11}$$

where $f = \Phi x + \Psi r$.

It is seen that (1.10) can be satisfied if

$$\dot{\Phi}_i^T = -x_e - P x_i \,, \qquad (i=1,...,n) \tag{1.12}$$

$$\dot{\Psi}_j^T = -x_e^T \mathrm{Pr}_j \,, \qquad (j=1,...,m) \tag{1.13}$$

Assuming that the elements A and B are directly adjustable, then (1.11) becomes

$$\dot{a}_i^{*T} = x_e^T P x_i \,, \tag{1.14}$$

$$\dot{b}_j^{*T} = x_e^T \mathrm{Pr}_j \,, \tag{1.15}$$

A_m and B_m are the model parameters and it is assumed that they are constant.

1.7 - THE REDUCED ORDER MODEL REFERENCE ADAPTIVE CONTROL DUE TO UNMODELLED DYNAMICS

Lyapunov equation method is very useful method to prove the global stability of the reduced order model reference adaptive controller, therefore it has been widely used in this case. A Lyapunov's second law equation was used to prove the stability of the system with unknown dynamics in [38]. Additionally, the use of the method was extended in the cases of reduced order adaptive systems, systems with disturbances, time varying systems, multivariable systems and adaptive observers. Consider a first order SISO nominal plant output with unmodelled dynamics which is given as

$$x_r(s) = \frac{b}{s + a_p} u(s) \tag{1.16}$$

where parameters b and a_p are unknown constants of the reduced order plant. The actual response is modelled as the output of the nominal plant, with some unstructured dynamics represented by a bounded operator D_a:

$$x_p(t) = x_r(t) + D_a u(t) \tag{1.17}$$

A reference model is defined as

$$x_m(s) = \frac{a_m}{s + a_m} r(s) \tag{1.18}$$

where $a_m > 0$ arbitrarily. Consider the linear model following control (LMFC) law which was studied in [39]. In the case of LMFC the feedforward part was represented by a positive (or strictly positive) real transfer function. This ensures the global stability (or global asymptotic stability) of the system. The LMFC law is

$$u = -k_x x + k_r r \tag{1.19}$$

where k_x , k_r are the feedback gain and the feedforward gain respectively, $k_x \in \mathbf{R}^{1x1}$, $k_r \in \mathbf{R}^{1x1}$. The input signal is given as

$$u = \theta^T \varphi \tag{1.20}$$

$$\frac{d\theta}{dt} = -k\varphi x_e \tag{1.21}$$

where $\theta = \begin{bmatrix} \theta_1 & \theta_2 \end{bmatrix}^T = \begin{bmatrix} k_r & k_x \end{bmatrix}^T$ is the adjustable parameter vector and $\varphi = \begin{bmatrix} r & -x_r \end{bmatrix}^T$ is the regression vector, r is the reference signal and x_r is the reduced order plant output signal in Fig. 1.3.

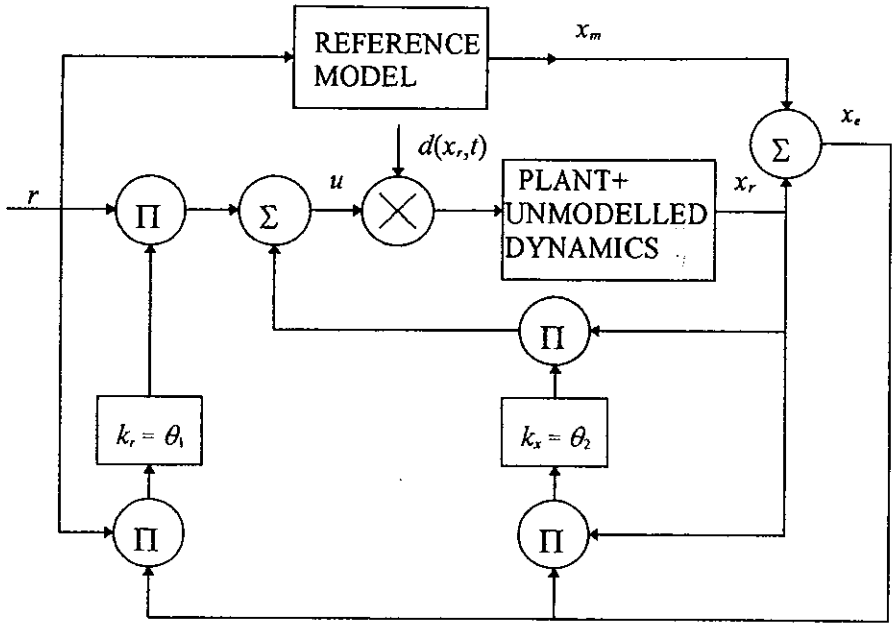

Fig. 1.3: Block diagram of a model reference adaptive control system (Taken from [42])

The controller generates the input $u(t)$ of the plant, using $x_m(t)$, $x_r(t)$ and $r(t)$. The error between the reduced order plant and reference model output, $x_e(t) = x_m(t) - x_r(t)$, tends to zero asymptotically. The output error signal is

$$x_e = x_m - x_r \tag{1.22}$$

Equation (1.21) can written as

$$\frac{d\theta}{dt} + k\varphi\left[G(p)\varphi^T\theta\right] = k\varphi x_m \tag{1.23}$$

Equation (1.23) separates the behaviour of the parameters from the other states which in this equation are hidden in G and φ. In this equation the rate of change of the parameters is governed by the constant k and the rate is quadratic in the components of φ. This indicates that there are problems in controlling the rate of change of the parameters unless the vector φ is bounded.

The sensitivity of an adaptive system in the presence of unmodelled dynamics and nonlinearities can be minimise if the real plant and model parameters converge during the operation. In general, exponential stability of adaptive algorithms is achieved when the reference input is PE; this will guarantee satisfactory stability properties of the adaptive systems. Stability of the adaptive control was studied in paper [40]. It was shown that the system is guaranteed to remain stable in the presence of unmodelled dynamics,

disturbances, nonlinearities and parameter changes. It was suggested that if the adaptive system is exponentially stable, it can tolerate certain levels of disturbances. In practice, it is commonly believed that parameter convergence is also an important condition for stability of the system.

In the case of model reference adaptive control, the designer selects an appropriate reference model transfer function. The control aim is to design a control system to get the plant output $x_r(t)$ to track the model output $x_m(t)$, in response to reference signal $r(t)$ driving the model.

The stability of the adaptive controller in the case of unmodelled dynamics very much depend on the condition when the parameters of the real plant and reduced order model are convergence [40]. The loop transfer function can be written as $L(s) = (a_m - a_p)/(s + a_p)$, then for the sake of stability the unmodelled dynamics and nonlinearities, $D_a(j\omega)$ should satisfied the following condition:

$$|D_a(j\omega)| < \left| \frac{j\omega + a_m}{(j\omega + a_p)} \times \frac{1}{(a_m - a_p)} \right| \tag{1.24}$$

for all $\omega > 0$. Condition (1.24) brings a bound on the model parameter, a_m, and in general, on the bandwidth of the model. After the plant and model parameters convergence:

$$u(j\omega) \sim \frac{j\omega + a_m}{j\omega + a_p} r(j\omega) \tag{1.25}$$

The term $D_a(j\omega)$ is negligible since its frequency is usually above the model and plant bandwidth, so that (1.25) can be written as:

$$u(j\omega) \sim r(j\omega) \tag{1.26}$$

Equation (1.26) suggests that the disturbances term due to unmodelled dynamics, nonlinearities and parameter variations can be minimise provided that the spectrum of the reference signal is chosen according to the model and the plant bandwidth.

The nature of the reference signal important in the case of adaptive systems with unmodelled dynamics. If the reference signal is square wave then only one parameter of the system can be determined [41]. The situation is different under sinusoidal reference signal In this case, it is possible to have an unique equilibrium point since a sinusoidal reference signal is persistently exciting of second order. Additionally, two parameters of the plant can be determined [42].

1.8 - THE REDUCED ORDER MCS CONTROL

The reduced order MCS control can be described as the nominal MCS control with some unmodelled dynamics. In this case, the unmodelled dynamics are considered as internal disturbances in the plant.

The Minimal Control Synthesis (MCS) algorithm was originally developed as an extension to the Model Reference Adaptive Control (MRAC) algorithm of Landau [43]. The MCS control does not requires plant dynamics parameters for implementation, and it still guarantees global asymptotic stability of the closed-loop system [44], [45]. The MCS control was first proposed in 1990 [46] as a form of direct adaptive control. The algorithm has been implemented on a variety of plants, such as robotic manipulator motion control, electrohydraulic servo system control, materials testing machine control (stroke/stress control), chaotic systems control,... etc.

The closed-loop stability proofs have been presented for a large class of electromechanical plants with Lagrangian dynamics, despite the fact that no prior knowledge was required concerning the nominal values of the plant parameters. The implementation of the MCS control requires a minimum amount of information about the plant parameters.

Since 1990, significant extensions to the basic MCS have been presented (including a decentralised version), together with sets of implementation studies. An overview of the algorithm and its extension was studied in [47]. In this paper, the predicted performance characteristics of MCS for all cases were matched in practice.

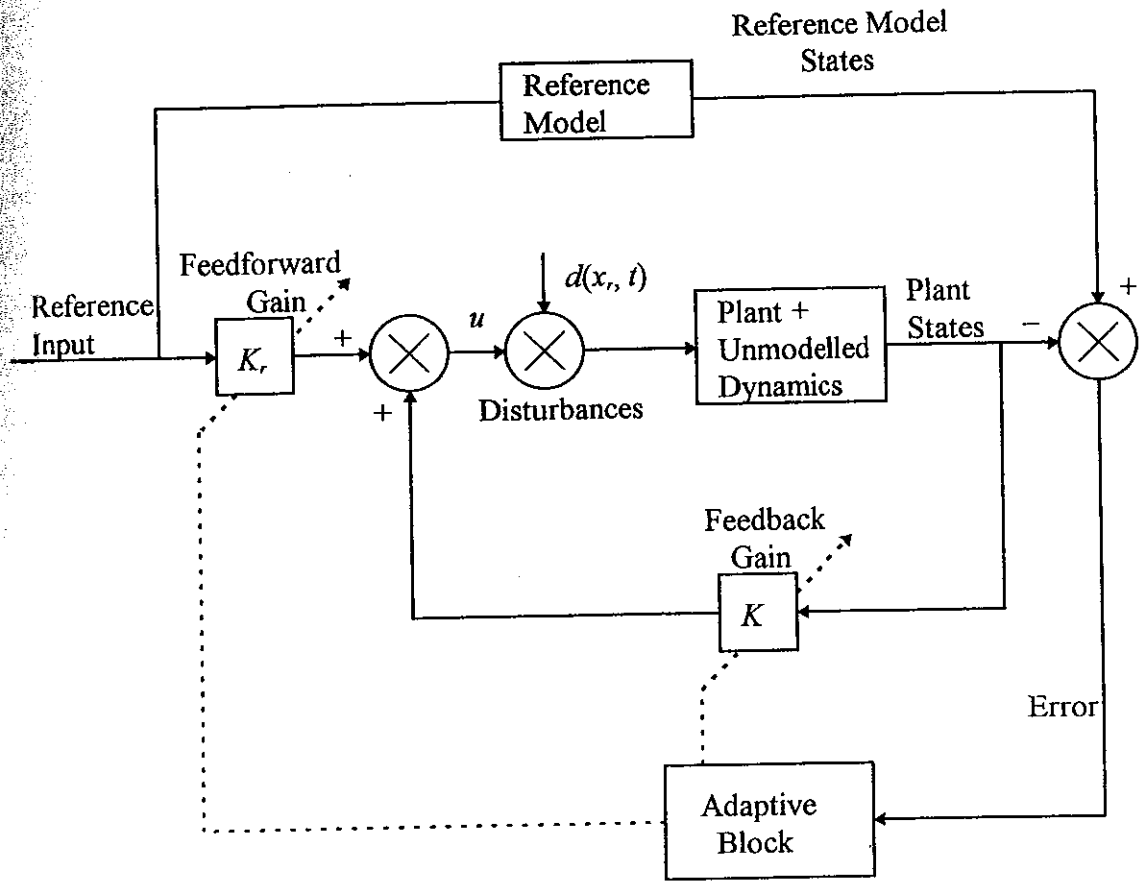

Fig. 1.5: The MCS with unmodelled dynamics

The reduced order MCS control can get unstable, if the MCS control weights α and β have very big values.

The Minimal Control Synthesis Identification (MCSID) algorithm [48], enables on-line identification of a linearised model of plants dynamics, based upon the MCS parameters (gain). It was emphasised that these parameters are not required for the MCS control to function; instead, the parameters might be required for simulation exercises, conventional controller designs and they can also be useful for plant diagnosis, monitoring and fault detection under closed-loop control.

The aim of MCS is to achieve an excellent closed-loop performance despite the presence of plant parameter variations, external disturbances, plant nonlinearities and dynamic coupling within plants, in a similar manner to MRAC. However the MRAC algorithm requires plant model identification. The designer is not required to synthesise the MCS control gain, since this is done automatically by the algorithm, given arbitrary (often

zero) initial conditions. The MCS control can adapt continuously to the unmodelled dynamics, plant parameter changes and external disturbances.

The MCS control will be implemented to the electrohydraulic actuator plant in a reduced order form in Chapter 5. The plant has a third order nominal transfer function. Normally third order MCS control is required, since the plant itself is third order, but the second order MCS will be implemented on the plant. Another application of the reduced order MCS control will be load control of the ESH material testing machine in Chapter 6. In this case the nominal plant had second order transfer function and the MCS control will be implemented in a first order form. It will be shown that the reduced order MCS control deals the nonlinearities and parameter changes in the plant.

1.9 - APPLICATIONS OF THE MCS CONTROL IN ELECTROHYDRAULIC FIELD

The MCS control was implemented first time on a servohydraulic materials testing machine in [49]. Comparative robustness tests were conducted between the MCS and P+I control, when the plant subject to supply pressure changes. Additionally, the reduced order MCS algorithm were introduced for the first time. The reduced order MCS control was implemented in SISO form and it preserved the system stability in the face of the unmodelled dynamics and parameter variations in specimens and the plant itself.

Adaptive control has been widely used in closed-loop materials testing application. Nonlinear nature of materials under load or strain control due to the changes molecular structure of the specimen and the changes in environment make this applications good candidates for adaptive control. Another example is low cycle fatigue testing in which the stiffness of materials changes each cycle and this can be represented by a nonlinear relationship [50] and using adaptive control in this case can prevent instability of the system due to the unknown disturbances, unmodelled dynamics and nonlinearities. The stability of the reduced order MCS control will be analytically proven in Chapter 4.

1.10 - CONCLUSIONS

In this chapter a review of model reference adaptive control (MRAC) and reduced order MRAC have been presented. Another important class of adaptive controllers is the self-tuning regulator. Compared to self-tuning controllers, MRAC algorithms are simple to implement due to the absence of on-line estimation techniques. Additionally, in the case of the MRAC approach, the error may still converge to zero without any need of estimating the plant parameters in real time. These advantages can clearly be seen in nonlinear plants.

In MRAC, the basic idea is to drive outputs of an unknown plant to a known reference model whereas in self-tuning controllers the basic procedure is to select a design for known plant parameters. Therefore, usual assumptions in self-tuning regulators are that the plant is linearisible and the control signal is sufficiently rich in frequencies. However, in real life these assumptions may not be valid e.g. the plant is nonlinear or the control signal may remain constant over a long period of time. These could lead to the generation of an incorrect estimator model.

Lyapunov functions are very useful tools to synthesise adaptation laws. The functions offer global stability properties for adaptively controlled systems without any restrictions either on the initial conditions of the errors or on the reference signal. The disadvantage of this approach is in finding an appropriate Lyapunov function.

It has been assumed that the reduced order adaptive controller is standard adaptive controller in which the controlled plant contains unmodelled parts in its dynamics and later on the unmodelled dynamics are treated as a disturbances in the plant. It is shown in this chapter that the reduced order model reference adaptive controller can be robust if the controller gains are tuned so as not to excite the frequencies in the unmodelled part of the plant and additionally, the input signal should be sufficiently enough in the mid-frequency range.

Hydraulic systems exhibit significant nonlinearities, therefore a linear controller is not good enough to give satisfactory results. The linear controller can only be optimised for one operating point. It has been shown that the model reference adaptive controller performs very well in electrohydraulic system control. The controller can adapt rapidly to changes in load and supply pressure.

A greater variety of material testing situations need to be considered, for instance, tests involving higher test frequencies and test involving nonlinear specimen deformation characteristics such as low cycle fatigue tests. Therefore using an adaptive controller in materials testing has many advantages, especially a model reference adaptive controller (e.g. the MCS control). In the case of self-tuning control, higher test frequencies would place greater demands on the on-line identification scheme since servovalve dynamics and hydraulic and structural resonance's may be excited by the test signal. For the MCS control this in not the case, since the MCS does not need on-line or off-line identification scheme.

The MCS control has been used to control the electrohydraulic actuator plant and ESH material testing machine. The MCS control is implemented in a reduced order form in both cases. Application of the MCS control to those systems will be studied in detailed in Chapter 5 and 6 respectively.

Much of the existing research concerns either algorithms, structures or specific applications and a great deal more needs to be understood about the dynamic behaviour of adaptive systems. Although, adaptive control has been used in large scale of systems, further development is required before it widely adopted in industry: Firstly, to have fast adaptation without large tuning transients. Secondly, it is important to develop an adaptive controller which preserves the stability under wide range of conditions with any demand signal. Finally, to have an adaptive controller which is easy to implement.

The MCS control has a very simple implementation procedure, hence the design of the controller is easy and as it will shown in Chapter 4, it is stable in the presence of external disturbances, plant parameter changes, nonlinearities and high frequency unmodelled dynamics in the plant. Therefore, the MCS control can be a good option for industrial systems control.

REFERENCES

[1] - **COOK, P. A. & Z. J. CHEN**, "Robustness Properties of Model-Reference Adaptive Control Systems", *IEE Proc.*, Vol. 129, Pt. D, No. 6, November 1982, pp. 305-309.

[2] - **TRUXAL, J. G.**, "Theory of Self-adjusting Control", *Proc. 2nd IFAC World Congress*, 1964.

[3] - **SARIDIS, G. N., J. M. MENDEL & Z. Z. NIKOLIC**, "Report on Definitions of Self-organising Control Processes and Learning Systems", *IEEE Control Systems Society Newsletter*, 1973.

[4] - **ASTROM, K. J.**, "Theory and Applications of Adaptive Control - A Survey", *Automatica*, Vol. 19, No. 5, pp. 471- 486, 1983.

[5] - **BELLMAN**, "*Dynamic Programming*", Princeton University Press, 1957.

[6] - **PARKS, P. C.**, "Lyapunov Redesign of Model Reference Adaptive Control Systems", *IEEE Trans. on Automatic Control*, AC-11, No. 3, pp. 362-367, 1966.

[7] - **EGARDT, B.** , *Stability of Adaptive Controllers*, Springer Verlag, New York, 1979.

[8] - **LANDAU, Y. D.**, *Adaptive Control - Model Reference Approach*, Marcel Dekker, New York, 1979.

[9] - **GOODWIN, G. C. & K. S. SIN**, *Adaptive Filtering Prediction and Control*, Prentice-Hall, Englewood Cliffs, New Jersey, 1984.

[10] - **NARENDRA, K. S., Y. H. LIN & L. S. VALAVANI**, "Stable Adaptive Controller Design, Part II: Proof of Stability", *IEEE Transactions on Automatic Control*, Vol. AC-25, No. 3, pp. 440-448, June 1980.

[11] - **K. S. NARENDRA & L. S. VALAVANI**, "Stable Adaptive Controller Design-Direct Control", *IEEE Transactions on Automatic Control*, Vol. AC-23, pp. 570-583, August 1978.

[12] - **NARENDRA, K. S. & S. S. TRIPHATI**, "The Choice of Adaptive Parameters in Model Reference Control Systems", *5th Asilomar Conference on Circuits and Systems*, pp. 596-600, 1971.

[13] - **LANDAU, I. D.** "A Survey of Model Reference Adaptive Techniques: Theory and Applications", *Automatica*, Vol. 10, pp. 353-379, 1974.

[14] - **NARENDRA, K. S. & R. V. MONOPOLI**, *Application of Adaptive Control*, Academic Press, New York, 1980.

[15] - **ROHRS, C. E., L. VALAVANI, M. ATHANS & G. STEIN**, " Robustness of Adaptive Control Algorithm in the Presence of Unmodelled Dynamics", *Proc. of the 21st IEEE Conference on Decision and Control*, Florida, pp. 3-11,1982.

[16] - **LINDORFF, D. P.**, "Effects of Incomplete Adaptation and Disturbance in Adaptive Control", *Proceedings of the Joint Automatic Control Conference*, pp. 562-567, 1972.

[17] - **IOANNAU, P. A. & P. V. KOKOTOVIC**, *Adaptive Systems with Reduced Models*, New York, Springer Verlag, 1983.

[18] - **PORTER, B. & M. L. TATNALL**, "Performance Characteristics of an Adaptive hydraulic Servo-mechanism", *International Journal of Control*, Vol. 11, No. 5, pp. 741- 757, 1970.

[19] - **WU, H.-W., & C.-B. LEE**, "Self-tuning Adaptive Speed Control of a Pump/Inverter Controlled Hydraulic Motor System", *Proc. Instn. Mech. Engrs.*, Vol. 209, pp. 101-114, 1995.

[20] - **WATTON, J.**, "A Digital Compensator Design for Electrohydraulic Single-Rod Cylinder Position Control Systems", *Transactions of the ASME, Journal of Dynamic Systems, Measurement, and Control*, Vol. 112, pp. 403-409, September 1990.

[21] - **FINNEY, J. M., A. DE PENNINGTON, M. S. BLOOR & G. S. GILL**, "A Pole-Assignment Controller for an Electrohydraulic Cylinder Drive", *Journal of Dynamic Systems, Measurement, and Control*, Vol. 107, pp. 145-150, 1985.

[22] - **VAUGHAN, N. D. & I. M. WHITING**, "Microprocessor Control Applied to a Nonlinear Electrohydraulic Position Servo System", *Proc. 7th Fluid Power Symposium*, pp. 187-198, Bath, UK, 1986.

[23] - **DALEY, S.**, "Application of a Fast Self-turning Control Algorithm to a Hydraulic Test Rig", *Proc. Instn. Mech. Engrs.*, Vol. 201, No C4, pp. 285-295, 1987.

[24] - **TSAO, T.-C., & M. TOMIZUKA**, "Robust adaptive and Repetitive Digital Tracking Control and Application to a Hydraulic Servo for Noncircular Machining", *Transactions of the ASME*, Vol. 116, pp. 24-32, March 1994.

[25] - **HUANG, C. H. & Y. T. WANG**, " The Simplified STR Applied For Hydraulic Systems, Part (I): Position Control of an Asymmetric Actuator Servo System", *Department of Mechanical Engineering, National Taiwan Institute of Technology, Taipei, Taiwan, Republic of China.*

[26] - **VAUGHAN, N. D. & A. R. PLUMMER**, "Robust Adaptive Control for Hydraulic Servosystems", *ASME, Winter Annual Meeting*, Texas, USA, November, 1990.

[27] - **ASTROM, K. J. & B. WITTENMARK**, "Self-tuning Controllers Based on Pole-zero placement", *IEE Proceedings*, Pt. D, 127(3), pp. 120-130, 1980.

[28] - **LEE, S. R. & K. SRINIVASAN**, "Self-Tuning Control Application to Closed-Loop Servohydraulic Material Testing", *Transactions of the ASME, Journal of Dynamic Systems, Measurements, and Control*, Vol. 112, pp. 680-689, December 1990.

[29] - **EDGE, K. A. & K. R. A. FIGUEREDO**, "An Adaptively Controlled Electrohydraulic Servo-Mechanism, Part 1: Adaptive Controller Design", *Proc. Instn. Mech. Engrs.*, Vol. 201, No. B3, pp. 175-180, 1987.

[30] - **EDGE, K. A. & K. R. A. FIGUEREDO**, "An Adaptively Controlled Electrohydraulic Servo-mechanism, Part 2: Implementation", *Proc. Instn. Mech. Engrs.*, Vol. 201, No. B3, pp. 181-189, 1987.

[31] - **UBEHAUEN, H., P. DU, & KEUCHEL, U.**, " Application of a Digital Adaptive Controller to a Hydraulic System", *International Conference on Control 88*, pp. 177-182, Oxford UK, 1988.

[32] - **SHIH, M.-C. & S.-N. HO**, "Hydraulic Variable Piston Motor Position Control by Using Model Reference Adaptive Control ", *Mechatronics*, Vol. 3, No. 6, pp. 689-704, 1993.

[33] - **DOYLE, J. & G. STEIN**, " Multivariable Feedback Design: Concepts for a Classical/Modern Synthesis," *IEEE Transaction on Automatic Control*, Vol. AC-26, No. 1, Feb. 1981, pp. 4-16.

[34] - **KREISSELMEIER, G. & K. S. NARENDRA**, "Stable Model Reference Adaptive Control in the Presence of Bounded Disturbances", *IEEE Transactions on Automatic Control*, Vol. AC-27, No. 6, December 1982, pp. 1169-1175.

[35] - **RIEDLE, B. D. & P. V. KOKOTOVIC**, "A Stability-Instability Boundary for Disturbances-Free Slow Adaptation with Unmodelled Dynamics", *IEEE Transactions on Automatic Control*, Vol. AC-30, No. 10, pp. 1027-1030, 1985.

[36] - **OSBURN, P. V., H. P. WHITAKER & A. KEZER**,."New Developments in the Design of Adaptive Control Systems", *Inst. Aeronautical Sciences*, Paper 61-39, 1961.

[37] - **MONOPOLI, R. V., J. W. GILBART & W. D. THAYER**, *Proc. 2nd I.F.A.C. Symposium on System Sensitivity and Adaptivity*, pp. 24, 1968.

[38] - **LINDORFF, D. P. & R. L. CARROLL**, "Survey of Adaptive Control Using Lyapunov Design", *International Journal of Control*, Vol. 18, No. 5, pp. 897-914, 1973.

[39] - **LANDAU, Y. D.** "*Adaptive Control, the Model Reference Approach*," Marcel Dekker, N. Y., 1979.

[40] - **BODSON, M. & S. SASTRY**., " Exponential Convergence and Robustness Margins in Adaptive Control," *Proceedings of 23rd Conference on Decision and Control*, Las Vegas, N V, December 1984.

[41] - **ASTROM, K. J. & T. BOHLIN**, " Numerical Identification of Linear Dynamic Systems from Normal Operating Records," *Proc. 2nd IFAC Symposium on the Theory of Self-Adaptive Control Systems*, NPL Teddington, England. Plenum Press, New York, pp. 96-111, 1965.

[42] - **ASTROM, K. J.,** " Interactions between Excitation and Unmodelled Dynamics in Adaptive Control," *Proceedings of 23rd IEEE Conference on Decision and Control*, Las Vegas, N V, December, 1984.

[43] - **LANDAU, I. D.,** *Adaptive Control, the Model Reference Approach*, Marcel Dekker, New York, 1979.

[44] - **STOTEN, D. P.,** *Model Reference Adaptive Control of Manipulators*, pp. 238, Research Studies Press Ltd., Taunton, England, 1990.

[45] - **STOTEN, D. P., & H. BENCHOUBANE,** "Empirical Studies of an MRAC Algorithm with Minimal Controller Synthesis," *International Journal of Control*, Vol. 51, No. 4, pp. 823-849, 1990.

[46] - **STOTEN, D. P., & H. BENCHOUBANE,** "Robustness of a Minimal Controller Synthesis Algorithm," *International Journal of Control*, Vol. 51, No. 4, pp. 851-861, 1990.

[47] - **STOTEN, D. P.** "An Overview of the MCS Algorithm," *International Mechanical Engineering Conference on Aerospace Hydraulics and Systems*, Ref. C474-033, London, 1993.

[48] - **STOTEN, D. P., & H. BENCOUBANE,** "The Minimal Control Synthesis Identification Algorithm," *International Journal of Control*, Vol. 58, No. 3, 1993.

[49] - **STOTEN, D. P.,** "Implementation of Minimal Control Synthesis on a Servo-Hydraulic Testing Machine", *Proc. Instn. Mech. Engrs.*, Vol. 206, pp. 189-194, 1993.

[50] - **SLOT, T., R. H. STENTZ, & J. T. BERLING,** "Controlled-Strain Testing Procedures, Manual on Low Cycle Fatigue Testing," *Manual on Low Cycle Fatigue Testing, ASTM STP 465, American Society for Testing and Materials*, pp. 100-128, 1969.

CHAPTER 2

HYDRAULIC SYSTEMS MODELLING

2.1 - INTRODUCTION

The propose of this chapter is to show the importance of hydraulic systems modelling and simulation. The simulation of a hydraulic system control helps the designer to choose the suitable parameters satisfying the desired closed loop response. Therefore, the determination of the ranges of the controller parameters enables the designer to set-up rules for building up an effective hydraulic system based on model reference adaptive control.

Hydraulic control systems have several advantages over other types of systems. A comparatively small size hydraulic actuator can produce very large forces or torques to provide rapid acceleration or deceleration of a heavy load. For the same power, hydraulic actuators are lighter than electrical motors and considerable reduction in size and weight can be achieved. This fact is making their use attractive in situations where lesser weight is more acceptable, such as aircraft and missiles. In addition, hydraulic fluid can be used to carry away the heat generated in the system and it also acts as a lubricant

Later in this chapter the electrohydraulic actuator plant is modelled and simulated by Simulink. The P+DFB and MCS controllers were implemented on the model in Simulink and good position responses are generated.

2.2 - SERVOHYDRAULIC SYSTEMS

The dynamics of servohydraulic systems are generally nonlinear and vary with time. The nonlinearity is mainly due to the fact that the hydraulic fluid flow rate through an orifice is proportional to the square root of the pressure difference across the orifice. Coulomb friction and stiction between the piston rod and the sealing are other sources of nonlinearity. The parameter of hydraulic systems change depending on many reasons, such as temperature changes of the hydraulic oil, air content, mechanical wear and leakage of the system. Nonlinear aspects of servohydraulic systems make adaptive controllers such a good candidate in this field [1].

Hydraulic systems are preferable in many cases due to the fact that for the same power they have less weight and smaller size in comparison with other types of systems. However, they have some disadvantages such as, the hydraulic power is not immediately available and leakage in the system can cause fire hazards. In order to prevent fire hazards fire resistant hydraulic fluids are commonly used in the mining industry and in power stations which are working in the high pressure.

For a quite hydraulic system, it is more desirable to have less transmission vibration from the pump. The hydraulic lines transmit both the pump vibration and the pressure fluctuations to other parts of the system such as, the actuator, the servovalve, the load mass [2]. As a result these parts of the systems vibrates more than the pump which cause the structural vibration.

Flexible hoses are normally in use to connect the pump to the actuator, which are causing some disturbance but they also provide isolation of vibration, and to a lesser extent, isolation of pressure fluctuation. Noises in hydraulic systems are a serious problem which can be prevented by decreasing pressure fluctuation. The isolating effect of hoses were investigated by using different types of wave transmission in [3]. The wave properties of a single steel braid hose, double steel braid hose, four spiral steel hose and synthetic fibre braid hose were compared in this work. In comparison with other type of hoses, the textile hose gave the best isolation of pressure fluctuation, although it was not much.

The steady-state error always exists in hydraulic actuator position control systems due to nonlinear relationship between the flow and the position of the actuator. The flow is proportional to the velocity of the actuator. Additional nonlinearity exists if the system has

a single rod actuator. In this case the flows to the first and second chambers of the actuator are not equal. Another nonlinearity in the system is the load mass. In [4], an underlapped servovalve was used to derive a single rod actuator hydraulic system and dynamics of the system were simplified and improved by neglecting the some parts of the system. It was suggested that the effects of load inertia and fluid compressibility can be neglected in this kind of system since the load mass is small.

A proportional relief valve was used in a single rod actuator electrohydraulic system to get a zero position error in [5]. The load force and supply pressure were adjusted according to the changes in the load force. The technique concentrated on the need to have symmetrical underlapping of the servovalve spool, which enables the position error to be eliminated. Using an adaptive controller can be a satisfactory choice in this case due to the fact that the controller can adapt itself changes in the plant dynamics.

Servovalve derived hydraulic systems have faster dynamics and high reliability therefore, they are in common use. However this kind of systems have low efficiency in comparison with load sensing electrohydraulic systems. In [6] load sensing was applied to an electrohydraulic system. It was demonstrated that the technique decreased the energy consumption and improved the dynamics the hydraulic system.

2.3 - MULTIVARIABLE HYDRAULIC SYSTEMS MODELLING AND SIMULATION

In order to have a reliable multivariable (MIMO) hydraulic system the following factors should considered: i.e. changes in the environment, the topology of the network, structure of computer modules, and the software quality. In a first place, a reliable system requires a good design method which will produce a model that will be close agreement with the real system. Hence, the use of an appropriate communication protocol and system scheduling become important in the case of MIMO hydraulic systems. Also, having a proper error detection mechanism can be very useful.

A multivariable Workmaster hydraulic robot was modelled in a simplified form for the computed-torque and variable-structure control applications both in simulation and in

practice in [7]. The mathematical model of the system was later examined to improve the working conditions of the real hydraulic robots.

A multivariable hydraulic system (multiarm forest or tunnelling machine) was controlled by using distributed computer control in [8]. It was demonstrated that the speed and reliability of the system can be improve due to distribution in the multivariable system structure. Additionally, the method reduced the use of cabling therefore, the cost of the system was decreased. In the case multivariable hydraulic systems, adaptive controller (in decentralised form) strategies can be a good alternative to overcome the delay and disturbance term due to large distribution of these sort of systems.

2.4 - HYDRAULIC SYSTEMS MODELLING AND SIMULATIONS

Modelling and simulations are very useful tools in hydraulic systems design and control due to the fact that it can help designer to choose suitable configuration of the real system. The system can build in the computers memory and necessary changes and improvements can be done very easily before the real system is build. The simulation of hydraulic systems can be also very helpful in the case of choosing suitable controller gains [9]. The simulation results will show how close the mathematical model is to the real plant.

In order to have satisfactory simulation results it is necessary to have detailed and accurate mathematical model of real systems. There are many different computer based design software package which have been used hydraulic systems modelling and simulations. Some of these methods are given below.

2.4.1.- Computational Fluid Dynamics (CFD) Simulation Techniques

Computational Fluid Dynamics (CFD) simulation techniques were used to model the impedance characteristics of simple cylindrical and sharp-edged orifices in [10]. It was demonstrated that the impedance characteristics was relatively independent of mean flow in non-cavitation condition. On the other hand the resistance is strongly dependent on the mean flow. Edge and Johnston have investigated the impedance characteristics of some

hydraulic components [11], [12]. They modelled restrictor valves, single-stage relief valves and accumulators simply by using inductive, capacitive and resistive characteristics of the components. For some complex components, such as two-stage relief valves, the impedance characteristics were developed based on the physical configuration of the real component. However satisfactory responses did not generated, the responses which was generated from simulations was not close agreement with the measured impedance of the relief valves.

2.4.2 - Using Neural Networks in Modelling of Hydraulic Systems

Neural networks have been used in the case nonlinear system modelling and simulation effectively. Hydraulics systems have nonlinear dynamics due to the nonlinear relationship between the flow and the position of the actuator and the nonlinear characteristics of hydraulic fluids For that reason, artificial neural networks can be used in the case hydraulic systems modelling and control [13]. In this work the method was also used to model the pressure relief valve and variety of servovalve controlled motor systems.

2.4.3 - Transmission Line Modelling Method

Over decades transmission line modelling (TLM) has been applied to variety of electrical, mechanical and fluid power systems. An electrohydraulic systems contains all these elements therefore, the method was used to model the hydraulic, mechanical and electrical parts of the plant in [14]. In this work the parallel simulation method was used together with TLM method which increased speed of the simulation. Accurate models for cavitation and friction were developed using TLM methods and verified experimentally. It was demonstrated that by using transmission line modelling technique the simulated model gave responses which are close agreement with the real plant. Normally, the method of characteristics (MOC) required more computational effort than TLM. In TLM, the component models were simplified due to use of the pressure and flow equations at the

transmission line and incorporated into the model. Hence, the line models were not solved separately therefore, the total number of models was reduced.

TLM method was proposed for modelling of the fluid flow in hydraulic pipelines by using the distributed parameter model in [15]. In this work, a method proposed to eliminate limit cycle conditions in hydraulic control systems. It was suggested that limit cycle conditions were a strong function of certain plant parameters such as backlash in the actuator and nonlinear transmission line therefore, it can be eliminated by ignoring (the unmodelled dynamics) the certain parts of the plant dynamics. It was pointed out that if the hydraulic control system consisting a nonlinear hydraulic transmission line or the hydraulic actuator secured by a mechanical structure, it may result in limit cycle conditions. Additionally oscillations along the pipelines may be excited by a nonlinear element which may lead instability. In order to overcome this problem the pipe length should be kept as short as possible.

2.4.4 - Fault Analysis Method

Transmission line modelling method tended to be based on heuristic knowledge (empirically derived shallow knowledge). It was suggested that, for the sake of more accurate models, detailed knowledge (deep knowledge) should also be considered [16]. The method was applied to an electrohydraulic control system modelling and simulation by using an object oriented library in which the components were modelled base on deep knowledge. It was pointed out that although the method has many useful features still there were problems describing the system in the software. Additionally, there were difficulties choosing the combination of unexpected and unwanted conditions.

2.4.5 - Failure Mode and Effects Analysis and Fault Tree Analysis

In [17] Failure Mode and Effects Analysis (FMEA) was used together with Fault Tree Analysis (FTA) to model the unwanted features of a electrohydraulic control system In this method, each component was modelled independent of any particular circuit configuration as a self-contained unit then, the connectivity information was used to form any type of hydraulic systems in the computers memory. The method did not only modelled the known unwanted effects of the component dynamics, it also modelled the normal effects of the component dynamics. In the case of qualitative simulation, some components were selected as active such as electric motors, accumulators, etc. which are capable of introducing energy into the system and when simulation started, the software activated components, for example an accumulator switched on. The software has the capacity to model the behaviour of the components by using the descriptive terms therefore it has comparatively less computation. Additionally it was observed that it is very flexible for hydraulic systems modelling, any type of systems can be formed by using object-oriented software, any changes can be made easily while the simulation running.

FMEA program was indicated the worst possible, or most extreme, effects of a fault. In real system, the effects may not as severe as predicted, due to the fact that the simulation method was based on very detailed qualitative reasoning of the system. The method was shown the more significant probabilities and features of the system. The method was performed manually which was subject to human mistakes. It was suggested, that FTA is necessary together with the application of heuristic knowledge and active testing of a hydraulic circuit, for a good modelling.

2.5 - CONSIDERING THE EFFECTS OF THE BULK MODULUS OF HYDRAULIC OILS IN THE CASE OF HYDRAULIC SYSTEMS MODELLING

If the pressure changes are significant in the electrohydraulic system then, using the pressure dependent bulk modulus can make models more accurate. In [18], the bulk modulus in high pressure pipes were measured pressure-volume-temperature methods which is given as follows

$$c_0 = \sqrt{\frac{N}{\rho}} \tag{2.1}$$

where c_0 is the speed of sound in the fluid, N is the effective bulk modulus and ρ is the density of the fluid.

Generally, a constant value of the effective bulk modulus have been used in hydraulic systems modelling. Therefore, it is assumed that the effective bulk modulus is constant during operation of the system. This assumption is not very accurate due to the fact that the system loading can vary significantly, e.g., the pressure in the actuator varies periodically from the supply pressure to the return pressure. If a hydraulic system is subject to large and sudden pressure changes, then it is more reasonable to use the pressure dependence effective bulk modulus for accurate plant modelling and simulation. It was demonstrated by Edge and Darling [19] that, if a constant effective bulk modulus value is used, satisfactory simulation results are difficult to obtain.

Following factors are considered to have influence on the effective bulk modulus: air content of the oil, oil pressure, oil temperature and pipe rigidity. Air content of a hydraulic oil depends on the pressure and temperature in the system. Air exists in hydraulic systems either in entrained or dissolved form and except very high pressures dissolved air does effect the performance of the system. The effective bulk modulus affected badly when entrained air present in the system due to the bigger size of the air bubbles in the hydraulic oil.

The temperature of the hydraulic oil influences the effective bulk modulus, because it effects the density of the air content inside the hydraulic oil. At high temperature, the effective bulk modulus increases due to the size of small air bubbles in the hydraulic oil. The effect of oil temperature can be ignored when the oil temperature is approximately constant during operation of systems. The affects of pipe rigidity also

ignored in many practical applications and it is assumed that either the affects are insignificant or rigid pipes are in use.

The effective bulk modulus value of the oil varies depending on oil pressure significantly. This was clearly demonstrated by Yu and Lu in [20]. According to the authors' experience, the effective bulk modulus value of a particular hydraulic system was determined to be 1132 MPa when the load pressure was equal to 1 atmosphere, 1631 MPa at 5 MPa and 1686 MPa at 10 MPa. The effective bulk modulus was increased when some entrained air become dissolved air due to increase in the hydraulic oil pressure.

Accurate modelling and simulation of an electrohydraulic system was achieved by using a pressure dependent effective bulk modulus in [21]. The work concentrated on the relationship between the effective bulk modulus and oil pressure in the hydraulic system and other factors such as oil temperature, air content of the oil were assumed to be constant. It was demonstrated that the method is efficient, convenient and produced more accurate model. Hence, if the pressure in the hydraulic system is varying dramatically with working conditions then using the pressure sensitive effective bulk modulus may produce more accurate models.

2.6 - MODELLING AND SIMULATION OF THE ELECTROHYDRAULIC ACTUATOR PLANT BY SIMULINK

Simulink is a program for simulating dynamic systems. Simulink has two phases of use: model definition and model analysis. As a extension to Matlab, it works inside of window's environment. To facilitate model definition, Simulink adds a new class of windows called block diagram windows. In these windows, the model is created and edited principally by mouse driven commands.

Extensive use can be made of Matlab's Control Systems Toolbox and Simulink throughout the design and modelling processes. The system can be modelled using Matlab and Simulink and subsequently the controller can be implemented using analogue models [22]. The paper describes the design methodology used to produce a multivariable control system and illustrates the differences between the predicted and actual performance of the real electrohydraulic actuator plant.

The model can be defined or analysed either by choosing options from the Simulink menus or by entering commands in Matlab's command window. With the simulation running, the results were directed to the Matlab workspace.

2.6.1 - The Electrohydraulic Actuator Plant

The electrohydraulic actuator plant, which is presented in this chapter, has been developed in the Aerospace Engineering Department at Bristol University. The increasing demands from modern control systems necessitate greater flexibility between controlling elements. This has resulted in the combining of electrical signalling with fluid power actuators.

The output from the servo amplifier actuates the torque motor attached to the pilot spool. Supply pressure is directed to both spool valves, so that the product of the supply pressure and the main spool area produces the force to move the main spool. The output flow from the main spool is used to drive the ram piston, which is also provided with a feedback loop. The flow force varies with the load pressure in the actuator. Switchable accumulators are situated either side of the actuator. The accumulator is an energy storage unit allowing hydraulic oil systems to use the energy storage capacity of compressed gas. The accumulators consist of a high pressure cylinder containing a rubber bag. The bag is normally charged with an inert gas (normally nitrogen). As oil is pumped into the cylinder around the bag the pressure will rise. The accumulators can be used as a reserve of power in circuits, in which there are short duration high flow demands. The accumulator can also be used as a low pass filter, helping to smooth out fluctuations in pressure and flow due to the pump action [23].

2.6.2 - Dynamics of the Plant

The dynamic analysis of the hydraulic system can be made by identifying their differential equations of motion. Forming an equation for a hydraulic system is the first step for design and control. Before building a real system, however, it is important to determine whether the system will be stable.

It is necessary to examine the parameters, variables and differential equations of the system. With the exceptions of geometric and kinematics relationships, the equations

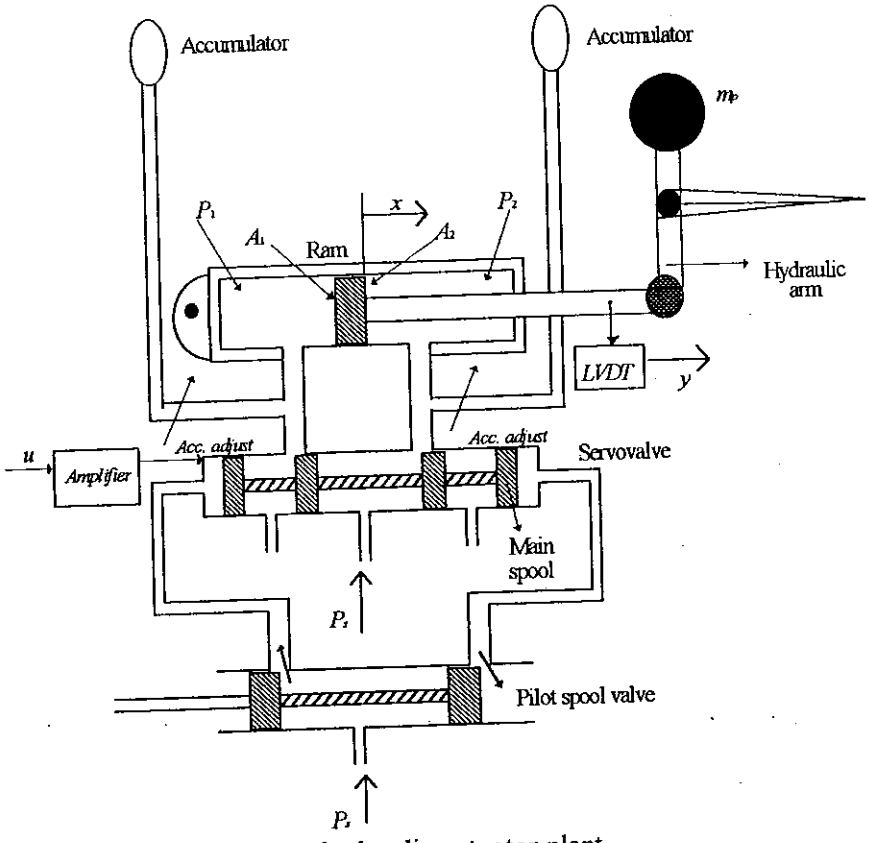

Fig. 2.1: The electrohydraulic actuator plant

reduce to either equations of flow (2.4) and to equations of force (or torque, 2.8). In this case of the electrohydraulic actuator plant, the equation describing the system dynamics were derived analytically using the equations for flow and torque [24].

The servovalve is described by a linear transfer function which is published by Moog [25]. The electrohydraulic servovalve is a highly nonlinear device that exhibits high order, nonlinear response. It has many parts which have so small shape and this is

analytically non-ideal. In many cases, it is appropriate for more accurate hydraulic system design to use empirical approximations of the measured servovalve response. A very adequate nonlinear representation for the servovalve is given in Fig. 2.5. The plant dynamics are described by using the actuator and servovalve dynamics.

2.6.3 - Dynamics of the actuator

The flow equations:

Flow in:

$$Q_1 = A_1\dot{x} + V_1\frac{\dot{P}_1}{N} \tag{2.2}$$

and flow out:

$$Q_2 = A_2\dot{x} - V_2\frac{\dot{P}_2}{N} \tag{2.3}$$

Q_1 and Q_2 are flows into chambers C_1 and C_2 in Fig. 2.2. The pressure difference is

$$\Delta P = P_1 - P_2$$

and similarly

$$\Delta\dot{P} = \dot{P}_1 - \dot{P}_2 \tag{2.4}$$

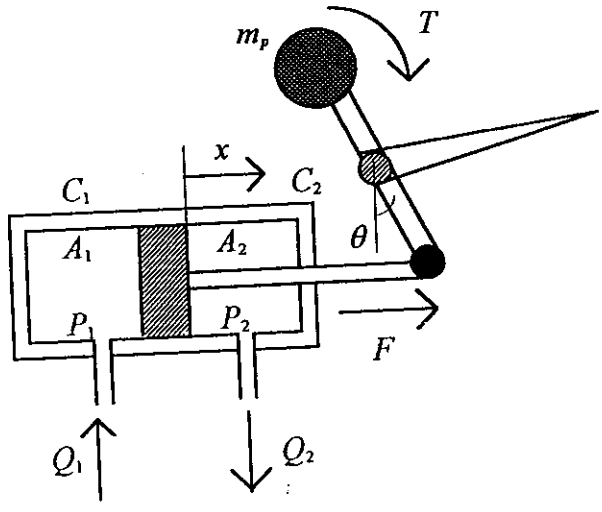

Fig. 2.2: Hydraulic ram

2.6.3.1 - Nonlinear Description of the Actuator

The force equation is:

$$A_1 P_1 - A_2 P_2 - f_s \dot{x} - T = m_p \ddot{x} \tag{2.5}$$

where $T = \frac{J\ddot{\theta}}{l\cos\theta}$, f_s is the coefficient of viscous friction, m_p is the mass and J is the moment of inertia. The system has a single rod actuator. The area in the first chamber of the actuator is:

$$A_1 = \frac{A_2}{0.84}$$

In this diagram $x = l\sin\theta$ and $p = l\cos\theta$ and $F = A_1 P_1 - A_2 P_2$. For the sake of simplicity the averaged value of Q_1 and Q_2 are used in modelling to produce the load force in the actuator. The averaged hydraulic volume flow:

$$Q_f = A_{av}\dot{x} + \frac{V_{av}\left(\dot{P}_1 - \dot{P}_2\right)}{2N} \tag{2.6}$$

where, A_1 and A_2 are the effective area of the first and second chambers of the ram respectively, N is the bulk modulus of the hydraulic oil and V_{av} is the average volume in the ram. The volume (V_{av}) is provided for the liquid downstream of the valve in one chamber or the other when the ram is in the middle piston (Fig. 2.2). The volumetric coefficient:

$$k_v = \frac{V_{av}}{V_e} \tag{2.7}$$

where V_e is the effective half volume, $V_e = A_{av} x_m$, where x_m is the maximum half travel of the ram and A_{av} is the average effective area of the ram. It is always desirable to decrease the total volume, V_{av}. In a linear actuator, $V_{av} = V_e + V_m$, where V_m is the dead volume corresponding to the ducting between the distributor and the actuator and to other intermediate volumes. The volumetric coefficient, k_v can be low as 1.2 for large rams, while for small rams it is rarely less than 1.5 or 1.6. For the servohydraulic plant k_v is taken 1.4 [24]. Q_1, Q_2 are flows into chamber C_1 and C_2. Equation (2.5) can be rewritten as:

$$A_{av}\left(P_1 - P_2\right) - f_s\dot{x} - T = m_p\ddot{x} \tag{2.8}$$

For the hydraulic system the transfer function of the ram is obtained by eliminating the intermediary pressure variable between the flow equation and the force equation.

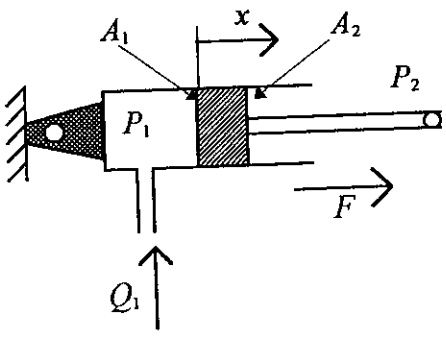

(a)

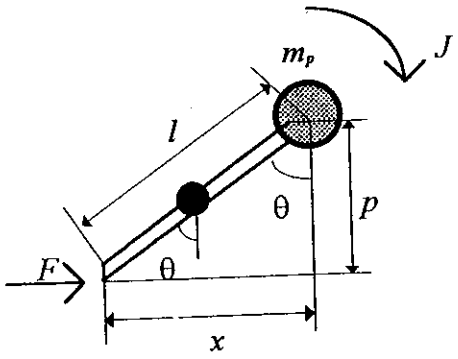

(b)

Fig. 2.3: The hydraulic actuator and load

From (2.6), the pressure difference across the actuators chambers is

$$\left(\dot{P}_1 - \dot{P}_2\right) = \frac{2N}{V_{av}}\left(Q_f - A_{av}\dot{x}\right) \tag{2.9}$$

Integrating (2.9) with respect to time gives:

$$\left(P_1 - P_2\right) = \int \frac{2N}{V_{av}}\left(Q_f - A_{av}\dot{x}\right)dx \tag{2.10}$$

From, (2.8) and (2.10)

$$A_{av}\left(\frac{2N}{V_{av}}\left(Q_f - A_{av}\dot{x}\right)dx\right) - f_s\dot{x} - \frac{J\ddot{\theta}}{lCos\theta} = m_p\ddot{x} \tag{2.11}$$

So, the dynamic equation of the actuator is:

$$\ddot{x} = \frac{A_{av}}{m_p}\left(\int \frac{2N}{V_{av}}\left(Q_f - A_{av}\dot{x}\right)dx\right) - \left(\frac{f_s}{m_p}\right)\dot{x} - \frac{1}{m_p}\left(\frac{J\ddot{\theta}}{l\cos\theta}\right) \tag{2.12}$$

which becomes:

$$x = \iint \left[\frac{A_{av}}{m_p} \left(\int \frac{2N}{V_{av}} \left(Q_f - A_{av} \dot{x} \right) dx \right) - \left(\frac{f_s}{m_p} \right) \dot{x} - \frac{1}{m_p} \left(\frac{J\ddot{\theta}}{l \cos\theta} \right) \right] dx dx \qquad (2.13)$$

This equation is described schematically in Simulink as follows:

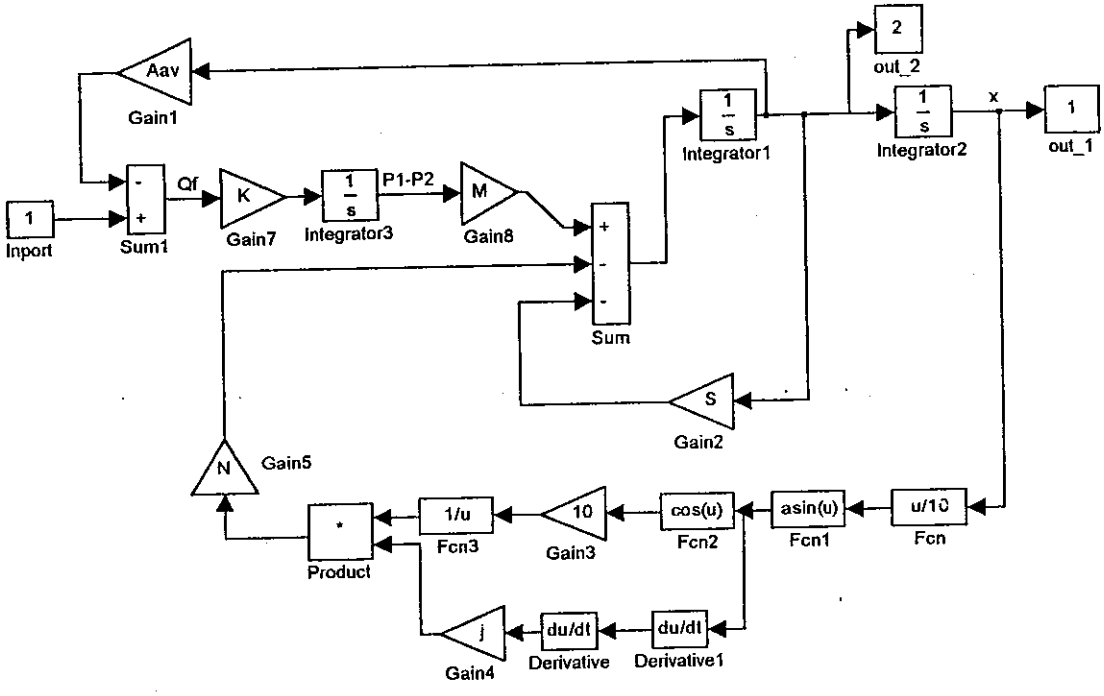

Fig. 2.4: The block diagram of the actuator in Simulink.

In this diagram: $K = \frac{2N}{V_{av}}$, $M = \left(\frac{A_{av}}{m_p} \right)$, $N = \frac{1}{m_p}$, J is the inertia of the system and $S = \frac{f_s}{m_p}$, where $f_s = \frac{4\zeta N A_p^2}{W_c V_{av}}$. The condition for stability can be represented fairly accurately by the relationship $\zeta \rangle \frac{\omega_f}{\omega_c}$ where, the critical frequency of the system, $\omega_c = \sqrt{\frac{2NA_p^2}{V_t m}}$. In this case the bulk modulus of the hydraulic oil, N is 2.9x10^{+9} N/m^2, the effective area of the ram, A_{av} is 11.57 cm^2, the mass, m_p is 6.7 kg, the total half volume, V_{av} is $V_{av} = 84$ cm^3. The value of ω_c is 94 rad/s and $\frac{\omega_c}{\omega_f} = 0.25$, and ω_f is the open loop gain.

Then, the damping coefficient, ζ was chosen to be 0.24. The flow rate of the rig, Q_{max} is 14.7 lt/min, the valve sizing constant, K is 0.0598 and the input current i, is 40 mA. The supply pressure of the electrohydraulic actuator plant P_s is 110 bar, and the inertia of the system is, J is 0.44 kgm^2. The servovalve is described by the nonlinear third order model shown as below:

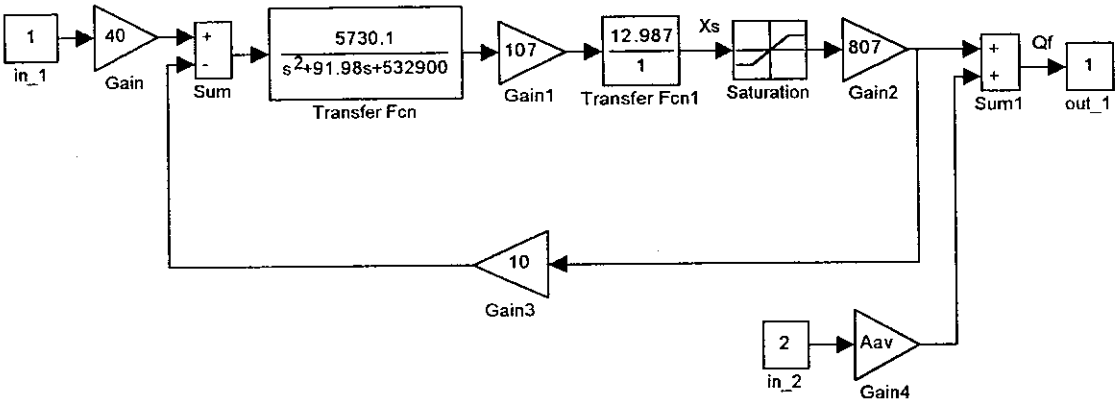

Fig. 2.5: The third order nonlinear dynamics of the servovalve

The servovalve is modelled by a third order transfer function (the data received from the manufacturing company). Using flow equations and Newton's law the actuator dynamics is described by a second order nonlinear model. This to separate model linked by using the relationship between the flow and force. Hence, electrohydraulic servo plant is described by a nonlinear fifth order model by using Simulink as shown in Figs. 2.4 and 2.5.

2.7 - SIMULATION TESTS RESULTS

The electrohydraulic actuator plant was modelled by Simulink. Dynamic simulation plays vital and very visible role in the hydraulic system design process. The modelling is important to investigate the dynamic behaviour of the system. The plant is modelled by a fifth order nonlinear model. The mathematical model of the plant controlled in Simulink under second order MCS control (Fig. 2.6).

The plant described by the following state-space equation:

$$\dot{x}(t) = Ax(t) + Bu + d(t) \tag{2.14}$$

For a given settling time, $t_s = 0.25$ s, the second-order MCS reference model is

$$\dot{x}_m(t) = A_m x(t) + B_m r(t) \tag{2.15}$$

where $A_m = \begin{bmatrix} 0 & 1 \\ -256 & -32 \end{bmatrix}$ and $B_m = \begin{bmatrix} 0 \\ 256 \end{bmatrix}$

The MCS control signal, u:

$$u(t) = K(t)x(t) + K_r(t)r(t) \tag{2.16}$$

together with

$$K(t) = \int_0^t \alpha y_e x^T d\tau + \beta y_e x^T$$
$$K_r(t) = \int_0^t \alpha y_e r d\tau + \beta y_e r \tag{2.17}$$

Form the output error signal:

$$y_e(t) = C_e(t)x_e(t) \tag{2.18}$$

The hyperstable condition is guaranteed if:

$$C_e = B_e^T P \tag{2.19}$$

where $B_e = diag\left[B_{e1}, \ \cdots \ , B_{ep}\right]$; $B_{ei} = \left[0, \ \cdots \ ,0 \ \ 1\right]^T$

For second order reference model

$$B_{e2} = \begin{bmatrix} 0 \\ 1 \end{bmatrix}$$

and P is the positive definite solution to the Lyapunov equation

$$PA_m + A_m^T P = -Q \ ; \ Q>0 \tag{2.20}$$

Q is the arbitrary positive-definite matrix, it was chosen as

$$Q = \begin{bmatrix} 10 & 0 \\ 0 & 1 \end{bmatrix}$$

then, the output error matrix is

$$C_e = \left[0.0195 \quad 0.0162\right]$$

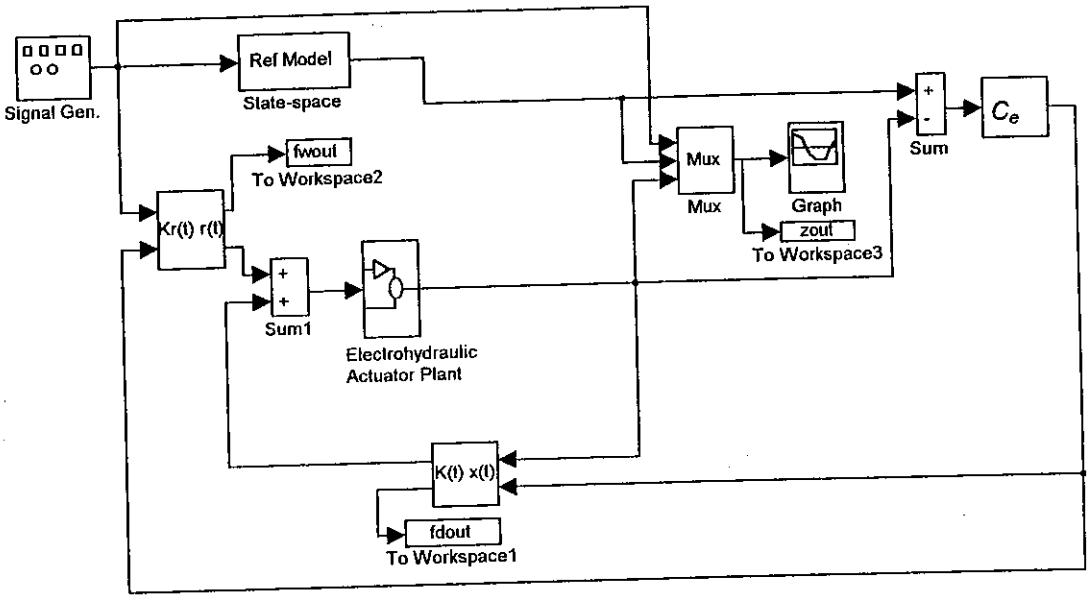

Fig. 2.6: Block diagram of the electrohydraulic actuator plant under second order MCS.

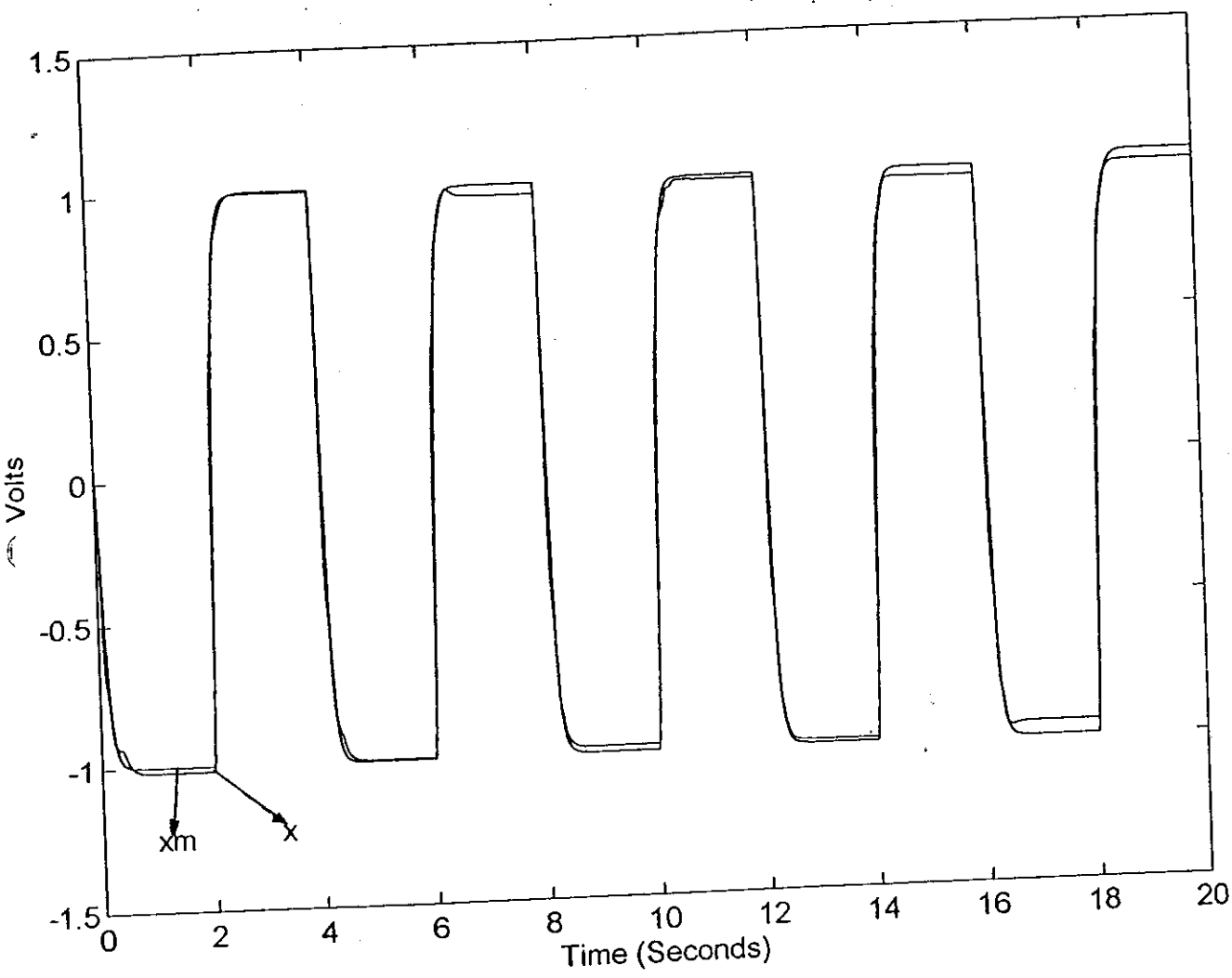

Fig. 2.7: The model of the plant under P+DFB control, supply pressure 110 bar

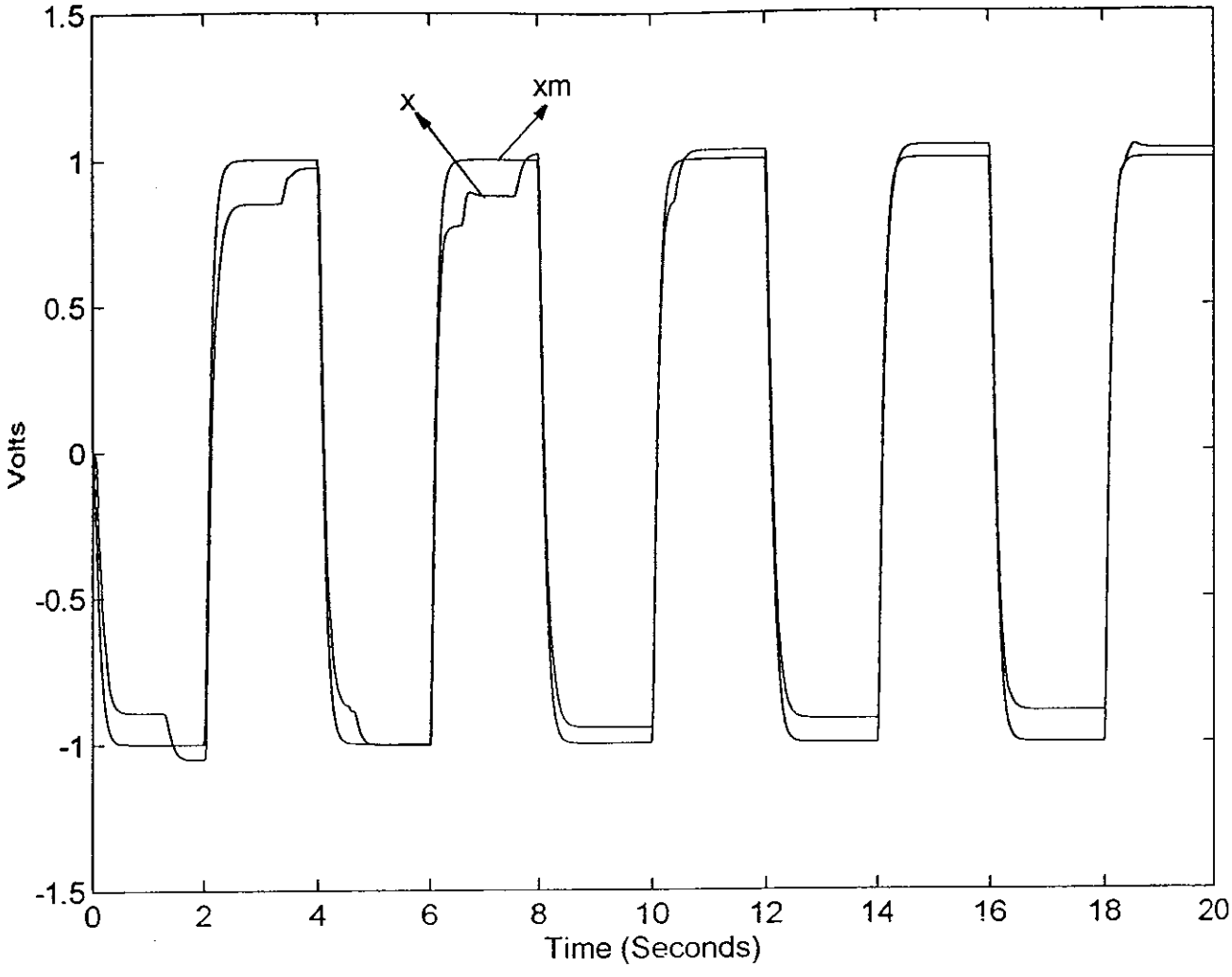

(a) Reference and output signals.

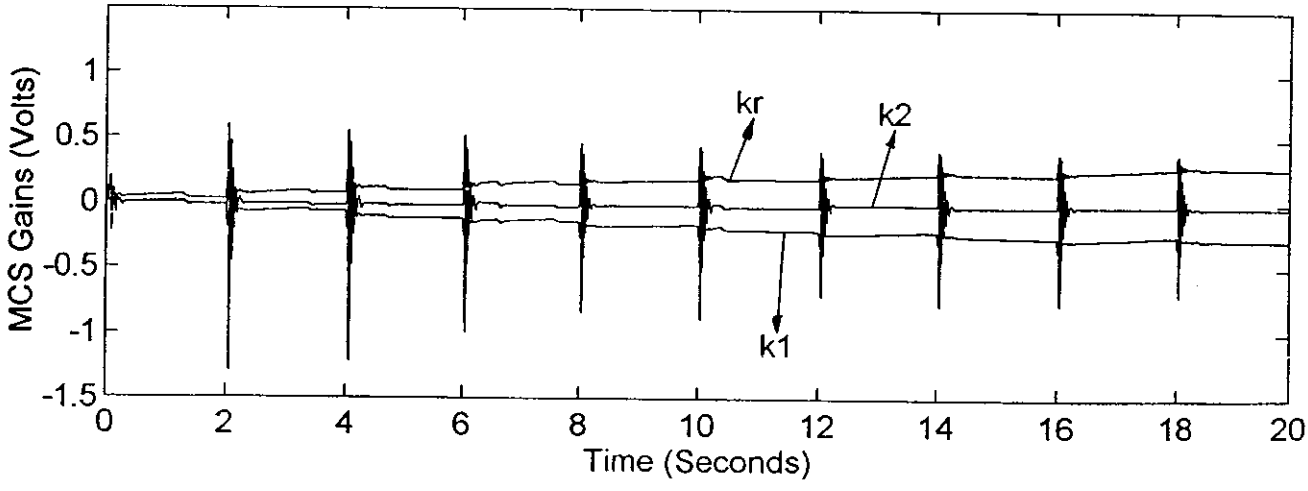

b) MCS gains

Fig. 2.8: The responses of the model of the plant under MCS control, supply pressure 110 bar.

The results of the model of the electrohydraulic actuator plant under P+DFB control are shown in Fig. 2.7. The settling time was t_s = 0.25 s, the reference signal was a square wave of frequency 0.25 Hz, k_p = 1 and k_d = 0.1 and the amplitude was 1 volt. The position responses and gains from the simulation of the electrohydraulic actuator plant behaviour under the MCS can be seen in Fig. 2.8 a, b. The settling time, t_s = 0.25 s, the values of α, β were {10, 1}, the reference signal was a square wave, the frequency was 0.25 Hz and the amplitude was 1 volt.

The position responses and gains of the real plant under the MCS can be seen in Fig. 5.12 (Chapter 5). The reference signal was a square wave, settling time was t_s = 0.25 s, frequency was 0.25 Hz, amplitude was 1 Volt and the values of α, β were {0.001, 0.0001},. The corresponding results of the real system under P+DFB are shown in Fig. 5.11 (Chapter 5), together with a proportional gain, k_p = 1 and a derivative feedback gain, k_d = 0.1.

There is reasonable correspondence between the simulated and the actual system responses, indicating that the mathematical model of the system, which was calculated analytically and modelled by Simulink, is accurate.

The steady-state error is occurred in both the real and model position responses due to the relationship between the flow and position. Additionally, the system has a single rod actuator and the mass at the end of the actuator has nonlinear effects. The real plant responses are more oscillatory in both the P+DFB and MCS control than the simulated plant responses. The reasons of this steady-state error are firstly, in modelling the volumes inside the actuator chambers are assumed constant during operation, then for the sake of simplicity the averaged form of these volumes is used as the effective volume. In fact, the volumes in the first and second chambers are not just equal (due to the use of single rod actuator) also they change during dynamic operation of the plant. Secondly, the constant bulk modulus was used in Simulink models to bring the simplicity in to modelling which is not the case in real plant operation. The bulk modulus changes due to the changes in the pressure inside the actuator and servovalve. There so many other factors which are not considered in this modelling like, the nonlinear dynamics of the accumulators (the accumulators dynamics are not included into the model), the plant rigidity and the cavitation in the fluid.

In the case of the P+DFB control both the real and simulated plant are controlled by using same controller gains. The adaptive weights of the MCS control was greater in the simulated model due to fact that the computation of the adaptive gains and controller itself take longer time in Simulink and using smaller adaptive weights makes this process even slower. In comparison to the MCS control P+DFB control has a simple structure therefore the calculation in Simulink was rather quick.

2.8 - CONCLUSIONS

At the most basic level, modelling of hydraulic systems can enable the users to explore the various configuration options and decide which system configuration needs to be used to ensure acceptable performance. Once this decision has been made, the sizes of the hydraulic system components such as hoses, hydraulic pump units and directional control valves can be established.

In the case of adaptive control of hydraulic systems, since both the controlled system and the controller are nonlinear, it is necessary to use simulation to confirm that the control strategy is correct. The results from the simulation must of course be validated with experiments.

For industrial fluid power systems, it is often possible to carry out much of the initial design work using steady state performance calculations. Simulation can then be used to refine performance.

Numerical simulation of hydraulic systems is used extensively as a design tool, but in order to investigate much larger and more complex systems, within an economic time frame, faster software and hardware required.

Reasonable good simulation results are generated in the case of both the P+DFB and the MCS controllers from the model of the electrohydraulic actuator plant, which are close to the real plant responses. This indicates that the mathematical model of the system is accurate and also that Simulink can be a good option for modelling hydraulic systems (or any other kind of systems).

REFERENCES

[1] - **EDGE, K. A. & K. R. A. FIGUERODO,** "Adaptively Controlled Electrohydraulic Servo-Mechanism, Part 2: Implementation," *Proc. I. Mech. E.*, Vol. 201, No. B3, pp. 181-189, 1987.

[2] - **LONGMORE, D. K. & A. SCHLEISINGER,** "Relative Importance of Various Vibration Transmitting Mechanisms in Horses in Typical Hydraulic System", *Proc. Instn. Mech. Engrs.*, Vol. 205, pp. 105-111, 1991.

[3] - **LONGMORE, D. K., & A. SCHLESINGER,** "Transmission of Vibration and Pressure Fluctuations Through the Hydraulic Hoses", *Proc. Instn. Mech. Engrs.*, Vol. 205, pp. 97-104, 1991.

[4] - **WATTON, J.,** "A Digital Compensator Design for Electrohydraulic Single-Rod Cylinder Position Control Systems," *Journal of Dynamics Systems, Measurement and Control*, Vol. 112, pp. 403-409, September 1990.

[5] - **WATTON, J., & R. A. H. AL-BALDAWI,** "Performance Optimisation of an Electrohydraulic Position Control System with Load Dependent Supply Pressure", *Proc. Instn. Mech. Engrs.*, Vol. 205, pp. 175-189, 1991.

[6] - **BACKÉ, W., & B. ZÄHE,** "Electrohydraulic Loadsensing-Analysis of Benefits," *Society of Automotive Engineering Transactions*, pp. 303-311, 1991.

[7] - **HABIBI, S. R., & R. J. RICHARDS,** " Computed -torque and Variable Structure Multi-variable Control of a Hydraulic Industrial Robot", *Proc. Instn. Mech. Engrs.*, Vol. 205, pp. 123-140, April 1991.

[8] - **RICHARD, W. U., & M. E. TORNGREN,** " Introducing Distributed Control in Mobile Machines Based on Hydraulic Actuators", *Mechatronics*, Vol. 4, No. 2, pp. 139-157, 1994.

[9] - **TANTAWY, H. S. & I. S. MOGHRAM,** "Digital Simulation of Hydraulic Position Control of a Robot Arm," *Modelling, Measurement and Control*, B, ASME Press, Vol. 51, No. 2, pp. 21-29, 1993.

[10] - **LAU, K. K., K. A. EDGE, & D. N. JOHNSTON,** "Impedance Characteristics of Hydraulic Orifices", *Proc. Instn. Mech. Engrs.*, Vol. 209, pp. 241-253, 1995.

[11] - **EDGE, K. A., & D. N. JOHNSTON,** "The Impedance Characteristics of Fluid Power Components: Relief Valves and Accumulators", *Proc. Instn. Mech. Engrs.*, Part I, Vol. 205 (11), pp. 11-22, 1991.

[12] - **JOHNSTON, D. N., & K. A. EDGE,** "The impedance Characteristics of Fluid Power Components: Restrictor and Flow Control Valves", *Proc. Instn. Mech. Engrs.*, Part I, Vol. 205 (II), pp. 3-10, 1991.

[13] - **XUE, Y., & J. WATTON**, "A Self-organising Neural Network Approach to Data-based Modelling of Fluid Power Systems Dynamics Using the GMDH Algorithm", *Proc. Instn. Mech. Engrs.* , Vol. 209, pp. 229-240, 1995.

[14] - **BURTON, J. D., K. A. EDGE, & C. R. BURROWS**, " Modelling Requirements for the Parallel Simulation of Hydraulic Systems", *Journal of Dynamic Systems, Measurement, and Control*, Vol. 116, pp. 137-145, March 1994.

[15] - **HEYNS, L. J., & J. J. KRUGER**, "Describing Function-Based Analysis of a Nonlinear Hydraulic Transmission Line", *IEEE Transactions on Control Systems Technology*, Vol. 2, No. 1, March 1994.

[16] - **ATKINSON, R. M., M. R. MONTAKHAB, K. D. A. PILLAY, D. J. WOOLLONS, P. A. HOGAN, C. R. BURROWS, & K. A. EDGE**, "Automated Fault Analysis for Hydraulic Systems, Part I: Fundamentals", *Proc. Instn. Mech. Engrs.*, Vol. 206, pp. 207-214, 1992.

[17] - **HOGAN, P. A., J. R. BURROWS, K. A. EDGE, R. M. ATKINSON, M. R. MONTAKHAB, D. J. WOOLLONS**, "Automated Fault Analysis for Hydraulic Systems, Part 2: Applications" *Proc. Instn. Mech. Engrs.*, Vol. 206, pp. 215-224, 1992.

[18] - **JOHNSTON, D. N. & K. A. EDGE**, "In-Situ Measurement of the Wavespeed and Bulk Modulus in Hydraulic Lines", *Proc. Instn. Mech. Engrs.*, Vol. 205, pp. 191-197, 1991.

[19] - **EDGE, K. A. & J. DARLING**, "Cylinder Pressure Transients in Oil Hydraulic Pumps with Sliding Plate Valves," *Proc. Instn. Mech. Engrs.*, Vol. 12, No. 4, 1986.

[20] - **JINGHONG Y., & L. YUANZHANG**, "The Cross-Correlation Method for Determining the Effective Bulk Modulus of Oil in Hydraulic Systems," *Machine Tool & Hydraulics* (Chinese), No. 5, pp. 29-32, 1991.

[21] - **JINHONG, Y. , C. ZHAONENG, & L. YUANZHANG**, "The variation of oil Effective Bulk Modulus with Pressure in Hydraulic Systems," *Journal of Dynamic Systems Measurement, and Control, Transactions of the ASME*, Vol. 116, pp. 146-150, 1994.

[22] - **WARDMAN, D. & R. RODDIS**, "Design of an Electro-Hydraulic Multivariable Control System Teaching Facility", *UKACC International Conference on CONTROL*, September 1996, Conference Publication No. 427, IEE 1996.

[23] - **MARTIN, H. R.**, *The control of fluid power* (Longman Group Limited 1973, London ISBN 058247003X).

[24] - **GUILLON, M.** translated by **GRIFFITHS, R. T.** Hydraulic Servo Systems Analysis and Design. Translated from French *Elude et determination des systemes hydrauliques* by M. Guillon, Paris, Dunod, 1961, Butterworth & Co. (Publishers) Ltd., 1969. Printed in Great Britain by J. W. Arrows.

[25] - **THAYER, W. J.**, *Transfer Functions for Moog Servovalves*. Moog Inc. Technical Bulletin 103, 1965.

CHAPTER 3

A REVIEW OF MODEL REDUCTION METHODS

3.1 - INTRODUCTION

The reduced order MCS has a reference model of lower order than the nominal plant model, and the modelled part of the plant matches the reference model in order. Hence, the unmodelled part of the plant, which represents the fast dynamics of the plant can be considered as a disturbance term. Together with the unmodelled dynamics the stability of the reduced order MCS incorporating unmodelled plant dynamics will be proven in Chapter 4 in the case of both SISO and MIMO systems. If the disturbance term is large in magnitude, using EMCS (Extended Minimal Controller Synthesis) may be an option to guarantee global asymptotic stability of the system.

Another possibility may be to use an averaging method, which gives good results in the case of SISO first order plant but it is rather difficult to derive the stability of the error equation if the relative degree of the plant is greater than one. It is also difficult to derive the stability error equation in the case of multivariable systems.

Later in this chapter, linear model reduction methods are presented. By using linear model reduction methods it is possible to reduce the order of the plant and then implement the MCS control according to the reduced order plant parameters. Although, the MCS control does not need the reduced order plant parameters, they can be still very useful when choosing the settling time and sampling interval of the controller. Additionally, plant parameters are required in the case of comparative studies, due to the fact that linear controller strategies need plant parameters for implementation.

In the case of the reduced order MCS control, the controller is implemented in such way that the controlled plant is higher order than the reference model in terms of degree. This procedure reduces the order of the plant automatically due to the fact that the

lower order reference model will activate only the dominant part (mid-frequency range) and it will ignore high order dynamics of the plant. For this reason, the implementation of the reduced order MCS control is very simple and easy.

The reduced order electrohydraulic actuator plant and ESH material testing machine transfer functions which are obtained by conventional model reduction methods are given in Tables 3.3-3.6. These transfer functions will be compared with the nominal model of the plants which are found from system identification tests in the case of step and impulse energy responses. The performances of conventional model reduction methods will be compared with the original plant transfer function by step and impulse response methods.

3.2 - MODEL REDUCTION METHODS

Model reduction methods are presented in two groups in this chapter. The first group is adaptive model reduction methods. In this case, the model reduction procedure takes place inside the adaptive algorithm. This is due to the fact that the adaptive control does not require the plant parameters directly (except the self-tuning regulator). For that reason, there is not a direct reduction in the plant order. Instead of that the algorithm uses a lower order reference model and the plant matches the reference model in order. Two adaptive model reduction methods are presented in this chapter: averaging method and extended MCS control algorithm which are studied in sections 3.3-3.4. The extended MCS algorithm is an extension of the standard MCS control and it may guarantee the stability of the system in the face of large unmodelled dynamics. The second group is linear model reduction methods. Most of these methods require a linear description of the plant in the state-space form and they are studied in sections 3.6-3.16. In this case, the reduction procedures approximate the plant transfer function to a lower order one directly.

The linear model reduction methods can be use together with the model reference adaptive controller as well. The model reference adaptive control algorithm does not require the reduced order plant parameters, still they can be very useful to have an idea about the suitable controller gains, the reference signal characteristics and comparative studies.

3.3 - AVERAGING THEORY

Averaging method was proposed to prove the stability of adaptive systems in the presence of unmodelled dynamics, nonlinearities in [1]. Later, the method was improved in [2], [3] and [4]. It was demonstrated in [5] that the averaged model of the system is stable in a larger scale than the nominal plant model. Additionally, the converge of the averaged and original plant model was investigated in this work.

The characteristic of the reference signal is important in the case of averaged adaptive systems. The system may become unstable depending on the property of the reference signal. The relationship between the unmodelled dynamics and high frequency reference signals were studied in [6]. It was shown that equilibrium is not a unique point when the input signal is not persistently exciting therefore, even small disturbances may lead unstable responses in the presence of the unmodelled dynamics and nonlinearities in the system. It was shown that if the input signal is persistently exciting than the equilibrium set will be a point and this will preserve the stability of the system [7], [8] and [9].

Averaging method was used to determine the stability of a reduced order adaptive systems with relative degree one in [10]. It was pointed out that the method is not easily applicable to adaptive systems which have higher order transfer functions or the relative degree greater than one. In addition, although the method works well with sinusoidal reference signal it does not produce the stable output responses for other types of input signal e.g., square wave signal.

3.4 - THE REDUCED ORDER EXTENDED MCS ALGORITHM (ROEMCS)

Model reduction methods are based on deriving lower order models of original higher order systems by simplifying their dynamic equations. Similarly, the reduced order MCS control uses a simpler mathematical approximation that retains the key features of the original systems. In the case of the reduced order MCS control, the simplicity of the controller is achieved by using a lower order reference model.

If the disturbance term is rapidly varying due to the high order unmodelled dynamics then it could be a good idea to use reduced order EMCS control instead of standard reduced order MCS control. It was shown that the effects of rapidly varying plant disturbances were substantially reduced in the EMCS [11]. The EMCS control signal has more active nature than the standard MCS signal due to the quasi-switching term. Hence, in some case the EMCS control may lead an undesirable oscillations of the plant states it may even cause instability due to excitement of the higher order unmodelled dynamics. The algorithm is applicable to the control of SISO and MIMO plants. It will be shown in Chapter 4 that the standard MCS algorithm is stable in the presence of rapidly varying disturbances; thus the plant-reference model signals remain bounded.

EMCS algorithm guarantees global asymptotic stability of the tracking errors in the case of plants, which are subject to unmodelled dynamics in comparison with the MCS algorithm. Consider a linear, SISO plant with unmodelled dynamics given as below

$$\dot{x}_r = A_r x_r(t) + B_r u(t) + d(x_r, t) \tag{3.1}$$

where $A_r(t) \in \mathbb{R}^{h\times h}$ and $B_r(t) \in \mathbb{R}^{h\times 1}$, $d(x_r, t)$ is the disturbance term due to the high order unmodelled dynamics and $x_r = [x_1 \ , \ x_2 \ , \ . \ . \ . \ . \ , \ x_h]^T$ $x_r \in \mathbb{R}^{h\times 1}$. The variables $x_r(t)$ and $u(t)$ denote the reduced order plant state vector and control input signal respectively, where

$$A_r(t) = \begin{bmatrix} 0 & 1 & 0 & \dots & 0 \\ 0 & 0 & 1 & \dots & 0 \\ \vdots & & & \ddots & \\ 0 & 0 & 0 & \dots & 1 \\ -a_1 & -a_2 & -a_3 & \dots & -a_h \end{bmatrix}, \quad B_r(t) = \begin{bmatrix} 0 \\ \vdots \\ 0 \\ b_1 \end{bmatrix} = \begin{bmatrix} 0 \\ \vdots \\ 0 \\ 1 \end{bmatrix} \tag{3.2}$$

and

$$d(x_r, t) = \begin{bmatrix} 0 \\ \vdots \\ 0 \\ d_1 \end{bmatrix} = bd_1$$

The stable, reference model is given by the following state-space equation.

$$\dot{x}_m(t) = A_m x_m(t) + B_m r(t) \tag{3.3}$$

where $A_m \in \mathbb{R}^{h\times h}$ and $B_m \in \mathbb{R}^{h\times 1}$. The matrix A_m and the vector B_m are given by

$$A_m = \begin{bmatrix} 0 & 1 & 0 & \dots & 0 \\ 0 & 0 & 1 & \dots & 0 \\ \vdots & & & \ddots & \vdots \\ 0 & 0 & 0 & \dots & 1 \\ -a_{m1} & -a_{m2} & -a_{m3} & \dots & -a_{mn} \end{bmatrix}, \quad B_m = \begin{bmatrix} 0 \\ \vdots \\ 0 \\ b_m \end{bmatrix} \tag{3.4}$$

The error dynamics of the closed-loop system determined by using (3.1) to (3.3) as follows

$$\dot{x}_e(t) = A_m x_e(t) - (A_r - A_m)x_r(t) - B_r u(t) + B_m r(t) - d(x_r, t) \tag{3.5}$$

where

$$x_e(t) = x_m(t) - x_r(t) \tag{3.6}$$

The MCS control signal is

$$u = K(t)x_r(t) + K_R(t)r(t) \tag{3.7}$$

with

$$K(t) = \int_0^t \alpha y_e x_r^T d\tau + \beta y_e x_r^T$$
$$K_R(t) = \int_0^t \varepsilon y_e r d\tau + \beta y_e r \tag{3.8}$$

$$y_e = C_e x_e \tag{3.9}$$
$$C_e = b^T P$$

where the vector b is of dimension (hx1), and is given as:

$$b = \begin{bmatrix} 0 & \dots & 0 & 1 \end{bmatrix}^T \tag{3.10}$$

and P is the symmetric positive definite matrix solution to the Lyapunov equation:

$$A_m^T P + P A_m = -Q; \quad P > 0; \quad Q > 0 \tag{3.11}$$

From equations (3.7), (3.5) and (3.11) a new error dynamics equation is determined as

$$\dot{x}_e = A_m x_e - b w^T \Phi - b w^T \Psi - b d_1 \tag{3.12}$$

where

$$\dot{\Phi} = b_1 \alpha b^T P x_e w \tag{3.13}$$

$$w = \begin{bmatrix} x_r^T & r \end{bmatrix}^T \tag{3.14}$$

and

$$\Psi = b_1 \beta b^T P x_e w \tag{3.15}$$

From Equation (3.1) the SISO EMCS control signal, u_s is determined in the following form:

$$u_s = \left[\theta^T + \frac{1}{b_1}\Psi^T\right] w + N sign(y_e) \tag{3.16}$$

where N is a constant scalar and the sign function is

$$sign(y_e) = \begin{cases} 1 & if \quad y_e > 0 \\ 0 & if \quad y_e = 0 \\ -1 & if \quad y_e < 0 \end{cases} \tag{3.17}$$

and

$$\theta^T = \left[\int_0^t \alpha y_e x_r^T d\tau, \quad \int_0^t \alpha y_e r d\tau\right] \tag{3.18}$$

b_1 is the last (and the only non-zero) entry of matrix b, where b, w, y_e and Ψ are respectively defined by (3.9), (3.10), (3.14) and (3.15). Following, the new MCS law (3.16) and (3.12) become:

$$\dot{x}_e = A_m x_e - bw^T\Phi - bw^T\Psi - b\left[d(x_r,t) + b_1 N sign(y_e)\right] \tag{3.19}$$

where Φ is given in (3.13) and $d(x_r,t)$ is the disturbance term then, the error x_e is globally asymptotically stable if following condition is satisfied for all $t \geq 0$ [11]:

$$d(x_r,t)sign(y_e) + b_1 N \frac{y_e}{|y_e| + \xi} \geq 0 \tag{3.20}$$

If the term $b_1 N$ is positive, then N is obtained from (3.19) as follows :

$$b_1 N \geq \max\left\{|d(x_r,t)|\frac{|y_e| + \xi}{|y_e|}\right\} \tag{3.21}$$

and $b_1 N > 0$ f or all $t \geq 0$. The above condition indicating that if ξ is sufficiently small then the term $\frac{|y_e| + \xi}{|y_e|}$ may be approximated to 1. Hence, it can be concluded that the SISO EMCS control law, (3.16) yields the globally asymptotically stability of the error, x_e for the suitable set values of N and ξ. The condition (3.21) is not related to the variation of d_1 therefore no matter how rapidly d_1 is varying, suitable values of N and ξ ensure the global asymptotic stability of the error x_e..

In similar manner to SISO systems, the global asymptotic stability of the MIMO EMCS control was proven in [11]. The EMCS algorithm was further extended as the purely adaptive EMCS algorithm in [12]. New algorithm estimated the amplitude of the discontinuous switching term adaptively.

3.5- LINEAR MODEL REDUCTION METHODS

The reduced order models have simpler mathematical structure compare to the nominal plant model which retains the crucial dynamics of the original system. There are great variety of ways to reduce the order of the higher order plant transfer function. The current linear model reduction methods uses either the time domain or the frequency domain approach. These methods are based on the classical theories of the mathematical approximation or mathematical concepts; such as Pade´ approximation, continued fraction method and time-moment matching method.

The model order reduction problem was very closely related to the stabilisation problem in [13]. In [14], a model reduction method was introduced based on the differentiation of the numerator and denominator polynomials of the higher order transfer function. The nominal transfer function of the plant were differentiated as many times as required to derive the coefficients of the reduced order transfer function polynomials.

Linear model reduction methods can be used together with adaptive controllers, e.g., a mixed method of Liaw was used to find the reduced order model of the interconnected power system in [15]. After model reduction process the plant was controlled under the proposed adaptive controller in [16]. The proposed adaptive controller implemented by using a reduced order reference model and it did not required the plant parameters for implementation. Although, the adaptive controller required minimum knowledge about the plant parameters for implementation still it produced good plant output responses.

A control system with a very high order linear model will be difficult to design and control. Therefore, using the reduced order form of the original system is more desirable in many cases. Some of linear model reduction methods are given as below

Routh Method

Pade´ Method

Initial Time Moments Method

Frequency Domain Model Reduction Method

Dominant Mode Model Reduction Method

Davison Method

Marshall's Method

Stability-Equation Method

Impulse Energy methods

Singular Value Decomposition

Stochastic Model Reduction Method

Balancing Method

Optimal Model Reduction Method

In practice most of the systems work in low or mid-frequency range therefore, in most of the applications only dominant dynamics of the plant are in use. Although, the plant can be modelled by a high order model, if it is not working in the high frequency range these high order dynamics will not contribute much to the plant output response. Hence, a high order model could lead to large steady-state errors due to the fact that the plant is over parameterised. Hence, the model reduction is vital in many control application for satisfactory results.

Now, each of these linear model reduction methods will reviewed in sections 3.6-3.14 and later in this chapter some of these methods will be used to produce the reduced order models in the case of both ESH material testing machine and electrohydraulic actuator plant.

3.6 - ROUTH METHOD

The method uses the expansion of the denominator and the numerator Routh array of the higher order original system [17]. The method produces stable reduced order models provided that the original plant model is stable. Routh method improves the impulse response of the reduced order models. Let us consider a linear time invariant SISO system having the transfer function

$$G_p(s) = \frac{b_1 s^{n-1} + \cdots + b_n}{a_0 s^n + a_1 s^{n-1} + \cdots + a_n} \tag{3.22}$$

The above equation is asymptotically stable and it can be further expanded into the following canonical form:

$$G_p(s) = \beta_1 C_1(s) + \beta_2 C_1(s)C_2(s) + \cdots + \beta_n C_1(s)C_2(s)\cdots C_n(s) \qquad (3.23)$$
$$= \sum_{l=1}^{n} \beta_l \prod_{j=1}^{l} C_j(s)$$

where the β_j (j = 1,2,...,n) are constants and the C_j are the continued fraction expansions. Equation (3.23) was described as the alpha-beta expansion of $G_p(s)$.

$$C_j = \cfrac{1}{\alpha_j s + \cfrac{1}{\alpha_{j+1} s + \cdots + \alpha_{n-1} s + \cfrac{1}{\alpha_n s}}} \qquad (3.24)$$

Alpha Routh Table	$a_0^0 = a_0$	$a_2^0 = a_2$	$a_4^0 = a_4$	$a_6^0 = a_6$
	$a_0^1 = a_1$	$a_2^1 = a_3$	$a_4^1 = a_5$	...
$\alpha_1 = a_0^0 / a_0^1$	$a_0^2 = a_2^0 - \alpha_1 a_2^1$	$a_2^2 = a_4^0 - \alpha_1 a_4^1$	$a_4^2 = a_6^0 - \alpha_1 a_6^1$	...
$\alpha_2 = a_0^1 / a_0^2$	$a_0^3 = a_2^1 - \alpha_2 a_2^2$	$a_2^3 = a_4^1 - \alpha_2 a_4^2$	...	
$\alpha_3 = a_0^2 / a_0^3$	$a_0^4 = a_2^2 - \alpha_3 a_2^3$	$a_2^4 = a_4^2 - \alpha_3 a_4^3$	...	
$\alpha_4 = a_0^3 / a_0^4$	...	...		
...				

Table 3.1: Alpha Routh table

The first two rows of the alpha Routh table were formed from the coefficients of the denominator of $G_p(s)$. The remaining elements were calculated as follows

$$\begin{aligned} a_0^{j+1} &= a_2^{j-1} - \alpha_j a_2^j \\ a_2^{j+1} &= a_4^{j-1} - \alpha_j a_4^j \\ &\cdots \\ a_{n-j-2}^{j+1} &= a_{n-j}^{j-1} - \alpha_j a_{n-j}^j, \qquad j = 1,\cdots,n-1 \end{aligned} \qquad (3.25)$$

If n-j odd, the last equation in (3.25) was replaced by

$$a_{n-j-1}^{j+1} = a_{n-j+1}^{j-1} \qquad (3.26)$$

and the α_j are given by

$$\alpha_j = \frac{a_0^{j-1}}{a_0^j}, \qquad j = 1,2,\cdots,n. \qquad (3.27)$$

Beta Routh Table	$b_0^1 = b_1$	$b_2^1 = b_3$	$b_4^1 = b_5$	...
	$b_0^2 = b_2$	$b_2^2 = b_4$	$b_4^2 = b_6$	...
$\beta_1 = b_0^1 / a_0^1$	$b_0^3 = b_2^1 - \beta_1 a_2^1$	$b_2^3 = b_4^1 - \beta_1 a_4^1$	...	
$\beta_2 = b_0^2 / a_0^2$	$b_0^4 = b_2^2 - \beta_2 a_2^2$	$b_2^4 = b_4^2 - \beta_2 a_4^2$	...	
$\beta_3 = b_0^3 / a_0^3$	...	...		
$\beta_4 = b_0^4 / a_0^4$				
⋮				

Table 3.2: Beta Routh table

The coefficients β_j were formed by using a tabular algorithm as shown in Table 3.2. The first two rows of beta Routh table were obtained from the coefficients of the numerator of $G_p(s)$. The following elements were computed from alpha Routh table as follows

$$\beta_j = b_0^j / a_0^j, \qquad j = 1,2,\ldots,n$$

$$b_{i-2}^{j+2} = b_i^j - \beta_j a_i^j, \quad i = \begin{cases} 2,4,\ldots,n-j \text{ for } n-j \text{ even} \\ 2,4,\ldots,n-j-1 \text{ for } n-j-1 \text{ odd} \end{cases} \qquad (3.28)$$

$$j = 1,2,\ldots,n-2$$

The reduced order models numerator and denominator $A_k(s)$ and $B_k(s)$ computed by the following algorithm

$$\begin{aligned} A_1(s) &= \alpha_1 + 1 \\ B_1(s) &= \beta_1 \\ A_2(s) &= \alpha_1\alpha_2 s^2 + \alpha_2 s + 1 \\ B_2(s) &= \alpha_2\beta_1 s + \beta_2 \\ &\cdots \end{aligned} \qquad (3.29)$$

Generally, $B_k(s)$ and $A_k(s)$ can be derived following equations

$$\begin{aligned} A_k(s) &= \alpha_k s A_{k-1}(s) + A_{k-2}(s) \\ B_k(s) &= \alpha_k s B_{k-1}(s) + B_{k-2}(s) + \beta_k \end{aligned}, \quad k = 1,2,\ldots \qquad (3.30)$$

$$A_{-1}(s) = 0 \quad B_{-1}(s) = 0$$
$$A_0(s) = 1 \quad B_0(s) = 0$$

where, k is the order of the reduced order model. It was suggested that the method is applicable to MIMO systems provided that it is modified.

A simplified form of Routh method used in [18] and [19]. In this method the reduced order transfer function was determined directly from elements of the high-order

denominator and numerator Routh stability arrays. The method is computationally simpler than the standard Routh method and it improves the frequency response of the reduced order models.

For systems which have imaginary roots or natural integrators in their dynamics the standard Routh method can not be apply. The Routh-Hurwitz criterion is suitable for such conditions which is one of the modified forms of Routh method [20]. In this method, a zero element of the alpha table was replaced by a small number ε and the Routh table completed in terms of ε.

In comparison with Routh method the reduced order MCS control will not give large time-response errors so long as the adaptive weights are big enough to reduce the steady-state error to zero. If the adaptive weights are too big then, they may excite the high order unmodelled dynamics of the plant which may then cause instability. Similarly, if the adaptive weights are very small then the plant response will be slow down and this may lead large steady-state error. Additionally, the reduced order MCS control uses the poles and zeros of the system which are closest to the imaginary axis automatically therefore there is no need to compute the roots of the higher order plant model.

3.6.1 - New Optimal Routh Method

The reduced order models produced by Routh method does not fit the time response of the original system therefore, they may give large time response errors. To overcome this problem while preserving the stability of the reduced order model, a new optimal Routh approximation method was proposed which combined Routh approximation method with an integral square error (ISE) method in [21]. In this method, the denominator of the reduced order transfer function was formulated by using the standard Routh method and the numerator was determined by minimising a time response integral square error (ISE) criterion. The method is applicable to both continuous and discrete time SISO systems. Although, the technique has simple formulation procedure the construction of a set of linear equation is rather time consuming.

In comparison with new optimal Routh method the reduced order MCS control is very simple due to the fact that it does not use plant parameter for implementation.

3.6.2 - Routh-Approximant Time Domain Model Reduction

Routh approximant time domain modelling is another modified form of Routh approximation method which produces reduced order models via a γ-δ expansion [22] similar to the α-β expansion of Hutton and Friedland [18]. The lower order time domain model matrices were derived from the original system dynamics parameters by a suitable truncation procedure. The method is a time domain model reduction technique based on the frequency domain Routh approximant procedure and it is applicable for both SISO and MIMO systems.

3.7 - PADE´ METHOD

Pade´ approximation technique or equivalently continued fraction methods has many useful features and it is easy to conduct. However, it may produce an unstable reduced order model, although the original plant is stable. In order to overcome this problem Pade´ method was used together with some additional approaches which were preserved the reduced order model stability. Firstly, Pade´ method was used together with Routh stability criteria in order to construct Hurwitz polynomials for the reduced order model. The second method was the generalised Pade´ approximation technique which retained specified dominant roots of the higher order original system in the reduced order model. Another approach proposed by Appiah in [23] in this method, the denominator of the reduced order transfer function was derived using the original Hurwitz characteristic polynomial and the numerator was obtained using Pade´ approximation. Let the Pade´ approximant be defined by

$$\frac{P_n(s)}{Q_n(s)} = G_p(s) = \frac{d_0 + d_1 s + \cdots + d_{n-1} s^{n-1}}{e_0 + e_1 s + \cdots + e_n s^n} \tag{3.31}$$

where $P_n(s)$ and $Q_n(s)$ are polynomials of the original plant transfer function. After model order reduction procedure, let us denote a reduced order model $R(s)$, of order k, is required, and let it be of the form

$$R(s) = \frac{a_0 + a_1 s + \cdots + a_{k-1} s^{k-1}}{b_0 + b_1 s + \cdots + b_k s^k} \tag{3.32}$$

In general, the coefficient of the numerator is given as follows

$$
\begin{aligned}
a_0 &= b_0 c_0 \\
a_1 &= b_0 c_1 + b_1 c_0 \\
&\cdots \quad \cdots \quad \cdots \quad \cdots \\
a_{k-1} &= b_0 c_{k-1} + b_1 c_{k-2} + \cdots + b_{k-1} c_1 + b_k c_0 \\
&\cdots \quad \cdots \quad \cdots \quad \cdots \quad \cdots \quad \cdots \quad \cdots \quad \cdots \quad \cdots \quad \cdots \\
0 &= b_0 c_{2k-2} + b_1 c_{2k-3} + \cdots + b_{k-1} c_k + b_k c_{k-1}
\end{aligned}
\tag{3.33}
$$

3.7.1 - Pade´ Approximant with Time Moments Method

In this method Pade´ approximation was used together with time moments method in order to derive a reduced order model which has the same initial time moments as the original plant [24]. The method retained the dominant poles, or any other desired poles of the system into the reduced model by using Koenig's theorem in [25]. The reduced order models generated from this method showed the significant characteristics of the original system by fitting the initial time moments of it.

In comparison with this method the reduced order MCS control is easy to apply and it produces stable and accurate reduced order models which have the initial time moments that is very close to the original plant without necessity of knowing the reduced order plant parameters.

3.7.2 - Pade´ Methods of Hurwitz Polynomial Approximation

Time moments and Markov parameters approaches were used to construct low-degree Hurwitz polynomial from the higher order original system in [17]. Using the Hurwitz polynomial, the numerator dynamics of the reduced order transfer function models were determined by partial Pade´ approximation of a given higher order model. It was claimed that reduced order models generated from this method are always stable.

3.7.3 - Routh- Pade´ Approximation

In this method, the denominator of the reduced order model was derived by using Routh stability criterion while the numerator was computed from Pade´ method in order to fit the initial time moments of the original plant [26]. It was demonstrated that the method can preserve the stability of the reduced order models.

3.7.4 - Stable Partial Pade´ Approximation

In stable partial Pade´method, the numerator of the reduced order model was obtained by using standard root locus plots [27]. It was shown that the reduced order model matched the original plant in the Taylor series accurately. The method improved the stability of Pade´ approach.

3.7.5 - The Constrained Suboptimal Pade´ Method

The suboptimal Pade´ method is based on the multipoint Pade´ approximation method [28]. It was shown that the method is not complex but it requires great deal of computation.

Constrained suboptimal Pade´ model reduction is an another type of Pade´ method which was developed as an extension to the suboptimal Pade´ method in [29]. The method uses the Lagrange multipliers theory in order to produce reduced order models which matches the original plant in the initial time response.

Pade´ approximation technique was used in the case of MIMO systems model reduction in [30]. The multivariable reduced order model was derived from the partial realisations of the system in state-space form. The method needs a great deal of numerical computation therefore, it is time consuming.

3.8 - REDUCTION OF TRANSFER FUNCTIONS BY THE STABILITY-EQUATION METHOD

The stability-equation model reduction method was performed by ignoring the largest poles and zeros of the nominal plant transfer function. It was observed that poles and zeros with smaller magnitudes are more dominant therefore, they should retained in the reduced order model [31]. Let a higher order system transfer function be given by

$$G(s)=\frac{b_m s^m+b_{m-1}s^{m-1}+\cdots+b_1 s+b_0}{a_n s^n+a_{n-1}s^{n-1}+\cdots+a_1 s+a_0}=\frac{N(s)}{D(s)} \tag{3.34}$$

where $n \geq m$ and $N(s)$ and $D(s)$ are the numerator and the denominator of $G(s)$, respectively. The above equation can be written as

$$G(s)=\frac{N_e(s)+N_o(s)}{D_e(s)+D_o(s)} \tag{3.35}$$

where

$$\begin{cases} N_e(s)=\sum_{i=0,2,\ldots}^{m} b_i s^i \\ N_o(s)=\sum_{i=1,3,\ldots}^{m} b_i s^i \end{cases} \tag{3.36}$$

and

$$\begin{cases} D_e(s)=\sum_{i=0,2,\ldots}^{n} a_i s^i \\ D_o(s)=\sum_{i=1,3,\ldots}^{n} a_i s^i \end{cases} \tag{3.37}$$

Later, Equations (3.36) and (3.37) were factored as

$$\begin{cases} N_e(s)=\prod_{i=1}^{m'}\left(s^2+z_i^2\right) \\ N_o(s)=s\prod_{i=1}^{m'}\left(s^2+z_i^2\right) \end{cases} \tag{3.38}$$

and

$$\begin{cases} D_e(s)=\prod_{i=1}^{n'}\left(s^2+p_i^2\right) \\ D_o(s)=s\prod_{i=1}^{n'}\left(s^2+p_i^2\right) \end{cases} \tag{3.39}$$

$m' = m / 2$ if m is even,

$= (m - 1) / 2$ m is odd;

$n' = n / 2$ if n is even,

$= (n - 1) / 2$ if n is odd;

and

$$p_1^2 \langle p_2^2 \langle p_3^2 \langle \cdots$$
$$z_1^2 \langle z_2^2 \langle z_3^2 \langle \cdots$$

The coefficients of the reduced stability equations were multiplied by the magnitudes of the selected poles and zeros. Hence, the reduced order model matched the original plant in steady-state response [34]. Following, the reduced stability equations of $G(s)$ were written as

$$N_e'(s) = z_n^2 \prod_{i=1}^{m'-1} \left(s^2 + z_i^2\right)$$
$$N_o'(s) = sp_n^2 \prod_{i=1}^{m'-1} \left(s^2 + p_i^2\right) \qquad (3.40)$$

The reduced order model was

$$G_{n-1} = \frac{N'(s)}{D'(s)} \qquad (3.41)$$

where

$N'(s) = N_o + N_e'$ if m is even

$N'(s) = N_o' + N_e$ if m is odd

and

$D'(s) = D_o + D_e'$ if n is even

$D'(s) = D_o' + D_e$ if n is odd

Then, the reduced models of the polynomials $N(s)$ and $D(s)$ were constructed and finally the reduced model of $G(s)$ was obtained.

3.9 - DOMINANT MODE MODEL REDUCTION METHOD

Davison's [32] and Marshall [33] methods are both dominant mode model reduction methods which retain the dominant roots of the original transfer function of the system in the reduced order models. It was shown that the reduced order models produced by these methods are stable provided that original plants are stable. However, these methods did not produced accurate reduced order models especially when the eigenvalues of the original higher order systems are widely separated. The computation of the eigenvalues of the original system can be a problem if the order is very high. In order to overcome this difficulty some other approaches were used to retain the most dominant part of the original system in the reduced order models without computing the eigenvectors and eigenvalues of the nominal plant model [34].

A multivariable system was composed of a number of slow and fast subsystems then the slow subsystems were used to form a reduced order model by using dominant mode model reduction method in [35]. It was pointed out that slow dynamics of the system are near the origin therefore they are dominant and will produce stable lower order models.

Similarly, Marshall's method retains only the dominant eigenvalues of the original plant in reduced order models [36]. In this work, after model reduction process by using the proposed method the difference between the higher order system and the reduced order model was evaluated by ISE criterion. It was shown that the method may produce a good reduced order model provided that most suitable eigenvalues are chosen.

In the case of the reduced order MCS control, there is no need to select the dominant eigenvalues and eigenvectors of the original plant since the reduced order MCS algorithm is activating the most dominant part itself. This is obviously an advantage due to the fact that it may be a problem to choose the suitable eigenvalues for the reduced order models if the eigenvalues of the original plant is widely separated.

3.10 - AGGREGATION METHOD

Aggregation method is also based on the dominant modes of the original system in a similar manner to the previous method. In this method the states of the original plant state vector was divided into parts to bring out the most significant dynamics of the system. This is usually time consuming process and needs a great deal of numerical computation. A simplified form of the method was used in [37] by using an equation which satisfies the optimal aggregation matrix.

Aggregation method applied to a higher order system by using Markov parameters in [38]. Markov parameters were used to form the aggregation matrix to match the time moments of the nominal and reduced order model of the system in order to produce accurate models.

The method have some disadvantages such as, the computation of the aggregation matrix can be complicated and if the chosen eigenvalues are not truly dominant then, the reduced order model may give large steady-state error.

3.11 - BALANCED MODEL REDUCTION METHOD

Balancing model reduction method uses the most controllable and observable part of the nominal plant model to produce reduced order models [39]. The method is based on the balanced state-space representation of the original plant and it is applicable to both continuous and discrete time system. It was shown in [40] there exists co-ordinate systems in which grammians were equal and diagonal. We are given a linear time invariant continuous system in the state-space form

$$\dot{x} = Ax + Bu \qquad (3.42)$$
$$y = Cx$$

where A is nxn, B is nxr and C is mxn. The controllability and observability grammians are

$$W_c = \int_0^{\tau} e^{At} BB^T e^{A^T t} dt \qquad (3.43)$$

$$W_o = \int_0^\tau e^{A^T t} C^T C e^{At} dt \tag{3.44}$$

are both non-singular for any $\tau > 0$. If the system is internally balanced then, (3.43) and (3.44) can be written as follows

$$W_c^2(P) = W_o^2(P) = \Sigma^2 \tag{3.45}$$

where, the matrix P is the similarity transformation and the matrix Σ^2 is diagonal and the diagonal positive elements were called the singular values of the system.

$$\Sigma^2 = diag\left(\sigma_1^2 \quad \sigma_2^2, \quad \cdots \quad ,\sigma_n^2\right) \tag{3.46}$$

The internally balanced system was partitioned as

$$\begin{pmatrix} \dot{x}_1 \\ \dot{x}_2 \end{pmatrix} = \begin{pmatrix} A_{11} & A_{12} \\ A_{21} & A_{22} \end{pmatrix} \begin{pmatrix} x_1 \\ x_2 \end{pmatrix} + \begin{pmatrix} B_1 \\ B_2 \end{pmatrix} u$$
$$y = \begin{pmatrix} C_1 & C_2 \end{pmatrix} \begin{pmatrix} x_1 \\ x_2 \end{pmatrix} \tag{3.47}$$

where A_{11} is kxk and the matrices A_{11} and A_{22} are square It was shown in [39] that

$$\frac{\int_0^\tau \|u_2\|^2 dt}{\int_0^\tau \|u_1\|^2 dt} \geq \frac{\sigma_k}{\sigma_{k+1}} \frac{\|x_2(\tau)\|^2}{\|x_1(\tau)\|^2} \tag{3.48}$$

If $\sigma_k \rangle\rangle \sigma_{k+1}$ then $\|x_2(\tau)\| \langle\langle \|x_1(\tau)\|$, suggesting that the part x_2 is much less affected by the input than the part x_1.

$$\|x_1(0)\| = \|x_2(0)\| \tag{3.49}$$

Equation (3.49) indicated that the x_2 part of the state affects the output much less than the x_1 part. Therefore, the system (A_{11}, B_1, C_1) may be a good reduced order model of the system (3.42). If the system (3.42) is balanced, then every subsystem is asymptotically stable and the diagonal grammian matrix W satisfies the Lyapunov equations

$$\begin{aligned} WA^T + AW &= -BB^T \\ WA + A^T W &= -CC^T \end{aligned} \tag{3.50}$$

The two subsystems (A_{ii}, B_i, C_i) in (3.47) are also balanced and the grammians are given as below

$$\begin{aligned} W_i A_{ii}^T + A_{ii} W_i &= -B_i B_i^T \\ W_i A_{ii} + A_{ii}^T W_i &= -C_i^T C_i \end{aligned} \qquad (i = 1,2) \tag{3.51}$$

where $W = \begin{pmatrix} W_1 & 0 \\ 0 & W_2 \end{pmatrix}$

For the balanced system the cross-grammian matrix, $W_{co}(P)$ is given by

$$W_{co}^2 = W_o^2 W_c^2 \qquad (3.52)$$
$$W_c^2(P) W_o^2 = W_{co}^2(P)$$

The cross-grammian matrix W_{co} contains information about both controllability and observability grammians matrices [41]. Balancing method was used in the case of the LQG (Linear Quadratic Gaussian) design problem in [42]. As it was pointed out in [43] that Moore's truncated balanced realisation is not close to the optimal reduced order model. The balancing method was used to generate reduced order models in the case of a unstable plant in [44]. Balancing method was used together with the singular perturbation model reduction approach in [45] which gave a new unified technique that combined advantages of both methods.

Balancing and aggregation model reduction methods were compared in [46]. It was pointed out that although, in many cases the eigenvalues retained in aggregation method were dominant still there were conditions in which the choice of the retained eigenvalues were not truly dominant therefore, balancing method is more reliable.

A stochastic balancing model reduction method was introduced by Desai in [47]. The method guaranteed the asymptotic stability of the reduced order models. Pernebo and Silverman proposed a new method for stochastic balancing in [48]. Later, this method was used to prove the stochastic reduced order model is stable, dissipative, minimal and positive real in [49].

The standard balancing method is not applicable systems which have natural integrators in their dynamics due to the fact that for such system grammians do not exist. However, if the system is controllable and observable then, antigramnians do exist. The antigrammians of the original system were used for the balancing and model order reduction in [50].

In comparison with balancing method using the reduced order MCS control has many advantages. Firstly, a great deal of numerical computation will be avoided due to the fact that the reduced order MCS control does not need the nominal plant parameters. Secondly, it will guarantee to get the most controllable and observable part as a reduced order model automatically due to the fact that the reduced order MCS control activates the

dominant part of the original plant. The reduced order MCS control can also be used in the case of unstable systems and systems with integrator. Using the reduced order MCS control in the case of systems with integrators has advantages compared with balancing method. The reduced order MCS control does not need to compute the antigammians to find out most controllable and observable part of the plant, therefore it is very straight forward and still it will guarantee the stability of the reduced order model. Additionally, the reduced order MCS will preserve the integrator in the reduced order plant dynamics therefore, it is computationally simple and practical implementation is very easy. The reduced order MCS control can be implemented in such way that it will guarantee the hyperstability of the reduced order models. The reduced order plant parameters will give a solution to Lyapunov equation. The implementation of the control is simple and does not need the reduced order model parameters of the system.

3.11.1 - A Fractional Approach to Model Reduction Method

A fractional model reduction method was used to balance and truncate an unstable system in [51]. The method produced stable reduced order models without dividing the nominal plant model into stable and unstable parts. The reduced order models generated by this method were minimal in terms of controllabilty and observabilty. The method preserved the reduced order models stability and retained the dominant part of the original system.

3.12 - IMPULSE ENERGY APPROXIMATION FOR MODEL REDUCTION

It was suggested that if the impulse response energies of the reduced order models and the original plant are close then, the reduced order model will be a good approximation of the real system [52]. Impulse energy method is based on selection of alpha and beta parameters in a similar manner to Routh method and it satisfies the impulse response energy criterion better than the ordinary Routh method. It was claimed by Lucas that the reduced order model derived by using impulse energy method is better than Routh

method [53], this is not true in general, it was shown that even though the impulse response energy of the reduced order model was very close agreement with the original plant still the lower order model was not good approximation of the full order system in [54]. However, if the reduced order model is a good approximation of the nominal plant model than it will give impulse response which is close to the real system impulse response as a natural consequence.

3.13 - SINGULAR VALUE DECOMPOSITION

A singular value decomposition model reduction method was formed by using a Hankel matrix which was generated from a set of Markov parameters in [55]. The Markov parameter sequence has a property of driving the steady-state error of the reduced order models to zero. The reduced order models produced by this method were stable and internally balanced. However, the method has some disadvantages such as numerical complexity. In comparison with this method the reduced order MCS control has minimum numerical computation and it guarantees the global stability of the reduced order model.

3.14 - OPTIMUM SOLUTION OF MODEL REDUCTION PROBLEM

An optimal model reduction method was used to generate a reduced order model in the case of an unstable plant in [44]. The method retained the unstable part of the plant without any changes therefore, only the stable part of the original plant is reduced. The method used an explicit solution of the Lyapunov in a Newton-Raphson algorithm. Accurate reduced order models were generated due to minimization of the integral-square difference between the impulse responses of the original and reduced order models.

The optimal steady-state reduced order estimator was described by one modified Riccati equation and two modified Lyapunov equations in [56]. The method generated accurate reduced order models. However, there were fixed order dynamic compensation problems which required iterative algorithms.

Although, these methods produced accurate reduced order models, they are analytically complex and numerical computation is time consuming. In comparison with the reduced MCS control algorithm the optimal model reduction methods require very accurate linear model of the original plant. For that reason the parameter uncertainties and nonlinearities in the plant can prevent obtaining accurate reduced order model in the case of the optimal model reduction methods which is obviously not a problem for the reduced order MCS control.

3.15 - FREQUENCY DOMAIN MODEL REDUCTION METHODS

Frequency domain model reduction methods are capable of deriving accurate reduced order models due to the fact that they can retain the dominant mid-frequency dynamics in the reduced order model. For that reason, these methods were used together with other approaches to improve the accuracy of the reduced order models, e.g., in [57], the denominator of the reduced order model was calculated by using the power decomposition method while the numerator was derived from the frequency response matching technique.

3.15.1 - Frequency Fitting (F-F) Pade´ Method

For the sake of generating an accurate reduced order model the high frequency dynamics of the system should retained in the model as well as the low frequency dynamics. Lower order models generated by the standard Pade´ technique gives accurate responses at the low frequency range, but they may get unstable when the plant is working in mid-frequency range. To overcome this problem Pade´ method was used together with the frequency-fitting method which are capable of matching the original plant at dominant mid-frequency range in [58]. The dominant part of the plant dynamics were retained in reduced order model by using the frequency fitting method while the lower frequency characteristic was retained by the Pade´ approximation method. It was suggested that

when the accurate fitting is achieved in the mid-frequency range, the stability problem will be solve as a natural consequence.

Frequency fitting method gives more accurate reduced order model than the classical model reduction methods (Routh method, Pade´ method, Routh-Pade´ method, Routh-Hurwitz and dominant eigenvalues method) due to the fact that it reflects the characteristic of the original system in the dominant-mid frequency range more accurately. For this reason, it guarantees the stability of the reduced order models.

3.16 - APPLICATION OF CONVENTIONAL MODEL REDUCTION METHODS ON THE ELECTROHDRAULIC ACTUATOR PLANT

The nominal transfer function of the electrohydraulic actuator plant was found from system identification tests as follows:

$$G_{p3}(s) = \frac{2830}{s(s+8.8+16j)(s+8.8-16j)} \tag{3.53}$$

The reduced second order models which are found by conventional model reduction methods are given in Table 3.3 and 3.4. The step and impulse responses of the nominal transfer function of the electrohydraulic actuator plant together with its reduced order models are given in Fig. 3.3 and 3.4 respectively.

Electro-hydraulic Actuator Plant	Routh-Hurwitz Method	Routh Stability of Pade´ Method	Impulse Energy Method	Pade´ Methods of Hurwitz Polynomial Method
Second Order Model	$Gp_1(s) = \frac{333.44}{s^2+17.7s+333.4}$	$Gp_2(s) = \frac{118}{s^2+12.3s}$	$Gp_2(s) = \frac{333.44}{s^2+17.6s+333.4}$	$Gp_1(s) = \frac{160.79}{s^2+18.95s}$

Table 3.3: Reduced order models of the electrohydraulic actuator plant

Electro-hydraulic Actuator Plant	Stability Equation Method	Pade´ Method with Dominant Mode Reduction	Balancing Method	Dominant Mode Model Reduction Method	Dominant Eigenvalue and Frequency Matching Method
Second Order Model	$Gp_1(s) = \frac{117.98}{s^2 + 12.3s}$	$Gp_1(s) = \frac{283}{s^2 + 14s}$	$Gp_2(s) = \frac{74.71}{s^2 + 8.8s}$	$Gp_1(s) = \frac{75}{s^2 + 8.8s}$	$Gp_1(s) = \frac{102}{s^2 + 12s}$

Table 3.4: The reduced order models of the electrohydraulic actuator plant

Discussions:

The Routh-Hurwitz and impulse energy methods are produced the same reduced second order model. This is mainly due to a free integrator inside of the plant dynamics which is treated similarly by both methods. As it is mentioned in section 3.6 and section 3.12 although these two methods based on Routh stability arrays they are different than each other. Similarly, the balancing and dominant mode model reduction methods gave the same reduced order model indicating that the selected eigenvalues of the original plant in the case of dominant mode model reduction method are truly dominant due to the fact that the balancing method retains the most controllable and observable part of the original plant in the reduced order model.

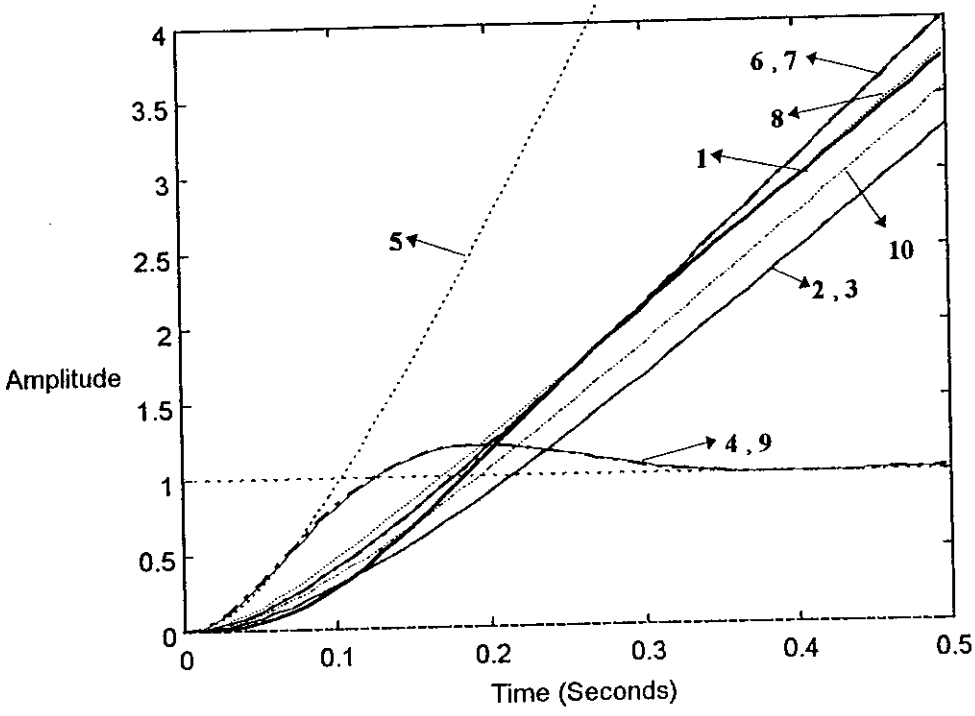

1 ——— Nominal Plant
2 ——— Balancing Method
3 -·-·-·- Dominant Mode Model Reduction Method
4 ——— Impulse Energy Response
5 ····· Pade´ Method with Dominant Mode Reduction
6 —·—·— Routh Stability of Pade´ Method
7 ——— Stability Equation Method
8 ------ Pade Methods of Hurwitz Polynomial Methods
9 —·——·— Routh Method
10 ····· Dominant Eigenvalue and Frequency Fitting Method

Fig. 3.1: Step responses of the electrohydraulic actuator plant and its lower order models

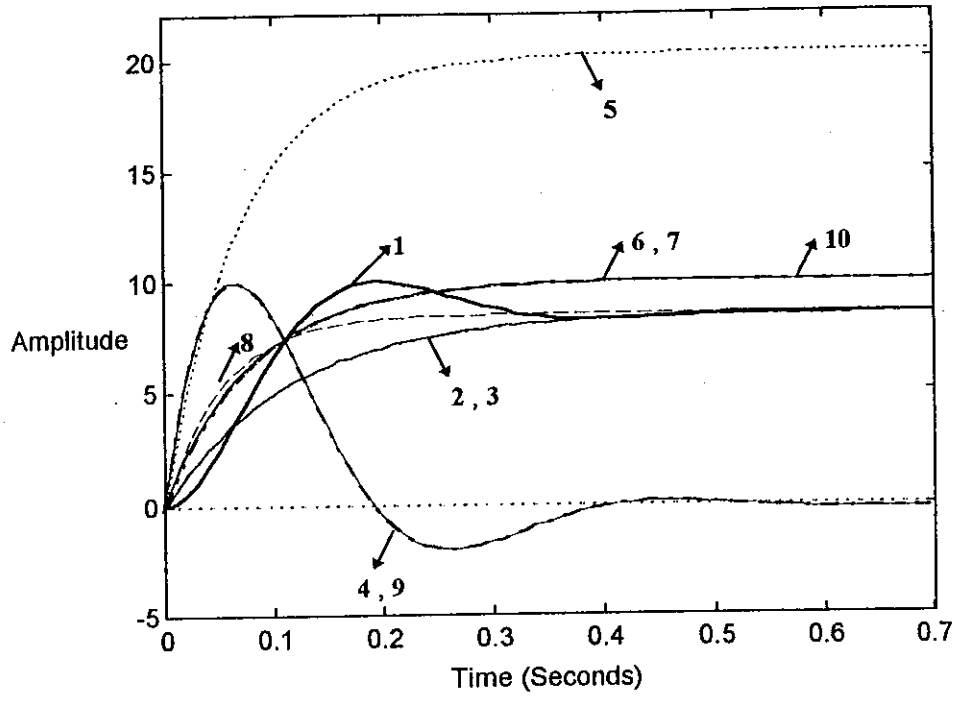

Fig 3.2: Impulse responses of the electrohydraulic actuator plant and its lower order models

In the case of the electrohydraulic actuator plant Routh method did not generate an accurate reduced order model due to a free integrator in the plant dynamics. Hence, the alpha table has a zero in its first column. In normal condition, Routh method can not be applied. In order to overcome this problem, Routh method is used together with Hurwitz criterion to produce an approximation. The zero element of the left column entry is replaced by a small number ε and the Routh table is completed in terms of ε. Another difficulty is encountered that was the numerator of the transfer function a constant. Later, this constant number is treated as the first element of the beta table.

In the case of balancing method, the order of the plant is reduced by using antigrammians of the plant instead of grammians. This is again due to a free integrator in the plant transfer function. As it is mentioned in section 3.10.3, for plants which have free integrators in their dynamics grammians do not exist but antigrammians do.

The first group which includes balancing method, Padé method of Hurwitz polynomial method and dominant mode model reduction method produced second order models with a free integrator in them. The model responses are very close agreement with the original plant output in both step responses and impulse energy responses as it is shown in Fig. 3.1 and 3.2.

Dominant eigenvalue and frequency matching method, Routh stability of Pade´ method and stability equation method produced reasonably accurate reduced order models. Although, the responses are reasonably good still they are not as good as the first group of model reduction methods responses.

The third group, including: impulse energy response method, Routh method and Pade´ method with dominant method did not produced good models. It can be seen in both step responses and impulse responses diagram in Fig. 3.1 and 3.2.

3.17 - REDUCING THE ORDER OF THE ESH PLANT BY CONVENTIONAL MODEL REDUCTION METHODS

The second order transfer function of the ESH materials testing machine is found by a system identification tests under load control, which is given below

$$G_{p2} = \frac{2900}{(s+87.01)(s+22.98)} \tag{3.54}$$

The reduced first order models that are found by conventional model reduction methods are given in Table 3.5 and 3.6. The step and impulse responses of the nominal transfer function of the servohydraulic ESH materials testing machine and its reduced order models are given in Fig. 3.3 and 3.4 respectively.

ESH Materials Testing Machine	Routh Method	Routh Stability of Pade´ Method	Balancing Method	Pade´ Methods of Hurwitz Polynomial Method
First Order Model	$Gp_1(s) = \frac{159.5}{s+110}$	$Gp_1(s) = \frac{26.36}{s+18.18}$	$Gp_1 = \frac{20.35}{s+12.37}$	$Gp_1 = \frac{159.5}{s+110}$

Table 3.5: The lower order models of the ESH materials testing machine

ESH Materials Testing Machine	Stability Equation Method	Pade´ Method with Dominant Mode Reduction	Impulse Energy Method	Dominant Mode Model Reduction Method	Dominant Eigenvalue and Frequency Matching Method
First Order Model	$Gp_1(s) = \frac{26.36}{s+18.18}$	$Gp_1(s) = \frac{32.32}{s+22.98}$	$Gp_1(s) = \frac{110}{s+110}$	$Gp_1(s) = \frac{45.29}{s+22.98}$	$Gp_1(s) = \frac{32.321}{s+22.98}$

Table 3.6: The lower order models of the ESH materials testing machine

Discussions:

Routh stability of Pade´method and stability equation methods are given the same reduced order model. Both methods are based on neglecting roots of the original plant model which have larger magnitudes. Pade´ method with dominant model reduction and dominant eigenvalue and frequency matching method are produced the same reduced first order model. In both method the denominator of the reduced order model is formed by choosing the dominant eigenvalues of the nominal plant model therefore, the denominator is obtained was the same. Subsequently, the denominator polynomials are used to form the numerator dynamics in both cases which lead the same constant number as a numerator. Routh and Pade´ methods of Hurwitz polynomial methods also generated the same reduced order models despite the fact that these two methods are considerable different than each other in terms model reduction procedure.

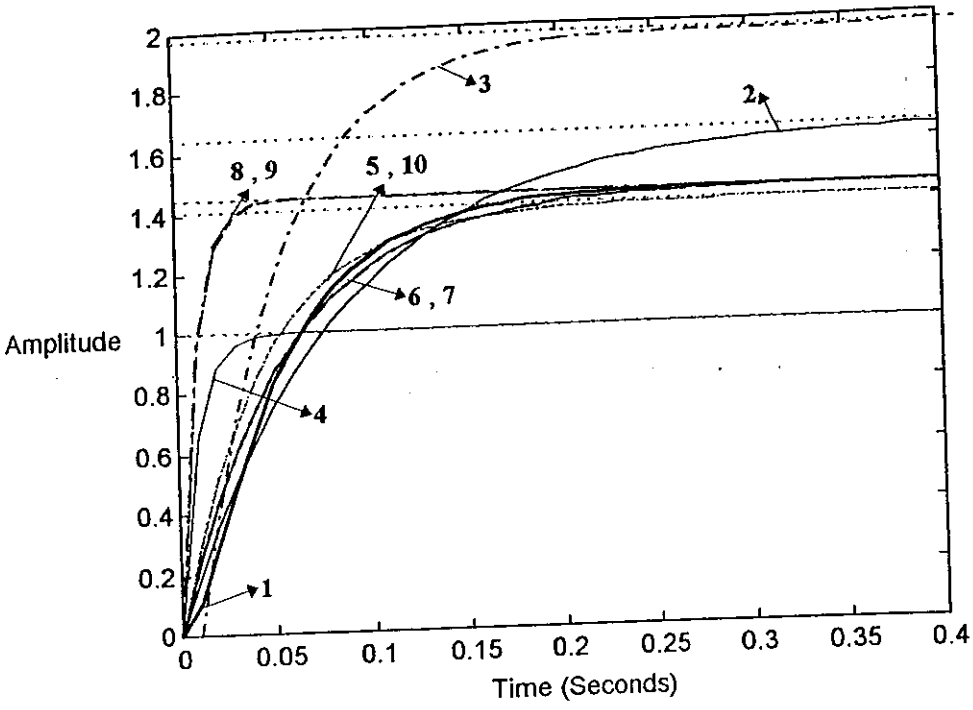

1 ——— Nominal Plant
2 ——— Balancing Method
3 -·-·-·- Dominant Mode Model Reduction Method
4 ——— Impulse Energy Response
5 ..... Pade´ Method with Dominant Mode Reduction
6 — - - — - Routh Stability of Pade´ Method
7 ——— Stability Equation Method
8 ------ Pade´ Methods of Hurwitz Polynomial Methods
9 — - — - - Routh Method
10 ..... Dominant Eigenvalue and Frequency Matching Method

Fig. 3.3: Step responses of the ESH plant and its lower order models

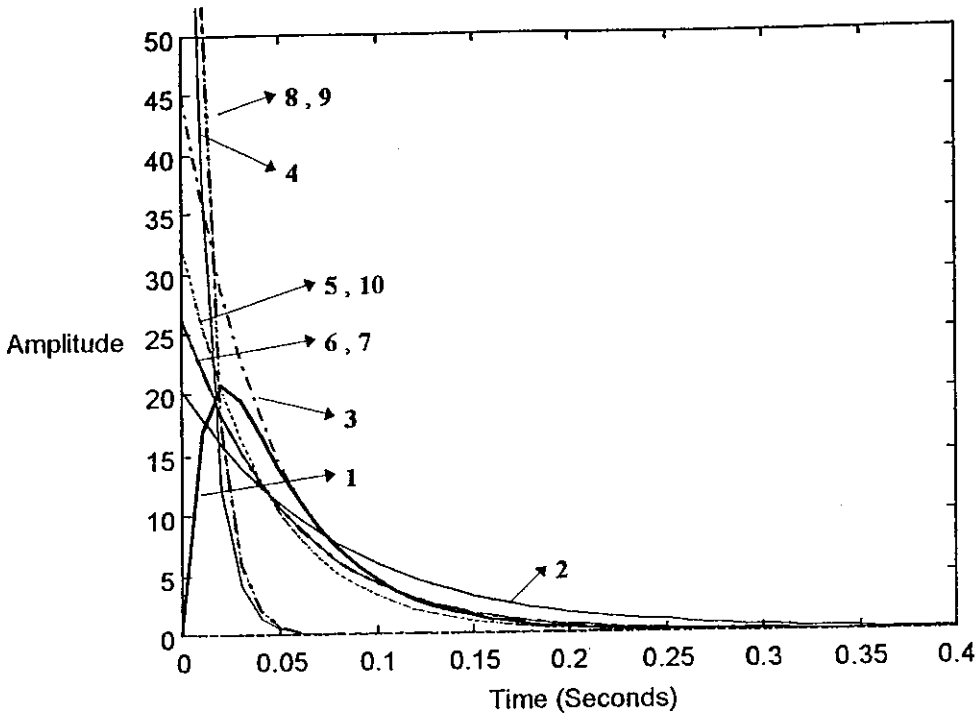

Fig. 3.4: Impulse responses of the ESH machine and its lower order models

In the case of the ESH materials testing machine, Routh stability of Pade´ method, stability equation method, dominant eigenvalue and frequency method and Pade´ method with dominant mode reduction method are produced step and impulse responses which are very closely following the nominal plant transfer function response of the system as shown in Fig 3.3 and 3.4.

Pade´ methods of Hurwitz polynomial method and Routh method produced acceptable responses. Balancing method, dominant mode model reduction method and impulse energy method did not produce very accurate models as shown in Fig 3.3 and 3.4.

3.18 - CONCLUSIONS

In this chapter model reduction methods are introduced in the case of both SISO and MIMO plants. In the first section of the chapter adaptive model reduction methods are presented. The first method was averaging method. Although the method was shown to be effective for model reduction, it is rather difficult to derive the error equation if the relative degree of the plant is higher than one. The second method was EMCS control. This is a

control strategy extension to the standard MCS control and it is a good option in the case of plants which are subjected to rapidly varying disturbances. The reduced order MCS control can be describe as the standard MCS algorithm in which the controlled plant contains high frequency unmodelled dynamics which is treated as the part of the disturbances term acting on the system. It is assumed that these unmodelled dynamics may lead to rapid variations in the disturbances term unless there is some limitations set on the reference model and input signal. Hence, using the reduced order EMCS control in the case can be an another option. The stability of the reduced order MCS control (MCS with unmodelled dynamics) will be investigated in chapter 4.

In the second part of this chapter, fifteen different conventional model reduction methods are presented. Subsequently, some of these model reduction methods are used to reduce the order of both the ESH materials testing machine and electrohydraulic actuator plant. Finally, the performance of conventional model reduction methods were compared with the original plant transfer function using step and impulse response in Figs. 3.1-3.4.

Classical model reduction methods are based on mathematical approximation such as Pade´ approximation, the continued fraction method and the time-moment matching method. Although, these methods are useful in many practical applications they have some disadvantages such as, the reduced order models obtained by those methods may be unstable although the original system is stable and they may not be accurate in the mid and high-frequency range.

Some of the conventional model reduction methods gave very close results to the real plant transfer function of the ESH materials testing machine, e.g., dominant eigenvalue and frequency matching method, balancing method, Routh stability of Pade´ method, stability equation method, Pade´ method with dominant mode reduction, shown in Fig. 3.3 and 3.4.

Routh's method and impulse energy method did not give a good approximation in the case of the electrohydraulic actuator plant, due to the fact that the plant contains a free integrator, therefore it is rather difficult to arrange the alpha as well as beta table. The models produced by dominant mode model reduction method, Pade´ method of Hurwitz polynomial and balancing method produced very accurate second order models with a free integrators inside of them. As it is shown in Fig. 3.1 and 3.2 step and impulse responses those models responses are very close agreement with the nominal plant model response.

It has been observed that the frequency domain model reduction methods and balancing methods produced very accurate reduced order models which are close agreement with the original plant responses. This is due to the fact that these methods are capable of retaining the most dominant part of the original higher order system.

It can be concluded that, conventional model reduction techniques may be used in the case of reduced order MCS control. In this case, it is useful to find the reduced order transfer function of the system to figure out the settling time and sampling interval of the MCS control. In addition, the reduced order plant parameters are required in the case of conventional controller implementation which are in common use in comparative studies.

REFERENCES

[1] - **BOGOLIUBOFF, N. N. & Y. A. MITROPOLSKII**, *Asymptotic Methods in the Theory of Nonlinear Oscillators*, Gordon & Breach, New York, 1961.

[2] - **VOLOSOV, V. M.**, "Averaging in Systems of Ordinary Differential Equations," *Russian Mathematical Surveys*, Vol. 17, No. 6, pp. 1-126, 1962.

[3] - **SETHNA, P. E.**, "Method of Averaging for Systems Bounded for Positive Time," *Journal of Mathematical Analysis and Applications*, Vol. 41, pp. 621-631, 1973.

[4] - **BALACHANDRA, M. & P. R. SETHNA**, "A Generalization of the method of Averaging for systems with two time Scales," *Archive for Rational Mechanics and Analysis*, Vol. 58, pp. 261-283, 1975.

[5] - **HALE, J. K.**, *Ordinary Differential Equations*, Krieger, Huntington, New York, 1980.

[6] - **ASTROM, K. J.**, "Analysis of Rohrs Counter Examples to Adaptive Control", *Proc. of the 22nd IEEE Conf. on Decision and Control*, pp. 982-987, San Antonio, Texas, 1983.

[7] - **ASTROM, K. J.**, "Interactions Between Excitation and Unmodelled Dynamics in Adaptive Control," *Proc. of the 23rd IEEE Conf. on Decision and Control*, pp. 1276-1281, Las Vegas, 1984.

[8] - **RIEDLE, B. D., P. V. KOKOTOVIC**, " A Stability-Instability Boundary for Disturbance-Free Slow Adaptation with Unmodelled Dynamics," *IEEE Trans. on Automatic Control*, Vol. AC-30, No. 10, pp. 1027-1030, 1985.

[9] - **MAREELS, I. M. Y., B. D. O. ANDERSON, R. R. BITMEAD, M. BODSON, & S. S. SASTRY**, "Revisiting the MIT Rule for Adaptive Control", *Proc. of the 22nd IFAC Workshop on Adaptive Systems in Control and Signal Processing*, Lund, Sweden, 1986.

[10]- **SASTRY, S. & M. BODSON**, *Adaptive Control Stability, Convergence, and Robustness*, Prentice-Hall International, Inc., 1989.

[11] - **STOTEN D. P. & H. BENCHOUBANE**, "The Extended Minimal Controller Synthesis Algorithm", *International Journal of Control*, 1992.

[12] - **DI BERNARDO, M. & D. P. STOTEN**, "A New Extended Minimal Control Synthesis Algorithm with an Application to the Control of Chaotic Systems" University of Bristol.

[13] - **OLIVIER, P. D.**, "On the Relationship Between the Model Order Reduction Problem and the Simultaneous Stabilisation Problem", *IEEE Transactions on Automatic Control*, Vol. AC-32, No. 1 January 1987.

[14] - **GUTMAN, P.-O., C. F. MANNERFELT & P. MOLANDER**, "Contributions to the Model Reduction Problem", *IEEE Transactions on Automatic Control*, Vol. AC-27, No. 2, pp. 454-455, April 1982.

[15] - **LIAW, C. M.**, "Mixed Method of Model Reduction for Linear Multivariable Systems", *International Journal of System Science*, Vol. 20, No. 11, pp. 2029-2041, 1989.

[16] - **LIAW, C. M.**, "Design of a Reduced Order Adaptive Load Frequency Controller for an Interconnected Hydrothermal Power System", *International Journal of Control*, Vol. 60, No. 6, pp. 1051-1063, 1994.

[17] - **HUTTON, M. F. & B. FRIEDLAND**, "Routh Approximations for Reducing Order of Linear, Time Invariant Systems", *IEEE Transactions on Automatic Control*, Vol. AC-20, No. 3, pp. 329-337, June 1975.

[18] - **KRISHNAMURTHY, V. & V. SESHADRI**, " Model Reduction Using the Routh Stability Criterion", *IEEE Transactions on Automatic Control*, Vol. AC-23, No. 4, pp. 729-731, August 1978.

[19] - **KRISHNAMURTHI, V. & V. SESHADRI**, "A Simple and Direct Method of Reducing Order of Linear Systems Using Routh Approximations in the Frequency Domain", *IEEE Transactions on Automatic Control, Technical Notes and Correspondence*, pp. 797-799, October 1976,

[20] - **SHAMASH, Y.**, "Comments on the Routh-Hurwitz Criterion", *IEEE Transactions on Automatic Control*, Vol. AC-25, No. 1, pp. 132-133, February 1980.

[21] - **HWANG, C., G. TONG-YI & L. S. SHEIH**, "Model Reduction using New Optimal Routh Approximant Technique", *International Journal of Control*, Vol. 55, No. 4, pp. 989-1007, 1992.

[22] - **RAO, A. S., S. S. LAMBA, S. V. RAO**, "Routh-Approximant Time Domain Reduced-Order Models for Single-Input Single-Output Systems", *Proc. IEE*, Vol. 125, No. 9, October 1978.

[23] - **APPIAH, R. K.**, 'Pade´ Methods of Hurwitz Polynomial Approximation with Application to Linear System Reduction', *International Journal of Control*, Vol. 29, No. 1, pp. 39-48, 1979.

[24] - **SHAMASH, Y.**, "Stable Reduced-Order Models Using Pade´-Type Approximations", *IEEE, Transactions on Automatic Control*, pp. 615-616, October 1974.

[25] - **SHAMASH, Y.**, "Linear System Reduction using Pade´ Approximation to Allow Retention of Dominant Modes", *International Journal of Control*, Vol. 27, No. 2, pp. 257-272, 1975.

[26] - **SHAMASH, Y.,** " Model Reduction Using the Routh Stability Criterion and the Pade´ Approximation Technique", *International Journal of Control*, Vol. 21, No. 3, pp. 475-484, 1975.

[27] - **ALEXANDRO, F. J.** "Stable Partial Pade´ Approximations for Reduced-Order Transfer Functions", *IEEE Transactions on Automatic Control*, Vol. AC-29, No. 2, pp. 159-162, February 1984.

[28] - **LUCAS, T. N.,** "Suboptimal Model Reduction by Multipoint Pade´ Approximation", *Proceedings of the Institution of Mechanical Engineers*, Part I, Vol. 204, No. 12, pp. 131-134, 1994.

[29] - **LUCAS, T. N.,** " Constrained Suboptimal Pade´ Model Reduction", *Proceedings of the Institution of Mechanical Engineers*, Part I, Vol. 209, pp. 35-39, 1995.

[30] - **HICKIN, J. & N. K. SINHA,** "New Method of Obtaining Reduced Order Models for Multivariable Systems", *Electronics Letters*, Vol. 12, No. 4, February 1976.

[31] - **CHEN, T. C. & C. Y. CHANG,** " Reduction of Transfer Functions by the Stability-Equation Method", *Journal of the Franklin Institute*, Vol. 308, pp. 389-404, 1979.

[32] - **DAVISON, E. J.,** "A Method for Simplifying Linear Dynamic Systems", *IEEE Transactions on Automatic Control*, Vol. AC. 11, No. 1, pp. 93-101, 1966.

[33] - **MARSHALL, S. A.,** "An Approximate Method for Reducing the Order of a Linear System", *Control*, Vol. 10, pp. 642-643, 1966.

[34] - **SHAMASH, Y.,** "Linear System Reduction Using Pade´ Approximation to Allow Retention of Dominant Modes", *International Journal of Control*, Vol. 21, N0. 2, pp. 257-272, 1975.

[35]- **VAZ, A. F. & E. J. DAVISON,** "Modular Model Reduction for Interconnected Systems", *Automatica*, Vol. 26, No. 2, pp. 251-261, 1990.

[36] - **IWAI, Z. &Y. KUBO,** "Determination of Eigenvalues in Marshall's Model Reduction", *International Journal of Control*, Vol. 30, No. 5, pp. 823-836, 1979.

[37] - **MASANAO, A.** "Control of Large-Scale Dynamic Systems by Aggregation", *IEEE Transactions on Automatic Control*, Vol. AC-13, No. 3, June 1968.

[38] - **HICKIN, J. & N. K. SINHA,** "Canonical forms for Aggregated Models", *International Journal of Control*, Vol. 27, No. 3, pp. 473-485, 1978.

[39] - **MOORE, B. C.,** "Principal Component Analysis in Linear Systems: Controllability, Observability and Model Reduction", *IEEE Transactions on Automatic Control*, Vol. AC-26, pp. 17-32, Feb., 1981.

[40] - **PERNEBO, L. & L. M. SILVERMAN**, "Model Reduction via Balanced State Space Representations", *IEEE Transactions on Automatic Control*, Vol. AC-27, No. 2, pp. 382-387, April 1982.

[41] - **FERNANDO, K. V. & H. NICHOLSON**, "On the Structure of Balanced and Other Principal Representations of SISO Systems", *IEEE Transactions on Automatic Control*, Vol. AC-28, No. 2, pp. 228-231, February 1983.

[42] - **VERRIEST, I. E.**, "Low sensitivity design and Optimal order Reduction for the LQG Problem", *Proc. 24th Midwest Symp. Circuits Syst.*, pp. 365-369, Albuquerque, N M, June 1981.

[43] - **BRYSON, A. E. & A. CARRIER**, "Second-Order Algorithm for Optimal Model Order Reduction", *Journal of Guidance*, Vol. 13, No. 5, pp. 887-892, September October 1990.

[44] - **KENNEY, C. & G. HEWER**, "Necessary and Sufficient Conditions for Balancing Unstable Systems", *IEEE Transactions on Automatic Control*, Vol. AC-32, No. 2, pp. 157-160, February 1987.

[45] - **FERNANDO, K. V., & H. NICHOLSON**, "Singular Perturbational Model Reduction of Balanced Systems", *IEEE Transactions on Automatic Control*, Vol. AC-27, No. 2, pp. 466-468, 1982.

[46] - **LASTMAN, G. J. & N. K. SINHA**, "A comparison of the Balanced Matrix Method and the Aggregation Method of Model Reduction", *IEEE Transactions on Automatic Control*, Vol. AC-30, No. 3, pp. 301-304, March 1985.

[47] - **DESAI, U. B. & D. PAL** ,"A Realisation Approach to Stochastic Model Reduction and Balanced Stochastic Realisations", *Proc. 16th Annual Conference on Inform. Syst.*, Princeton, Univ. of Princeton, N J, 1982.

[48] - **PERNEBO, L. & L. M. SILVERMAN**, "Model Reduction via Balanced State Space Representation", *IEEE Transactions on Automatic Control*, Vol. AC-27, pp. 382-387, 1982.

[49] - **HARSHAVARDHANE, P., E. A. JONCKHEERE & L. M. SILVERMAN**, "Stochastic Balancing and Approximation Stability and Minimality", *IEEE Transactions on Automatic Control*, Vol. AC-29, No. 8, pp. 744-746, 1984.

[50] - **GAWRONSKI, W. & J. A. MELLESTROM**, "Model Reductions for Systems with Integrators", *Journal of Guidance, Engineering Notes*, Vol. 15, No. 5, pp. 1304-1306, 1991.

[51] - **MEYER, D. G.**, "Fractional Approach to Model Reduction", *Proceedings American Control Conference*, pp. 1041-1047, 1988, Atlanta.

[52] - **LUCAS, T. N.**, "Linear System Reduction by Impulse Energy Approximation", *IEEE Transactions on Automatic Control*, Vol. AC-30, No. 8, pp. 784-786, August 1985.

[53] - **LUCAS, T. N.**, "Further Discussion on Impulse Energy Approximation", *IEEE Transactions on Automatic Control*, Vol. AC-32, No. 2, February 1987.

[54] - **RAO, A. S.**, "On Linear System Reduction by Impulse Energy Approximation", *IEEE Transactions on Automatic Control*, AC-31, No. 6, pp. 551-552, June 1986.

[55] - **KUNG, S.**, "A New Identification and Model Reduction Algorithm via Singular Value Decompositions", *Proceedings 12th Annual Asilomar Conference, Circuits, Systems Computer*, pp. 705-714, 1979.

[56] - **BERNSTEIN, D. S. & D. C. HYLAND**, "The Optimal Projection Equations for Reduced Order State Estimation", *IEEE Transactions on Automatic Control*, Vol. AC-30, No. 6, pp. 583-585, June 1985.

[57]- **OUYANG, M., C. M. LIAW & T. PAN**, "Model Reduction by Power Decomposition and Frequency Response Matching", *IEEE Transactions on Automatic Control*, AC-32, No. 1, pp. 59-62, January 1987.

[58] - **XIHENG, H.** "FF-Pade´ Method of Model Reduction in Frequency Domain", *IEEE Transactions on Automatic Control*, Vol. AC-32, No. 3, pp. 243-246, March 1987.

CHAPTER 4

THE STABILITY ANALYSIS OF THE REDUCED ORDER MCS CONTROL

4.1 - INTRODUCTION

In this chapter the stability of the reduced order SISO and MIMO MCS control system will be proven by using Popov's and the Lyapunov equation method. Normally, the dominant frequencies are in the range of the slow part of the plant which can be matched by the reduced order model. In the case of the reduced order MCS control, the reference model which has lower order than the nominal plant model has been used and the modelled part of the plant matched the reference model in order to represent the slow dynamics of the plant. Hence, the fast dynamics of the plant are unmodelled, and included into the disturbance term in the state-space representation of the plant.

The stability of the reduced order MCS to unmodelled plant dynamics is proven by both the Popov's hyperstability theory or the Lyapunov function depending on the nature of the disturbances. If the disturbances and the plant parameters are slowly varying, then Popov's hyperstability theory is used to prove the stability of the system. If the disturbances are rapidly varying then the Lyapunov function is needed to prove the stability of the system.

The stability analysis of the reduced second order electrohydraulic actuator plant is proven by the Popov's hyperstability theory and the Lyapunov function. In the normal operation case, the nominal plant transfer function is of third order, including a free

integrator. In the case of MCS, the plant is represented by a second order transfer function (including a free integrator) together with a disturbance term, in a state-space form.

In a similar manner, the stability of the ESH servohydraulic material testing machine is analysed by both methods. Under the MCS control the plant is described by a first order transfer function together with a disturbance term in state-space form. It is shown that MCS guarantees stability of systems with unmodelled dynamics. Reduced order MCS controllers is used very effectively in the case of the higher order plants due to simplified dynamics of them. The stability of the reduced order MCS control will be proven in the case of both SISO and MIMO systems in this chapter.

4.2 - THE REDUCED ORDER ADAPTIVE CONTROL

Adaptive control has been researched for a number of decades. In recent years, the algorithm has been applied to variety of systems. The frequency content and magnitude of the reference input signal, adaptive gains and initial conditions have crucial effects on the stability of the adaptive controls.

Reduced order adaptive control is described as an standard adaptive control together with unmodelled dynamics. Many efforts have been made to formulate and analyse reduced order adaptive control schemes. In [1] the stability was proven for a reduced order indirect adaptive regulator. The efforts of reduced order direct adaptive control were studied in [2], [3] and [4].

In order to prove the stability of adaptive control it is convenient to assume that the controlled plant is lower order. The dominant frequencies are slow and are in the mid frequency range of the plant which can be matched by the reduced order model. The unmodelled dynamics effect the closed loop system dynamics different in adaptive control than the conventional controller due to the fact that the plant input which is generated by adaptive feedback incorporates the unknown plant with the unmodelled fast dynamics.

If the input signal has more action in the high frequency range the adaptive control may become unstable due to excitement in the unmodelled part of the system. This simple but fundamental observation has led us to the restriction of the inputs to the class of persistently exciting inputs which has more action in the mid frequency range. High

frequencies in the input signal can excite high order unmodelled parts of the system and hence can lead to instability.

In the case of MIMO systems each local controller faces the uncertainty of unmodelled interactions with other subsystems as well as the unmodelled dynamics in its own subsystems. When high order unmodelled dynamics are present, all signals converge to a stability set that size depends on controller parameters, the magnitude of disturbances, and the reference input signal.

4.3 - PERSISTENTLY EXCITING INPUTS

The adaptive control is considered to be stable provided that the input signal is persistently exciting, which means it has more action in the mid frequency range but does not contain high frequencies in the unmodelled part of the plant.

The requirement for asymptotic stability is that the input signal $u(t)$ be sufficient enough to persistently excite all the modes of the plant, as shown in [5], [6] and [7]. The main aim is to consider only the dominant and to neglect the higher order dynamics of the system. Hence, input signal will only activate the dominant part of the system. An example of a persistently exciting input signal is

$$u(t) = \sum_{i=1}^{k} a_i \sin \omega_i t \tag{4.1}$$

where ω_i are all distinct and positive and $a_i \neq 0$. High frequencies can be avoided since they excite the unmodelled higher order dynamics. It was illustrated in [6] that in the presence of high order unmodelled dynamics, high input frequencies may destroy the persistently excitation of the input signal.

4.4 - THE REDUCED ORDER MCS CONTROL

It is usually an advantage to obtain a reduced order controller by neglecting the high order dynamics of the plant. Using lower order model may produce more accurate

results due to the fact that in many cases the generated model of the higher order plant may be over parameterised.

The reduced order MCS control is standard MCS control in which the reference model is lower order than the controlled plant therefore the controller contains high order unmodelled dynamics which are included into the disturbance terms. The stability of the reduced order MCS control will be proven in this section, first by Popov's hyperstability theory in the case of small variations, then by Lyapunov function in the case of rapid variation in plant parameters and disturbance terms. If the plant is subjected to rapidly varying external disturbances and plant parameters, then the boundedness of different signals of the plant-reference model is guaranteed.

4.5 - STABILITY ANALYSES OF THE REDUCED ORDER MCS CONTROL BY POPOV'S HYPERSTABILITY THEORY

4.5.1 - The Reduced Order SISO MCS Algorithm

The reduced order SISO MCS algorithm is an standard SISO MCS control in which the controlled plant contains some high frequency unmodelled dynamics and these unmodelled dynamics are included into the disturbance term. Consider a linear, nominal plant model described by the following state-space equation

$$\dot{x} = Ax(t) + Bu(t) \tag{4.2}$$

where $A(t) \in \mathbf{R}^{nxn}$ and $B(t) \in \mathbf{R}^{nxl}$ and $x = [x_1 \ , \ x_2 \ , \ \ldots \ , \ x_n]^T \ x \in \mathbf{R}^{nxl}$. The variables $x(t)$ and $u(t)$ denote the plant state vector and the control input respectively, where

$$A(t) = \begin{bmatrix} 0 & 1 & 0 & 0 & \ldots & 0 \\ 0 & 0 & 1 & 0 & \ldots & 0 \\ \cdot & \cdot & \cdot & \cdot & \cdot & \cdot \\ 0 & 0 & 0 & 0 & \ldots & 1 \\ -a_1 & -a_2 & -a_3 & -a_4 & \ldots & -a_n \end{bmatrix}, \quad B(t) = \begin{bmatrix} 0 \\ 0 \\ \cdot \\ \cdot \\ b_1 \end{bmatrix} = \begin{bmatrix} 0 \\ 0 \\ \cdot \\ \cdot \\ 1 \end{bmatrix} \tag{4.3}$$

The reduced order plant model together with unmodelled dynamics may be written as

$$\dot{x}_r = A_r x_r(t) + B_r u(t) + d(x_r, t) \tag{4.4}$$

where

$$A_r(t) = \begin{bmatrix} 0 & 1 & 0 & 0 & \dots & 0 \\ 0 & 0 & 1 & 0 & \dots & 0 \\ & & \cdot & & & \\ \cdot & \cdot & \cdot & \cdot & \cdot & \cdot \\ & & \cdot & & & \\ 0 & 0 & 0 & 0 & \dots & 1 \\ -a_1 & -a_2 & -a_3 & -a_4 & \dots & -a_h \end{bmatrix}, \quad B_r(t) = \begin{bmatrix} 0 \\ 0 \\ \cdot \\ \cdot \\ \cdot \\ b_1 \end{bmatrix} = \begin{bmatrix} 0 \\ 0 \\ \cdot \\ \cdot \\ \cdot \\ 1 \end{bmatrix} \tag{4.5}$$

and

$$d(x_r, t) = \begin{bmatrix} 0 \\ 0 \\ \vdots \\ d_1 \end{bmatrix} \tag{4.6}$$

The unmodelled dynamics are included into the disturbances term $d(x_r,t)$. The reduced order model has a transfer function of h'th order. Hence, the order of the reduced order plant model is n-h degrees lower than the original plant model. It has been observed that the plant states are available and the order of the plant is known. Moreover, the coefficients a_i (i=1,2,...,h), d_1 are unknown and assumed to be bounded and time varying. The reference model is defined by the following state-space equation.

$$\dot{x}_m(t) = A_m x_m(t) + B_m r(t) \tag{4.7}$$

where $A_m \in \mathbb{R}^{h\times h}$ and $B_m \in \mathbb{R}^{h\times 1}$. The matrix A_m and the vector B_m are given by

$$A_m = \begin{bmatrix} 0 & 1 & 0 & 0 & \dots & 0 \\ 0 & 0 & 1 & 0 & \dots & 0 \\ & & \cdot & & & \\ \cdot & \cdot & \cdot & \cdot & \cdot & \cdot \\ & & \cdot & & & \\ 0 & 0 & 0 & 0 & \dots & 1 \\ -a_{m1} & -a_{m2} & -a_{m3} & -a_{m4} & \dots & -a_{mh} \end{bmatrix}, \quad B_m = \begin{bmatrix} 0 \\ 0 \\ \cdot \\ \cdot \\ \cdot \\ b_m \end{bmatrix} \tag{4.8}$$

The error dynamics of the closed-loop system given by Equations (4.4) to (4.7) are

$$\dot{x}_e(t) = A_m x_e(t) - (A_r - A_m)x_r(t) - B_r u(t) + B_m r(t) - d(x_r, t) \tag{4.9}$$

where

$$x_e(t) = x_m(t) - x_r(t) \tag{4.10}$$

According to Stoten and Benchoubane [8], the disturbance term, $d(x_r,t)$ due to unmodelled dynamics is bounded and it can be written as below.

$$d(x_r,t) = \delta A_r(t) r \tag{4.11}$$

where $\delta A_r(t) = \begin{bmatrix} 0 \\ \vdots \\ 0 \\ \delta a_r(t) \end{bmatrix}$ and $\delta A_r(t) \in \mathbb{R}^{hx1}$ and r is the reference input $r(t) \neq 0$, for all t.

Normally, the reference signal is a slowly varying therefore, the nature of the disturbance $d(x_r,t)$ is depend on the variations of $\delta a_r(t)$. By partitioning the matrices A_r, A_m and the vectors B_r, B_m and $d(x_r,t)$ into

$$A_r = \begin{bmatrix} 0_{h-1,1} & I_{h-1} \\ A_{r1} & \end{bmatrix}, \quad A_m = \begin{bmatrix} 0_{h-1,1} & I_{h-1} \\ A_{m1} & \end{bmatrix},$$

$$B_r = \begin{bmatrix} 0_{h-1,1} \\ b_1 \end{bmatrix}, \quad B_m = \begin{bmatrix} 0_{h-1,1} \\ b_m \end{bmatrix} \text{ and } d(x_r,t) = \begin{bmatrix} 0_{h-1,1} \\ d_1 \end{bmatrix} \tag{4.12}$$

and

A_{r1}. = (1x h) vector, $A_{r1} = \begin{bmatrix} -a_1 & -a_2 & \ldots, & -a_h \end{bmatrix}$

A_{m1} = (1x h) vector, $A_{m1} = \begin{bmatrix} -a_{m1} & -a_{m2} & \ldots, & -a_{mh} \end{bmatrix}$

where $\delta A_1(t)$ term is the unknown variation and unmodelled dynamics in the A_r matrix in (4.11). Then, (4.4) can be rewritten as:

$$\dot{x}_r(t) = \left(A_r + \delta A_1(t)\right)x_r(t) + B_r u(t) \tag{4.13}$$

The changes in A_r, and B_r due to the parameter variations and unmodelled dynamics are denoted by $\delta A_2(t)$ and $\delta B_r(t)$ respectively, then (4.13) becomes:

$$\dot{x}_r(t) = \left(A_r + \delta A_r(t)\right)x_r(t) + \left(B_r + \delta B_r(t)\right)u(t) \tag{4.14}$$

where $\delta A_r(t) = \delta A_1(t) + \delta A_2(t)$.

The control signal in the case of MRAC is given as

$$u(t) = \left(-K + \delta K(t)\right)x_r(t) + \left(K_R + \delta K_R\right)r(t) \tag{4.15}$$

In the case of MCS (4.15) is determined by using $K = 0_{n,m}$ and $K_R = 0_{n,m}$

$$u(t) = \delta K(t) x_r(t) + \delta K_R(t) r(t) \tag{4.16}$$

where K and K_R the linear model reference controller gains. Then, the closed-loop plant dynamics can be written from (4.14) and (4.15)

$$\dot{x}_r(t) = \left(A_r + \delta A_r(t)\right)x_r(t) + \left(B_r + \delta B_r(t)\right)\left(\delta K(t) x_r(t) + \delta K_R(t) r(t)\right) \tag{4.17}$$

which becomes

$$\dot{x}_r(t) = \left(A_r^*(t) + B_r^*(t)\delta K(t)\right)x_r(t) + B_r^*(t)\delta K_R(t)r(t) \tag{4.18}$$

where, $A_r^*(t) = A_r + \delta A_r(t)$ and $B_r^*(t) = B_r + \delta B_r(t)$.

The error dynamics of the closed-loop system is derived from (4.7) and (4.18) as follows

$$\begin{aligned}\dot{x}_e(t) = A_m x_e(t) &+ \left(A_{r0}(t) - B_r^*(t)\delta K(t)\right)x_r(t) \\ &+ \left(B_{r0}(t) - B_r^*(t)\delta K_R(t)\right)r(t)\end{aligned} \tag{4.19}$$

where

$$x_e(t) = x_m(t) - x_r(t)$$

$$A_{r0}(t) = A_m(t) - A_r^*(t)$$

$$B_{r0}(t) = B_m(t)$$

Equation (4.19) can be rewritten as

$$\dot{x}_e(t) = A_m x_e(t) + I_h W(t) \tag{4.20}$$

where

$$W(t) = \left(A_{r0}(t) - B_r^*(t)\delta K(t)\right)x_r(t) + \left(B_m(t) - B_r^*(t)\delta K_R(t)\right)r(t) \tag{4.21}$$

The feedback system (4.20) was represented by the standard form of two blocks for the stability analyses see [9] and Appendix 1: A linear time invariant feedforward block, and nonlinear time varying feedback block as shown in Fig. 4.1.

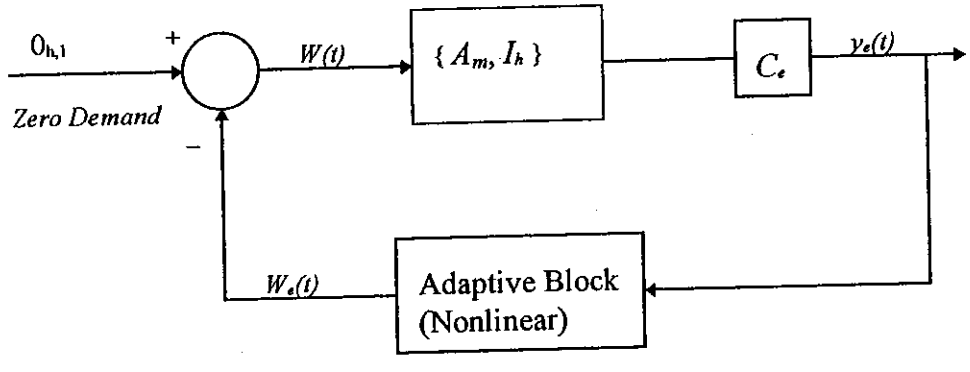

Fig. 4.1: Error dynamics presented as a nonlinear feedback system

In Fig. 4.1 $W(t) = -W_e(t)$, and the system is hyperstable if:

1 - The feedforward transfer function matrix $C_e[sI - A_m]^{-1} I_h$ is strictly positive real (SPR), (4.22)

2 - The nonlinear feedback path satisfies Popov's criterion, which is given below:

$$\int_{t_0}^{t_1} y_e(t)W_e(t)dt \geq -c^2 \ , \ \text{for all } t_1 \geq t_0 \tag{4.23}$$

where c is a constant independent of t_1. Thus, by using the Kalman-Yacubovitch lemma which is given in Appendix 2, we obtain

$$y_e = B_e^T P x_e = C_e x_e \tag{4.24}$$

where C_e is the output error matrix, which is determined from the positive definite solution of the Lyapunov equation

$$PA_m + A_m^T P = -Q \ , \qquad Q > 0 \tag{4.25}$$

as

$$C_e = B_e^T P \ , \qquad B_e^T = [0, \ \ldots \ ,0 \quad 1] \tag{4.26}$$

Substituting (4.21) into (4.23), we get

$$\int_{t_0}^{t_1} y_e^T(t)\left(B_r^*(t)\delta K(t) - A_{r0}(t)\right)x_r(t)dt \geq -c_1^2 \tag{4.27a}$$

$$\int_{t_0}^{t_1} y_e^T(t)\left(B_r^*(t)\delta K_R(t) - B_m(t)\right)r(t)dt \geq -c_2^2 \tag{4.27b}$$

where

$$c_1^2 + c_2^2 = c^2$$

From (4.15) and (4.16), the adaptive gains are [10];

$$\delta K(t) = \int_0^t \phi_1(\tau)d\tau + \phi_2(t)$$
$$\delta K_R(t) = \int_0^t \psi_1(\tau)d\tau + \psi_2(t) \tag{4.28}$$

where,

$$\phi_1(\tau) = \alpha y_e(\tau)x_r^T(\tau) \ ; \ \phi_2(t) = \beta y_e(t)x_r^T(t)$$
$$\psi_1(\tau) = \alpha y_e(\tau)r(\tau) \ ; \ \psi_2(t) = \beta y_e(t)r(t) \tag{4.28a}$$

and

$$\alpha = [\alpha_1 \quad \alpha_2 \quad \ldots \quad \alpha_h] \ ; \quad \beta = [\beta_1 \quad \beta_2 \quad \ldots \quad \beta_h]$$
$$y_e^T = [y_{e1} \quad y_{e2} \quad \ldots \quad y_{eh}] ; \quad x_r^T = [x_1 \quad x_2 \quad \ldots \quad x_h] \tag{4.28b}$$

Equations (4.27a)-(4.27b) are satisfied by the following choices of α and β

$$\left.\begin{aligned}\alpha &= [0 \quad \ldots \quad 0 \quad \alpha_h] \\ \beta &= [0 \quad \ldots \quad 0 \quad \beta_h]\end{aligned}\right\} \tag{4.29}$$

where α_h and β_h are both of the same sign as b_{r1}^*. Hence the Popov criterion (4.27a) expands to

$$\int_{t_0}^{t_1} b_{r1}^* \alpha_h \sum_{i=1}^{h} y_{eh} x_i \left[\int_0^t y_{eh} x_i d\tau - a_{r0i} / \left(b_{r1}^* \alpha_h \right) \right] dt \geq -c_{11}^2 \tag{4.30a}$$

together with

$$\int_{t_0}^{t_1} b_{r1}^* \beta_h y_{eh}^2 \sum_{i=1}^{h} x_i^2 dt \geq -c_{12}^2 \tag{4.30b}$$

where b_{r1}^* is the last and the only non-zero entry of $B_r^*(t)$ and a_{r0i} is the last row elements of $A_{r0}(t)$ and

$$c_{11}^2 + c_{12}^2 = c_1^2$$

Following the same pattern (4.27b) is written as below

$$\int_{t_0}^{t_1} b_{r1}^* \alpha_h y_{eh} r \left[\int_0^t y_{eh} r d\tau - b_m / \left(b_{r1}^* \alpha_h \right) \right] dt \geq -c_{21}^2 \tag{4.31a}$$

$$\int_{t_0}^{t_1} b_{r1}^* \beta_h y_{eh}^2 r^2 dt \geq -c_{22}^2 \tag{4.31b}$$

where b_m is the last and the only non-zero entry of $B_m(t)$, indicating that inequalities (4.30b) and (4.31b) are satisfied. In order to satisfy (4.30a) and (4.31a) the following integral property is used

$$\int_{t_0}^{t_1} k \dot{f} f dt \geq -k f^2(t_0)/2 \tag{4.32}$$

where k is a constant. Comparison with equation (4.30a) gives

$$f_i = \int_0^t y_{eh} x_{ri} d\tau - a_{r0i} / \left(b_{r1}^* \alpha_h \right) \text{ and } k = b_{r1}^* \alpha_h \tag{4.33}$$

If the variations in a_{r0i} and b_{r1}^* are not significant then differentiating (4.33) with respect to time gives

$$\dot{f}_i \cong y_{eh} x_{ri} \tag{4.34}$$

then (4.30a) becomes

$$\int_{t_0}^{t_1} k\sum_{i=1}^{h} \dot{f}_i f_i dt \geq -k\sum_{i=1}^{h} f_i^2(t_0)/2 \tag{4.35}$$

Similarly, comparison with (4.31a) gives

$$f_{i1} = \int_0^t y_{eh} r d\tau - b_m / \left(b_{r1}^* \alpha_h\right) \tag{4.36}$$

Again if b_{r1}^* vary less rapidly than the adaptive process, then

$$\dot{f}_{i1} \cong y_{eh} r \tag{4.37}$$

Equation (4.31a) can written as

$$\int_{t_0}^{t_1} k\dot{f}_{i1} f_{i1} \geq -kf_{i1}^2(t_0)/2 \tag{4.38}$$

The system will remain stable provided that plant parameter variations slower than the adaptive process. The inequalities (4.34) and (4.37) can be made arbitrarily close to an equality. Therefore, inequalities (4.27a) and (4.27b) are satisfied, since each term in the summations satisfies an inequality of the type given in (4.32). Bringing together (4.30a)-(4.31b) the Popov criterion (4.23) is satisfied, indicating that the reduced order MCS control guaranteed asymptotic hyperstability of the SISO system. The SISO plant parameter matrices $A(t)$, $B(t)$ and the plant state matrix x are represented in the reduced order plant model as $A_r(t)$, $B_r(t)$ and x_r and unmodelled dynamics due to the reduction in the plant order are included into the disturbance term $d(x_r, t)$. In this case, it is assumed that the disturbances due to the unmodelled dynamics are slowly varying therefore the Popov's hyperstability theory is used to prove the stability of the reduced order plant.

4.5.1.1 - Stability Analyses of the ESH Materials Testing Machine by Popov's Hyperstability Theory

The second order nominal transfer function may be written in a phase canonical form as:

$$\begin{bmatrix} \dot{x}_1(t) \\ \dot{x}_2(t) \end{bmatrix} = \begin{bmatrix} 0 & 1 \\ -2000 & -110 \end{bmatrix} \begin{bmatrix} x_1(t) \\ x_2(t) \end{bmatrix} + \begin{bmatrix} 0 \\ 1 \end{bmatrix} u(t) \tag{4.39}$$

$$y(t) = \begin{bmatrix} 2900 & 0 \end{bmatrix} \begin{bmatrix} x_1(t) \\ x_2(t) \end{bmatrix} + [0]$$

The ESH materials testing machine parameters and plant state are represented in the reduced first order model as A_{r1}, B_{r1} and x_{r1}. Then, the reduced first order plant model is described by the following state space equation:

$$\dot{x}_{r1}(t) = A_{r1}x_{r1}(t) + B_{r1}u(t) + d(x_{r1}, t) \tag{4.40}$$

where $A_{r1} = -a_1$, $B_{r1} = b_1$, then (4.40) becomes

$$\dot{x}_{r1}(t) = (-a_1)x_{r1}(t) + (b_1)u(t) + d(x_{r1}, t) \tag{4.41}$$

where a_1 and b_1 are unknown first order plant parameters. The first order reference model is:

$$\dot{x}_m(t) = A_m x_m(t) + B_m r(t)$$

$$\dot{x}_m(t) = (-4/t_s)x_m(t) + (4/t_s)r(t) \tag{4.42}$$

According to [11], the bounded disturbance vector is written as:

$$d(x_{r1}, t) = \delta A_{r1}(t)r \tag{4.43}$$

where

$r \neq 0_{n,1}$, for all t

In the case of reduced first order SISO ESH plant

$$\delta A_{r1}(t) = \delta(a_{11}(t))$$

$$d(x_{r1}, t) = \delta a_{11}(t)r \tag{4.44}$$

The plant parameters A_{r1} and B_{r1} vary due to the unmodelled dynamics and nonlinearities in the plant. These changes can be denoted by $\delta A_{r2}(t) = \delta a_{12}(t)$ and $\delta B_{r1}(t) = \delta b(t)$, respectively, then (4.41) can be written as

$$\dot{x}_{r1}(t) = (a_1 + \delta a(t))x_{r1}(t) + (b_1 + \delta b(t))u(t) \tag{4.45}$$

where $\delta a(t) = \delta A_{r1}(t) = \delta A_1 + \delta A_2 = \delta a_{11}(t) + \delta a_{12}(t)$. The MCS control signal is

$$u(t) = \delta K(t)x_{r1}(t) + \delta K_R(t)r(t) \tag{4.46}$$

From (4.45) and (4.46) the closed-loop plant dynamics can be written as

$$\dot{x}_{r1}(t) = (A_r^*(t) + B_r^*(t)\delta K(t))x_{r1}(t) + B_r^*(t)\delta K_R r(t) \tag{4.47}$$

where

$$A_r^*(t) = a_r^*(t) = a_1 + \delta a$$
$$B_r^*(t) = b_r^*(t) = b_1 + \delta b$$

The error dynamics of the closed-loop system are given by

$$\dot{x}_e = A_m x_e(t) + \left(a_{r0}(t) - b_r^*(t)\delta K(t)\right)x_{r1}(t) + \left(B_m(t) - b_r^*(t)\delta K_R(t)\right)r(t) \qquad (4.48)$$

where

$$\dot{x}_e(t) = \dot{x}_m(t) - \dot{x}_{r1}(t); \quad x_e = x_m - x_{r1}$$

$$a_{r0}(t) = A_{r0}(t) = A_m - a_r^*(t)$$

From (4.48), the error dynamics can be written as

$$\dot{x}_e(t) = (-4/t_s)x_e(t) + I_1 w(t) \qquad (4.49)$$

where,

$$w(t) = \left(a_{r0}(t) - b_r^*(t)\delta K(t)\right)x_{r1}(t) + \left((4/t_s) - b_r^*(t)\delta K_R(t)\right)r(t)$$

The system is hyperstable if $\{A_m, I_1, C_e\}$ is a hyperstable block, i.e.

$$PA_m + A_m^T P = -Q\ , \qquad Q > 0$$

where P is the symmetric positive definite solution of the Lyapunov equation and Q is chosen for the first order plant as:

$$Q = [1]$$

so that

$$C_e = B_e^T P$$

where

$$B_e^T = [1]$$

The required closed loop settling time for the ESH machine is t_s = 0.35 s. The reference model parameters are:

$$A_m = -4/t_s = -11.402$$
$$B_m = 4/t_s = 11.402$$
$$C_e = t_s/8 = 0.0438$$

and Popov's criterion is satisfied if

$$\int_{t_0}^{t_1} y_{e1}^T(t)w(t)dt \geq -c^2, \forall t_1 \geq t_0 \qquad (4.50)$$

The Lyapunov equation can be solved to yield a positive-semidefinite matrix C_e. It remains to satisfy (4.50), which can be rewritten as

$$\int_{t_0}^{t_1} y_{e1}^T(t)\left(b_r^*(t)\delta K(t) - a_{r0}(t)\right)x_{r1}(t) \geq -c_1^2 \qquad (4.51a)$$

$$\int_{t_0}^{t_1} y_{e1}^T(t)\left(b_r^*(t)\delta K_R(t) - (4/t_s)\right)r(t) \geq -c_2^2 \tag{4.51b}$$

where

$$c_1^2 + c_2^2 = c^2$$

Writing

$$y_e^T = [y_{e1}]\ ,\ x_{r1}^T = [x_1],\ \alpha = [\alpha_1] \text{ and } \beta = [\beta_1]$$

the Popov criterion (4.51a) expands to

$$\int_{t_0}^{t_1} b_{r1}^* \alpha_1 y_{e1} x_1 \left[\int_0^t y_{e1} x_1 d\tau - a_{r01}/\left(b_{r1}^*\alpha_1\right)\right] dt \geq -c_{11}^2 \tag{4.52a}$$

where b_{r1}^* is the only entry of $b_r^*(t)$ and similarly a_{r01} is the only entry of $a_{r0}(t)$.

$$\int_{t_0}^{t_1} b_{r1}^* \beta_1 y_{e1}^2 x_1^2 dt \geq -c_{12}^2 \tag{4.52b}$$

and (4.51b) expands to

$$\int_{t_0}^{t_1} b_{r1}^* \alpha_1 y_{e1} r \left[\int_0^t y_{e1} r d\tau - 4/\left(b_{r1}^*\alpha_1 t_s\right)\right] dt \geq -c_{21}^2 \tag{4.53a}$$

together with

$$\int_{t_0}^{t_1} b_{r1}^* \beta_1 y_{e1}^2 r^2 dt \geq -c_{22}^2 \tag{4.53b}$$

By inspection, inequalities (4.52b) and (4.53b) are satisfied. To confirm that (4.52a) and (4.53a) are satisfied, we use (4.32) integral property, then from (4.52a) one can assign

$$f_1 = \int_0^t y_{e1} x_1 d\tau - a_{r01}/\left(b_{r1}^*\alpha_1\right) \text{ and } k = b_{r1}^*\alpha_1$$

It is assumed that a_{r01} and b_{r1}^* vary less rapidly than the transient terms in the adaptive laws (4.28), $\dot{f}_1 \cong y_{e1}x_1$. Therefore, in practice the above approximation can be made arbitrarily close to an equality. In a same manner, (4.52a) can be rewritten as

$$\int_{t_0}^{t_1} k\dot{f}_1 f_1 \geq -k f_1^2(t_0)/2 \tag{4.54}$$

In a similar manner, (4.53a) becomes

$$\int_{t_0}^{t_1} k\dot{f}_2 f_2 dt \geq -k f_2^2(t_0)/2 \tag{4.55}$$

where,

$$k = b_{r1}^{*}\alpha_1,\ f_2 = \int_0^t y_{e1} r d\tau - 4/\left(b_{r1}^{*}\alpha_1 t_s\right) \text{ and } \dot{f}_2 \cong y_{e1} r$$

Hence, inequalities (4.51a) and (4.51b) are satisfied since we may now ensure (4.52a) and (4.53a) satisfy an inequality of the type given in (4.32). Therefore the Popov criterion (4.50) is also satisfied, as required, together with the strictly positive realness of the feedforward transfer function matrix, implying that MCS guarantees the asymptotic hyperstability of a reduced first order SISO ESH materials testing machine.

4.5.1.2 - Stability Proof of the Electrohydraulic Actuator Plant by Popov's Hyperstability Theory

The nominal linearised model is third order, including a free integrator. The third order plant transfer function is given in Chapter 5 as:

$$G_p(s) = \frac{2830}{s^3 + 17.6s^2 + 333.44s} \tag{4.56}$$

The phase canonical form of the nominal plant model is

$$\begin{bmatrix} \dot{x}_1(t) \\ \dot{x}_2(t) \\ \dot{x}_3(t) \end{bmatrix} = \begin{bmatrix} 0 & 1 & 0 \\ 0 & 0 & 1 \\ 0 & -333.44 & -17.6 \end{bmatrix} \begin{bmatrix} x_1(t) \\ x_2(t) \\ x_3(t) \end{bmatrix} + \begin{bmatrix} 0 \\ 0 \\ 1 \end{bmatrix} u(t)$$

$$y(t) = \begin{bmatrix} 2830 & 0 & 0 \end{bmatrix} \begin{bmatrix} x_1(t) \\ x_2(t) \\ x_3(t) \end{bmatrix} + [0] \tag{4.57}$$

The reduced second order plant model is described by the following state-space equation:

$$\dot{x}_{r2}(t) = A_{r2} x_{r2}(t) + B_{r2} u(t) + d(x_{r2}, t) \tag{4.58}$$

where $A_{r2} = \begin{bmatrix} 0 & 1 \\ 0 & -a_1 \end{bmatrix}$, $B_{r2} = \begin{bmatrix} 0 \\ b_1 \end{bmatrix}$, then the reduced second order plant model including a free integrator is described by the following phase canonical form

$$\begin{bmatrix} \dot{x}_{r2_1}(t) \\ \dot{x}_{r2_2}(t) \end{bmatrix} = \begin{bmatrix} 0 & 1 \\ 0 & -a_1 \end{bmatrix} \begin{bmatrix} x_{r2_1}(t) \\ x_{r2_2}(t) \end{bmatrix} + \begin{bmatrix} 0 \\ b_1 \end{bmatrix} u(t) + d(x_{r2}, t) \tag{4.59}$$

where a_1 and b_1 are unknown reduced second order plant parameters and $d(x_{r2},t)$ represents the disturbance due to the unmodelled dynamics, plant nonlinearities and external disturbances. The bounded disturbance vector can always be written as:

$$d(x_{r2},t) = \delta A_r(t) r \tag{4.60}$$

The term $\delta A_r(t)$ can be considered as an unknown variation and unmodelled dynamics in the A_{r2} matrix, structured according to any variation in A_{r2}. Equation (4.60) can be rewritten as:

$$d(x_{r2},t) = \begin{bmatrix} 0 \\ \delta a(t) \end{bmatrix} r$$

Then, (4.57) becomes

$$\begin{bmatrix} \dot{x}_{r2_1}(t) \\ \dot{x}_{r2_2}(t) \end{bmatrix} = \begin{bmatrix} 0 & 1 \\ 0 & -a_1 \end{bmatrix} \begin{bmatrix} x_{r2_1}(t) \\ x_{r2_2}(t) \end{bmatrix} + \begin{bmatrix} 0 \\ b_1 \end{bmatrix} u(t) + \begin{bmatrix} 0 \\ \delta a(t) \end{bmatrix} r \tag{4.61}$$

Let

$$\delta A_{r1}(t) = \begin{bmatrix} 0 & 0 \\ 0 & \delta a_{12}(t) \end{bmatrix}$$

where $\delta a_{11}(t) = 0$, due to a free integrator in the plant, so that

$$\delta a_{12}(t) x_{r2_2}(t) = \delta a(t) r \tag{4.62}$$

which gives

$$\delta a_{12}(t) = \delta a(t) r \,/\, x_{r2_2}(t)$$

For the sake of simplicity it is more suitable to have the first row of $\delta A_{r1}(t)$ zero. For the cases where $d(t) \neq 0_{n,1}$ whilst $x_{r2}(t) = 0_{n,1}$ for some $x_{r2} \geq 0$. Then, (4.58) can be rewritten in the state-space form as:

$$\dot{x}_{r2}(t) = \left(A_{r2} + \delta A_{r1}(t)\right) x_{r2}(t) + B_{r2} u(t) \tag{4.63}$$

Consider that parameter changes will occur in $\{A_{r2}, B_{r2}\}$, due to the unmodelled dynamics and nonlinearities in the plant. Let these changes be denoted by $\delta A_{r2}(t)$ and $\delta B_r(t)$ respectively; also let $\delta A_r(t) = \delta A_{r1}(t) + \delta A_{r2}(t)$, so that the state equation is now written as

$$\dot{x}_{r2}(t) = \left(A_{r2} + \delta A_r(t)\right) x_{r2}(t) + \left(B_{r2} + \delta B_r(t)\right) u(t) \tag{4.64}$$

Thus, we define the MCS control input u as

$$u(t) = \delta K(t) x_{r2}(t) + \delta K_R(t) r(t) \tag{4.65}$$

The second order reference model is known exactly as

$$\ddot{x}_m + 2\zeta\omega_n^2\dot{x}_m + \omega_n^2 x_m = \omega_n^2 r \tag{4.66}$$

where, ω_n is the natural frequency and ζ is the damping ratio of the system, for critical damping $\zeta = 1$ and $t_s = \dfrac{4}{\zeta\omega_n}$

$$\begin{bmatrix}\dot{x}_{m1}(t)\\ \dot{x}_{m2}(t)\end{bmatrix} = \begin{bmatrix}0 & 1\\ -a_{m1} & -a_{m2}\end{bmatrix}\begin{bmatrix}x_{m1}(t)\\ x_{m2}(t)\end{bmatrix} + \begin{bmatrix}0\\ b_m\end{bmatrix} r(t) \tag{4.67}$$

In (4.67) reference model parameters $-a_{m1} = -\omega_n^2, -a_{m2} = -2\omega_n$ and $b_m = \omega_n^2$ are known for a given settling time. In the case of the electrohydraulic actuator plant t_s = 0.25 s. Hence, (4.67) can be written for the plant as

$$\begin{bmatrix}\dot{x}_{m1}(t)\\ \dot{x}_{m2}(t)\end{bmatrix} = \begin{bmatrix}0 & 1\\ -256 & -32\end{bmatrix}\begin{bmatrix}x_{m1}(t)\\ x_{m2}(t)\end{bmatrix} + \begin{bmatrix}0\\ 256\end{bmatrix} r(t)$$

Therefore, the closed-loop plant dynamics are given by (4.64) and (4.65)

$$\dot{x}_{r2}(t) = \left(A_r^*(t) + B_r^*(t)\delta K(t)\right)x(t) + B_r^*(t)\delta K_R(t)r(t) \tag{4.68}$$

where

$$A_r^*(t) = A_{r2} + \delta A_r(t) \text{ and } B_r^*(t) = B_{r2} + \delta B_r(t)$$

From (4.67) and (4.68) the error dynamics of the closed loop system are given by

$$\begin{aligned}\dot{x}_e(t) = {} & A_m x_e(t) + \left(A_{r0}(t) - B_r^*(t)\delta K(t)\right)x_{r2}(t)\\ & + \left(B_m - B_r^*(t)\delta K_R(t)\right)r(t)\end{aligned} \tag{4.69}$$

where

$$A_{r0}(t) = A_m - A_r^*(t)$$

From (4.69), let

$$W(t) = \left(A_{r0}(t) - B_r^*(t)\delta K(t)\right)x_{r2}(t) + \left(B_m - B_r^*(t)\delta K_R(t)\right)r(t)$$

then (4.69) can be rewritten as

$$\dot{x}_e(t) = A_m x_e + I_2 W(t) \tag{4.70}$$

The stability of (4.70) is investigated by the Popov's hyperstability theory. The system is hyperstable if $\{A_m, I_2, C_e\}$ is a hyperstable block, i.e.

$$PA_m + A_m^T P = -Q, \qquad Q > 0 \tag{4.71}$$

where P is the positive definite solution to the Lyapunov equation and Q is chosen as:

$$Q = \begin{bmatrix} 10 & 0 \\ 0 & 1 \end{bmatrix}$$

so that

$$C_e = B_e^T P$$

where

$$B_e = [0 \quad 1]^T$$

For a given settling time $t_s = 0.35$ s

$$A_m = \begin{bmatrix} 0 & 1 \\ -256 & -32 \end{bmatrix}, \qquad B_m = \begin{bmatrix} 0 \\ 256 \end{bmatrix}, \qquad C_e = [0.0195 \quad 0.0162]$$

and it remains to satisfy (4.23), which can be rewritten as

$$\int_{t_0}^{t_1} y_e^T(t)\left(B_r^*(t)\delta K(t) - A_{r0}(t)\right)x_{r2}(t)dt \geq -c_1^2 \tag{4.72a}$$

$$\int_{t_0}^{t_1} y_e^T(t)\left(B_r^*(t)\delta K_R(t) - B_m\right)r(t)dt \geq -c_2^2 \tag{4.72b}$$

where

$$c_1^2 + c_2^2 = c^2$$

and

$$\delta K(t) = \int_0^t \alpha y_e(\tau)x_{r2}^T(\tau)d\tau + \beta y_e(t)x_{r2}^T(t)$$

$$\delta K_R(t) = \int_0^t \alpha y_e(\tau)r(\tau)d\tau + \beta y_e(t)r(t)$$

together with

$$y_e^T = [y_{e1} \quad y_{e2}], \qquad x_{r2}^T = [x_1 \quad x_2]$$
$$\alpha = [0 \quad \alpha_2], \qquad \beta = [0 \quad \beta_2]$$

Equation (4.72a) is further expanded to:

$$\int_{t_0}^{t_1} b_{r2}^* \alpha_2 \sum_{i=1}^{2} y_{e2}x_i \left[\int_0^t y_{e2}x_i d\tau - \alpha_{r02_i} / b_{r2}^* \alpha_2\right]dt \geq -c_{11}^2 \tag{4.73a}$$

where b_{r2}^* is the second and the only non-zero entry of $B_r^*(t)$

$$\int_{t_0}^{t_1} b_{r2}^* \beta_2 y_{e2}^2 x_1^2 x_2^2 dt \geq -c_{12}^2 \tag{4.73b}$$

Similarly (4.72b) is expanded respectively as

$$\int_{t_0}^{t_1} b_{r2}^{*}\alpha_2 y_{e2} r\left[\int_0^t y_{e2} r d\tau - b_{m2}/\left(b_{r2}^{*}\alpha_2\right)\right]dt \geq -c_{21}^2 \tag{4.74a}$$

$$\int_{t_0}^{t_1} b_{r2}^{*}\beta_2 y_{e2}^2 r^2 dt \geq -c_{22}^2 \tag{4.74b}$$

where b_{m2} is the second and only non-zero entry of $B_m(t)$. The above equations (4.73b) and (4.74b) are satisfied. In order to satisfy (4.73a) and (4.74a) the integral property (4.32) can be used. Then (4.73a) can be written as

$$\int k\dot{f}_i f_i dt \geq -kf^2(t_0)/2 \tag{4.75}$$

where

$$k = b_{r2}^{*}\alpha_2, \qquad f_i = \int_0^t y_{e2} x_i\, d\tau - a_{r02_2}/b_{r2}^{*}\alpha_2 \text{ and } (i = 1,2)$$

Similarly (4.74a) can be written as

$$f = \int_0^t y_{e2} r - b_{m2}/b_{r2}^{*}\alpha_2$$

Again, it has been assumed that, b_{r2}^{*}, a_{r02_2} and b_{m2} vary less rapidly than, the transient terms in the adaptive laws and parameter variations occur on a longer time scale than the adaptive process. The Popov criteria (4.74a) and (4.74b) are satisfied. Therefore MCS ensures asymptotic hyperstability of the reduced second order (including a free integrator) electrohydraulic actuator plant.

The nominal plant parameters and plant states appear in the reduced second order model as A_{r2}, B_{r2} and x_{r2} together with unmodelled dynamics which are treated as disturbances.

4.5.2 - Stability Analyses of the Reduced Order MCS in the Case of MIMO Systems

Stability of the MCS algorithm will be investigated in the case of Multi Input Multi output (MIMO) systems. The structure of plants under consideration is a generalisation of the SISO phase canonical form previously investigated at the beginning of

this chapter. Consider the disturbances of a free MIMO plant described by the following state space equation:

$$\dot{x}(t) = A(t)x(t) + B(t)u(t) \tag{4.76}$$

where, $x = [x_1, \quad x_2, \quad . \quad . \quad . \quad ., \quad x_n]$, $x \in \mathbb{R}^{nx1}$ and $u \ \mathbb{R}^{kx1}$

The matrices $A(t)$, $B(t)$ are given as below

$$A(t) = \begin{bmatrix} A_{11} & \cdots & A_{1k} \\ \vdots & \ddots & \vdots \\ A_{k1} & \cdots & A_{kk} \end{bmatrix}, \quad B(t) = \begin{bmatrix} B_{11} & \cdots & B_{1k} \\ \vdots & \ddots & \vdots \\ B_{k1} & \cdots & B_{kk} \end{bmatrix} \tag{4.76a}$$

where k is the number of degrees of freedom in the plant and ni is the state dimension of each degree of freedom. It assumed that $k \leq n$. Also:

$$A_{ii} = \begin{bmatrix} 0 & 1 & 0 & 0 & \cdots & 0 \\ 0 & 0 & 1 & 0 & \cdots & 0 \\ \vdots & \vdots & \vdots & \vdots & \vdots & \vdots \\ 0 & . & . & . & 0 & 1 \\ -a_{ii1} & -a_{ii2} & . & . & . & -a_{iini} \end{bmatrix}; \quad A_{ij} = \begin{bmatrix} 0 & \cdots & 0 \\ \vdots & \vdots & \vdots \\ 0 & \cdots & 0 \\ a_{ij1} & \cdots & a_{ijnj} \end{bmatrix} \tag{4.76b}$$

$$B_{ii} = \begin{bmatrix} 0 \\ \vdots \\ 0 \\ b_{ii} \end{bmatrix}; \ B_{ij} = \begin{bmatrix} 0 \\ \vdots \\ 0 \\ b_{ij} \end{bmatrix} \qquad \begin{matrix} (i = 1,\ldots,n) \\ (j = 1,\ldots,k) \end{matrix} \tag{4.76c}$$

$$u^T = [u_1 \quad u_2 \quad \cdots \quad u_k] \tag{4.77}$$

$$\sum_{i=1}^{k} ni = n \tag{4.78}$$

and

$$\begin{aligned} x^T &= [x_{11} \quad \ldots \quad x_{1n} \quad x_{21} \quad \ldots \quad x_{2n} \quad \ldots \quad x_{k1} \quad \ldots \quad x_{kn}] \\ y_e^T &= [y_{11} \quad \ldots \quad y_{1n} \quad y_{21} \quad \ldots \quad y_{2n} \quad \ldots \quad y_{k1} \quad \ldots \quad y_{kn}] \end{aligned} \tag{4.79}$$

The reduced order plant model together with unmodelled dynamics may be written as:

$$\dot{x}_r(t) = A_r(t)x_r(t) + B_r(t)u(t) + d(x_r, t) \tag{4.80}$$

where the matrices $A_r(t)$ and $B_r(t)$ are

$$A_r(t) = \begin{bmatrix} A_{11} & \cdots & A_{1k} \\ \vdots & \ddots & \vdots \\ A_{k1} & \cdots & A_{kk} \end{bmatrix}, \quad B_r(t) = \begin{bmatrix} B_{11} & \cdots & B_{1k} \\ \vdots & \ddots & \vdots \\ B_{k1} & \cdots & B_{kk} \end{bmatrix} \tag{4.80a}$$

where k is the number of degrees of freedom in the plant and hi is the state dimension of each degree of freedom. Also:

$$A_{iir} = \begin{bmatrix} 0 & 1 & 0 & 0 & \cdots & 0 \\ 0 & 0 & 1 & 0 & \cdots & 0 \\ \vdots & \vdots & \vdots & \vdots & \vdots & \vdots \\ 0 & . & . & . & 0 & 1 \\ -a_{ii1} & -a_{ii2} & . & . & . & -a_{iihi} \end{bmatrix}; \quad A_{ijr} = \begin{bmatrix} 0 & \cdots & 0 \\ \vdots & \vdots & \vdots \\ 0 & \cdots & 0 \\ a_{ij1} & \cdots & a_{ijhj} \end{bmatrix} \tag{4.80b}$$

and $d(x_r,t)$ is defined as:

$$d(x_r,t) = \begin{bmatrix} d_1 \\ d_2 \\ \vdots \\ d_h \end{bmatrix}; \quad d_j = \begin{bmatrix} 0 \\ \vdots \\ 0 \\ d_{jj} \end{bmatrix} \qquad \begin{matrix} (i = 1,\ldots,h) \\ (j = 1,\ldots,k) \end{matrix} \tag{4.80c}$$

The matrix $d(x_r,t)$ represents the bounded effect of unmodelled dynamics, plant parameter variations and nonlinearities in the plant. The integers hi (i= 1,...,h) are assumed to be known. The plant parameters and the disturbances d_j (j = 1,...,h) are assumed to be unknown and time varying. The term $\sum_{i=1}^{k} hi = h$, together with

$$\begin{aligned} x_r^T &= \begin{bmatrix} x_{11} & \ldots & x_{1h} & x_{21} & \ldots & x_{2h} & \ldots & x_{k1} & \ldots & x_{kh} \end{bmatrix} \\ y_{re}^T &= \begin{bmatrix} y_{11} & \ldots & y_{1h} & y_{21} & \ldots & y_{2h} & \ldots & y_{k1} & \ldots & y_{kh} \end{bmatrix} \end{aligned} \tag{4.81}$$

The stable reference model is given as:

$$\dot{x}_m = A_m x_m + B_m r \tag{4.82}$$

where

$$A_m = \begin{bmatrix} A_{m11} & \cdots & 0 \\ \vdots & \ddots & \vdots \\ 0 & \cdots & A_{mkk} \end{bmatrix}; \quad B_m = \begin{bmatrix} B_{m11} & \cdots & 0 \\ \vdots & \ddots & \vdots \\ 0 & \cdots & B_{mkk} \end{bmatrix} \tag{4.82a}$$

and

$$A_{mii} = \begin{bmatrix} 0 & 1 & 0 & \cdots & 0 \\ 0 & 0 & 1 & 0 \cdots & 0 \\ \vdots & \vdots & \vdots & \vdots & \vdots \\ 0 & 0 & \cdots & 0 & 1 \\ -a_{mii1} & -a_{mii2} & -a_{mii3} & \cdots & -a_{miihi} \end{bmatrix}; \quad B_{mii} = \begin{bmatrix} 0 \\ \vdots \\ 0 \\ b_{mhi} \end{bmatrix} \tag{4.82b}$$

Then, (4.83) can be rewritten as

$$\dot{x}_r(t) = \left(A_r + \delta A_r(t)\right)x_r(t) + \left(B_r + \delta B_r(t)\right)u(t) \tag{4.83}$$

where, $\delta A_r(t)$ and $\delta B_r(t)$ are the effect of the unmodelled and unknown dynamics in $A_r(t)$ and $B_r(t)$ respectively. The MCS control signal is given in (4.16) then, (4.83) becomes

$$\dot{x}_r(t) = \left(A_r^*(t) + B_r^*(t)\right)x_r(t) + B_r^*(t)\delta K_R(t)r(t) \tag{4.84}$$

where, $A_r^*(t) = A_r + \delta A_r(t)$ and $B_r^*(t) = B_r + \delta B_r(t)$. The model-following error x_e is defined as:

$$x_e(t) = x_m(t) - x_r(t) \tag{4.85}$$

so that from (4.82) and (4.84), the error dynamics of the closed loop system becomes:

$$\begin{aligned}\dot{x}_e(t) = {} & A_m(t)x_e(t) + \left(A_{r0}(t) - B_r^*\delta K(t)\right)x_r(t) \\ & + \left(B_{r0}(t) - B_r^*(t)\delta K_R(t)\right)r(t)\end{aligned} \tag{4.86}$$

where, $A_{r0}(t) = A_m - A_r^*(t)$ and $B_{r0}(t) = B_m$. $A_{r0}(t)$ will take the following form

$$A_{r0}(t) = \begin{bmatrix} 0 & \cdots & 0 \\ & \vdots & \\ 0 & \cdots & 0 \\ a_{11}^1 & a_{12}^1 \cdots & a_{kh}^1 \\ \cdots & \cdots \cdots \cdots & \cdots \\ & \vdots & \\ \cdots & \cdots \cdots \cdots & \cdots \\ 0 & \cdots & 0 \\ & \vdots & \\ 0 & \cdots & 0 \\ a_{11}^k & a_{12}^k \cdots & a_{kh}^k \end{bmatrix} \tag{4.87}$$

The disturbance term due to the unmodelled dynamics may be written as

$$d(x_r, t) = B_r^* r \tag{4.88}$$

where, the reference inputs r_i $(i = 1,\ldots,h)$ are different from zero and the matrix B_r^* can be written as follows

$$B_r^* = \begin{bmatrix} 0 & \cdots & 0 \\ & \vdots & \\ b_{r11} & \cdots & b_{r_{1k}} \\ \cdots & \cdots \cdots \cdots & \cdots \\ & \vdots & \\ 0 & \cdots & 0 \\ & \vdots & \\ b_{r_{k1}} & \cdots & b_{r_{kk}} \end{bmatrix} \tag{4.89}$$

The matrix (4.89) is bounded and time varying depend on $d(x_r,t)$ and $r(t)$. By using (4.86) and (4.88) each disturbance term d_{jj} $(j = 1,...,k)$ can be written as:

$$d_{jj} = \sum_{i=1}^{h} b_{r_{ji}} r_i \tag{4.90}$$

In general, the reference inputs r_i $(i = 1,...,k)$ are slowly varying, for example a step function. Equation (4.86) can be rewritten as:

$$\dot{x}_e = A_m x_e - I_h W_e \tag{4.91}$$

where

$$W_e = (A_r - A_m)x_r + B_r u + (B_r^* - B_m)r \tag{4.92}$$

The argument "t" has been dropped for the sake of simplicity and the control input is given as

$$u_p = \sum_{i=1}^{h}\left(K_{1(pi)} + K_{2(pi)}\right)x_i + \sum_{j=1}^{k}\left(K_{r1(pi)} + K_{r2(pi)}\right)r_j \tag{4.93}$$

with

$$\begin{aligned} K_{1pi} &= \int_0^t \alpha_{pi} y_{php} x_i d\tau \\ K_{2pi} &= \beta_{pi} y_{php} x_i \qquad\qquad p = 1,...,k \\ K_{r1pi} &= \int_0^t \alpha(r)_{pi} + y_{php} r_j d\tau \qquad\qquad i = 1,...,h \\ K_{r2pj} &= \beta(r)_{pj} y_{phk} r_j \qquad\qquad j = 1,...,k \end{aligned} \tag{4.94}$$

The sign conditions associated with the application of (4.23) are

$$\begin{aligned}
&\alpha_{pi} b_{pp} > 0 \\
&\beta_{pi} b_{pp} \geq 0 \\
&\alpha(r)_{pj} b_{pp} > 0 \\
&\beta(r)_{pj} b_{pp} \geq 0
\end{aligned} \tag{4.95}$$

The vector W_e is further expanded to:

$$W_e = \begin{bmatrix}
0 \\
\vdots \\
\sum_{i=1}^{h}(a_{1i} - a_{m11})x_i + \sum_{j=1}^{k} b_{1j} u_j + \sum_{j=1}^{k} b_{r_1 j} r_j - b_{m11} r_1 \\
\cdots \quad \cdots \quad \cdots \quad \cdots \quad \cdots \quad \cdots \quad \cdots \quad \cdots \quad \cdots \\
\vdots \\
\cdots \quad \cdots \quad \cdots \quad \cdots \quad \cdots \quad \cdots \quad \cdots \quad \cdots \quad \cdots \\
0 \\
\vdots \\
\sum_{i=1}^{h}(a_{ki} - a_{mkk})x_i + \sum_{j=1}^{k} b_{kj} u_j + \sum_{j=1}^{k} b_{r_k j} r_j - b_{mkk} r_k
\end{bmatrix} \tag{4.96}$$

In order to proof the hyperstability of the reduced order MCS control in the case of MIMO systems by Popov's criterion, (4.91) is split into two parts as shown in Fig. 4.1: A feedforward block and a feedback block. For the asymptotic hyperstability of x_e, the following two conditions must be satisfied.

(a) - the forward block represented by the triple $\{A_m, I_h, C_e\}$ is SPR,

(b) - the feedback block ensures the integral inequality

$$\int_{t_0}^{t_1} y_{re}^T W_e dt \geq -c_0^2 \tag{4.97}$$

The B matrix is replaced with B_r^* due to the unmodelled dynamics and external disturbances, with entries b_{ii}^* and $-b_{ij}^*$. Let

$$B^{*'} u = B_r^* u$$

where $B^{*'}$ is a block diagonal matrix given by

$$B^{*'} = diag\left[B_{11}^{*'} \mid B_{22}^{*'} \mid \cdots \; B_{kk}^{*'}\right]$$

and

$$B_{ii}^{*'} = \left[0 \quad \cdots \quad 0 \quad b_{ii}^{*'}\right]^T$$

It is assumed that along control trajectories,

$$b_{ii}^{*'} = b_{ii}^{*} - \sum_{\substack{j=1 \\ j\neq i}}^{h} b_{ij}^{*} / u_i$$

The adaptive weights are described in the following forms

$$\begin{aligned} \alpha &= diag\left(\begin{bmatrix} 0 & \cdots & 0 & \alpha_1 \end{bmatrix} \begin{bmatrix} 0 & \cdots & 0 & \alpha_2 \end{bmatrix} \cdots \begin{bmatrix} 0 & \cdots & 0 & \alpha_k \end{bmatrix}\right) \\ \beta &= diag\left(\begin{bmatrix} 0 & \cdots & 0 & \beta_1 \end{bmatrix} \begin{bmatrix} 0 & \cdots & 0 & \beta_2 \end{bmatrix} \cdots \begin{bmatrix} 0 & \cdots & 0 & \beta_k \end{bmatrix}\right) \end{aligned} \tag{4.98}$$

There are four integral inequalities to satisfy, which are given in (4.30a)-(4.31b). Following inequality (4.30a) can be expanded, with the introduction of $B^{*'}$ instead of, B_r^* as

$$\begin{aligned} &\int_{t_0}^{t_1} \Bigg\{ b_{11}^{*'}\alpha_1 \Bigg[y_{1h}x_{11}\int_0^t y_{1h}x_{11}d\tau - a_{11}^1 / \left(b_{11}^{*'}\alpha_1\right) + \cdots + \\ &y_{1h}x_{kh}\int_0^t y_{1h}x_{kh}d\tau - a_{kh}^1 / \left(b_{11}^{*'}\alpha_1\right)\Bigg] + \cdots + \\ &b_{kk}^{*'}\alpha_k \Bigg[y_{kh}x_{11}\int_0^t y_{kh}x_{11}d\tau - a_{11}^k / \left(b_{kk}^{*'}\alpha_k\right) \\ &+ \cdots + y_{kh}x_{kh}\int_0^t y_{kh}x_{kh}d\tau - a_{kh}^k / \left(b_{kk}^{*'}\alpha_k\right)\Bigg]\Bigg\} dt \geq -c_{11}^2 \end{aligned} \tag{4.99a}$$

Each term in Equation (4.99a) can be written as:

$$\int_{t_0}^{t_1} b_{ii}^{*'}\alpha_i \left[y_{ih}x_{jk}\int_0^t y_{ih}x_{jp}d\tau - a_{jp}^i / \left(b_{ii}^{*'}\alpha_i\right)\right] dt$$

which satisfies a Popov criterion provided that α_i has the same sign as $b_{ii}^{*'}$. Bringing together all such terms in (4.99a) and (4.30a), the Popov's hyperstability criterion will be satisfied. Similarly (4.30b), (4.31a) and (4.31b) can be expanded as follows:

$$\int_{t_0}^{t_1} \left\{ b_{11}^{*'}\beta_1 \left[y_{1h}^2 x_{11}^2 + \cdots + y_{1h}^2 x_{kh}^2 \right] + \cdots + b_{kk}^{*'}\beta_k \left[y_{kh}^2 x_{11}^2 + \cdots + y_{kh}^2 x_{kh}^2 \right] \right\} dt \geq -c_{12}^2 \tag{4.99b}$$

In a similar manner to (4.30b), each term in (4.99b) can be written as

$$\int_{t_0}^{t_1} b_{ii}^{*'}\beta_i \left(y_{ih}^2 x_{jp}^2 \right) dt$$

satisfies a Popov criterion. Taking together all such terms in (4.99b), inequality (4.30b) will be satisfied. Then (4.31a) becomes

$$\int_{t_0}^{t_1}\Big\{b_{11}^{*'}\alpha_1\Big[y_{1h}r\int_0^t y_{1h}rd\tau - b_{mh1}/\left(b_{11}^{*'}\alpha_1\right)$$
$$+\cdots+y_{1h}r\int_0^t y_{1h}rd\tau - b_{mh1}/\left(b_{11}^{*'}\alpha_1\right)\Big]$$
$$+\cdots+b_{kk}^{*'}\alpha_k\Big[y_{kh}r\int_0^t y_{kh}rd\tau - b_{mhk}/\left(b_{kk}^{*'}\alpha_k\right)$$
$$+\cdots+y_{kh}r\int_0^t y_{kh}rd\tau - b_{mhk}/\left(b_{kk}^{*'}\alpha_k\right)\Big]\Big\}dt \geq -c_{21}^2 \qquad (4.100a)$$

Each term in (4.100a) can be expressed as:

$$\int_{t_0}^{t_1} b_{ii}^{*'}\alpha_i\Big[y_{ih}r\int_0^t y_{ih}rd\tau - b_{mhi}/\left(b_{ii}^{*'}\alpha_i\right)\Big]dt$$

Taking together all such terms in (4.100a), inequality (4.30a) and (4.31a) will be satisfied. Together with

$$\int_{t_0}^{t_1}\left\{b_{11}^{*'}\beta_1\left(y_{1h}^2r^2\right)+\cdots+b_{kk}^{*'}\left(y_{kh}^2r^2\right)\right\}dt \geq -c_{22}^2 \qquad (4.100b)$$

Each term in expression (4.100b) i.e. $\int_{t_0}^{t_1} b_{ii}^{*'}\beta_i\left(y_{ih}^2r^2\right)dt$ ensures a Popov criterion. Collecting together (4.99a), (4.100b) Popov's criterion (4.23) is satisfied therefore, the given MCS adaptive law (4.97) guarantees the asymptotic hyperstability of reduced order MIMO closed loop systems as required.

The nominal plant parameters of the MIMO systems are replaced with lower order plant parameters in the reduced order model together with unmodelled dynamics and the unmodelled dynamics are treated as disturbances. It is assumed that the disturbance term due to unmodelled dynamics is slowly varying (may be the plant is over parameterised), therefore Popov's method is used to prove the stability of the reduced order MIMO MCS control.

4.6 - STABILITY ANALYSES OF THE REDUCED ORDER MCS CONTROL BY THE LYAPUNOV EQUATION

The MCS algorithm is stable in the presence of slowly varying disturbances. In the previous section the stability of the reduced order MCS control was proven by Popov's hyperstability theory. In this section stability of the reduced order MCS control in the presence of rapidly varying disturbances due to unmodelled dynamics and nonlinearities in plants will be proven by the Lyapunov equation method. The Lyapunov function is an important method to prove the stability of plants which are subjected to rapidly varying disturbances and it is very suitable in examining the upper bounds of convergence of the error.

4.6.1 - Stability Proof of the Reduced Order MCS Control in the Case of SISO Systems by the Lyapunov Equation

From (4.4) and (4.7) we obtain:

$$\dot{x}_e = A_m x_e - (A_r - A_m)x_r - B_r u + B_m r - d(x_r, t) \tag{4.101}$$

where, the disturbance term is $d(x_r, t) = \delta A(t) r$. Then, equation (4.101) can be written as

$$\dot{x}_e = A_m x_e - I_h W_e \tag{4.102}$$

where

$$W_e = (A_r - A_m)x_r + B_r u + (\delta A_r - B_m)r \tag{4.103}$$

(4.103) can be further expanded to:

$$W_e = \begin{bmatrix} 0 \\ \vdots \\ 0 \\ \sum_{i=1}^{h}(-a_i + a_{mi})x_i + b_1 u + (\delta a - bm)r \end{bmatrix}; \quad W_e \in \mathbf{R}^{hx1} \tag{4.104}$$

The MCS control input u is

$$u = K(t)x_r + K_R(t)r \tag{4.105}$$

The adaptive gains are written as

$$\begin{aligned} K(t) &= [k_1 \quad k_2, \quad \ldots \quad , k_h] = K_{i\alpha}(t) + K_{i\beta}(t) \\ K_R(t) &= [k_{r1} \quad k_{r2}, \quad \ldots \quad , k_h] = K_{R\alpha}(t) + K_{R\beta}(t) \end{aligned} \tag{4.106}$$

where $K_{i\alpha}(t)$, $K_{R\alpha}(t)$ are the integral gains and $K_{i\beta}(t)$, $K_{R\beta}(t)$ are the proportional gains.

$$\begin{aligned} K_{i\alpha}(t) &= \int_{t_0}^{t} \alpha_i y_h x_i d\tau \\ K_{i\beta}(t) &= \beta_i y_h x_i \qquad\qquad i = 1,\ldots,h \\ K_{R\alpha}(t) &= \int_{t_0}^{t_1} \alpha_r y_h r d\tau \\ K_{R\beta}(t) &= \beta_r y_h r \end{aligned} \tag{4.107}$$

The output error equation is derived from (4.104), (4.105) and (4.106) as follows

$$\dot{x}_e = A_m x_e - bw^T\Phi - bw^T\Psi - d(x_r,t) \tag{4.108}$$

with

$$d(x_r,t) = [0 \quad 0 \quad \ldots \quad d]^T; \quad d(x_r,t) = \delta A(t)r \tag{4.109}$$

where

$$\delta A(t) = [0 \quad \cdots \quad 0 \quad \delta a(t)]^T = [0 \quad \ldots \quad 0 \quad d_1]^T \tag{4.110}$$

This disturbance is assumed to act only on h^{th} state, therefore (4.110) can be written as

$$d(x_r,t) = bw^T d_1 \tag{4.111}$$

Then, the error equation becomes

$$\dot{x}_e = A_m x_e - bw^T(\Phi + \Psi + d_1) \tag{4.112}$$

Equation (4.112) defines a hyperstable system, shown in Fig. 4.2.

$$b = [0 \quad \cdots \quad 0 \quad 1]^T \tag{4.113}$$

$$w = [x_r^T \quad r]^T \tag{4.114}$$

$$\begin{aligned} \Phi = \Bigg[& b_1 \int_0^t \alpha y_h x_1 d\tau + am_1 - a_1, \ldots, b_1 \int_0^t \alpha y_h x_h d\tau + am_h - a_h, \\ & b_1 \int_0^t \alpha y_h r d\tau - bm \Bigg]^T \end{aligned} \tag{4.115}$$

$$\dot{\Phi} = b_1 \alpha b^T P x_e w \tag{4.116}$$

where, Φ is integral gain vector and b_1 is the last and the only non-zero entry of the B_r matrix, and proportional gains vector is

$$\Psi = \left[b_1 \beta y_h x_1, \ldots, b_1 \beta y_h x_h, b_1 \beta y_h r\right]^T \tag{4.117}$$

The system defined from (4.108), (4.114), (4.116) and (4.117) is an asymptotically hyperstable provided that $d \in L^2$, hence Popov's hyperstability criterion (4.23) becomes:

$$\begin{aligned} \alpha b_1 &> 0 \\ \beta b_1 &\geq 0 \end{aligned} \tag{4.118}$$

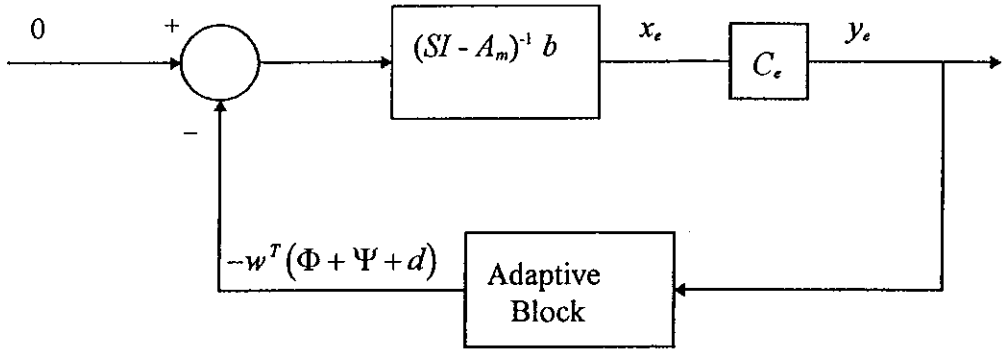

Fig. 4.2: Error dynamics represented as a nonlinear feedback system

It is assumed that the disturbances term $d(x_r,t)$ due to the unmodelled dynamics is rapidly varying therefore, the stability of the system is proven by using the Lyapunov equation method which is given in Appendix 3. The Lyapunov function can be written for SISO plant as below

$$V(x_e, \Phi) = x_e^T P x_e + \frac{1}{b_1 \alpha} \Phi^T \Phi \tag{4.119}$$

Equation (4.119) is positive for all $x_e \neq 0$ and $\Phi \neq 0$ since P is a symmetric positive definite matrix and $(b_1 \alpha)$ is positive scalar. For the sake of simplicity $V(x_e, \Phi)$ is denoted by V in the following section

$$\frac{dV}{dt} = \dot{x}_e^T P x_e + x_e^T P \dot{x}_e + \frac{2\dot{\Phi}^T \Phi}{b_1 \alpha}$$

$$= \left(A_m x_e - b w^T \Phi - w^T \Psi\right)^T P x_e + x_e^T P\left(A_m x_e - b w^T \Phi - b w^T \Psi\right) + \frac{2}{b_1 \alpha} \dot{\Phi}^T \Phi$$

$$\frac{dV}{dt} = \left(-\Psi^T w b^T - \Phi^T w b^T + x_e^T A_m^T\right) P x_e + x_e^T P\left(A_m x_e - b w^T \Phi - b w^T \Psi\right) + \frac{2}{b_1 \alpha} \dot{\Phi}^T \Phi \qquad (4.120)$$

$$= - x_e^T Q x_e - 2 b_1 \beta x_e^T P b b^T P x_e w^T w$$

The above equation is rearranged by using (4.113), (4.4), (4.6) and (4.25) as follows:

$$\frac{dV}{dt} = -x_e^T Q x_e - 2 b_1 \beta x_e^T P b b^T P x_e w^T w - 2 x_e^T P b d_1 \qquad (4.121)$$

where, Q is positive definite and $Pbb^T P$ is positive. The Lyapunov equation will be satisfied provided that (4.121) is negative in the x_e space. Then, using norm $\dot{V}$ can be written as follows

$$\dot{V}(x_e, \Phi) \le -\lambda_{\min}(Q)\|x_e\|^2 + 2\|x_e\|\lambda_{\max}(P)|d_1| \qquad (4.122)$$

From (4.113) $\|b\| = 1$

It was shown in [12] that if $\|x_e\| \ge \frac{2\lambda_{\max}(P)|d_1|}{\lambda_{\min}(Q)}$, then $\dot{V}$ is negative and x_e will be in the hypersphere stability region Λ determined by:

$$\Lambda = \left\{ x_e \ \mathbf{R}^n / \|x_e\| \le \frac{2\lambda_{\max}(P)|d_1|_{\max}}{\lambda_{\min}(Q)} \right\} \qquad (4.123)$$

where $|d_1|_{\max}$ is the maximum value of $|d(x_r, t)|$ and $\lambda_{\max}(P)$, $\lambda_{\min}(Q)$ are the largest and the smallest eigenvalues.of P and Q, respectively.

A SISO plant is represented in the reduced order MCS control by reduced order plant parameters together with the unmodelled and unknown dynamics which are assumed as disturbances acting on the system.

4.6.1.1 - Derivation of a Lyapunov Equation in the Case of ESH Materials Testing Machine

The plant has a second order transfer function during normal operation: under load control, the supply pressure is 13.8 MPa. The MCS control algorithm is implemented on the machine in a reduced first order form. Therefore, the plant is described by a first order model including some unmodelled dynamics which are assumed acting on the system as a part of disturbances. In the case of the ESH materials testing machine an arbitrary 'weighting' matrix chosen as $Q = [1]$, for a given settling time, t_s = 0.35 s and the positive definite matrix P, which is a solution to the Lyapunov equation, is found to be

$$P = [0.0438]$$

Equation (4.121) can be written in the case of the ESH materials testing machine as

$$\frac{dV}{dt} = -x_{e1}^T[1]x_{e1} - 2b_1\beta x_{e1}(0.0438)(0.0438)x_{e1}w^T w - 2x_{e1}^T(0.0438)d_1 \qquad (4.124)$$

where $x_e = [x_{e1}] = [x_e]$, $b_1 = 1$, $w = \begin{bmatrix} x_r \\ r \end{bmatrix}$, $\beta = 0.001$

Then (4.124) can be rewritten as

$$\frac{dV}{dt} = -x_e^2 - 3.8369 \times 10^{-6} x_e^2\left(x_r^2 + r^2\right) - 0.0876 x_e d_1 \qquad (4.125)$$

In this equality $-x_e^2$ and $-x_e^2\left(x_r^2 + r^2\right)$ are negative definite terms. Therefore, if $d_1 = 0$ then the first derivative of the Lyapunov function (4.124) is strictly negative; hence asymptotic stability is assured. When d1 $\neq$ 0, it was shown in [12] that a residual tracking error is present whose estimate is given by

$$\|x_e\| \leq 0.0876|d_1| \qquad (4.126)$$

From (4.125), it is observed that if $\|x_e\| \geq 0.0876|d_1|$, then $\dot{V}$ is negative. It can be concluded that x_e enters the hypersphere region Λ defined by:

$$\Lambda = \left\{ x_e \ \mathbf{R}^n / \|x_e\| \leq 0.0876|d_1|_{\max} \right\} \qquad (4.127)$$

where $|d_1|_{\max}$ denotes the maximum value of $|d(x_r, t)|$.

As it is shown above the Lyapunov's method is used to prove the stability of the reduced first order ESH materials testing machine.

4.6.1.2 - Derivation of a Lyapunov Equation in the Case of the Electrohydraulic Actuator Plant

The plant has a third order transfer function in normal operation (accumulators on, supply pressure 110 bar). The MCS control is implemented in a second order SISO form. In fact, the plant is higher order than MCS. It has been observed that MCS possesses a degree of robustness to mismatches in orders, e.g. [12], [13]. The plant can be described by a second order transfer function together with a disturbance term due to the unmodelled terms and nonlinearities in the plant as shown below

$$\begin{bmatrix}\dot{x}_1\\ \dot{x}_2\end{bmatrix}=\begin{bmatrix}0 & 1\\ 0 & a_1\end{bmatrix}\begin{bmatrix}x_1\\ x_2\end{bmatrix}+\begin{bmatrix}0\\ 1\end{bmatrix}u+\begin{bmatrix}0\\ d_1\end{bmatrix} \tag{4.128}$$

An arbitrary "weighting" matrix was chosen as $Q=\begin{bmatrix}10 & 0\\ 0 & 1\end{bmatrix}$ and for a given settling time, $t_s = 0.25$ s a positive definite matrix to the Lyapunov equation solution, P was where

$$P=\begin{bmatrix}4.7812 & 0.0195\\ 0.0195 & 0.0162\end{bmatrix}$$

From (4.121), the Lyapunov function for the electrohydraulic actuator plant can be written as

$$\begin{aligned}\frac{dV}{dt}=&-\begin{bmatrix}x_{e1} & x_{e2}\end{bmatrix}\begin{bmatrix}10 & 0\\ 0 & 1\end{bmatrix}\begin{bmatrix}x_{e1}\\ x_{e2}\end{bmatrix}\\ &-2b_1\beta\begin{bmatrix}x_{e1} & x_{e2}\end{bmatrix}\begin{bmatrix}4.7812 & 0.0195\\ 0.0195 & 0.0162\end{bmatrix}\begin{bmatrix}0\\ 1\end{bmatrix}\begin{bmatrix}01 & 1\end{bmatrix}\begin{bmatrix}4.7812 & 0.0195\\ 0.0195 & 0.0162\end{bmatrix}\\ &\begin{bmatrix}x_{e1}\\ x_{e2}\end{bmatrix}\begin{bmatrix}x_1 & x_2 & r\end{bmatrix}\begin{bmatrix}x_1\\ x_2\\ r\end{bmatrix}-2\begin{bmatrix}x_{e1} & x_{e2}\end{bmatrix}\begin{bmatrix}4.7812 & 0.0195\\ 0.0195 & 0.0162\end{bmatrix}\begin{bmatrix}0\\ 1\end{bmatrix}d_1\end{aligned} \tag{4.129}$$

The adaptive weight β was $\beta = 0.0001$, then (4.129) becomes

$$\begin{aligned}\frac{dV}{dt}=&-\left(10x_{e1}^2+x_{e2}^2\right)-0.0002\left(0.0195x_{e1}+0.0162x_{e2}\right)^2\left(x_1^2+x_2^2+r^2\right)\\ &-\left(0.0390x_{e1}+0.0324x_{e2}\right)d_1\end{aligned} \tag{4.130}$$

In (4.130), $-\left(10x_{e1}^2+x_{e2}^2\right)$ and $-0.0002\left(0.0195x_{e1}^2+0.0162x_{e2}^2\right)^2\left(x_1^2+x_2^2+r^2\right)$ are negative definite. If $d_1 = 0$, then the first derivative of the Lyapunov function (4.130) is

strictly negative, hence asymptotic stability assured. When $d_1 \neq 0$, then a residual tracking error is presented by

$$\|x_e\| \leq 0.9562|d_1|_{\max} \tag{4.131}$$

From (4.131), it is observed that if $\|x_e\| \geq 0.9562|d_1|$, then $\dot{V}$ is negative. It can be concluded that x_e enters the hypersphere region Λ defined by:

$$\Lambda = \{x_e \ \mathbb{R}^n / \|x_e\| \leq 0.9562|d_1|_{\max} \ \} \tag{4.132}$$

where $|d_1|_{\max}$ denotes the maximum value of $|d(x_r,t)|$. The stability of the reduced second order electrohydraulic actuator plant is proved by Lyapunov equation method.

4.6.2 - Derivation of the Lyapunov Equation in the Case of MIMO Systems

As for SISO plants, Lyapunov functions can be used in the case of the reduced order MIMO MCS control systems stability analysis. The general structure of the reduced order MIMO systems was given in section 4.5.2. Consider (4.80) with $d(x_r,t) = 0$ and with the reference input elements slowly varying, then the error equation (4.86) with the multivariable MCS law of (4.93) is rewritten as:

$$\dot{x}_e = A_m x_e - B_r \Phi W - B_r \Psi W \tag{4.133}$$

where B_r and A_m matrices are given in (4.80a) and (4.82a) respectively. Furthermore, Φ, Ψ and W are defined as:

$$\Phi = \begin{bmatrix} \Phi_1 & \Phi_2 & \dots & \Phi_k \end{bmatrix}^T$$

with

$$\Phi_p = \left[b_{pp} \int_0^t \alpha_{pi} y_{ph} x_i d\tau + a_{mpi} - a_{pi}, \dots, \quad b_{pp} \int_0^t \alpha_{pj} y_{ph} r_{pj} d\tau + b_{mpj} \right]^T \tag{4.134}$$

$$p = (1,\dots,k) \qquad i = (1,\dots,h) \qquad j = (1,\dots,k)$$

$$\Psi = \begin{bmatrix} \Psi_1 & \Psi_2 & \dots & \Psi_k \end{bmatrix}^T$$

$$\Psi_p = \left[b_{pp} \beta_{pi} y_{ph} x_r^T, b_{pp} \beta_{pj} y_{ph} r^T \right] \tag{4.135}$$

$$W = \left[x_r^T, \quad r\right]^T \tag{4.136}$$

In order to satisfy the Lyapunov equation, the feedforward transfer function matrix $C_e[SI - A_m]^{-1} B_r$ must be strictly positive real. Hence, by using Kalman-Yakubovitch lemma, we obtain

$$\begin{bmatrix} y_{1n} \\ y_{2n} \\ \vdots \\ y_{kh} \end{bmatrix} = B_r^T P x_e = C_e x_e \tag{4.137}$$

where P is the solution to the Lyapunov equation

$$\begin{aligned} &A_m^T P + P A_m = -Q \\ &P > 0 \\ &Q > 0 \end{aligned} \tag{4.138}$$

Subsequently, the matrices Φ, Ψ are written as:

$$\dot{\Phi} = \Gamma_\alpha B_r^T P x_e W^T \tag{4.139}$$

$$\Psi = \Gamma_\beta B_r^T P x_e W^T \tag{4.140}$$

where

$$\Gamma_\alpha = \begin{bmatrix} \alpha_1 b_{11} & 0 & \cdots & 0 \\ 0 & \alpha_2 b_{22} & 0\cdots & \vdots \\ \vdots & \vdots & \ddots & 0 \\ 0 & \cdots & 0 & \alpha_k b_{kk} \end{bmatrix}$$

$$\Gamma_\beta = \begin{bmatrix} \beta_1 b_{11} & 0 & \cdots & 0 \\ 0 & \beta_2 b_{22} & 0\cdots & \vdots \\ \vdots & \vdots & \ddots & 0 \\ 0 & \cdots & 0 & \beta_k b_{kk} \end{bmatrix}$$

From (4.133), the Lyapunov function is defined as

$$V(\Phi, x_e) = x_e^T P x_e + \sum_{p=1}^{k} \frac{1}{\alpha_p b_{pp}} \Phi_p^T \Phi_p \tag{4.141}$$

For the asymptotic hyperstability, all p (p = 1, ...,k) should satisfy following condition, $\alpha_p b_{pp} > 0$. When differentiating (4.141) along the trajectories (4.133), we obtain

$$\dot{V} = \dot{x}_e^T P x_e + x_e^T P \dot{x}_e + 2\sum_{p=1}^{k} \frac{1}{\alpha_p b_{pp}} \dot{\Phi}_p^T \Phi_p$$
$$= \left(-W^T \Psi^T B^T - W^T \Phi^T B^T + x_e^T A_m^T\right) P x_e + \qquad (4.142)$$
$$x_e^T P\left(A_m x_e - B\Phi W - B\Psi W\right) + 2\sum_{p=1}^{k} \frac{1}{\alpha_p b_{pp}} \dot{\Phi}_p^T \Phi_p$$

By using (4.138), (4.139) and (4.140) the above equation is simplified to:

$$\dot{V} = -x_e^T Q x_e - 2W^T W x_e^T P B \Gamma_\beta^T B^T P x_e \qquad (4.143)$$

where $PB\Gamma_\beta^T B^T P$ is positive semidefinite matrix. In (4.143) the terms, $-x_e^T Q x_e$ and $-W^T W x_e^T P B \Gamma_\beta^T B^T P x_e$ are a negative definite and a negative semidefinite respectively. Indicating that $\dot{V}$ is always negative in the x_e space, provided that $x_e \neq 0$ and x_e, Φ are bounded, then

$$\int_0^\infty \dot{V} dt < \infty$$

Let us consider (4.133), if $\dot{x}_e$ is bounded then x_e is uniformly continuous, hence $\dot{V}$ is uniformly continuous and following we have

$$\lim_{t\to\infty} \dot{V} = 0, \quad \lim_{t\to 0} x_e = 0, \quad \lim_{t\to 0} \Phi = 0$$

The above results indicate that the Lyapunov equation method guaranteed the stability of the reduced order MIMO MCS control in the presence of rapidly varying disturbances due to the unmodelled dynamics, plant parameters change and nonlinearities in the plant.

4.7 - CONCLUSIONS

In this chapter the stability of the reduced order MCS algorithm has been proven for SISO and MIMO plants. The reduced order MCS is considered as the standard MCS control in which the controlled plant contains some unmodelled dynamics and the unmodelled dynamics is treated as a part of the disturbances term which is acting on the system. Therefore, disturbances have a crucial importance in the case of the reduced order MCS algorithm stability analyses.

In the first section, disturbances due to unmodelled dynamics are considered slowly varying (maybe the plants are over parameterised), hence parameters variation are

very slow, almost insignificant. In this case the stability of the systems are proven by Popov's hyperstability theory. In the second section the disturbances due to unmodelled dynamics are considered as rapidly varying and a Lyapunov function is proposed to prove the hyperstability of SISO and MIMO systems.

It has been proven in both cases MCS guarantees the hyperstability of the reduced order plant. In practice MCS appears to be quite insensitive and robust to mismatches in orders. The stability of the reduced second order MCS control in the case of the electrohydraulic actuator plant is proven both by Popov's hyperstability theory and the Lyapunov function. Similarly, the stability of the reduced first order MCS control is proven in the case of the electrohydraulic ESH materials testing machine by using both methods.

In practice, the order of systems are limited. Most of the systems have an order less than 5. The MCS control can be very effectively implemented in only first or second order form hence, in many cases the reduced order models are maximum 2 or 3 degrees lower order than the estimated original plant model.

The adaptive system with higher order unmodelled dynamics are gain sensitive and even small disturbances can cause instability. To overcome instability problem in the case of the reduced order MCS, the adaptive weights (α and β) should not be increased beyond a certain point. The larger adaptive weights will activate the higher order unmodelled part of the system and this could lead a instability. In addition, if the reference signal is rich in high frequency content this will also excite higher order dynamics of the system.

In practice, using the reduced order MCS control has several advantages as follows: Firstly most of the systems work in the low or mid frequency range, therefore implementing lower order controllers or modelling systems with a lower order model can be very effective since the high order dynamics of the system are not contributing much into the plant output response. Secondly, if the system model is more than 5^{th} order the implementation of the controller can be computationally very cumbersome and it may not give a sensible result due to the fact that the plant is over parameterised. Thirdly, the implementation of the reduced order MCS controller is very easy and it does not require lower order plant parameters for implementation. In the case of the reduced order MCS control implementation, the control scheme uses a reference model which is lower order

than the estimated nominal plant model and the reference model matches the dominant part of the plant in order.

It can be concluded that in practice initial states, parameters and disturbances can not be beyond certain bounds, therefore it is not necessary to guarantee stability beyond these bounds and it has been proven that the reduced order MCS is robust in the presence of bounded disturbances due to the unmodelled dynamics, plant parameter changes and nonlinearities in the plant.

REFERENCES

[1]- **KREISSELMEIER, G.** "On Adaptive State Regulation," *IEEE Transaction on Automatic Control*, Vol. AC-27, February 1982.

[2] - **JOHNSON, C. R., & M. S. BALAS**, "Reduced Order Adaptive Controller Studies," *Proc. of Joint Automatic Control Conference*, San Francisco, CA, August 1980.

[3] - **ROHRS, C. E., L. S. VALAVANI & M. ATHANS**, " Convergence Studies of Adaptive Control Algorithms," Part I: Analysis, *Proc. 19th IEEE Conf. on Decision and Control*, Albuquerque, NM, December 1980.

[4] - **ROHRS, C. E., L. S. VALAVANI, M. ATHANS, & G. STEIN**, "Analytical Verification of Undesirable Properties of Direct Model Reference Adaptive Control Algorithms," *Proc. 20th IEEE Conf. on Decision and Control*, San Diego, CA, December 1981.

[5] - **MORGAN, A. P. & K. S. NARENDRA**, "On the Uniform Asymptotic Stability of Certain Linear Nonautonomous Differential Equations," *SIAM J. Control and Optimisation*, Vol. 15, No. 1, pp. 5-24, January 1977.

[6] - **ANDERSON, B. D. O.**," Exponential Stability of Linear Equations Arising in Adaptive Identification," *IEEE Trans. on Automatic Control*, Vol., AC-22, pp. 83-88, February 1977.

[7] - **YUAN, J. C. & W. M. WONHAM**, " Probing Signals for Model Reference Identification," *IEEE Trans. on Automatic Control*, pp. 530-538, August 1977.

[8] - **STOTEN, D. P. , & BENCHOUBANE, H.**, 'Robustness of a Minimal Controller Synthesis Algorithm', *International Journal of Control*, Vol. 51, No. 4, pp. 851-861,1990.

[9] - **POPOV, V. M.** , *Hyperstability of Control Systems*, Springer Verlag, Berlin, 1973.

[10] - **STOTEN, D. P.**, 'Discrete Adaptive Control of a Manipulator Arm', *Optimal Control Application and Methods*, Vol. 3, pp. 423-433, 1982, *Model Reference Adaptive Control, and the Control of Manipulators* (Taunton, U. K.: Research Studies Press), 1989.

[11] - **BENCHOUBANE, H.**, "*Investigations into a Minimal Controller Synthesis Algorithm*", PhD Thesis, Faculty of Engineering, University of Bristol, U. K., 1991.

[12] - **STOTEN, D. P.** "Implementation of MCS on a Servohydraulic Testing Machine", *Proc. I Mech. E-Part I, Journ. Sys Cont Eng.*, 206, No. 13, pp. 189 -194, 1992.

[13] - **STOTEN, D. P. & S. BULUT**, " Application of the MCS Algorithm to the control of an Electrohydraulic System", *Euriscon*, pp. 1861-1871, Malaga, Spain, August 1994.

CHAPTER 5

APPLICATION OF MCS TO AN ELECTROHYDRAULIC ACTUATOR PLANT TOGETHER WITH COMPARATIVE IMPLEMENTATION STUDIES

5.1 - INTRODUCTION

The purpose of this chapter is to present the results of the application of the Minimal Controller Synthesis (MCS) algorithm on an electrohydraulic actuator plant. The results obtained using the MCS algorithm are compared with those produced by Proportional Plus Derivative Feedback (P+DFB) control in the latter part of this chapter.

The aim of the MCS is to achieve excellent closed loop control despite the presence of plant parameter variations, external disturbances, plant nonlinearities and dynamic coupling within the plant, in a similar manner to MRAC.

The Minimal Controller Synthesis (MCS) algorithm has been shown to be effective in a number of diverse areas. The MCS algorithm is a good control strategy. In particular, this chapter shows how the algorithm is successfully applied to the control of an electrohydraulic actuator plant. The MCS algorithm appeared to be robust against the unknown plant dynamics, external disturbances and parameter variations within the plant.

In this chapter, the MCS is implemented in a second order reduced order form. In its nominal condition, the plant has a third order transfer function. For the electrohydraulic actuator plant, MCS can be recommended as a robust controller against the plant parameter changes, external disturbances and nonlinearities in the plant.

5.2 - THE ELECTROHYDRAULIC ACTUATOR PLANT

The electrohydraulic actuator plant consists of a hydraulic pump, a two-stage servo valve, two accumulators, a single rod actuator and a hydraulic arm in Fig. 2.1. The gas charged accumulators placed either side of the actuator have a high compliance and suppress high frequency supply pressure fluctuations at the servovalve resulting from high frequency fluctuations in the load flow.

The hydraulic pump can supply a maximum pressure of 172 bar. During the tests, the maximum pressure supplied by the hydraulic pump is limited to 110 bar. The constant pressure hydraulic power supply is an integral part of the actuation system, with flexible hoses connecting this power supply to the valves which direct the flow to the actuator. The electrohydraulic servovalve consists of a pilot spool valve and main spool, having an electrical feedback path to the servo amplifier.

From the system identification tests, it is found that the numerator term is a gain and this gain term is very sensitive to changes in operating conditions. The position error problem occurred when operating with a load force.

5.2.1 - The Actuator Linearization

From Newton's second law and Equation (2.9) (in Chapter 2) we can obtain:

$$A_p(P_1 - P_2) - f_s\dot{x} - T = m_p\ddot{x} \tag{5.1}$$

where f_s is the coefficient of friction, m_p is the mass of the hydraulic arm as shown in Fig. 2.1, F is the force on the actuator piston, A_p is the effective mean area of the actuator, and T is the force due to the mass of inertia which is comparable small therefore it can be neglected. The actuator is a single rod actuator therefore, the effective area of the first chamber is larger than the second one. The ratio of the effective area of the actuator chambers can be represented accurately by the relationship

$$A_1 = 0.86A_2 \tag{5.2}$$

and the effective mean area of the actuator, $A_{av} = \dfrac{A_1 + A_2}{2}$.

From equation (5.1), it follows that:

$$(P_1 - P_2) = \frac{1}{A_{av}}\left(m_p\ddot{x} + f_s\dot{x}\right) \tag{5.3}$$

Differentiating (5.3) with respect to time gives:

$$(\dot{P}_1 - \dot{P}_2) = \frac{1}{A_{av}}\left(m_p\dddot{x} + f_s\ddot{x}\right) \tag{5.4}$$

From Equations (2.2) and (2.3), the hydraulic flow equations

Flow in:

$$Q_1 = A_1\dot{x} + \frac{V_t\dot{P}_1}{N} \tag{5.5}$$

Flow out:

$$Q_2 = A_2\dot{x} - \frac{V_t\dot{P}_2}{N} \tag{5.6}$$

The tank pressure is assumed atmospheric hence, mean flow rate is

$$Q_f = A_{av}\dot{x} + \frac{V_{av}\left(\dot{P}_1 - \dot{P}_2\right)}{N} \tag{5.7}$$

where V_{av} is the average volume, $V_{av} = \frac{V_1 + V_2}{2}$. Although, the volume changes during the operation of the system it is assumed constant in this case for the sake of simplicity. From equation (5.4) and (5.7)

$$Q_f = A_{av}\dot{x} + \frac{V_{av}}{NA_{av}}\left(m_p\ddot{x} + f_s\ddot{x}\right) \tag{5.8}$$

Taking the Laplace transform of (5.8)

$$\frac{NA_{av}Q_f}{V_{av}m_p} = x\left(s^3 + \frac{f_s}{m_p}s^2 + \left(\frac{NA_{av}^2}{V_{av}m_p}\right)s\right) \tag{5.9}$$

which gives:

$$\frac{x}{Q_f} = \frac{\left(\frac{NA_{av}}{V_{av}m_p}\right)}{s^3 + \left(\frac{f_s}{m_p}\right)s^2 + \left(\frac{NA_{av}^2}{V_{av}m_p}\right)s} \tag{5.10}$$

The linear representation of the system is constructed from Equations (5.1), (5.3), (5.4), (5.7) and (5.10) as shown in Fig. 5.1.

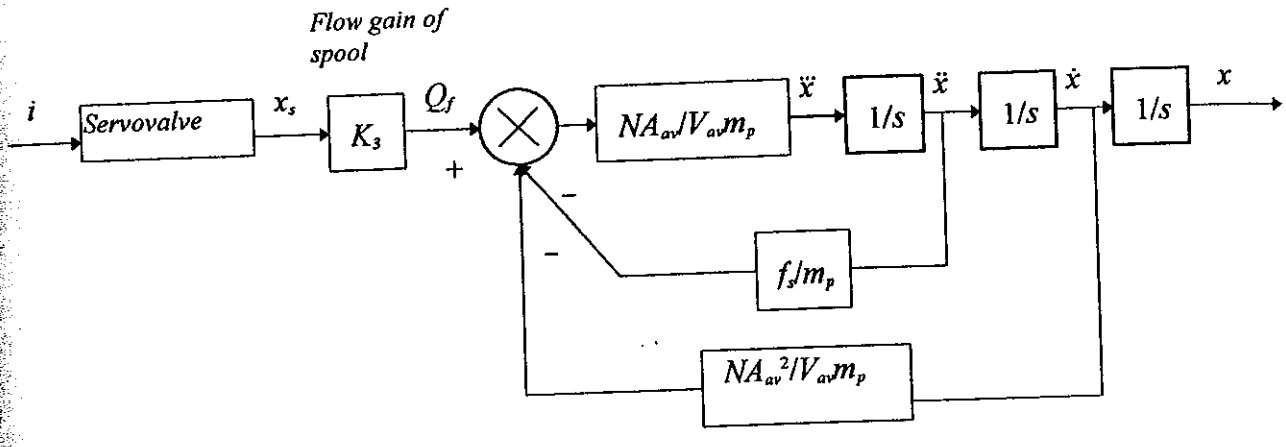

Fig. 5.1: Linear description of the electrohydraulic actuator plant.

The control flow, Q_f will change with valve sizing constant, electrical input current and pressure drop. These characteristics are modelled well by the theoretical square-root relationship for sharp-edged orifices:

$$Q_f = Ki\sqrt{P_v} \tag{5.11}$$

where K is the valve sizing constant, i is the input current to the servovalve and P_v is the pressure drop.

5.2.2 - Flow Control Servovalve (E760 Moog Valve)

The plant is actuated by a standard Moog E760 four way double acting servovalve which is operated by a torque motor/flapper. The servovalve is connected to the cylinder/actuator arm. In flow control servovalves under constant load the control flow is proportional to the electrical input current. The load pressures effect the flow of the servovalve as shown in Fig. 5.2. The centre of this plot is the null stability region in which the load effects is negligible.

Appropriate transfer functions for standard Moog E760 servovalve were given in [1]. The electrohydraulic servovalve has many nonlinear characteristics. In addition, many parts of the servovalve is so small therefore it is not easy to analyse.

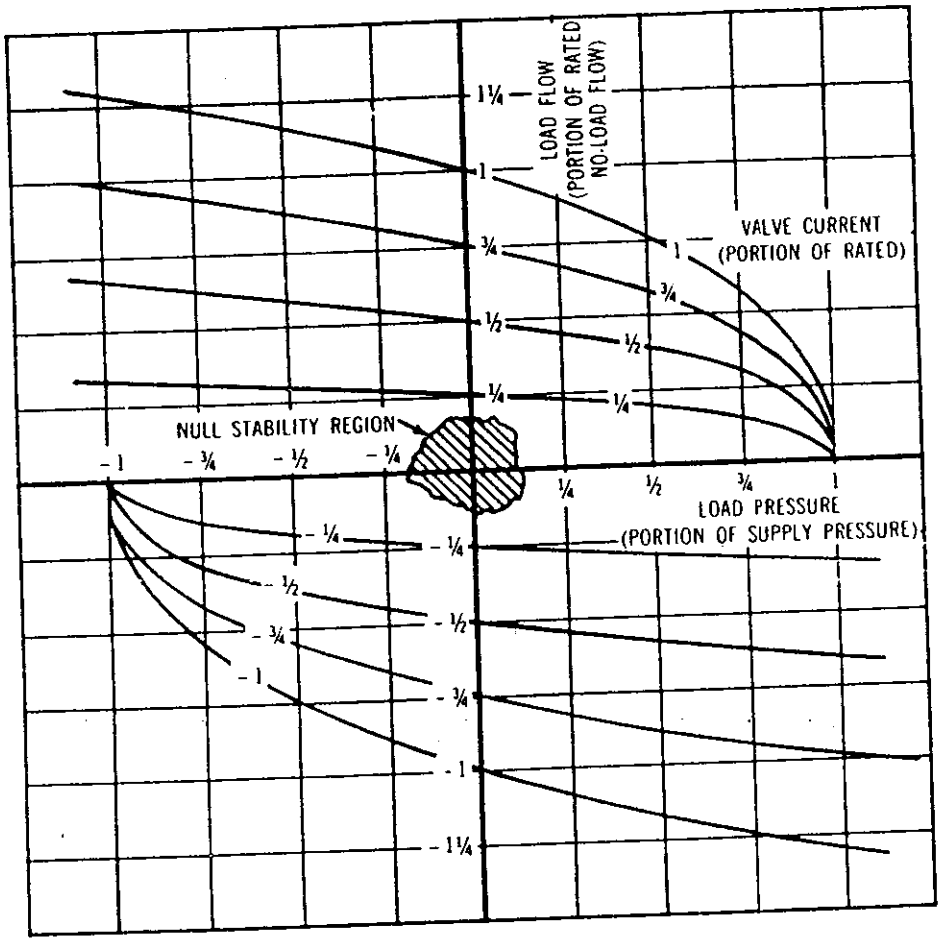

Fig. 5.2: Flow control servovalve (flow-load pressure)

The dynamic response of Moog flow control servovalve was described in the low frequency range by the following first order transfer function:

$$\frac{Q_f(s)}{i(s)} = K\left(\frac{1}{1+\tau s}\right) \tag{5.12}$$

where K is the servovalve static flow gain at zero load frequency drop and τ is the apparent servovalve time constant (seconds). In the mid frequency range, the servovalve was represented by a second order transfer function. Most of these transfer functions were linear, which approximated the response of actual servovalve when operating without saturation shown in Fig. 5.3.

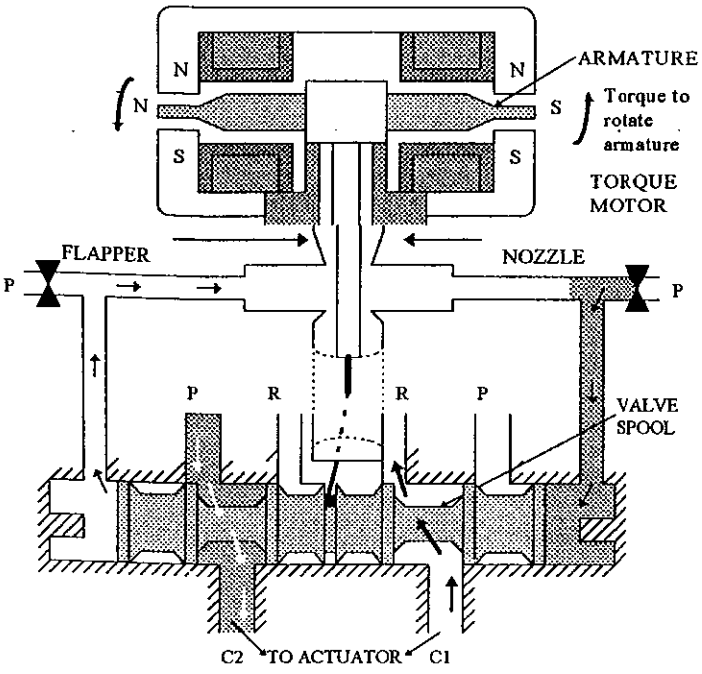

(a) Valve responding to change in electrical input

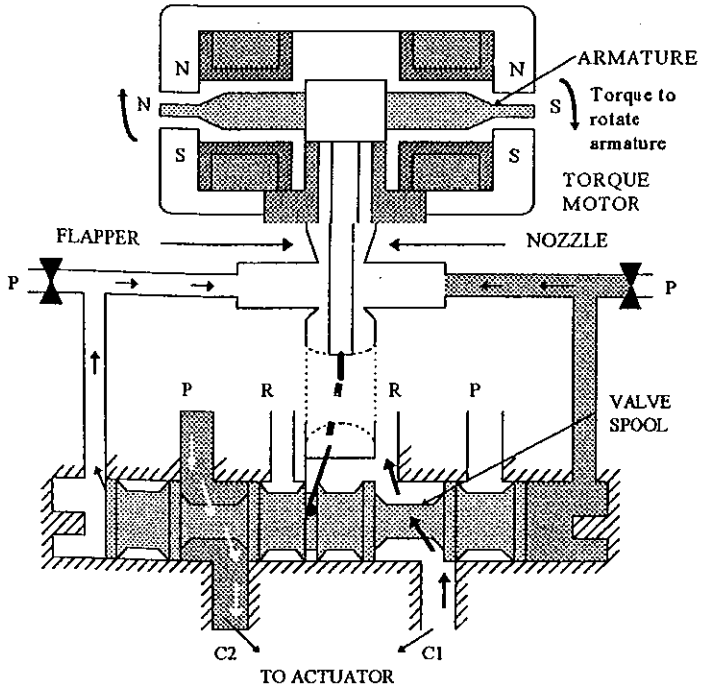

(b) Valve condition following change

Fig. 5.3: Torque motor and valve spool operation.

5.3 - LINEARIZATION OF THE SYSTEM

The electrohydraulic actuator plant contains significant nonlinear elements (servovalve, mass of the hydraulic arm). It is necessary to know a linearised representation of the plant for the design of a conventional fixed gain controller for the comparative test [2]. The transfer function of the plant can be written from the input/output relationship as:

$$G_p(s) = \frac{y(s)}{u(s)} = G_1(s)G_2(s) \tag{5.13}$$

where $G_1(s)$ is the actuator transfer function and $G_2(s)$ is the servovalve transfer function. Each part of the plant modelled as follows:

$$G_1(s) = \frac{\left(\frac{NA_{av}}{V_{av}m_p}\right)}{s^3 + \left(\frac{f_s}{m_p}\right)s^2 + \left(\frac{NA_{av}^2}{V_{av}m_p}\right)s} \tag{5.14}$$

$$G_2(s) = \frac{K_1}{\frac{s^2}{\omega_n^2} + \frac{2\zeta s}{\omega_n} + 1} \tag{5.15}$$

where K_1 is the servovalve gain, ω_n is the natural frequency, ζ is the damping coefficient of the servovalve, m_p is the mass of the actuator hydraulic arm, f_s is the coefficient of friction of the actuator cylinder, V_{av} is the average volume of the cylinder and N is the bulk modulus of the hydraulic oil.

As a result of this description, the linearised model of the plant is of 5th order, including a free integrator. In this case various further simplifications can justifiably be made. For instance, the pole of the $G_2(s)$ is typically much faster than those of $G_1(s)$, so that the plant can be modelled by a 3rd order transfer function. Another possibility is in the low frequency range the servovalve can be represented by a first order transfer function therefore, the plant can be described by a 4th order model. And similarly, the relative locations of the servovalve and actuator arm poles can lead to 2nd order models with a free integrator.

5.4 - SYSTEM IDENTIFICATION TESTS

The system identification program is a part of the "WinCtrl". "WinCtrl" is a windows based controller software package developed by [3] and it runs under Windows 3.1. The software is very flexible, it allows the user to conduct the system identification tests on systems under conventional controllers or the MCS control. Controller hardware is a 386 PC machine equipped with 12-bit D/A and A/D converters.

Several system identifications tests are conducted on the open loop plant, which yielded number of transfer function models for different operating conditions which are listed below:

[1] - Supply pressure 110 bar, accumulators on;

[2] - Supply pressure 110 bar, accumulators off;

The system identification tests are implemented on the plant under a proportional control using different amplitudes (low and high amplitudes) and frequency ranges (low and mid-frequency ranges).

Order	Condition [1]: 110 bar; Accum. on	Condition [2]: 110 bar; Accum. off
5	num=$5.6746\text{x}10^{6}$ den roots: 0;-7.9-j26;-7.9+j26; -24+j15;-24-j15	num=$1.31\text{x}10^{6}$ den roots: 0;-35+j25;-35-j25; -24;-3.2
4	num=$9.11\text{x}10^{4}$ den roots: 0;-15.5;-7.51+j22.9; -7.51-j22.9	num=$7.08\text{x}10^{4}$ den roots: 0;-4.32;-35.8+j23.1; -35-j23.1
3	num=$2.83\text{x}10^{3}$ den roots: 0;-8.80+j16; -8.80-j16	num=$17.9\text{x}10^{3}$ den roots: 0;-40.9+j20.3; -40-j20.3
2	num=62.4 den roots: 0;-4.58	num=108 den roots: 0;-10.3

Table 5.1: Identified plant transfer function data.

The transfer function of the electrohydraulic actuator plant is found by a system identification test. The system is subjected to a swept sinusoidal input signal u, which

produced a corresponding output y under the proportional controller. The test signal was a swept sinusoidal signal of frequency 1 to 12 Hz and amplitude 1 Volt. The proportional controller gain was $k_p = 7$ and sampling interval $\Delta = 5$ ms. Hence, the system identification tests are carried out in mid-frequency range. In this way, the dominant part of the plant is modelled as the transfer functions of the system.

For Condition [1], the 5th order model poles are dominated by the conjugate pair at $s = 7.9 \pm j26$ for this reason the actuator arm poles at $s = -24 \pm j15$ may be ignored. Similarly the 4th order model poles are dominated by the conjugated pair at $s = 7.51 \pm j22.9$ so that the actuator arm pole at s = -15 can (as an approximation) be ignored. This ensures that the given 3rd order model is relevant in Condition [1] for the normal operation case.

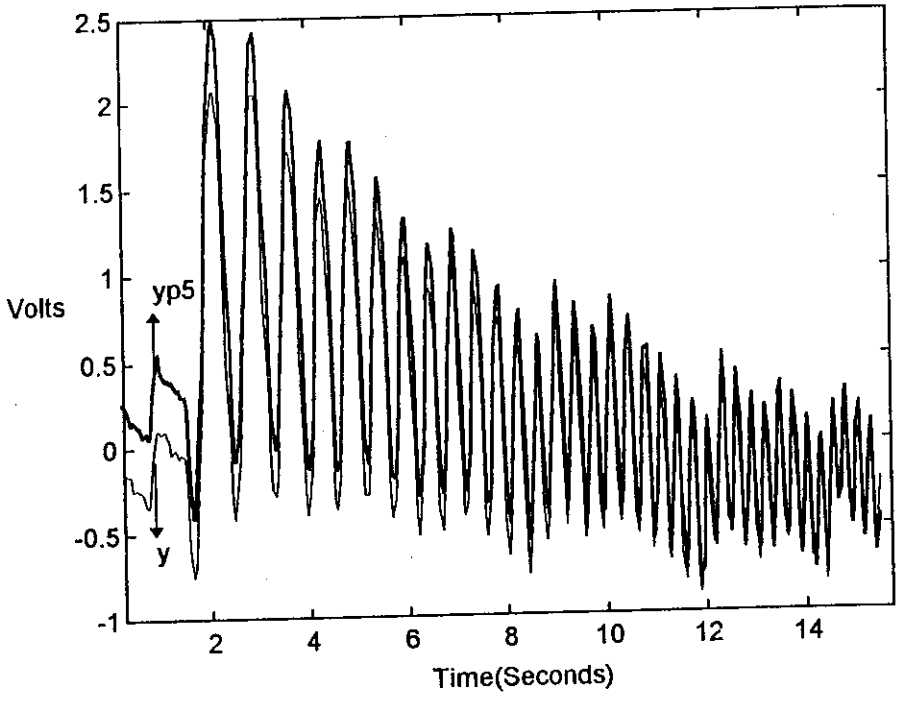

Fig. 5.4: Fifth order model (supply pressure is 110 bar, accumulators on)

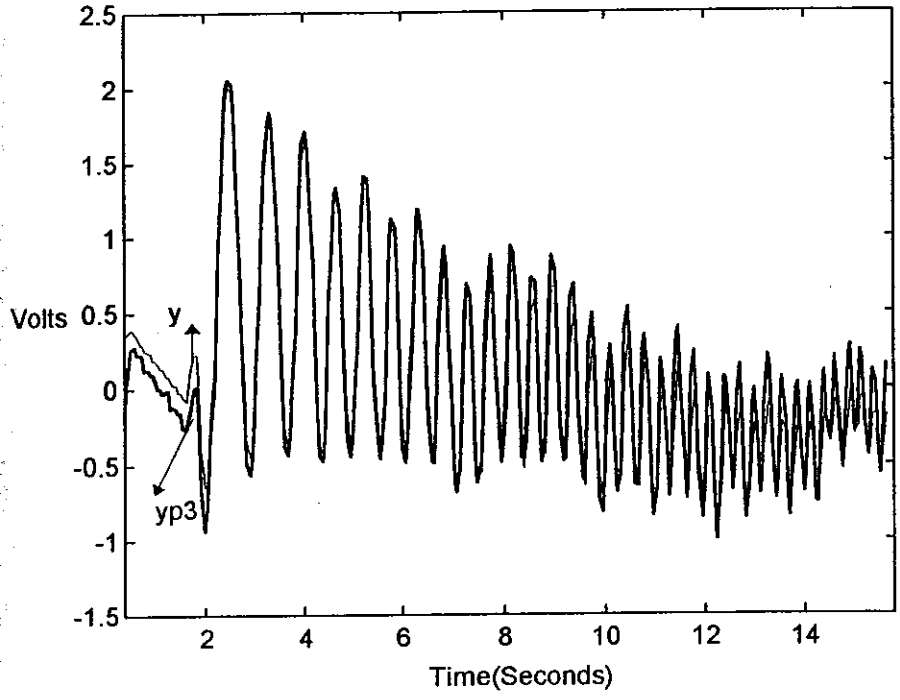

Fig. 5.5: The nominal third order plant model (supply pressure is 110 bar, accumulators on)

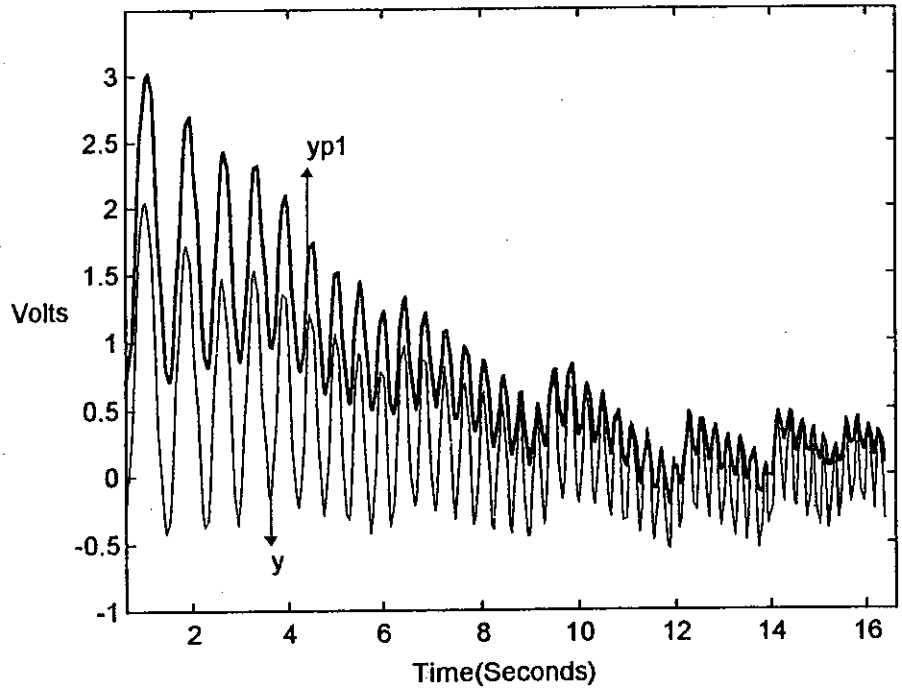

Fig. 5.6: The second order model (supply pressure is 110 bar, accumulators off)

For Condition [2], the given 2nd order model is a justifiable approximation of these condition dynamics. The fourth and fifth order models are not matched by any of these conditions, showing such models are over parameterised. It is observed that the plant has a nominal third order transfer function in the mid frequency range with a free integrator. Therefore the second order model which are derived from system identification tests can be considered as lower order models of the original system which is the most relevant approximation for condition [2].

It is possible to compare the reduced order models of the original plant which are derived from system identification tests with the models produced from linear model reduction methods. It is assumed that the second order model that is derived from system identification tests is a good second order approximation of the original plant therefore, it is compared with the lower second order models which are derived from linear model reduction methods in Chapter 3. It is observed that Routh stability of Pade´ method, dominant eigenvalue and frequency matching method, balancing method and stability equation method are produced second order models which are very close agreement with the second order model that is derived from system identification tests. This indicates that some of linear model reduction methods can be used very effectively in the case of producing lower order models from the nominal transfer function of the original plant. Hence, the reduced order models are derived without conducting system identification tests which are comparatively easy and need less time so, in many cases using linear model reduction methods may be preferable.

The plant dynamics are changed by changing the plant supply pressure and/or the accumulators settings. The plant has higher bandwidth when the accumulators are switched off. As it is shown in Fig. 5.7, the system is more stable when accumulators are switched off having higher bandwidth is the indication of it. Although, the plant is little more noisy when it is working in this condition still, it shows its full performances due to the fact the hydraulic fluid can be fully compress and the nonlinear effect of accumulator can be avoided when they are in off position.

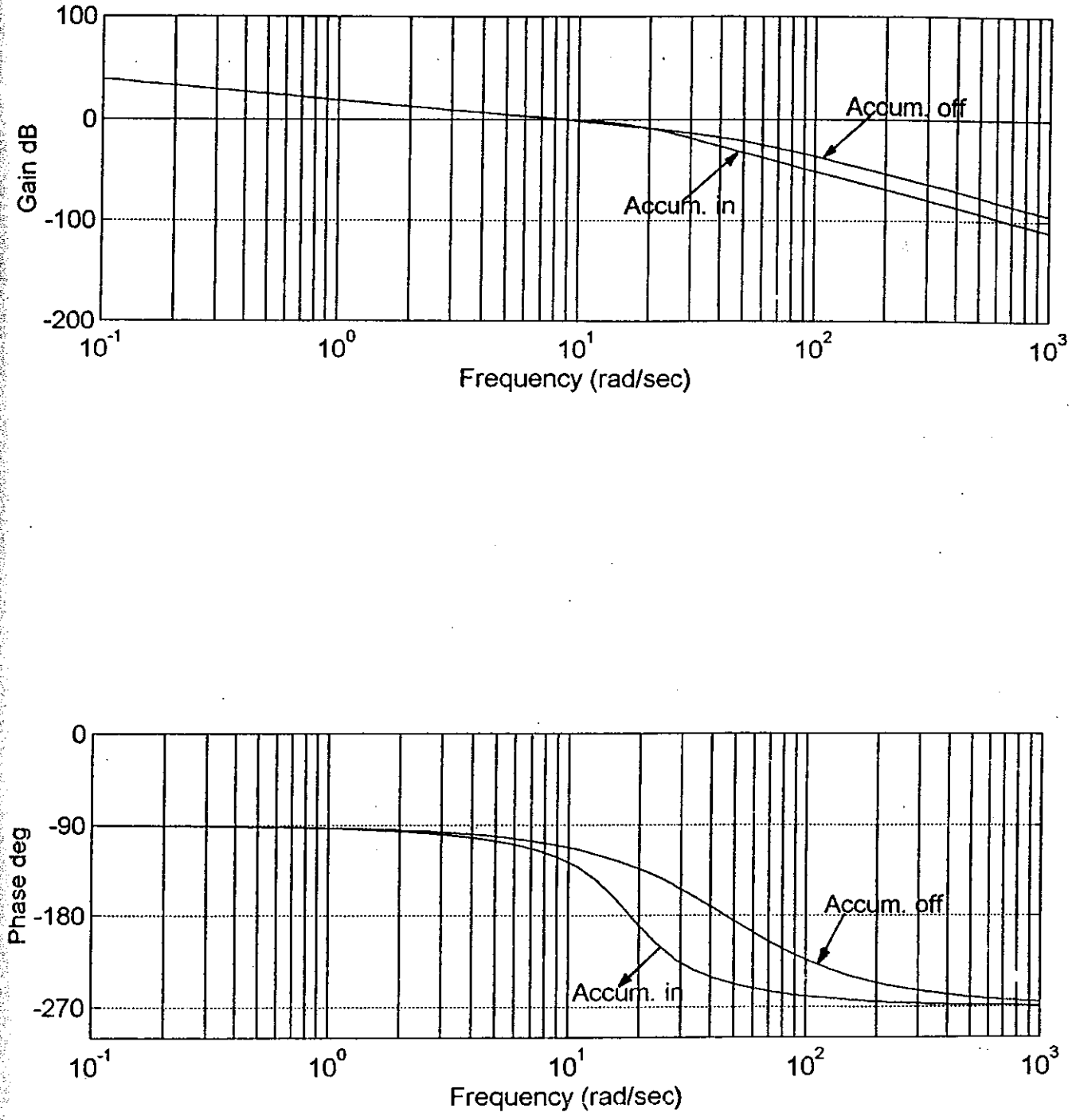

Fig. 5.7: The effect of the accumulators position on the system dynamics (on or off)

5.5 - IMPLEMENTATION OF CONTROLLERS

In this case the reference r is chosen as a square wave. "WinCtrl" software package is used to implement both the Proportional Plus Derivative Feedback control and the MCS control strategies.

During the experiments, the control problem is to ensure that the measured distance y closely tracks a given reference signal r, despite changes in servohydraulic characteristics.

5.5.1 - Proportional Plus Derivative Feedback Control (P+DFB)

Firstly, the Proportional Plus Derivative Feedback Control is implemented to control the electrohydraulic actuator rig. This control strategy requires knowledge of the plant dynamics, in the same way as do other conventional controllers. The third order model is chosen as the nominal (condition [1]) transfer function of the system and is shown in Fig. 5.8 (labelled 'Gp'), which indicates sufficient low frequency gain (the free integrator is the main reason), but a requirement to increase the margins (from 2.1 dB and 55°) and closed-loop bandwidth (from 10 rad/s). A P+DFB Controller is implemented with a proportional gain k_p = 1.0 and a derivative feedback gain k_d = 0.1. The resulting open loop transfer function plots are also shown in Fig. 5.8 (labelled 'GH'), which yield margins of ∞ dB and 61°, plus the bandwidth is raised to 18.2 rad/s. The closed-loop step response settling time is predicted to be $t_s \approx \frac{4}{(0.61 \times 18.2)} \approx 0.4$ s, with an oscillatory component containing approximately two overshoots, this is assumed to be an acceptable performance. The controller is implemented in discrete-time as follows:

$$u(k) = k_p e(k) - k_p k_d \left[y(k) - y(k-1) \right] / \Delta \qquad (5.16)$$

where $u(k)$ is the current control signal, $e(k)$ the current tracking error, $y(k)$ the current measured actuator arm position and Δ is the sampling interval.

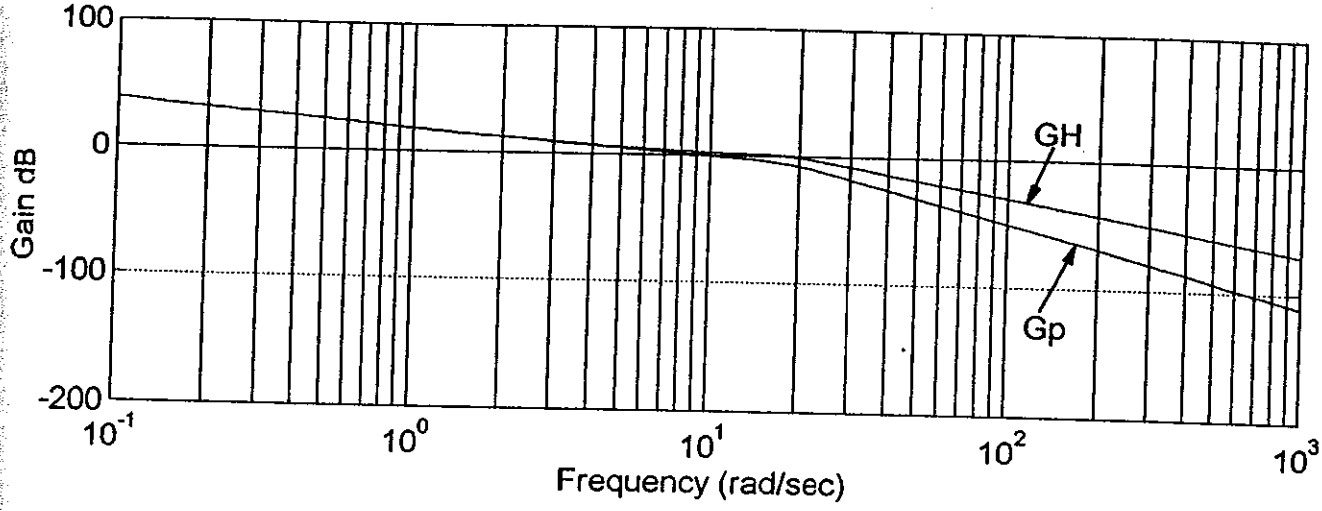

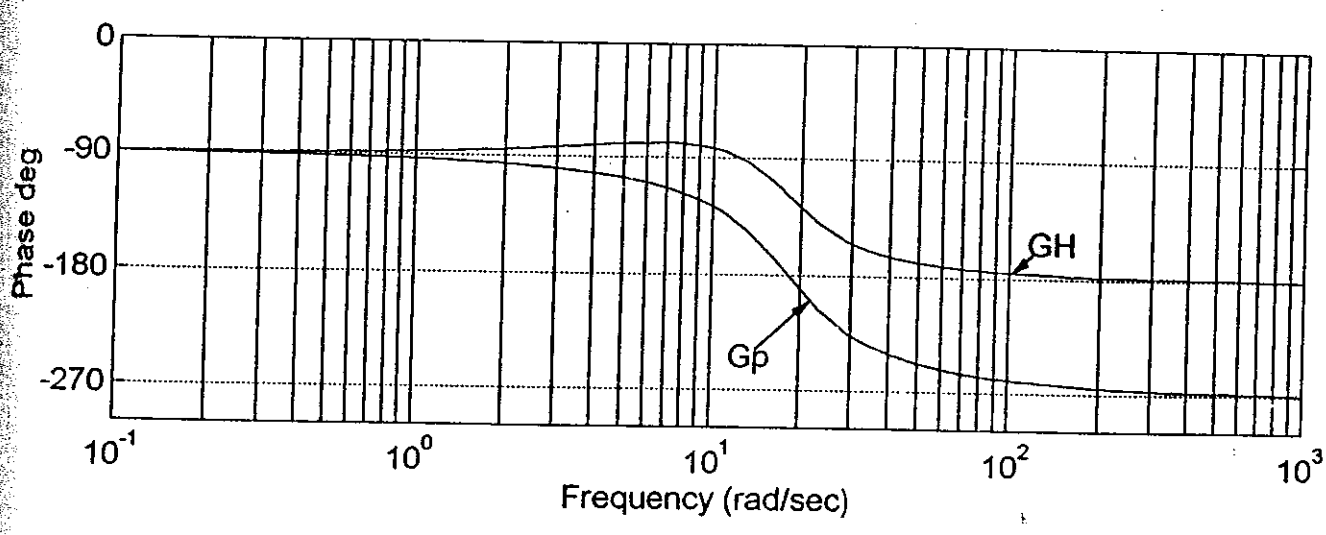

Fig. 5.8: Plant and plant controller (P+DFB) bode plots: Gp: plant;
GH: plant-controller

5.5.2 - The MCS Control

For the MCS case, the plant model is not required. The synthesis procedure commences with the derivation of a reference model equation. The reference model parameters $\{A_m, B_m\}$ are deduced from the settling time t_s together with zero steady-state errors. Firstly, an estimate is made of the nominal plant order and the order of the MCS algorithm matches this figure. The plant would normally expect to implement a 3rd-order algorithm. A third order MCS formulation would normally be necessary, since the plant is itself third order. The second order MCS reference model is used to control the system. The MCS control possesses a degree of robustness to such mismatches in orders. It is claimed that the reference model could even be removed from the design and the reference signal r could be fed directly into the adaption algorithm [4]. The second order MCS control is implemented to control the plant. The discrete-time second order MCS equations are: Second order MCS control equations (i =1,2) are summarised below, in discrete-time scalar form:

$$u(k) = k_r(k)r(k) + k_1(k)x_1(k) + k_2(k)x_2(k) \tag{5.17}$$

$$k_r(k) = k_r(k-1) + \beta y_e(k)r(k) - \sigma y_e(k-1)r(k-1) \tag{5.18}$$

$$k_i(k) = k_i(k-1) + \beta y_e(k)x_i(k) - \sigma y_e(k-1)x_i(k-1); \quad i = 1,2 \tag{5.19}$$

$$y_e(k) = \left(16/t_s^2\right)x_{e1}(k) + (4/t_s)x_{e2}(k) \tag{5.20}$$

$$x_{ei}(k) = x_{mi}(k) - x_i(k) \tag{5.21}$$

$$x_{mi}(k) = x_{mi}(k-1) + \Delta x_{m2}(k-1) \tag{5.22}$$

$$x_{m2}(k) = \left(-16\Delta/t_s^2\right)x_{m1}(k-1) + (1 - 8\Delta/t_s)x_{m2}(k-1) + \left(16\Delta/t_s^2\right)r(k-1) \tag{5.23}$$

where, $\sigma = \beta - \alpha\Delta$, where $\{\alpha, \beta\}$ are the adaptive weights, with a ratio of $\alpha/\beta = 10$ and $\alpha > 0$. The adaptive weights are chosen empirically. Values found to be suitable in this case are $\alpha = 0.001$ and $\beta = 0.0001$, the values having been deduced to be a good compromise between the speed of adaption and noise propagation. The values of $\{k_r, k_1, k_2\}$ are the adaptive forward, position and velocity gains, r is the reference signal, x_1 $(=y)$ is the measured actuator arm position, y_e is the output error, x_m is the reference

model states and t_s is the step response settling time of the reference model, $t_s = 0.25$ in the following tests together with the sampling interval, $\Delta = 5$ ms.

Second Order MCS Reference Model

Second order system can be describe as:

$$\ddot{x}_m + 2\zeta\omega_n^2\dot{x}_m + \omega_n^2 x_m = \omega_n^2 r \tag{5.24}$$

Here, ω_n is the natural frequency, ζ is the damping coefficient of the system, where $\zeta = 1$ (i.e., the critically damping) and $t_s = \dfrac{4}{\zeta\omega_n}$.

The reference model is

$$\dot{x}_m = A_m x_m + B_m r \tag{5.25}$$

where $A_m = \begin{bmatrix} 0 & 1 \\ -\omega_n^2 & -2\omega_n \end{bmatrix}$, $B_m = \begin{bmatrix} 0 \\ \omega_n^2 \end{bmatrix}$

The required closed-loop step response settling-time is $t_s = 0.25$. The reference model parameters are:

$$A_m = \begin{bmatrix} 0 & 1 \\ -256 & -32 \end{bmatrix}, \quad B_m = \begin{bmatrix} 0 \\ 256 \end{bmatrix}$$

The output error matrix is

$$C_e = \begin{bmatrix} 16/t_s^2 & 4/t_s \end{bmatrix}$$

$$C_e = \begin{bmatrix} 256 & 16 \end{bmatrix}$$

5.6 - COMPARATIVE IMPLEMENTATION TESTS

5.6.1 - Step Response Tests

In these cases the supply pressure is kept to 110 bar and accumulators were on-line. The conventional P+DFB Controller is implemented with the rig in the nominal condition (condition [1]) in steady state form. The result of the plant displacement is shown in Fig. 5.9. In this plot 'xm' is the desired response and 'x1' is the actual response of the system. There is good correspondence between the desired and actual responses apart from small steady-state errors due to the fact that the flow is proportional to the velocity of the actuator. In addition, the effect of other nonlinearities existing in the system such as, the spool valve stiction, the friction of the actuator and leakage of the plant.

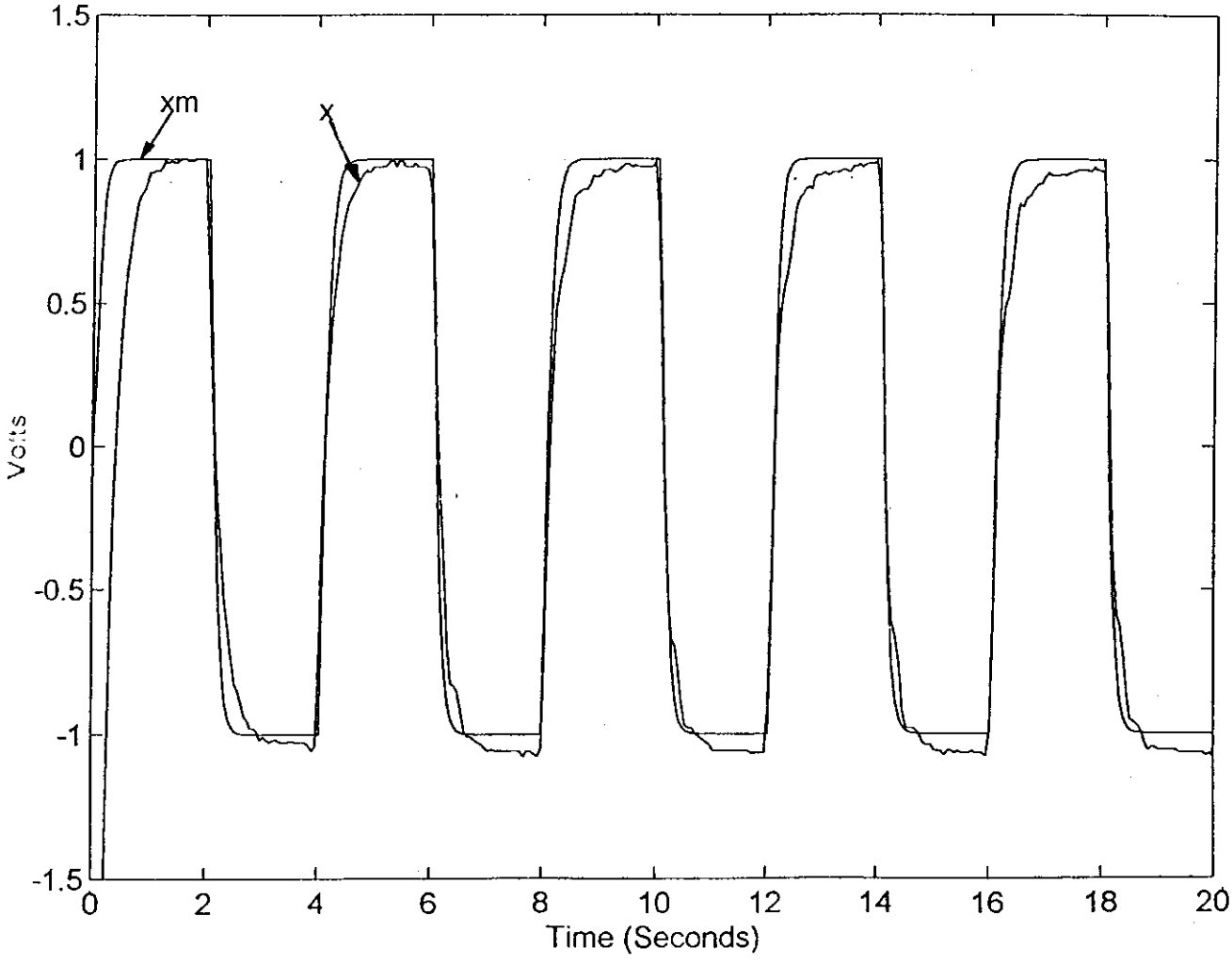

Fig. 5.9: P+DFB result for the nominal case (steady-state condition)

The result of the system under P+DFB control is shown in Fig. 5.9. The corresponding system responses under the MCS control are shown in Fig. 5.10a, b. There are no significant differences in response between the P+DFB case and the MCS. So, MCS matches the performance of this well-tuned conventional controller, without the need for system identification and controller synthesis.

This shows that the third order model and also P+DFB synthesis are well designed. The initial adaptive stage of the MCS control response is shown in Fig. 5.11a and the gains themselves are shown in Fig. 5.11b. One should note that in this case, for the MCS control, there is no requirement for the system identification and controller synthesis.

In the case of both controller there is a spike at the beginning of each step and following a steady state error due to the nonlinear relationship between the flow from the servovalve and the position of the actuator. The flow is proportional to the velocity of the hydraulic actuator arm. The plant responses in both cases is nonlinear due to nonlinear nature of the hydraulic systems such as, nonlinear behaviour of the hydraulic fluid, friction in the actuator and leakage in the system. Another nonlinearity in the system was the accumulators were on-line during the tests.

In case of both controllers the steady state error is positive when the piston of the actuator is extract and it is negative when it is retract position due to the nonlinear effects of the mass. The mass is rather heavy (6.7 kg) when the amplitude is negative the piston of the actuator is in the retract position and the mass of the hydraulic arm pushes the piston back in to the another end of the actuator forcefully beyond the demand signal. When the piston in the extract position the force due to the mass of inertia opposes against the load force.

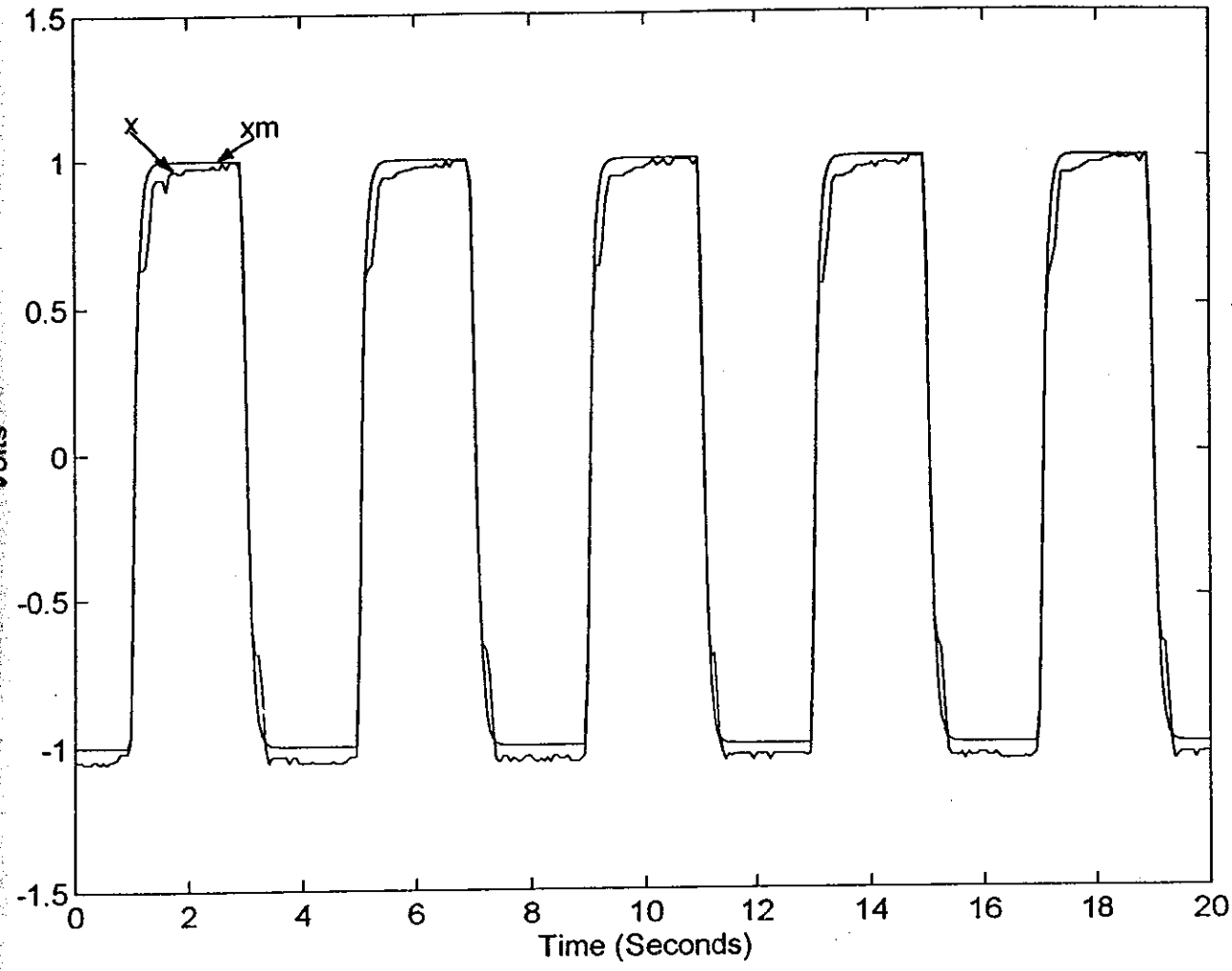

(a) Plant and reference model output

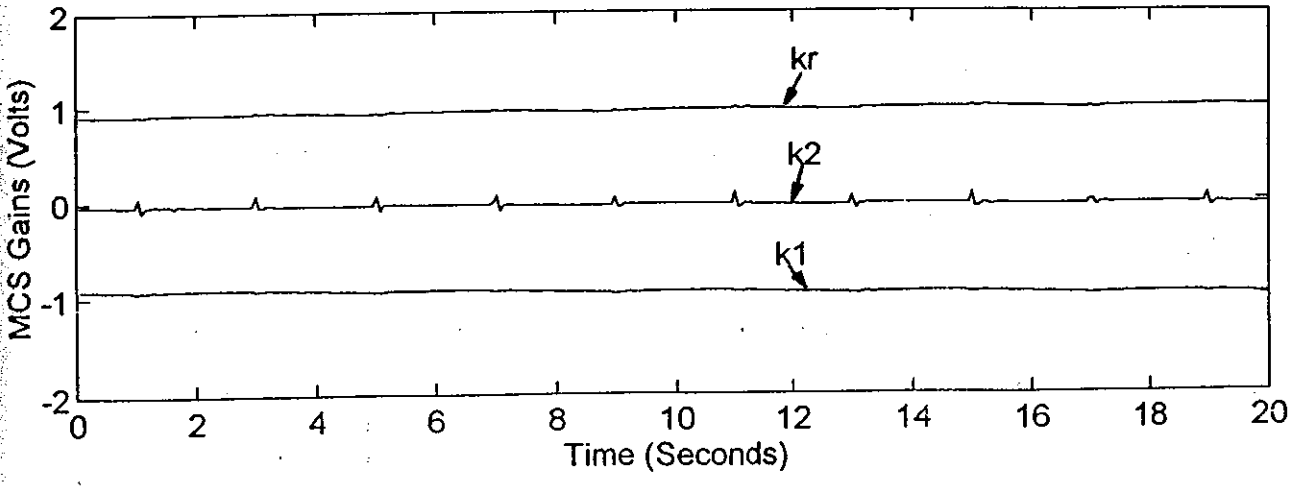

(b) MCS gains

Fig. 5.10: MCS step response for the nominal case (in steady-state condition)

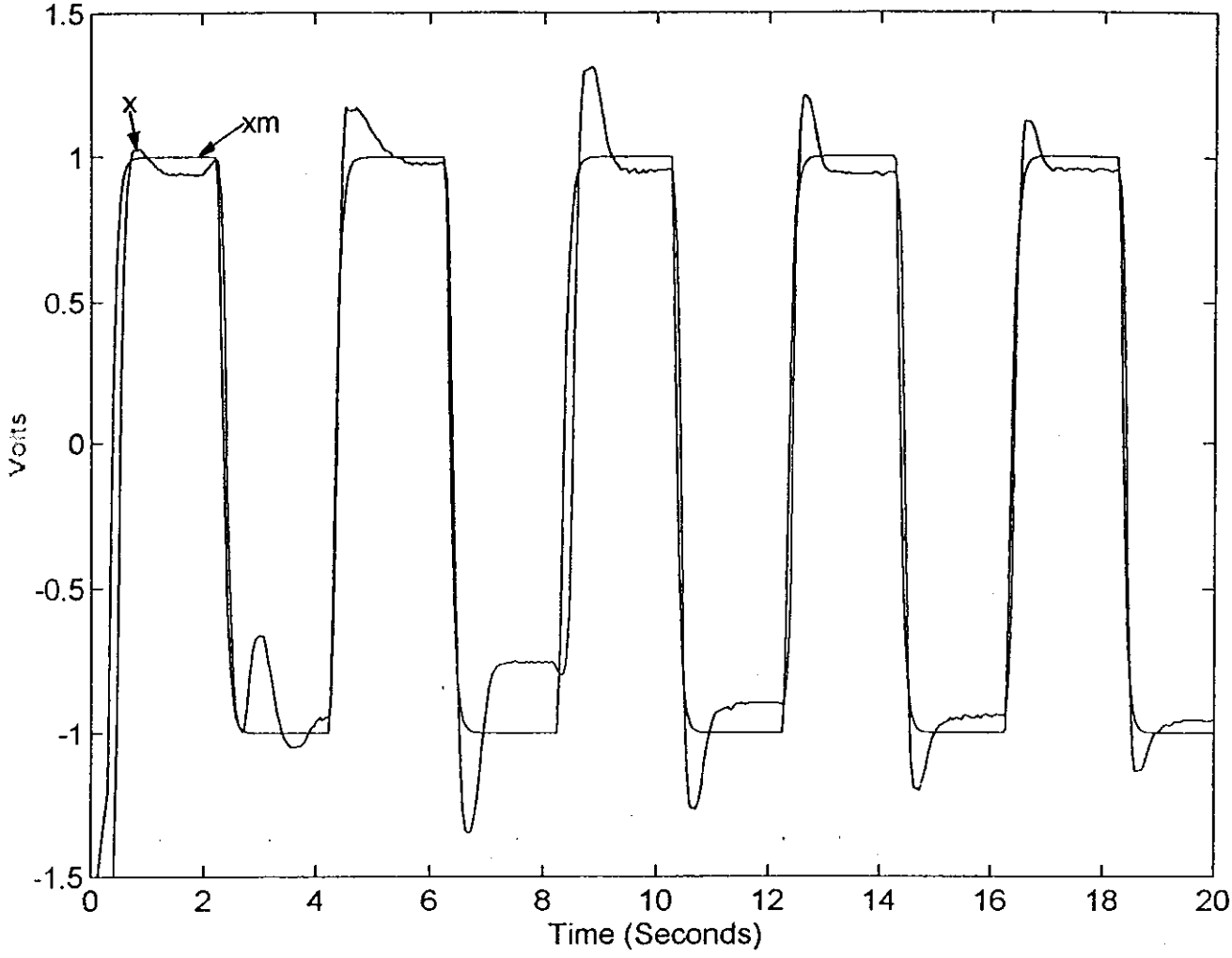

(a) Plant and reference model output

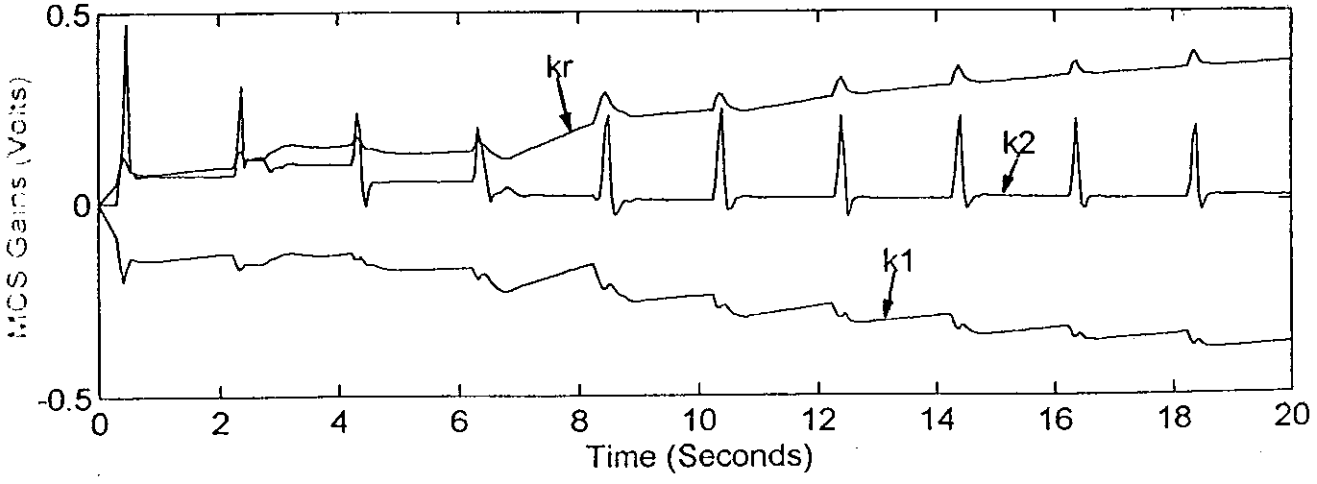

(b) Initial MCS control gains.

Fig. 5.11: Initial adaption for the nominal case of the MCS step response.

5.6.2 - Sinusoidal Tests; Condition [1] to [2]; Supply Pressure is 110 Bar; Accumulators Switched Off and On

Changing the accumulators to be suddenly off-line and then on-line again produces significant changes in the plant dynamics. The aim of this set of tests is to compare the efficiency of MCS in the face of such changes, when compared with the P+DFB controller.

The bandwidth of the closed-loop control system is an excellent measurement of the range of stability of the system. The plant has a reasonable high bandwidth when the accumulators are in the circuit. If the accumulators are switched on, then the plant responses to the sudden changes in the pressure, frequency an amplitude are rather smooth and less noisy compare to the condition in which the accumulators are switched off.

When the accumulators are switched off the plant has a larger bandwidth therefore it is more steady and the nonlinear effect of the accumulators are neglected. However, the plant responded to the sudden changes in the pressure, amplitude and frequency rather roughly together with noise. In addition, relatively large bandwidths mean that the settling time of the system is sufficiently small.

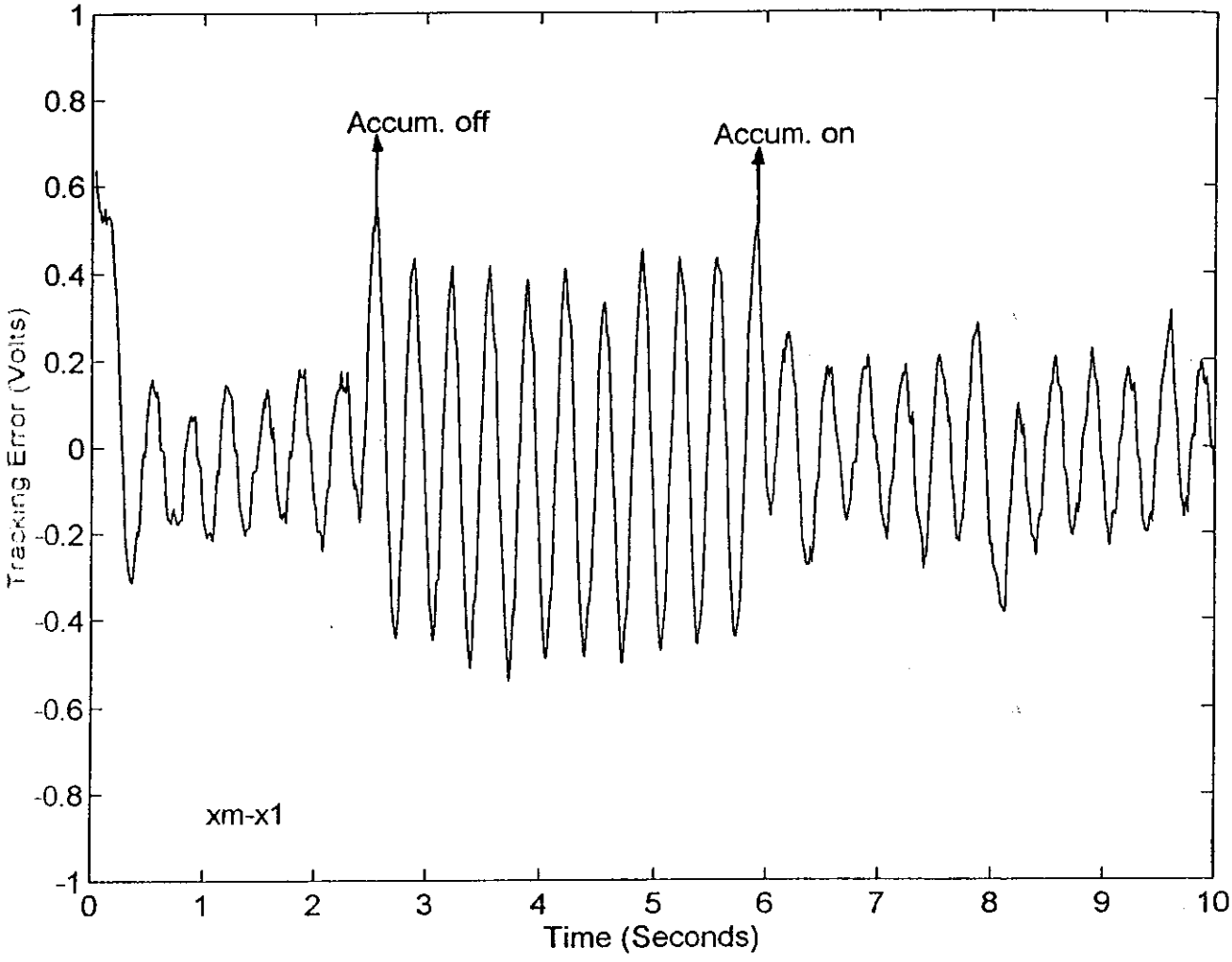

Fig. 5.12: The P+DFB controller tracking error, accumulators switched off and on, supply pressure is 110 bar.

The tracking error ('xm-x1') response for the P+DFB control is showed in Fig. 5.12. The reference signal was a sine wave of frequency 3 Hz, amplitude was 2 volt, k_p = 1.2 and k_d = 0.1. The corresponding MCS result is shown in Fig. 5.13. with a sine wave reference signal of the settling time was t_s = 0.25s, frequency was 3 Hz, amplitude was 2 Volt and the values of α, β were {0.01, 0.001}. A comparison of these figures shows that the

MCS controller outperformed the P+DFB. Fig. 5.14 reveals that the MCS produces a control signal with a greater amplitude and with more effect. The corresponding integral square error (ISE) criterion for each closed-loop response shows in Fig. 5.15, that shows MCS has less slope than P+DFB whether the accumulators are on-line or off-line. When accumulators are off position the plant responses has larger amplitude in the case of both controllers, indicating that the plant has higher performance and it is more robust.

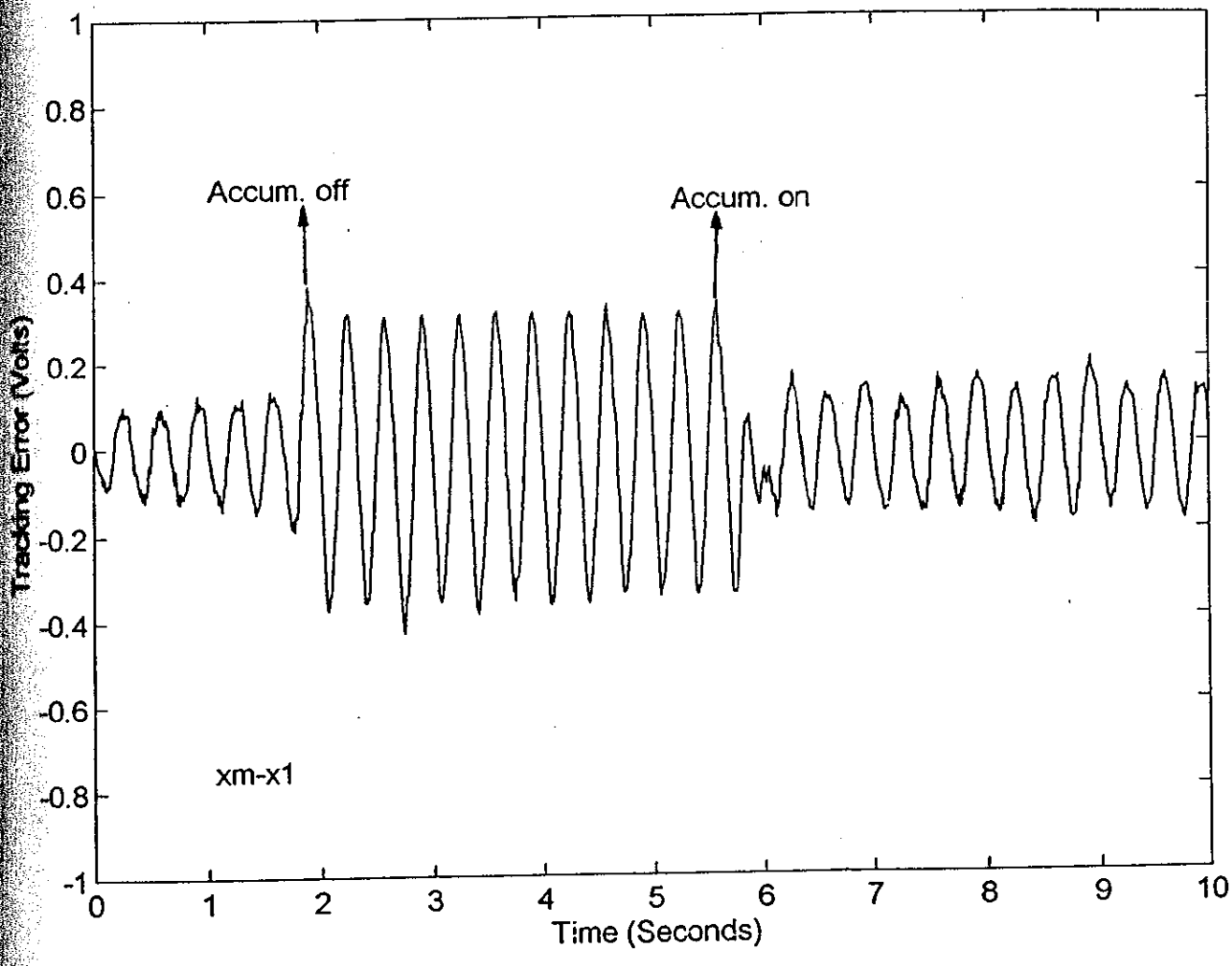

Fig. 5.13: MSC control tracking error, supply pressure 110 bar, accumulators switched off and on.

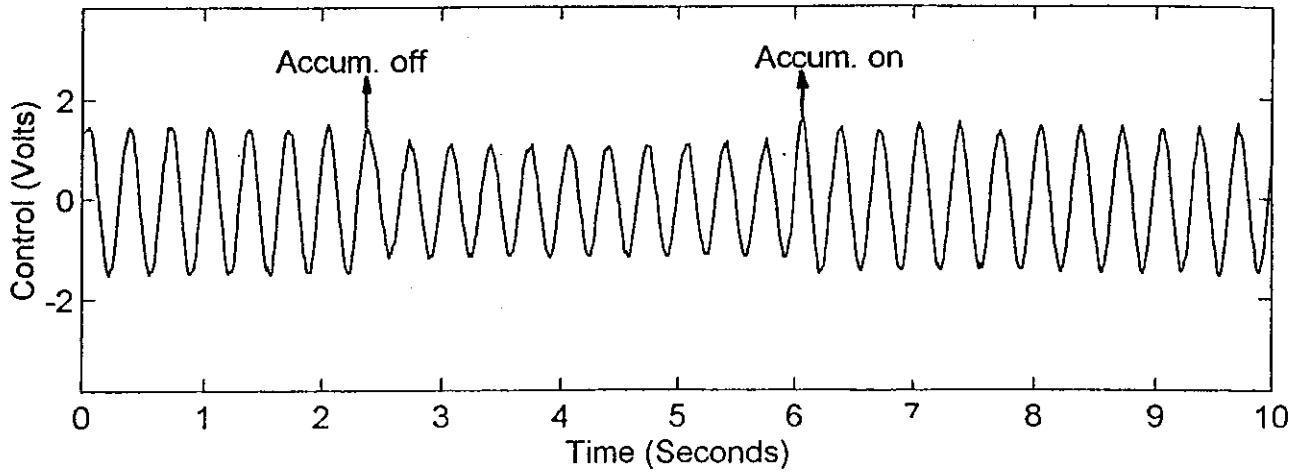

(a) P+DFB control

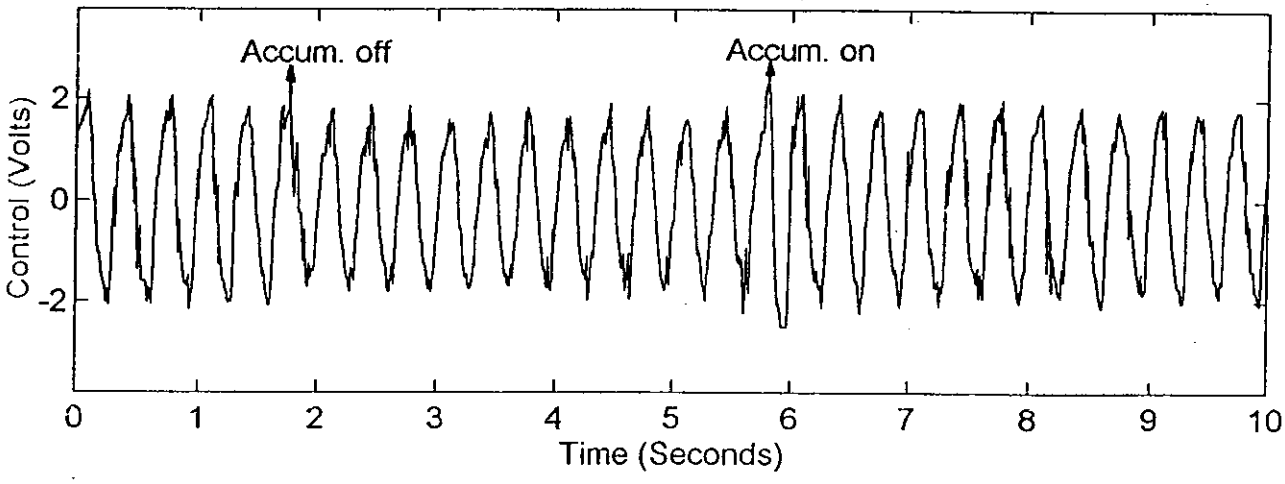

(b) MCS control

Fig. 5.14: Control signals; supply pressure is 110 bar; accumulators switched off and on

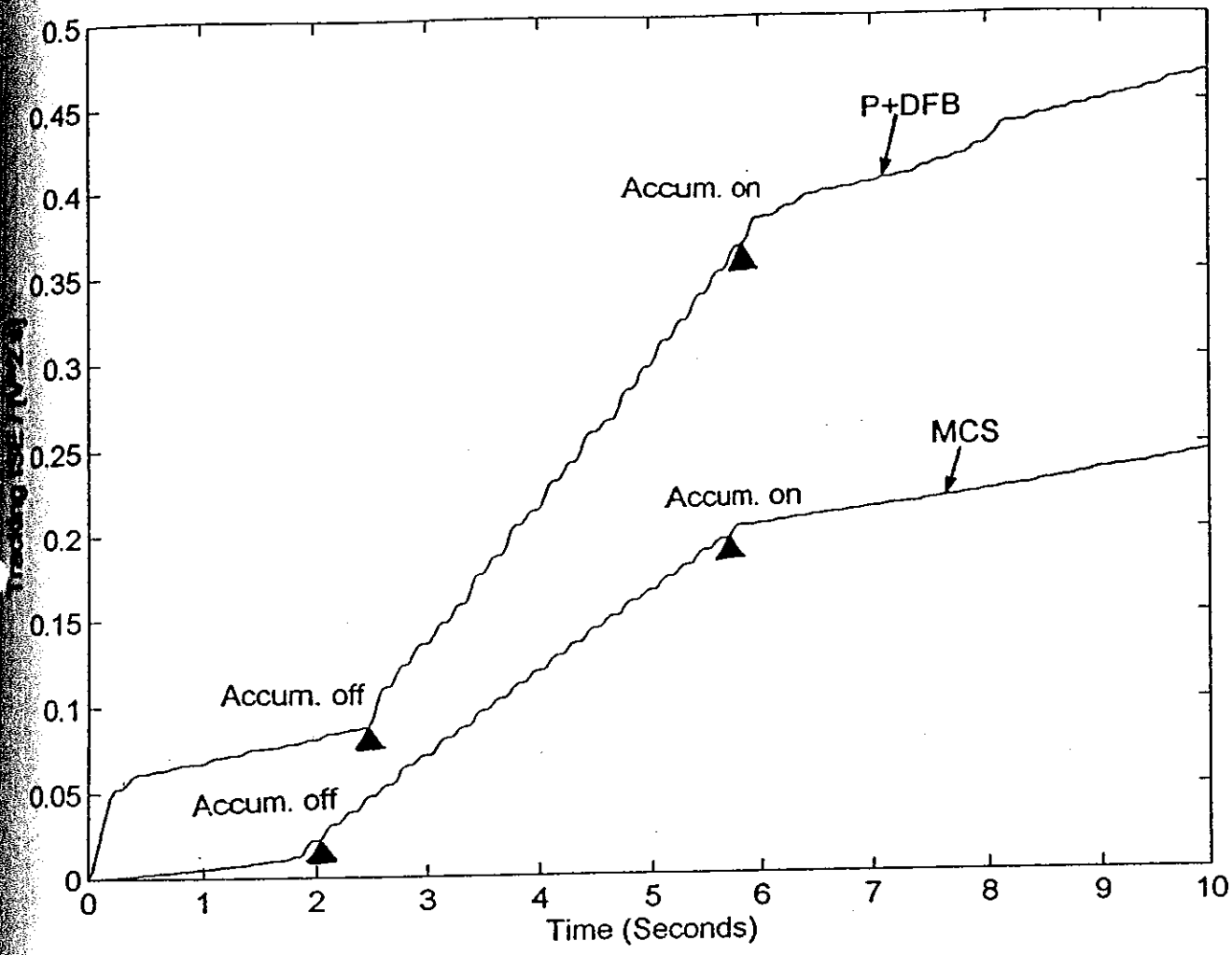

Fig. 5.15: ISE criteria response; supply pressure is 110 bar, accumulators switched off and on.

In the case of P+DFB control the error is twice larger than the MCS control. When accumulators are switched off the error increased more rapidly in the case of both controllers as it is shown in Fig. 15. Under the MCS controller the plant responded to the changes in its dynamics rather smoothly and rapidly. The plant parameter changes is introduced by varying accumulators position (on or off). The responses to this sudden changes in the case of P+DFB control are more rough and noisy. Indicating that the MCS control can be a good candidate in the case of systems which are subject to sudden changes in their working environments or their dynamics e.g., aeroplane.

5.7 - CONCLUSIONS

In this chapter the MCS algorithm has been applied to an electrohydraulic actuator plant. The MCS algorithm is applied in Single Input Single Output (SISO) form. For the nominal operation case, the third order transfer function model is seen to be an appropriate choice, and this model is used to design a P+DFB controller for the plant. The P+DFB control matched the design expectations when the plant is operated under the nominal condition.

The MCS algorithm is implemented on the plant and the closed loop results are compared with those produced by P+DFB. Under the nominal operating condition, the two controllers produced very similar responses, despite the MCS controller not requiring the plant dynamic parameters. Like other conventional controllers, the P+DFB control design requires the plant parameters for implementation.

This is the second known application of the MCS to the servohydraulic field. The first known application of the MCS to a servohydraulic problem was given in the paper by Stoten [4]. Excellent implementation results were also generated from this application.

The MCS algorithm is implemented in a simplified reduced order form. The electrohydraulic actuator plant has a third order transfer function and the MCS reference model was second order. The plant was higher order than the MCS controller. This indicates that the MCS can be quite insensitive to such mismatches.

It has been experienced that the plant can be controlled under the reduced first order MCS control as well, in this condition smaller adaptive weights, α and β are required. In addition, the settling time of the system will be larger to cope with high order unmodelled dynamics. The high order unmodelled dynamics are larger in the case of the reduced first order MCS compare to the reduced second order one. The plant works in the low-frequency range under the reduced first order MCS control. However, the plant output response gets rather slow and noisy, indicating that the reduced first order MCS control is not capable of showing the whole features of the plant therefore it is not the ideal solution for electrohydraulic actuator plant.

The nominal plant model has the third order transfer function. It is observed that the reduced second order MCS control is able to activate the dominant part of the plant

and it guarantees the asymptotic stability of the system. The plant output response is rapid together with comparatively small noise.

Simulation and experimental studies have been presented and these indicated that the MCS control produces excellent results. The MCS control is shown to produce excellent controlled responses which are in close agreement with the desired responses.

As it is shown by the ISE plot in Fig. 5.15 the MCS controller performed better than a conventional control strategy, indicating that, for the electrohydraulic actuator plant the MCS control algorithm can be recommended as a robust controller against the effects of plant parameter variations, external disturbances and plant nonlinearities on closed-loop performances.

REFERENCES

[1] - **THAYER, W. J.**, *Transfer Functions for Moog Servovalves.* Moog Inc. Technical Bulletin, 103, 1965.

[2]- **STOTEN, D. P. & S. BULUT**, 'Application of the MCS Algorithm to the Control of an Electrohydraulic System', *Euriscon*, pp. 1861-1871, August 1994, Malaga, Spain.

[3] - **DYE, M. G. & STOTEN, D. P.**, *WinCtrl-Implementation of Real Time Controllers in Windows 3.1*, Department of Mechanical Engineering, University of Bristol, BS8 1TR.

[4] - **STOTEN, D. P.**, "Implementation of Minimal Controller Synthesis on a Servohydraulic Testing Machine." *Proc. I. Mech. E. Part I*, Vol. 206, pp. 189-194, 1992.

CHAPTER 6

IMPLEMENTATION OF MCS ON A SERVOHYDRAULIC MATERIALS TESTING MACHINE UNDER LOAD CONTROL

6.1 - INTRODUCTION

The main objective of this chapter is to present the application of the Minimal Controller Synthesis (MCS) algorithm on a servohydraulic materials testing machine. The algorithm has been shown to be effective in a number of areas. It has a simple structure with relatively few computational requirements per time step. The MCS controller has been shown to be robust in the presence of unknown external disturbances and unmodelled dynamics in the plant.

MCS requires no prior knowledge of the plant parameters for implementation, and yet is guaranteed to provide global asymptotic stability of the closed-loop system, unlike conventional, linear control strategies e.g. P+I. Additionally, the designer is not require to synthesize the MCS controller gains, since this done automatically by the algorithm, given arbitrary (often zero) initial conditions.

The chapter starts with properties of materials being tested. Then, the MCS and P+I control algorithms are sythesized and implemented on the ESH material testing machine under load control. During these tests, only the 10 mm diameter aluminium specimens were used. It is shown that the MCS produces better results than those produced by an equivalent P+I control algorithm.

6.2 - PROPERTIES OF MATERIALS

A thorough understanding of mechanical behaviour is essential for the safe design of all structures, whether buildings, bridges or machines. This is the reason why mechanics of materials is used in many engineering fields. In materials testing applications, the static and dynamic properties of materials are measured by conducting tension, compression and temperature tests.

To investigate the stress and strains of a specimen it is loaded in tension as shown in Fig. 6.1. The specimen has a cylindrical cross-sectional area. To investigate the stress and strains in this specimen, it is loaded by axial forces P either side of it. In Fig. 6.1a, the first plot is showing the original length of the specimen (L) before the loads are applied and the second one is showing the elongated specimen after the loads are applied. The axial forces are produced the internal stress in the specimen which are shown in Fig. 61b, for the sake of clarity the specimen is cut at the section *mn* imaginatively The force per unit area is called the stress which is denoted by σ and given by the equation

$$\sigma = \frac{P}{A_p} \tag{6.1}$$

where A_p is the cross-sectional area of the bar and P is the applied load. The axial stress σ in the specimen is calculated by dividing the load P by the cross-sectional area, A_p. For the specimen with a cylindrical cross-sectional area, A_p is given below

$$A_p = \frac{\pi D^2}{4} \tag{6.2}$$

where D is the diameter of the specimen. The strain can be described as the elongation of the per unit length, denoted by ε (epsilon) and given by the equation

$$\varepsilon = \frac{\delta}{L} \tag{6.3}$$

where δ is the elongation of the bar and L is the unloaded length of the bar. If the material is linearly elastic then, it follows Hooke's law, so that the longitudinal stress and strain can be related by the equation $\sigma = E\varepsilon$, where E is the modulus of the elasticity. Then the elongation of the specimen can be written as follows

$$\delta = \frac{PL}{EA} \tag{6.4}$$

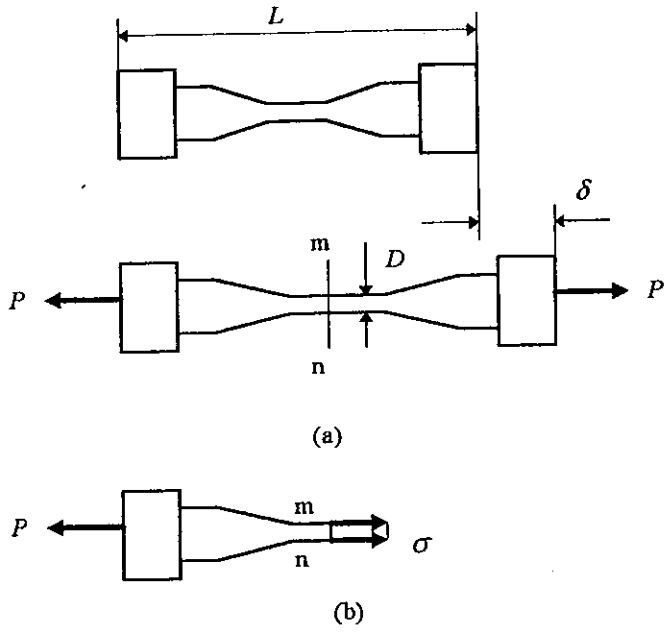

Fig. 6.1: Prismatic bar in tension.

Under the action of the force P, the specimen elongates an amount δ, so that the total length becomes $L+\delta$, where L is the original length. The stiffness k is described as the force to produce a unit elongation, that is, $k = P/\delta$.

6.2.1 - Stiffness in Elastic Region

Consider the specimen in Fig. 6.1 is loaded statically in tension or compression tests in its elastic region and then it is unloaded as shown in Fig. 6.2. In elastic region no matter how many times this task is repeated it will return to its original dimension without significant changes in its properties. This is called elasticity. In this case, the applied load is below the elastic limit of the material. In general, the elastic limit is slightly beyond, or nearly the same as, the proportional limit of materials.

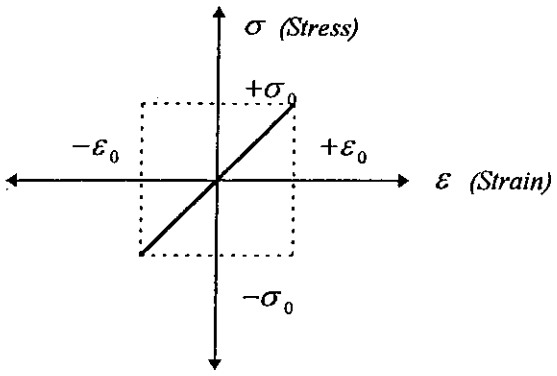

$$\sigma = \begin{cases} +\sigma_0; \varepsilon = +\varepsilon_0 \\ -\sigma_0; \varepsilon = -\varepsilon_0 \end{cases}$$

Fig. 6.2: Stress-strain diagram

If we consider ε and σ representing strain and stress respectively and ε_0 and σ_0 their maximum values, the hysteresis representation may be represented as in Fig. 6.3.

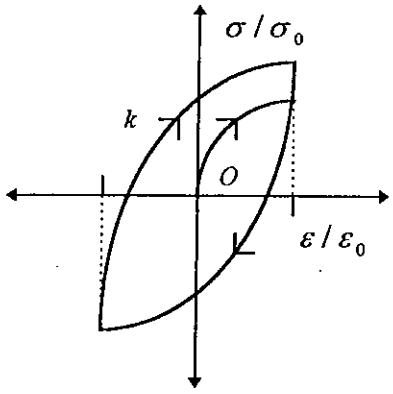

Fig 6.3: Hysteresis loop resulting from fully-reversed stress cycling when the material is in elastic region

6.2.2 - Stiffness in Elastic-Plastic Region

If the specimen is loaded statically in tension then, unloaded statically and loaded again in compression in its plastic region the stress-strain curve for a such deformation sequence will form a hysteresis loop, which is shown in Fig. 6.4.

In Fig. 6.5, the specimen is repeatedly loaded in tension/compression tests (fatigue) in the plastic region then, the internal structure and physical dimensions of the specimen will be changed. In this plot $\Delta\varepsilon$ represents the plastic strain range, since elastic

strains are comparatively small. When a material such as steel or aluminium is loaded under a reversed fatigue test into the plastic region, after the first cycle the ductility will be reduced.

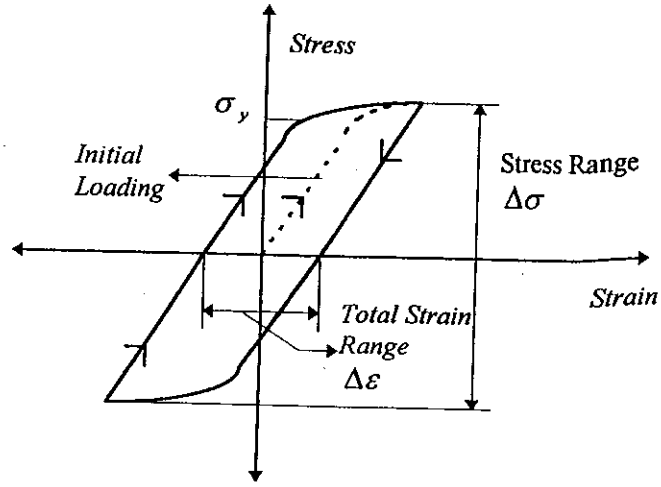

Fig. 6.4: Hysteresis loop resulting from fully-reversed stress cycling when the maximum stress reached in each cycle greater than the yield stress.

Under a reversed fatigue tests in plastic region fatigue will finally take place starting from one to a few thousand cycles depending on the load force and properties of the material. This type of failure is called as low cycle fatigue.

6.2.3 - Stress-Strain Diagram

The stress-strain diagram gives important information about the mechanical properties of materials. In general when materials are loaded under the load force the diagram starts with a slope. In this case the stress is proportional to the strain until the proportional limit and materials behave elastically. Beyond this point the proportionality no longer exist. After the proportional limit even a little increment in the load can cause rapid increase in strain. If materials are loaded in tension or compression beyond the proportional limit considerable amount of elongation occurs without increment in the load force. This is called as yielding and the corresponding stress is the yielding stress [1]. In the yielding region materials behave perfectly plastic.

6.3 - ADVANTAGES OF USING THE MCS CONTROL IN MATERIALS TESTING APPLICATIONS

Adaptive control techniques are often used for a plant with unknown and time varying dynamics. Especially a Model Reference Adaptive Control (MRAC) technique can make the plant output coincide with a reference output. Since electrohydraulic servo system are often used under varying conditions, the application of this technique to an servohydraulic materials testing machine is expected to be very powerful and useful [2]. The Minimal Controller Synthesis (MCS) algorithm was originally developed by Stoten and Benchoubane [3] as an extension to the Model Reference Adaptive Control algorithm of Landau [4]. However, the MCS control algorithm does not requires plant model identification, unlike the MRAC control.

In recent years, adaptive controller have been used in the case of electrohydraulic systems. Using digital controller have many advantages over analogue controllers therefore, they have been widely used in many industries and in the area of materials testing applications due to their consistency, flexibility and ease of use. The adaptive control is implemented in both discrete and continuous time. Digital controller benefits from new developments in electronic hardware. By using faster computers the efficiency and the capacity of the materials testing applications can be improved considerably.

In the manually controlled analogue controller parameters such as the demand mean level and amplitude, limit setting and controller gains are set using potentiometers. In the case of the ESH materials testing machine, analogue signals are restricted to the area of the transducers, servovalve, LVDT's and load cell, as shown in Fig. 6.5. In this diagram a 486 PC machine equipped with 12 bit D/A and A/D converters, that converts analogue output signals from the LVDT, load cell or extensometer into digital form and digital signal from computer into analogue form and sends to the plant. Every parameter can be manually adjusted from computer keyboard and complete test set up can be stored and recalled from the computer. A major advantage of digital systems for materials testing machines is that the intelligence of the system can be used to make the machine easier and safer to operate.

The specimens have sometimes nonlinear properties. In addition, the properties of materials change when they are tested in their plastic region. The stiffness of the specimen

decreases during fatigue tests. Using adaptive controllers in such applications have many advantages due to the fact that they can adapt themselves to the changes in the specimen properties and in the testing machine itself.

In this case, the controller problem is to ensure there is a good correspondence between the desired and actual responses despite changes in specimen (for example crack growths, effects of high temperatures and modulus variations) and in the test machine itself. During most materials tests the characteristic of the specimen changes, therefore adaptive control is needed.

6.4 - THE ESH MATERIALS TESTING MACHINE

In order to measure the mechanical properties of materials a small specimens of the material is tested by using materials testing machine under tension, compression, fatigue testing. The ESH materials testing machine which is presented in this chapter, has been developed in the Material Laboratory, the Mechanical Engineering Department at Bristol University. The plant consists of servo hydraulics, a load cell and a test specimen, with input u and output y and induced loads are measured by a load cell in series with the actuator ram.

The rig, shown schematically in Fig. 6.5, is actuated by a standard servohydraulic system. During materials testing, the control problem is to ensure that the measured force y closely tracks for a given reference signal despite changes in specimen and servohydraulic characteristics.

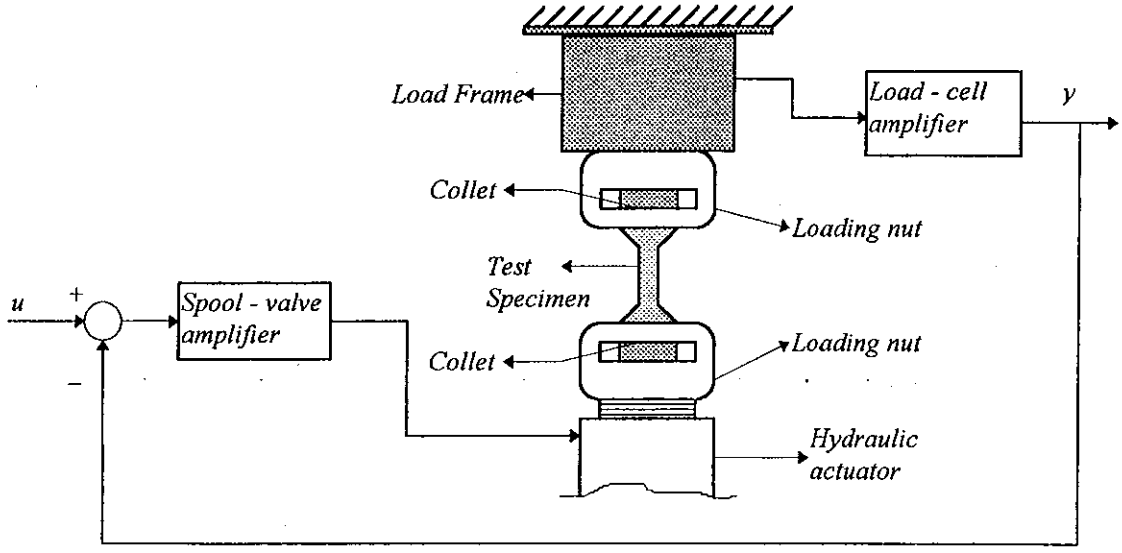

Fig. 6.5: Servo-hydraulic materials testing machine (in tension).

6.5 - DYNAMICS OF THE ESH MATERIALS TESTING MACHINE

The dynamics analysis of the ESH materials testing machine can be made by identifying its differential equation of motion. The dynamics of the system as depicted in Fig. 6.6, contains significant nonlinear elements due to the nature of hydraulic systems: servovalve dynamics, nonlinear effects of hydraulic fluids. The system consists of a double ended, balanced actuator, a servovalve, a fixed displacement pump. The hydraulic pump produces constant supply by using a pressure control valve.

The test specimen is analysed by a mass-spring-damper combination in Fig. 6.6, including the effect of the mass of the actuator, this combination is symbolised as M_a , k_s , and B_p respectively.

The servovalve is a highly nonlinear device. The load flow is represented by the square-root relationship for the servovalve therefore, the relationship between the flow and the pressure is nonlinear. In the case of materials testing applications the effects of the servovalve can be neglected since the load flow variations are very small in such tests.

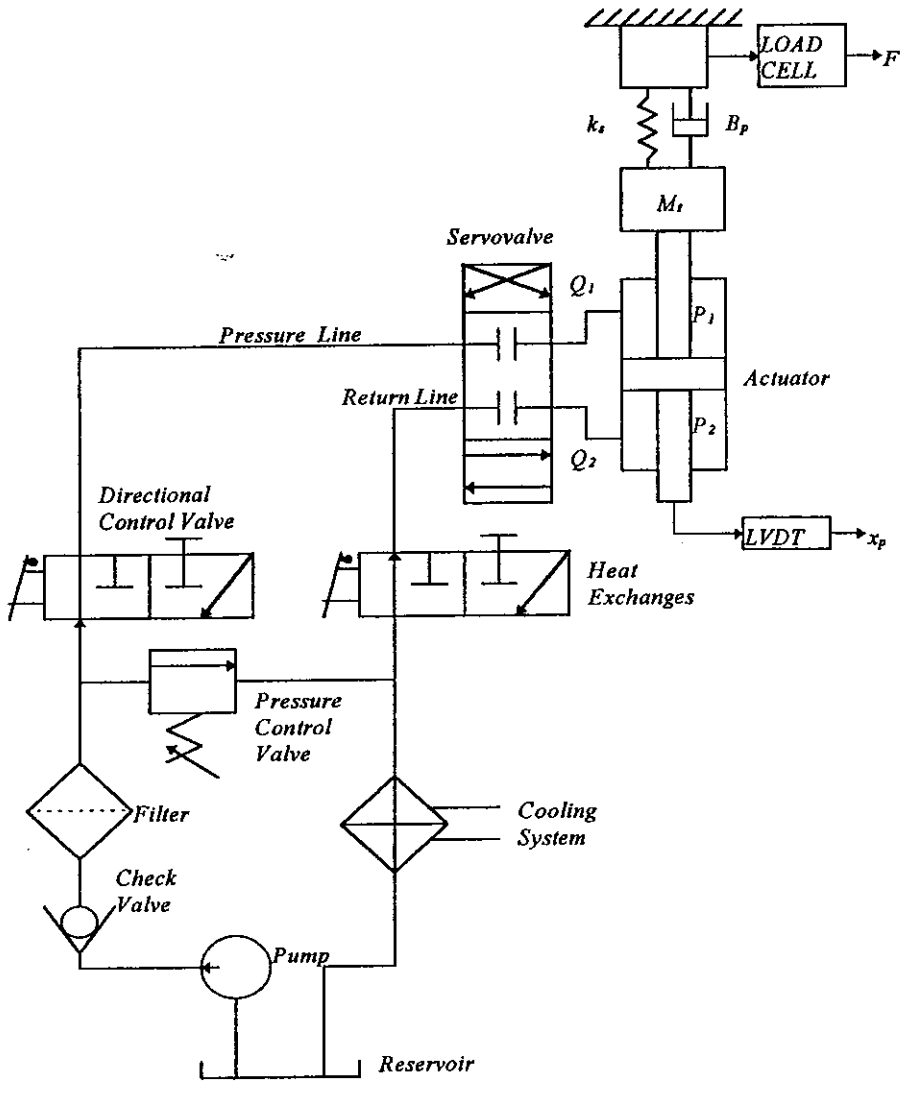

Fig. 6.6: Hydraulic system of materials testing machine

In this diagram Q_1, Q_2 are flows into the first and second chambers of the actuator. The leakage flow Q_l and the flow due to compressibility Q_c from the actuator are written as follows:

$$Q_l = C_p P_L \tag{6.5}$$

$$Q_c = \frac{V_t}{4NC_p}\dot{P}_L \tag{6.6}$$

where C_p is total actuator leakage coefficient, V_t is total volume of hydraulic oil in the actuator, N is bulk modulus of hydraulic oil. The load flow from the actuator can be written as below

$$Q_L = Q_l + Q_c \tag{6.7}$$

The load pressure is:

$$P_L = P_1 - P_2 \tag{6.8}$$

where, P_1 and P_2 are pressures into first and second chambers of the actuator. The plant dynamics were depicted in Fig. 6.7. In this diagram Q_L is load flow, s is Laplace variable, ε is strain, A_p is actuator cross-sectional area and L is gage length of test specimen.

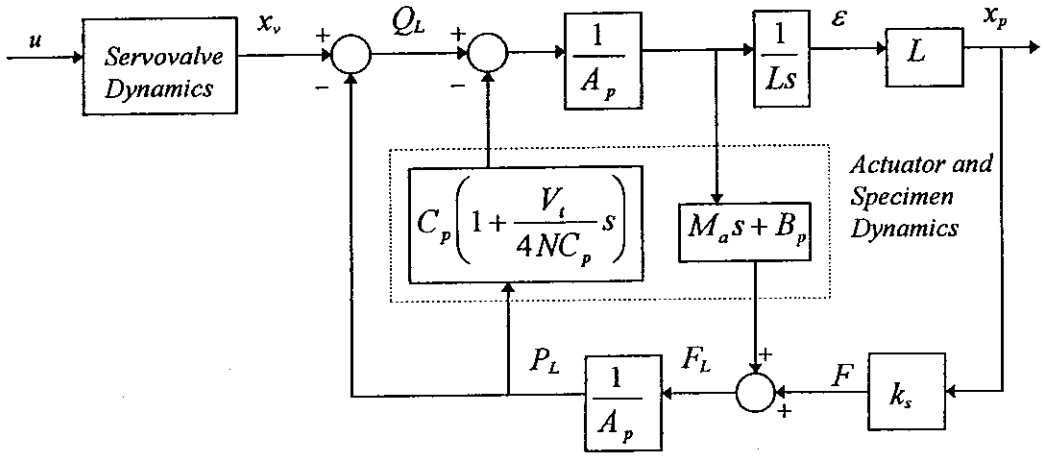

Fig 6.7: Block diagram of linearized materials testing machine dynamics

6.5.1 - Under Load Control

The nominal linearization model is of second order under load control. From Newton's law the actuator dynamics together with specimen can be written as:

$$F_L - F_k - F_r = M_a a \tag{6.9}$$

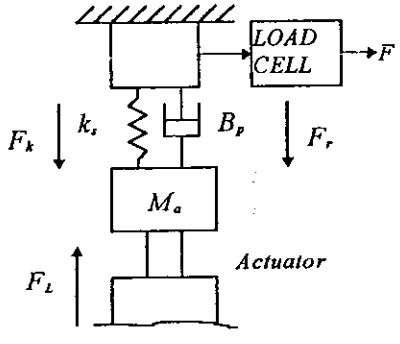

Fig. 6.8: Dynamics of the actuator and specimen

In Equation (6.9)

$$F_L = P_L A_p$$
$$F_k = k_s x_p \tag{6.10}$$
$$F_r = B_p \dot{x}_p$$

where F_L is load force, F_k is spring force, and F_r is the friction force, and M_a is total mass of the piston and load referred to piston, k_s is specimen spring constant. Then, Equation (6.9) becomes

$$F_L = M_a \ddot{x}_p + B_p \dot{x}_p + k_s x_p \tag{6.11}$$

In Equation (6.11), B_p is viscous damping coefficient for actuator and load, x_p is actuator displacement. Load force can be written as:

$$F_L = A_p P_L \tag{6.12}$$

where P_L is the load pressure. From (6.7), the load flow can be written as follows

$$Q_L = P_L C_p + \frac{V_t}{4NC_p} \dot{P}_L \tag{6.13}$$

If we take the Laplace transform of the above equation

$$Q_L = P_L \left(C_p + \frac{V_t}{4NC_p} s \right) \tag{6.14}$$

From (6.14) the load pressure can be written as

$$P_L = \frac{Q_L}{\left(C_p + \frac{V_t}{4NC_p} s \right)} \tag{6.15}$$

$$F = F_k = k_s x_p \text{ and } x_p = \frac{F}{k_s}, \ \dot{x}_p = \frac{\dot{F}}{k_s}, \ \ddot{x}_p = \frac{\ddot{F}}{k_s}$$

Equation (6.11) can written as:

$$P_L A_p - B_p \dot{x}_p - k_s x_p = M_a \ddot{x}_p \tag{6.16}$$

then,

$$P_L A_p - F\left(\frac{k_s}{M_t} \right) - \left(\frac{B_p}{M_t} \right) \dot{F} = \ddot{F} \tag{6.17}$$

Taking the Laplace transform of Equation (6.17) becomes:

$$P_L A_p = F\left(s^2 + \left(\frac{B_p}{M_t} \right) s + \left(\frac{k_s}{M_t} \right) \right) \tag{6.18}$$

Substituting (6.15) into (6.18) we get

$$\frac{Q_L A_p}{\left(C_p + \frac{V_t}{4NC_p}s\right)} = F\left(s^2 + \left(\frac{B_p}{M_t}\right)s + \left(\frac{k_s}{M_t}\right)\right) \tag{6.19}$$

So, the dynamics of the plant under load control can written from :

$$\frac{F}{Q_L}(s) = \frac{\dfrac{A_p}{\left(C_p + \dfrac{V_t}{4NC_p}s\right)}}{s^2 + \left(\dfrac{B_p}{M_t}\right)s + \left(\dfrac{k_s}{M_t}\right)} \tag{6.20}$$

In this model the servovalve dynamics is ignored as shown in Fig. 6.8.

6.6 - THE ALUMINIUM TEST SPECIMENS

The test specimen is installed between the two grips of the testing machine and then loaded in tension or compression. The specimens are made of aluminium (stress is $\sigma = 150$ MPa and Young's modulus is E = 72 GPa), with diameter D_1 = 10 mm and length L=120 *mm* and gauge length of 22 mm is shown in Fig. 6.9.

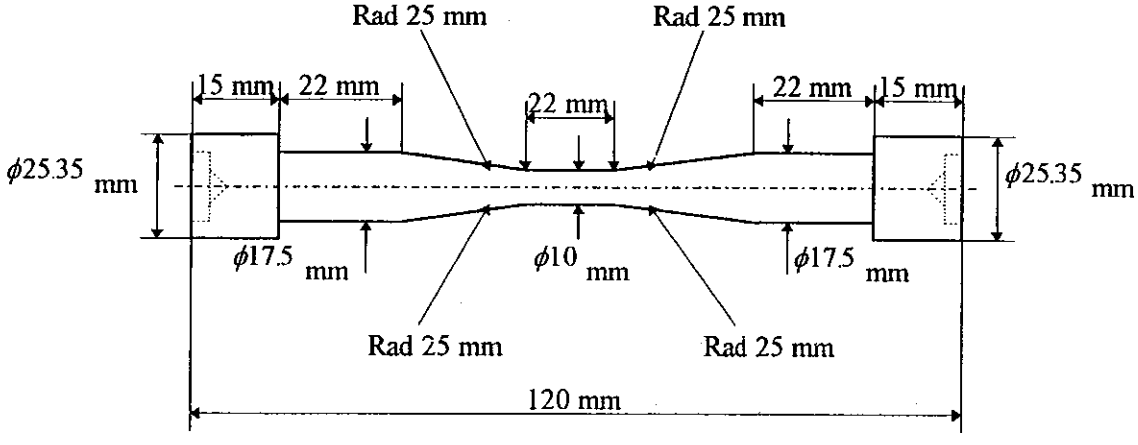

Fig. 6.9: The aluminium specimens

Aluminium and many of its alloys do not have a clearly determinable yielding point and they show considerable amount of ductility*. A typical stress-strain diagram for aluminium alloy is shown in Fig. 6.10. In this diagram, there is a linear region that is starting from point O to P, in which Hooke's Law holds and stress is proportional to strain. Then, a non-linear region follows starting from point P in Fig. 6. 10 which can be defined by an appropriate mathematical function.

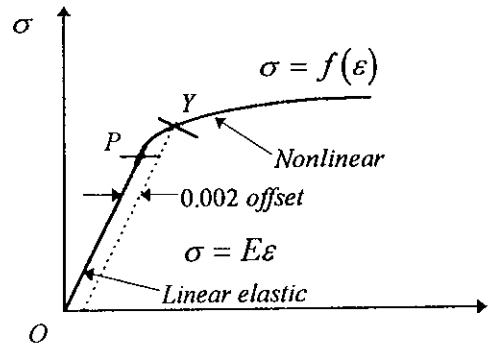

Fig. 6.10: Types of idealised non-linear stress-strain diagram for aluminium alloys.

In this diagram: E is the elasticity modulus that is often called *Young's Modulus*, δ is the elongation, σ is the stress and ε is the strain of the material. Aluminium alloys have proportional limit in the range of 70 to 420 MPa and ultimate stress of 140 to 560 MPa. The yielding stress of the material is determined by the offset method since it does not have a clearly definable yielding point. The method is based on an arbitrary rule therefore its is not depending on the properties of the material. As it shown in Fig. 6.10 an offset line drawn on the stress-strain diagram parallel to the first part of the diagram (starting from point O to P in Fig. 6.10) together with offset strain of 0.002 (%0.002). The intersection of the offset line and the stress-strain line is determined the yielding stress (point Y in Fig. 6.10). This is called the offset yielding stress. For aluminium, the offset yield stress is slightly above the proportional limit.

* Materials that undergo large strains before failure are classified as ductile.

6.7 - THE ESH SERVOHYDRAULIC MATERIALS TESTING MACHINE UNDER FATIGUE TESTS

Servohydraulic materials testing machines are widely used in the case of high frequency reversal load tests such as fatigue tests. These types of machines are capable of applying high-frequency alternating loads on specimens in tension or compression control. Electromechanical machines are not well suited for this kind of tests. The main mechanical components of a servohydraulic materials testing machine is shown Fig. 6.11. In this diagram, the crosshead can be moved and clamped at any position up and down the columns to tests specimens of different lengths. In general, grips are normally hydraulically operated. In the case of ESH materials testing machine the lower and upper grips are mechanically operated. The top part of the actuator is a large screw bolt, and a loading nut can be moved up and down to clamp test specimen at its length and collets (the smaller rings, see in Fig. 6.9) the ends of the specimen firmly to prevent slipping. The columns are fixed to the base platen which also carries the hydraulic actuator.

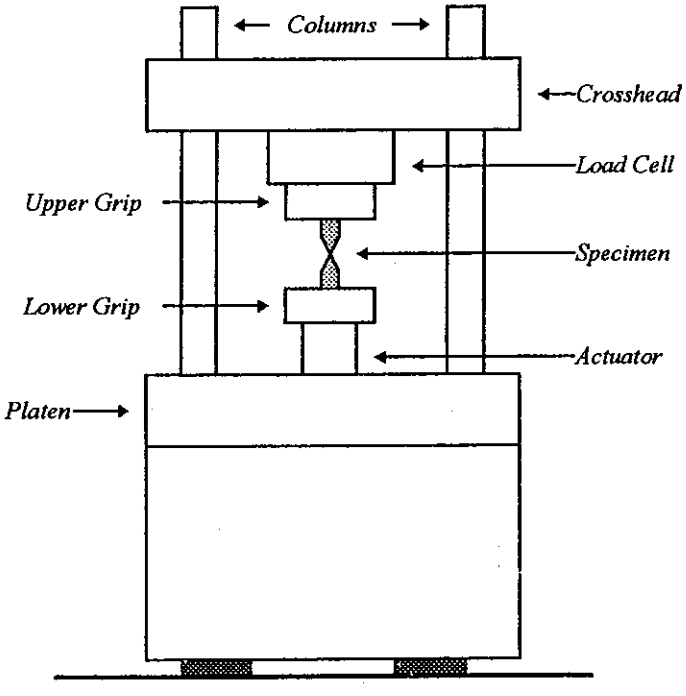

Fig. 6.11: Servohydraulic materials testing machine

The actuator piston position is monitored and controlled using an internal linear variable differential transformer (LVDT) as the feedback transducer, and the force applied to the specimen is measured by the load cell mounted beneath the crosshead.

In the case of strain measurement, an extensometer is attached to the specimen to provide a more accurate measure of extension than can be obtained from the LVDT which is sensitive to load frame deflections. For ESH materials testing machine 1 Volt corresponds 5 kN. The dynamics of the servohydraulic machine are effected by the following parameters: The capacity of the actuator, the flow rate of the servovalve, the stiffness of the load frame, grip mass, the stiffness of the specimen, transducers accuracy, the applied load. Under load control, when the stiffness of the specimen decreased the steady-state error will increase due to the lower controller gain.

6.7.1 - Dynamic and Static Loading

Dynamic loading is different than static loading. In dynamic tension or compression loading the elongation and the stress in the specimen are initially zero then, with suddenly applied load they will reach to a certain value. Dynamically applied load causes vibrations in the specimen. During this kind of tests the kinetic energy of the mass produces additional elongation in the specimen. For that reason dynamic loads may produce an elongation which is twice larger than the elongation that is produced the equivalent static load. In contrast static load applies slowly, gradually increasing from zero to its maximum value, and then remaining constant therefore, the equilibrium between the applied load and the resisting force in the specimen always exist.

6.8 - THE CONTROL LOOP

The Fig. 6.12 shows control loops of the ESH materials testing machine. Three control modes are provided: actuator position control, specimen load control and specimen strain control.

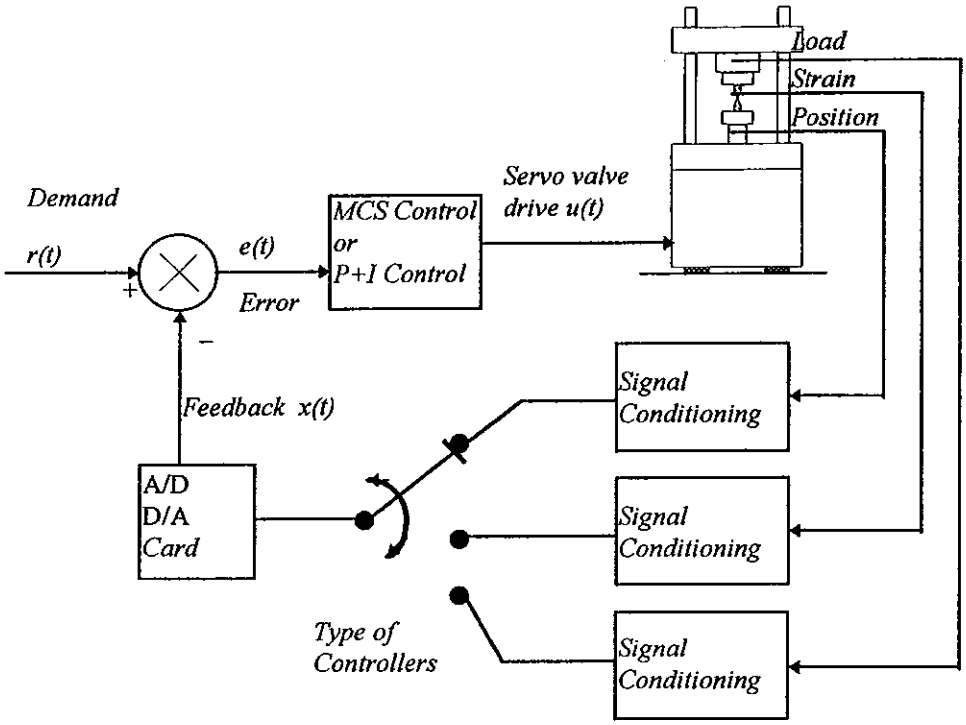

Fig. 6.12: Position, load and strain control.

A mode selector used to select which conditioned transducer signal is to be controlled variable $x(t)$. The function of the MCS control is to produce an appropriate control signal $u(t)$ to drive the testing machine actuator in a direction which minimises the error $e(t)$:

$$e(t) = x_m(t) - x(t) \tag{6.21}$$

where $x_m(t)$ is the demand signal which is usually derived from a computer. The output goes directly to the servovalve which controls the actuator, i.e. it acts as the power amplifier.

6.9 - SYSTEM IDENTIFICATION

Conventional control synthesis requires prior knowledge of the plant dynamics. In this case, a series of system identification tests are conducted on the open-loop plant. Test specimens are made of aluminium with $D_1 = \phi 10$ mm. During these tests, the plant is subjected to a swept sinusoidal input signal $\boldsymbol{u}$ under Proportional load control using the

aluminium specimens which produced a corresponding output y (load). The supply pressure is kept at its nominal value of 13.8 MPa during these tests and amplitude was 0.8 V (a corresponding load of 4.5 kN).

The compliance of the supporting structure on which the actuator, test specimen, and associated fixtures dynamics are negligible for the low frequency test considered, but could be significant if the test signal frequencies are increased. Therefore, at high frequencies a second order model is relevant for the ESH materials testing machine.

The test results are generated from a swept sinusoid input signal, with data analysed by the Matlab System Identification Toolbox macro *oe* (output-error method). At high frequencies, the average second order transfer function is found to be:

$$G_P(s) = \frac{2900}{s^2 + 110s + 2000} \tag{6.22}$$

The response ***yp2*** predicted from the original input $\boldsymbol{u}$ in Fig. 6.13. The second order model is judged to be acceptable for the high frequencies, due to given very close correspondence between ***yp2*** and $\boldsymbol{y}$.

At low test frequencies the plant can be modelled as a first order. This is because of the servovalve dynamics and load inertial and friction effects are negligible at low frequencies.

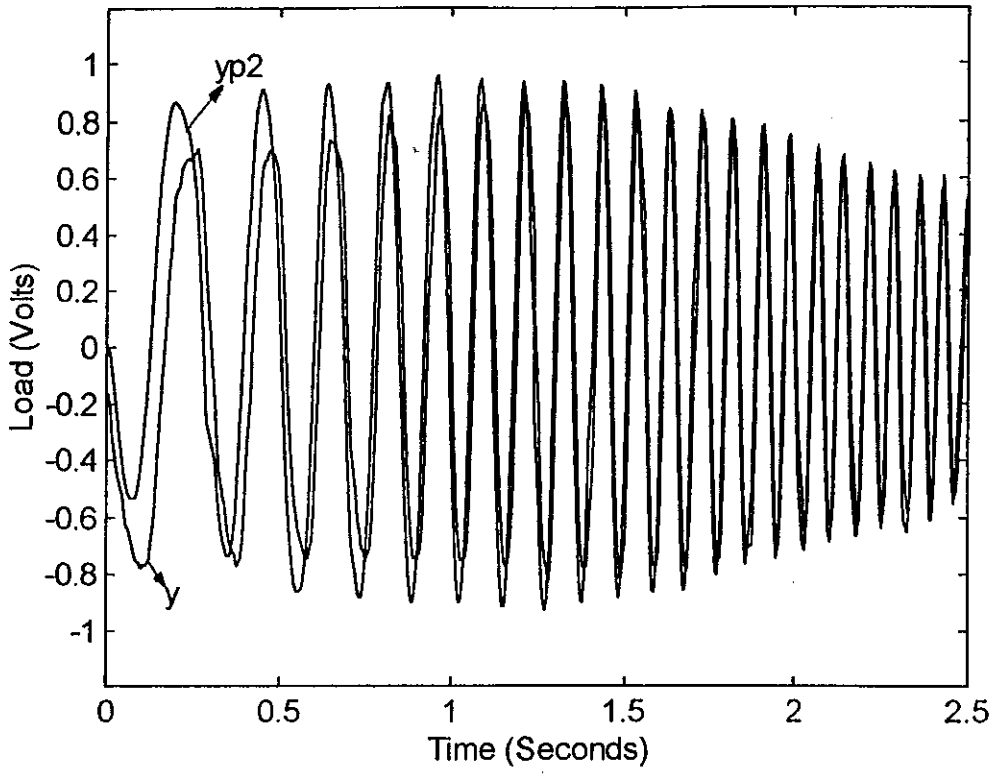

Fig. 6.13: The nominal second order plant model (supply pressure 13.8 MPa, under proportional load control, aluminium specimen with ϕ 10 mm)

6.10 - CHOOSING THE LINEAR CONTROLLER STRATEGIES FOR THE ESH MACHINE

A suitable set proportional gain reduces the steady-state error. The servovalve opening is proportional to the servo error. When the gain increased the error gets smaller. If the proportional gain is high enough materials testing machine is much more able to closely follow demand signal. Too high proportional gain value could result, though, in oscillatory plant response, it can even cause instability.

Integral gain is necessary in materials testing applications to apply static loads accurately and drive the steady-state error to zero. In addition, it also removes other offsets (the servovalve null offset) in the control loop. Integral action essentially affects the performance of the machine in the low-frequency range. In the high-frequency range it does not have significant affect. If integral gain is too high then, the plant response becomes though together with low-frequency overshoot.

The plant response becomes faster with derivative action due to the fact it makes possible to set higher proportional gain and introduces damping into the control loop. It also increases the systems accuracy. An unwanted effect of derivative gain is that it can make systems noisy in the high frequency range due to increase in the proportional gain.

Therefore, P+I controller is chosen as a good option in the case of controlling the ESH materials testing machine.

6.11 - IMPLEMENTATION OF CONTROLLERS (P+I, MCS CONTROLLERS)

Running under Windows 3.1, all controllers are implemented via *Winctrl4*. *Winctrl4* is a windows based controller software package developed and improved by [5]. It is used to implement the various controller strategies including conventional and adaptive controllers. Controller hardware was a 486 PC machine equipped with 12 bit D/A and A/D converters.

6.11.1 - Proportional Plus Integral (P+I) Controller

Proportional Plus Integral (P+I) controller is a linear, conventional control synthesis. This control strategy requires a plant transfer function for implementation. A P+I controller implemented for the aluminium specimens with $D_1 = 10$ mm diameter under load control.

Increasing the derivative gain at high frequency exaggerates signal noise. The resonance in the actuator and the load frame affect the performance of the materials testing machine badly. Especially, under load control the mass attached to the load cell moves with any frame resonance. As a result of this, the measured load will be different from the actual load which is imposed on the specimen. In addition, the detected inertia force reduces stability of the machine. In fact, derivative action actually makes the resonance worse and in this condition using P+I control can be a better option.

The P+I controller strategy is implemented to reduce steady-state errors to zero. The second order plant roots are placed at $s_1 = -22.9844$ and $s_2 = -87.016$. The

corresponding first order dominant root is then assigned to $s = -11$ rad/s, corresponding a step-response settling time of about 0.35 s. This design is summarised in the root's loci plot of Fig. 6.14, where the parameter along the loci is $k = 2900\ k_p$. To get a reasonably damped response, the controller zero is placed at:

$$s = -\frac{k_i}{k_p} = -12 \text{ rad/s}$$

Thus, suitable values of the integral and proportional gains are $k_i = 24$, $k_p = 2$. The P+I controller is implemented in a discrete time (ZOHDE) form, with the gains as $k_p = 2$ and $k_i = 24$, thus

$$u(k) = u(k-1) + k_p x_e(k) - (k_p - k_i \Delta) x_e(k-1)$$

$$x_e(k) = r(k) - y(k)$$

where $u(k)$ is the current control signal, $x_e(k)$ the current tracking error between reference and plant output signal, $y(k)$ the current measured load signal which is applied on specimens and Δ is the sampling interval.

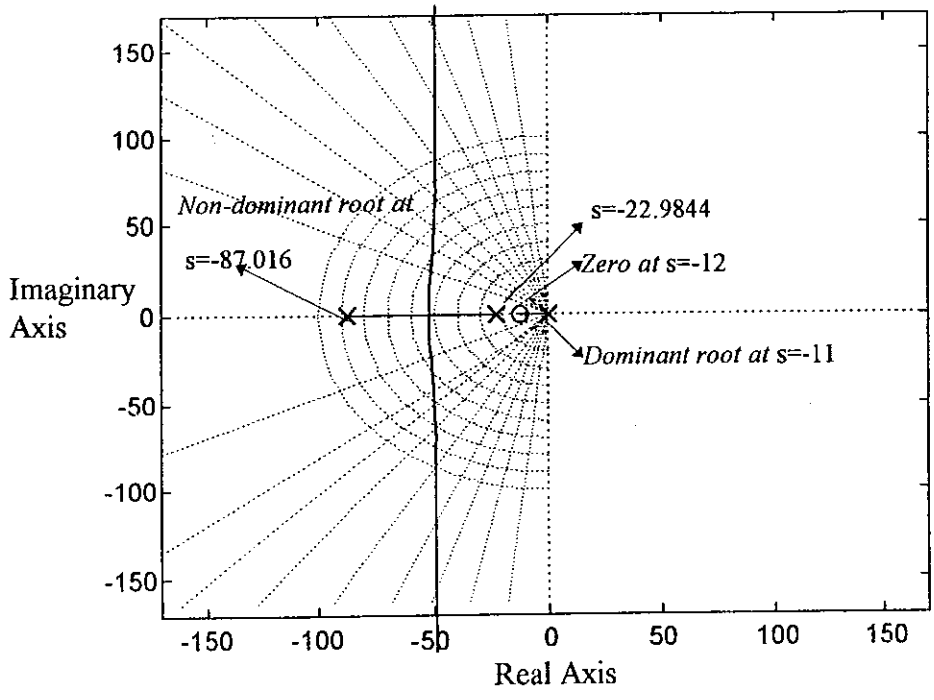

Fig. 6.14: Loci of roots for P+I control with $k_i / k_p = 12$

Given the desired closed-loop settling time of 0.35 s, a reasonable choice of Δ was $\Delta \leq 0.35/10 = 35$ ms. In fact, the actual choice was $\Delta = 20$ ms.

6.11.2 - The MCS Control

For the MCS case, the plant transfer function is not required by the control algorithm. Details of the MCS algorithm, including stability proofs, have been presented in [6], [7] and Chapter 4. As mentioned before, the aluminium specimens with $\phi 10$ mm used in this set of tests under the MCS load control. Firstly, an estimate is made of the nominal plant order, and order of the MCS matches this figure.

In this case the ESH material testing machine has second order plant dynamics, therefore a second-order MCS formulation would normally be necessary. The MCS control was implemented in a simplified reduced first order form. The fact that the plant was higher order than the MCS algorithm indicates that the MCS control possesses a degree of robustness to mismatches in orders. In Particular, relatively low order MCS controllers can be very effective in the control of higher order plants. First order MCS control equation is summarised below, in discrete time scalar form:

$$u(k) = K(k)x(k) + K_r(k)r(k) \tag{6.23}$$

$$K(k) = K(k-1) + \beta y_e x^T(k) - \sigma y_e(k-1)x^T(k-1) \tag{6.24}$$

$$K_r(k) = K_r(k-1) + \beta y_e r^T(k) - \sigma y_e(k-1)r^T(k-1) \tag{6.25}$$

$$y_e(k) = C_e x_e(k) \tag{6.26}$$

$$x_e(k) = x_m(k) - x(k) \tag{6.27}$$

where $\sigma = \beta - \alpha\Delta$ and Δ is the sampling interval of the discrete time process. The reference model parameters are chosen in order to have stable plant state trajectories x, which is guaranteed to follow reference model state trajectories x_m closely. The first order MCS reference model is

$$\dot{x}_m(t) = A_m x(t) + B_m r(t) \tag{6.28}$$

where $A_m = -4/t_s$ and $B_m = 4/t_s$

Equation (6.28) can be written as

$$\dot{x}_m(t) = (-4/t_s)x(t) + (4/t_s)r(t) \tag{6.29}$$

The hyperstable condition is guaranteed if:

$$C_e = \not{\sigma}^T P \tag{6.30}$$

In this equation

$$\mathcal{B} = [1]$$

and P is the positive definite solution to the Lyapunov equation

$$PA_m + A_m^T P = -Q \; ; \; Q > 0 \tag{6.31}$$

and the 'weighting' matrix Q in the Lyapunov equation , which was chosen as Q = [1]. The values of adaptive weights were α = 0.01 and β = 0.001. The first order reference model parameters are:

$$A_m = -4/t_s = -11.4286, B_m = 4/t_s = 11.4286 \text{ and } C_e = t_s/8 = 0.0438$$

6.12 - COMPARATIVE TESTS

6.12.1 - Step Response Tests

The conventional P+I controller was implemented on the plant. In this case the reference signal was a square wave of amplitude 1.5 V and frequency 0.25 Hz. The controller gains was k_p = 2 and k_i = 24. The P+I controller yielded the steady state responses shown in Figs. 6.15. There is good correspondence between the desired and actual responses indicating that the second order plant model from system identification tests is well founded and the P+I control is well implemented. The load was applied on specimens gradually (static loading).

With the initial conditions on the adaptive gains set to zero, the adaptive rates are chosen empirically; values found to be suitable in this case are α = 0.01 and β = 0.001, the values having been deduced as providing a good compromise between the rate of adaption and noise propagation. The MCS yielded the steady-state responses shown in Fig. 6.16a and MCS controller gains and input signal shown in Fig. 6.16b and c, indicating that the MCS control performs better than P+I, without the necessity for system identification and controller synthesis. The initial adaptive stage of the MCS controller is shown in Fig. 6.17a, b and c, the adaption and response tracking are seen to be both rapid and accurate.

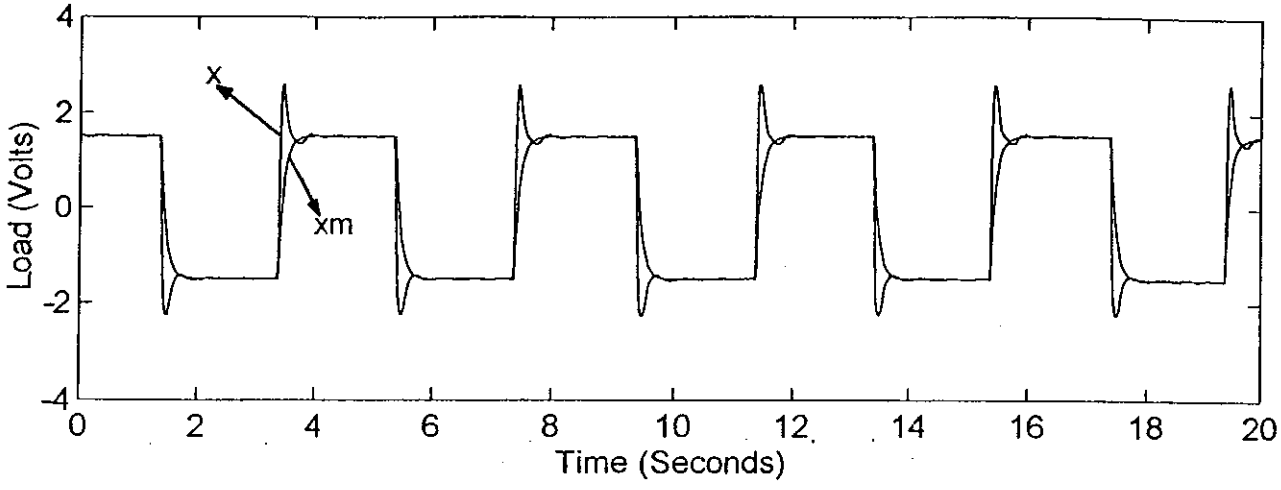

(a) The plant and reference model responses

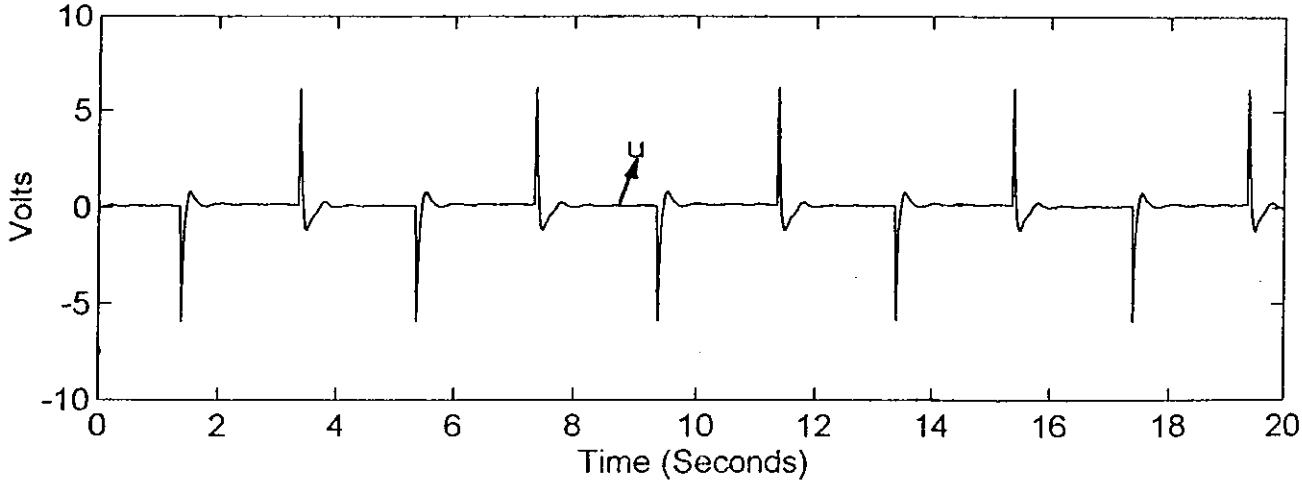

(b) Control signal

Fig. 6.15: P+I step response, supply pressure 13.8 MPa, load 7.5 kN.

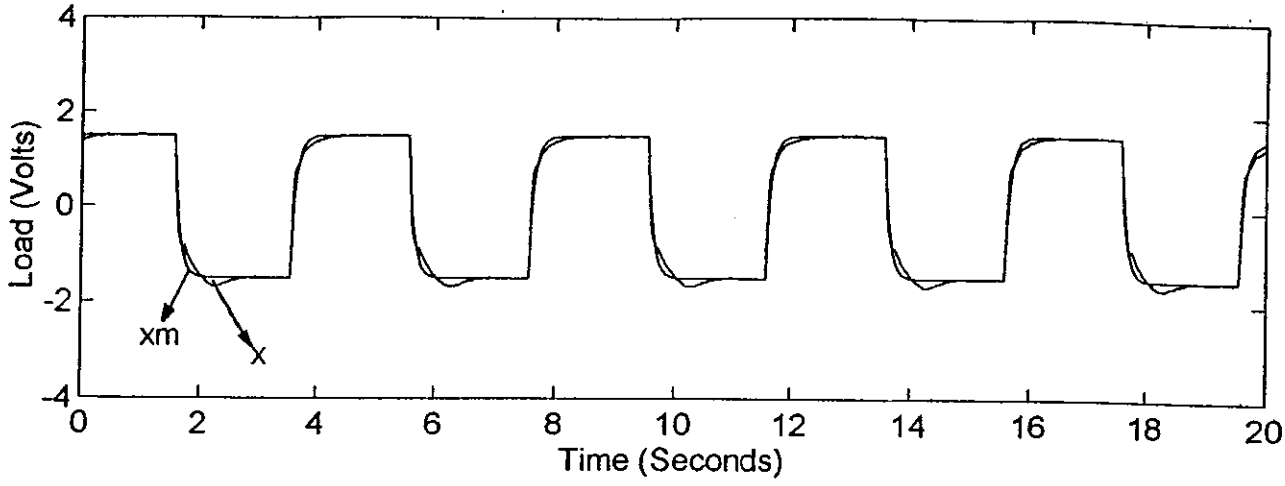

(a) The plant and reference model outputs

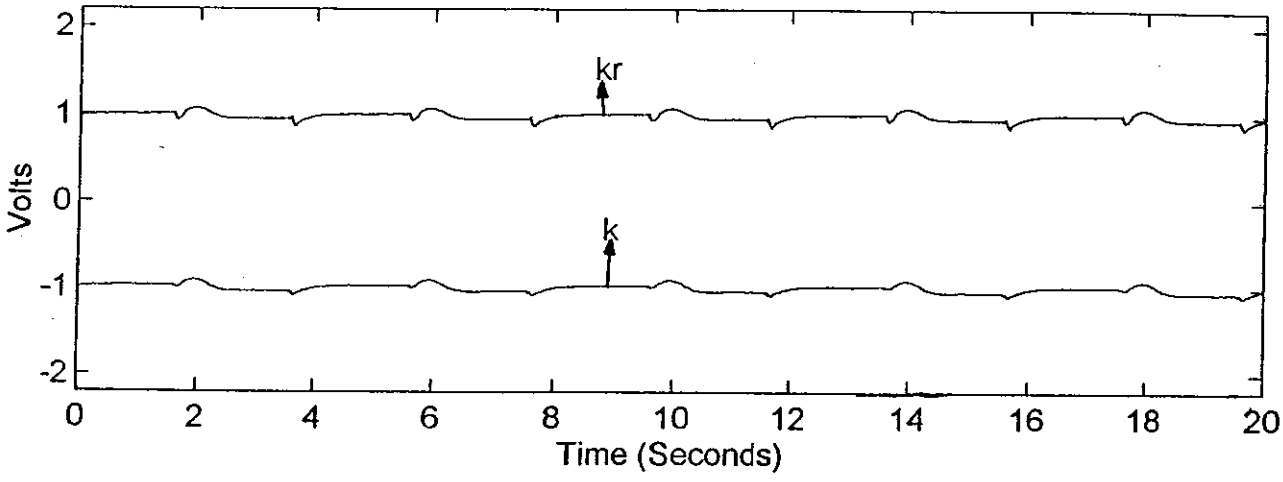

(b) MCS gains

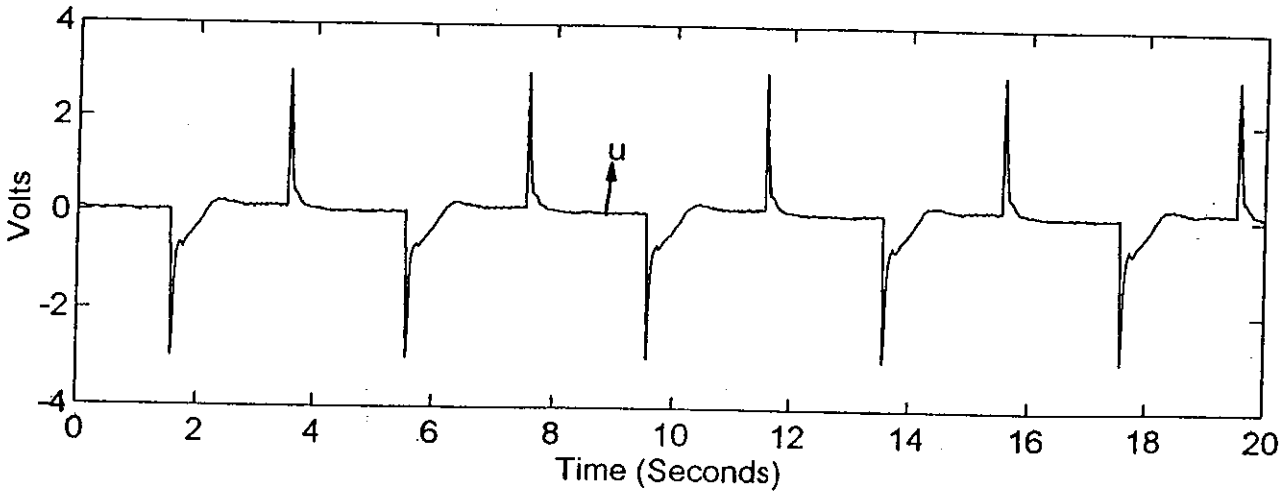

(c) Control signal

Fig. 6.16: MCS step response, supply pressure 13.8 MPa, load 7.5 kN.

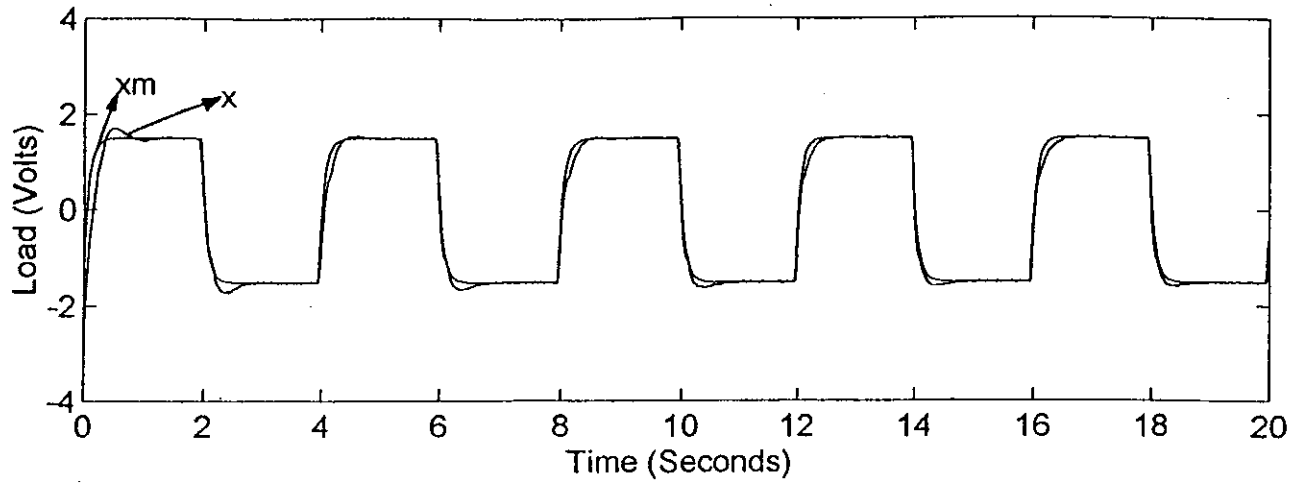

(a) The plant and reference model outputs

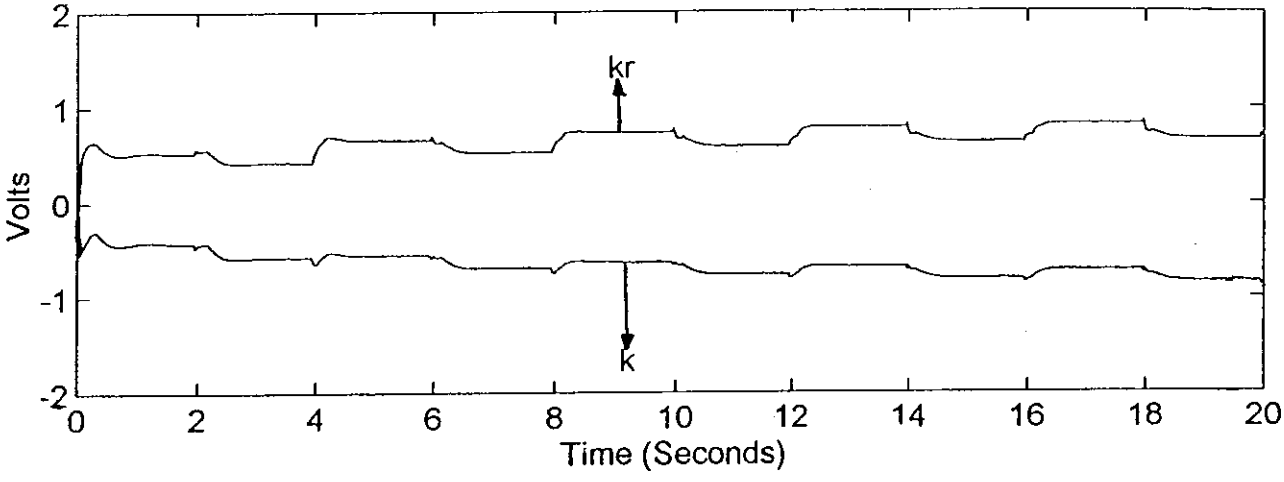

(b) MCS gains

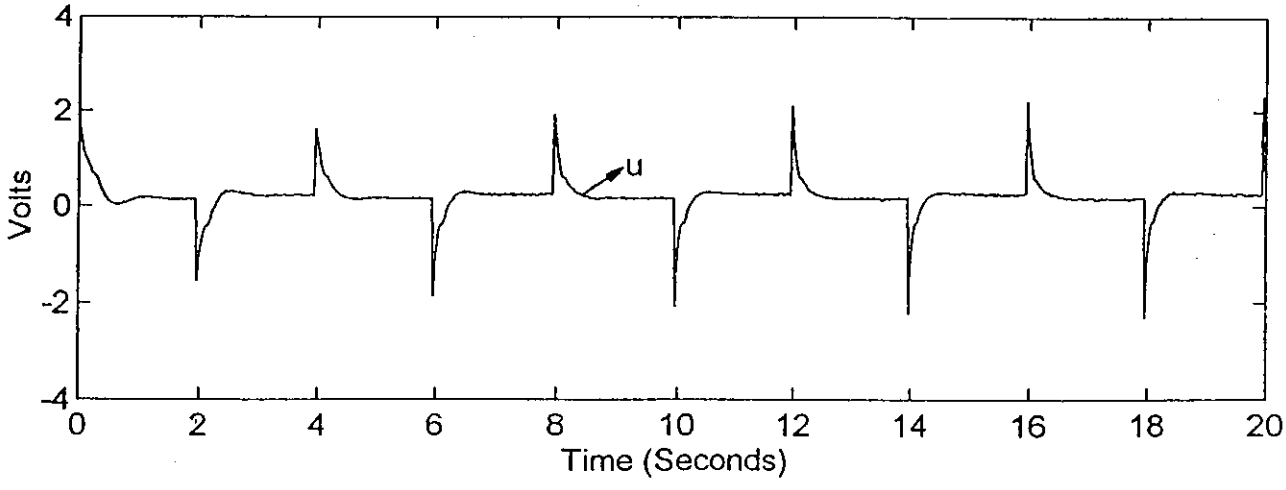

(c) Control signal

Fig. 6.17: MCS step response, supply 13.8 MPa, load 7.5 kN, initial adaption

Discussions

Both controller are implemented by using an aluminium specimen with ϕ 10 mm. In the case of step response tests there is a spike at the beginning of each step changes, then the steady-state error becomes zero. The spikes occurs due to the nonlinear relationship between the flow and the position of the actuator and sudden changes in the amplitude of the input signal. In the case of P+I controller spikes are higher than the MCS controller indicating that the MCS controller can cope better with changes in the input signal and the plant parameters than the P+I controller as it can be seen in Fig. 6.16. The steady-state error driven to zero by integral gain. Initial MCS control results are shown in Fig. 6.17, the plant response under load controller shown in Fig. 6.17a, spikes get smaller after 14 seconds, which is more suitable in materials testing. At the beginning the adaptive gains are zero as shown in Fig. 6.17b and they gradually increased. After approximately 14 seconds the gains did not increase much indicating that the controller preserves the stability of the system.

6.12.2 - Sinusoidal Tests

In this case supply pressure was set at 13.8 MPa during the tests. The reference signal was chosen as a sine wave of frequency 0.25 Hz and amplitude of 2 V (10 kN). A reasonable choice of Δ was $\Delta = 20$ ms.

The resulting transient response for P+I control is shown in Fig. 6.18. There is a good correspondence between the desired and actual responses. The reference model shown as 'xm', together with the actual response 'x'. Plots of corresponding MCS results are shown in Fig. 6.19a. In this diagram the desired response shown as 'xm' together with the actual response 'x'. MCS controller gains and input signal shown in Fig. 6.19b and c.

In order to show the effectiveness of MCS during the initial adaption phase, the supply pressure kept at 13.8 MPa and the amplitude of the reference signal was 2 V (10 kN). Initially, only small control signal and gain values generated by the controller, after 2 s, the adaption and response tracking are seen to be both rapid and accurate; see Figs. 6.20a, b and c.

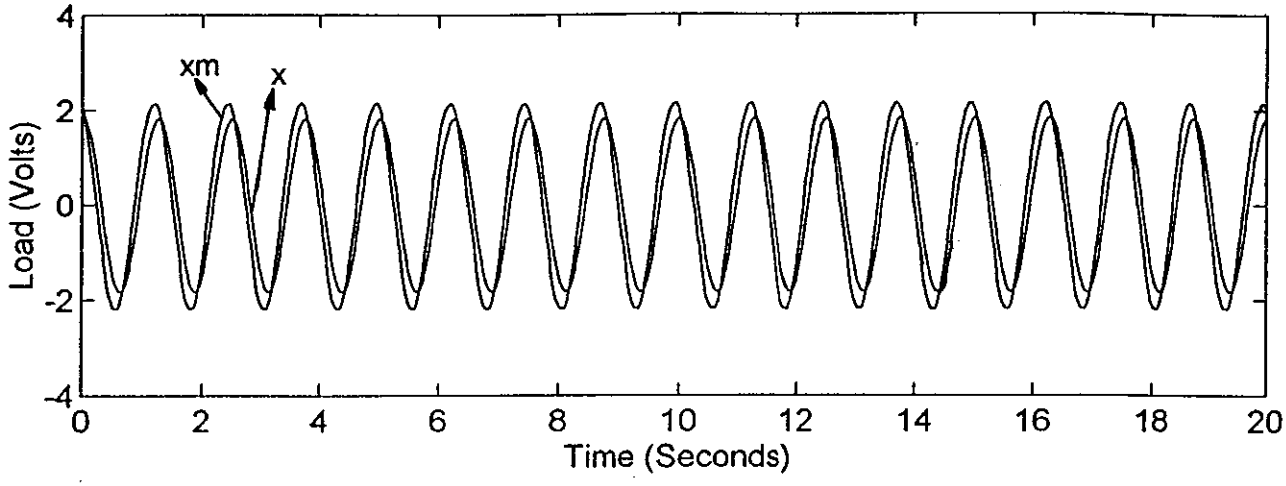

(a) The plant and reference model outputs

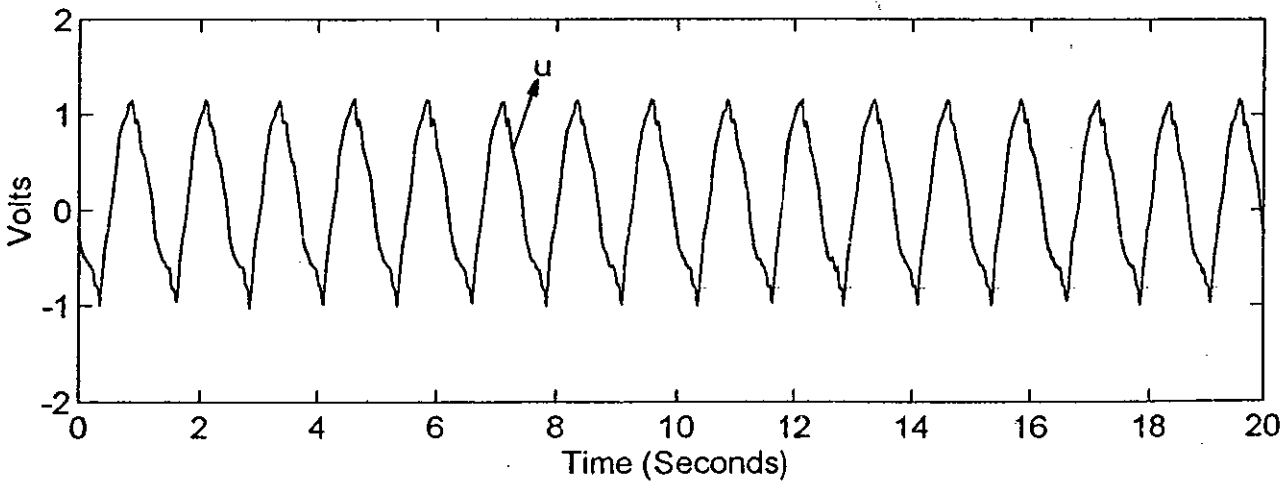

(b) Control signal

Fig. 6.18: P+I transient response, supply pressure 13.8 MPa, load 10 kN.

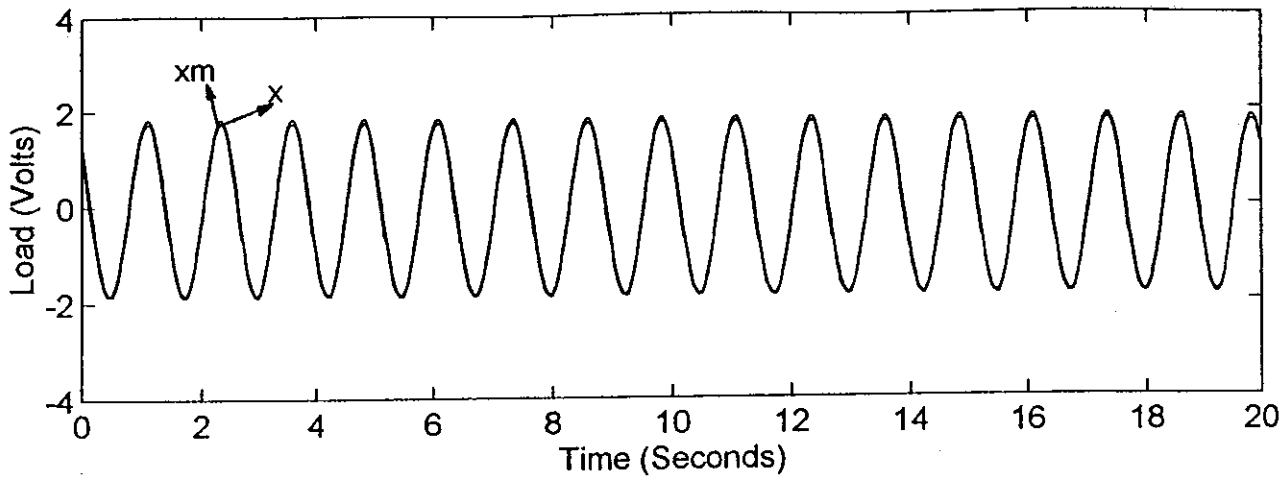

(a) The plant and reference model output responses

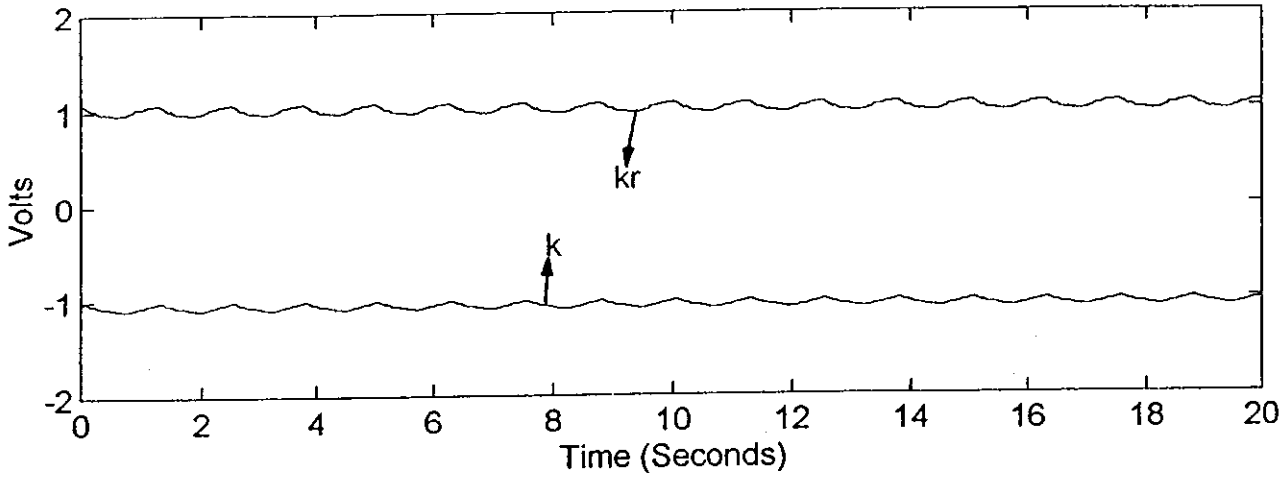

(b) MCS gains

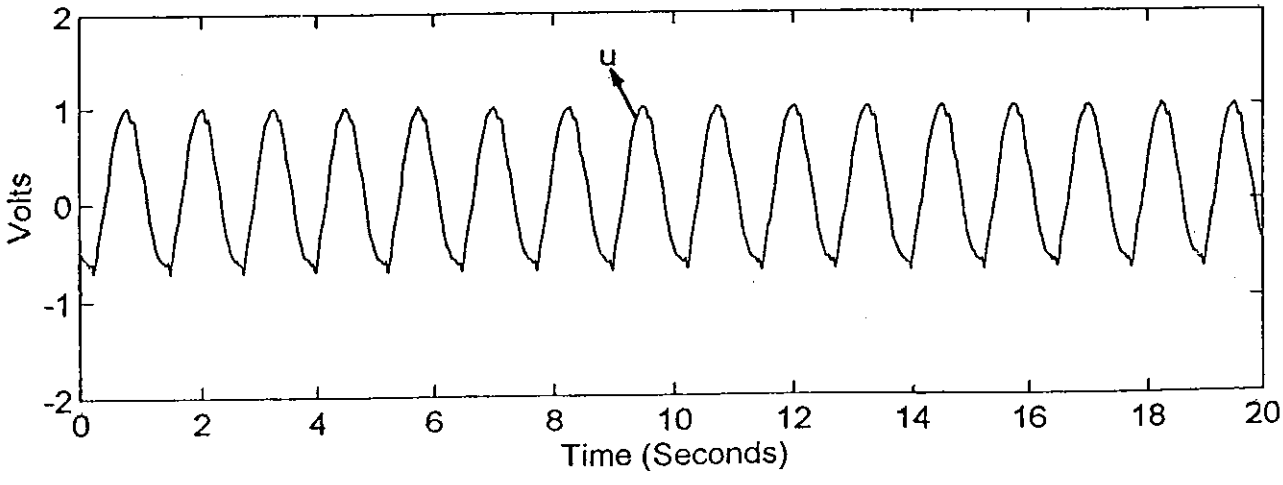

(c) Control signal

Fig. 6.19: MCS transient response, supply pressure 13.8 MPa, load 10 kN.

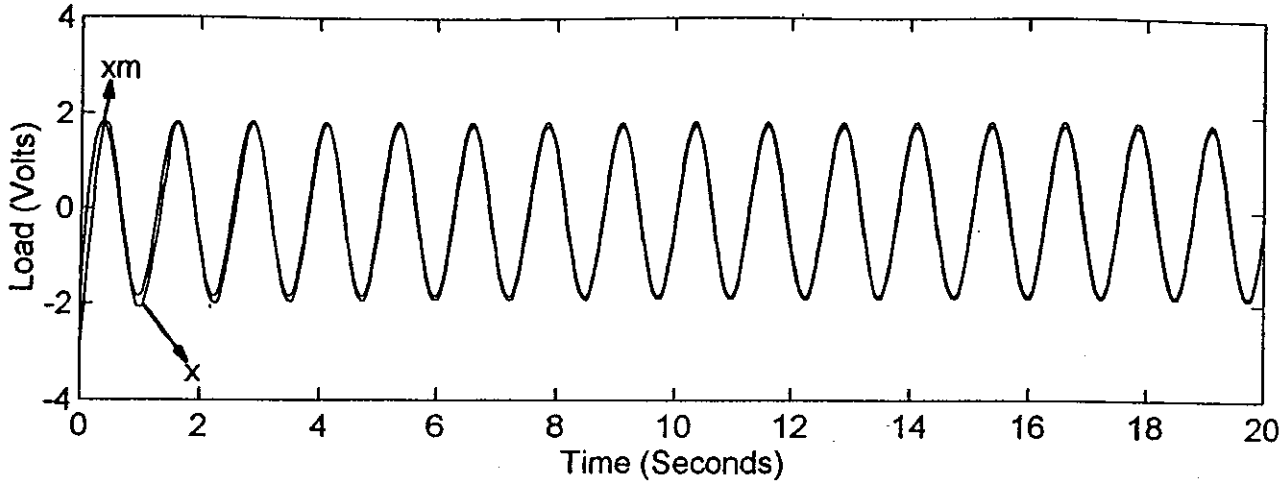

(a) The plant and reference model output responses

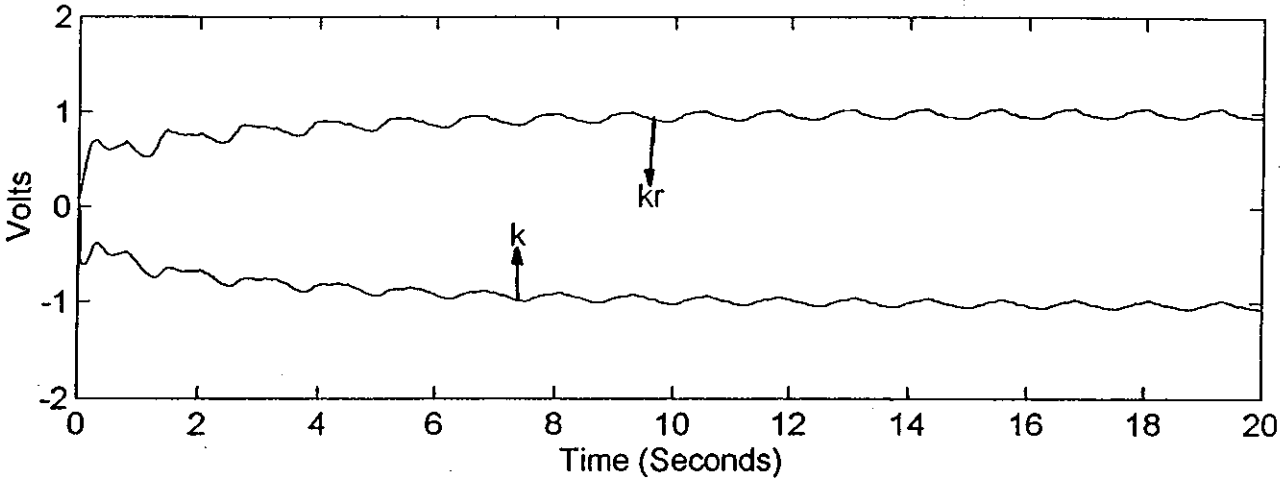

(b) MCS gains

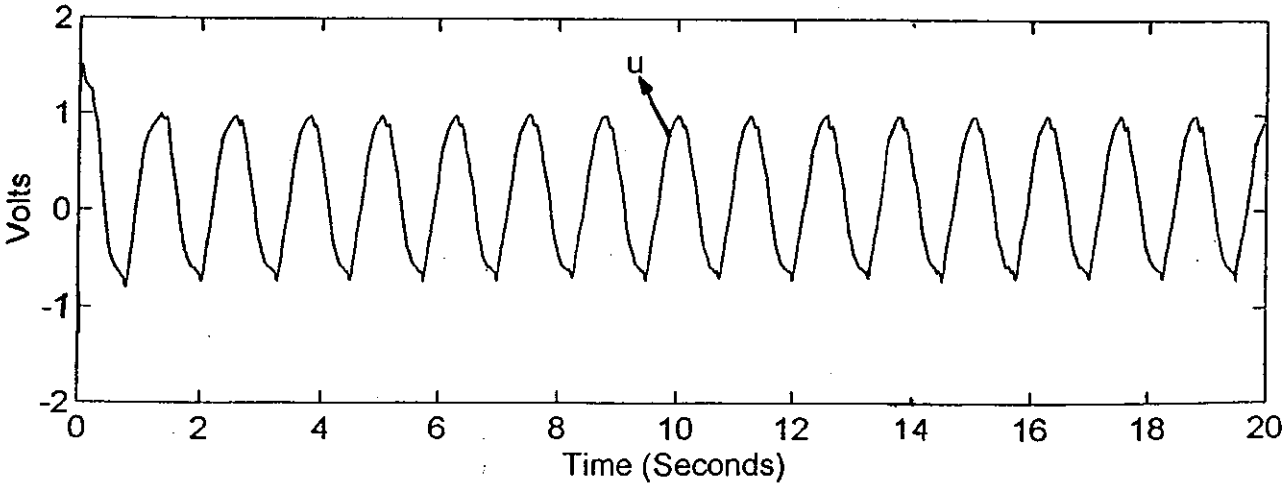

(c) Control signal

Fig. 6.20: Initial MCS transient response, supply pressure 13.8 MPa, load 10 kN.

Discussions

In the case sinusoidal tests the plant responses are smoother than step response tests due to gradual changes in the sinusoidal input signal for both controllers. The steady-state error in the case of the MCS controller is smaller than the P+I controller as shown in Figs. 6.18 and 6.19. It is observed that small plant parameter variations occurs when the amplitude of the input signal is changed. Initial sinusoidal MCS results shown in Fig. 6.20, the controller gains started from zero, rapidly adapt to the changes in the plant and environment. After 16 seconds gains are settle down and did not increased much afterwards as shown in Fig. 6.20b.

6.13 - CONCLUSIONS

In this chapter the Minimal Controller Synthesis (MCS) algorithm has been applied to the ESH Servo-hydraulic Materials testing machine. The MCS algorithm was applied in Single Input Single Output (SISO) form. For nominal operating conditions (supply pressure 13.8 MPa, load 7.5 kN), the second order transfer function model was seen to be an appropriate choice, and this model was used to design a P+I controller for the plant. Proportional Plus Integral controller (P+I) matched the design expectations. The MCS algorithm was implemented on the servo-hydraulic rig, and the closed-loop results compared with those produced by P+I control under load control. The MCS controller performed better than a well designed P+I, despite MCS requiring no plant dynamic parameters. Proportional Plus Integral controller design requires plant system identification, like other conventional controllers. The MCS algorithm was implemented in a simplified reduced-order form. The servo-hydraulic rig has a second-order transfer function and the MCS reference model was first-order. The plant was higher order than the MCS controller. This indicates that MCS appears to be quite insensitive to such mismatches. The MCS algorithm can be recommended as a robust controller for the servohydraulic materials testing machine. The algorithm copes with parameter variations in specimens (small plant parameters variation introduced when the amplitude of the input signal is changed) and in the test machine itself (nonlinear effects of the hydraulic fluids

and servovalve dynamics). 'Bumpless transfer' between load, strain and position control can be accommodated with ease, and simultaneous MCS control of temperature cycles is perfectly viable [8].

Adaptive control is suitable for use with materials testing machines which have to test a variety of specimen of very different, and sometimes non-linear, stiffness. Additionally, during the fatigue tests, the stiffness of the specimen decreases as fatigue cracks propagate and a controller which can continuously adapt to the changing specimen characteristics has obvious advantages. The MCS control can be recommended for the materials testing machines as a robust controller against the effects of plant parameter variations, external disturbances and plant nonlinearities (which are high pressure and temperature changes, aeration and cavitation problems) on closed-loop performances. This feature of the MCS control will be detailed in the following chapter (Chapter 7).

REFERENCES

[1] - **GERE, J. M.,& S. P. TIMOSHENKO**, *Mechanics of Materials* , Third SI Edition Published by Chapman & Hall, 1991.

[2] - **YAMAHASHI, Y., K. TAKAHASHI, Y. TAMOTO & S. IKEO**, 'The Improvement of the Frequency Response of an Electrohydraulic Servo System Using Model Reference Adaptive Control Techniques', *Fourth International Fluid Power Workshop*, September 1991.

[3] - **STOTEN, D. P.,& H. BENCHOUBANE**, 'Robustness of a Minimal Controller Synthesis Algorithm', *Internatinal Journal of Control*, Vol. 51, No. 4, pp. 851-861, 1991.

[4] - **LANDAU, I. D.**, *Adaptive Control, the Model Reference Approach*, Marcel Dekker, New York, 1979.

[5] - **DYE, M. G., & STOTEN, D. P.**, *Winctrl4 - Implementation of Real Time Controllers in Windows 3.1*, Department of Mechanical Engineering, University of Bristol, BS8 1TR, U.K., 1995.

[6] - **STOTEN, D. P.**, *Model Reference Adaptive Control of Manipulators*, 1990 (Research Studies Press, Taunton, U.K.).

[7] - **STOTEN, D. P., & H. BENCHAUBANE**, 'Empirical Studies of an MRAC algorithm with Minimal Controller Synthesis', *International Journal of Control*, Vol. 51, pp. 823-849, 1990.

[8] - **STOTEN, D. P.**, 'Implementation of Minimal Control Synthesis on a Servohydraulic Testing Machine', *Proc I Mech E-Part I, Journal of the System Control Engineering*, Vol. 206, No. 13, pp. 189-194, 1992.

CHAPTER 7

COMPARATIVE ROBUSTNESS TESTS AND STRAIN MEASUREMENT UNDER MCS LOAD CONTROL

7.1 - INTRODUCTION

The purpose of this chapter is to show the robustness of the MCS control, in the presence of plant parameters changes, plant nonlinearities, external disturbances and unmodelled dynamics, under load control. The results of the MCS control will be compared with a conventional, linear P+I load control.

The MCS and P+I control algorithms have been implemented on the ESH materials testing machine as detailed in Chapter 6. It has been shown that the MCS control outperformed a well designed P+I control. In this chapter, the robustness of the MCS control will be investigated in the presence of plant parameter changes due to use of different types of specimen. The chapter begins with a linear description of the plant under load control. Then, the results of the MCS and P+I control algorithms on the ESH materials testing machine are presented. During the tests presented in this chapter, four different specimens in terms of materials and diameters have been used. It is shown that the MCS control performed better than P+I control algorithm, in both elastic and elastic-plastic region, despite MCS requiring no plant dynamic parameters.

The MCS control algorithm can be recommended as a robust controller for servo hydraulic materials testing machine. The algorithm coped with various specimens, which have different materials and diameters under equivalent implementation condition (same

controller gains, reference signal and reference model). It is shown that the MCS algorithm outperforms a well-designed conventional controller, especially when the plant is subjected to gross parameter changes and unmodelled dynamics. Finally, the main conclusions of this chapter are listed.

7.2 - PROCESS DYNAMICS IN CLOSED-LOOP MATERIALS TESTING AND MODELLING UNDER LOAD CONTROL

Closed-loop control accuracy is crucial in materials testing applications due to the fact that even smaller overshoots or undershoots can cause undesirable result in tension or compression tests therefore, controller tuning is also important in such tests. The suitable controller parameter values for any one test depend on the nature of the test, the specimen characteristics and the dynamics of the materials testing machine. Normally, these values vary from test to test. Manual tuning of the controller parameters can be a serious problem especially many controller parameters need to be reset during the operation of the machine. For that reason it is more desirable to use digital controller in material testing applications.

The controller parameters needs to adjusted according to the changes in the plant parameters for satisfactory plant output response. The plant dynamics changes enormously during materials testing due to the changes in specimens and the machine characteristics. Using adaptive control in this field have many advantages, such as adaptivity to the changes in the working condition. Users do not redesign the controller for new condition since the controller itself doing this task automatically.

7.3 - USING THE MCS LOAD CONTROL IN THE CASE OF STRAIN MEASUREMENT

7.3.1 - Strain Measurement by Contacting Specimens

In general, strain measurement techniques uses direct contact with the test specimen surface which requires high degree of skill and patience by the users [1]. Surface

preparation of the testpiece is particularly important for the accuracy of the test. In tension or compression, strain is defined as the elongation per unit of the gauge length, and described as follows

$$\varepsilon = \frac{l - l_0}{l_0} \tag{7.1}$$

where l is the gauge length at any time and l_0 is the original gauge length. This expression is satisfactory for elastic strains since l-l_0 is small. For plastic deformation the gauge length will change considerably, therefore using natural strain, ε_n is more suitable in such cases which is given below

$$\varepsilon_n = \ln \frac{l}{l_0} \tag{7.2}$$

$$\varepsilon_n = \ln(\varepsilon + 1)$$

Equations (7.1) and (7.2) give similar results for strains less than 0.1. If strain is below this value, it is reasonable to use the first equation to measure strain. For larger strains, and depending on the application, it is more appropriate to use (7.2) when converting output signals. There are many contact strain measurement techniques which are currently in use, some of this methods are given as follows: capacitance strain gauge; foil strain gauge; the electrical, wire resistance strain gauge; servo controlled strain gauge. Transducers are converted displacement into an electrical voltage output and they have been widely used in the case of strain measurement.

7.3.2 - The LVDT Extensometer (5 mm)

Linear Variable Differential Transformer (LVDT) device, with good linearity and low cost they have become very common in creep laboratories. Under load control, the device produces an error when the direction of the loading changes.The internal spring of the LVDT is the source of this error. Additionally, LVDT devices are also sensitive to ambient changes and the presence of magnetic fields. The long standing LVDT's are best used in their more traditional role in the low temperatures (below 250 °C), but they are not effective at high temperatures.

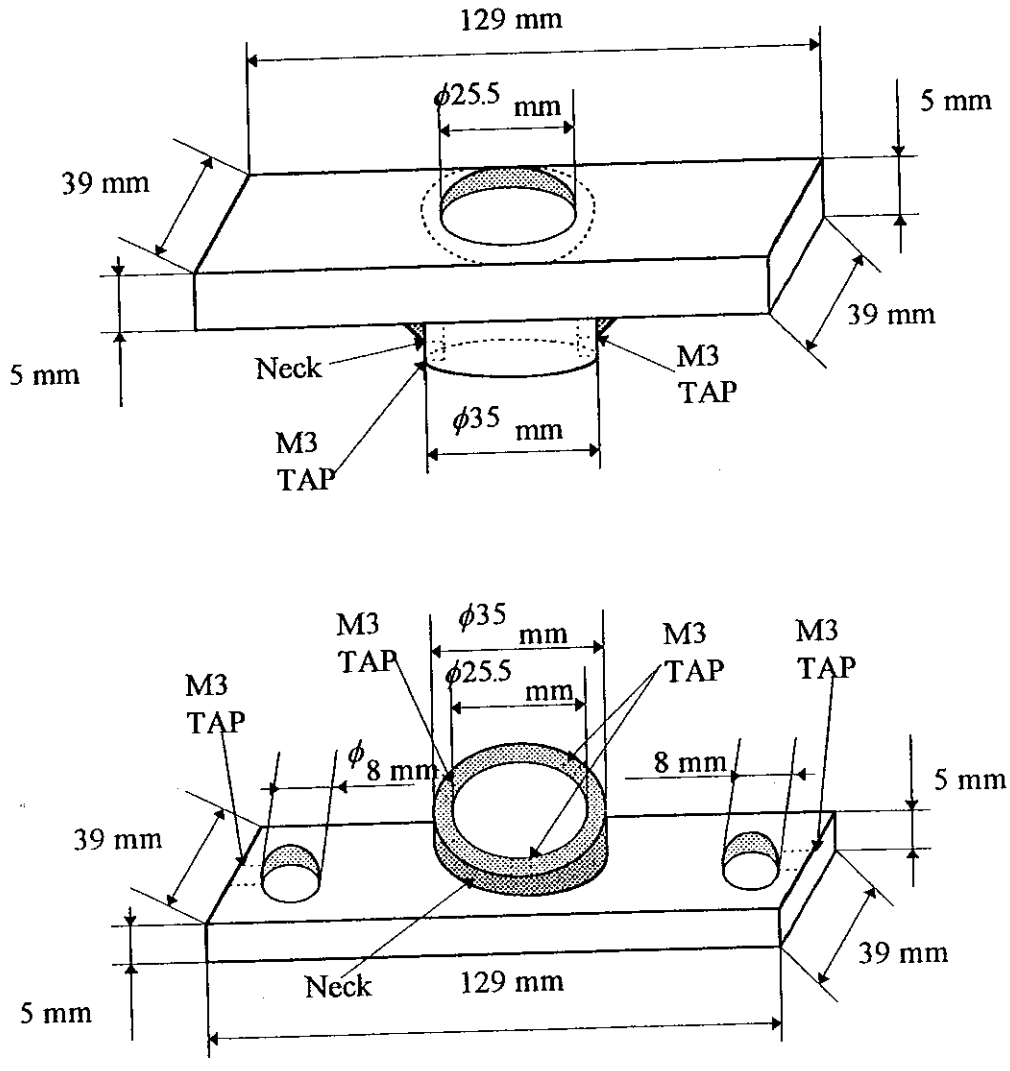

Fig 7.1: The top and bottom plates of the LVDT extensometer.

The LVDT extensometer, which is presented in this section, has been made in the Mechanical Engineering Department Workshop at Bristol. The extensometer consists of two parallel rectangular plates each of width 39 mm and height 5 mm and two LVDT's which are placed either side of the bottom plate, shown in Fig. 7.1. The bottom plate has two holes with $\phi 8$ mm either side of each corner which is 5 mm away from the plate edges, so that two LVDT's can be placed in these holes and fixed by two M3 screws at zero position. The two LVDT's have a range of 5 mm which corresponds to ± 10 V. Both plates have a hole in the middle of them with $\phi 25.5$ mm which will help to drag these plates on the specimens. Two plates are fixed in the middle of the specimens with ~15 mm gauge length. In order to get fixed gauge length two collets had been used during the installation of the plates on the specimens, which have 10 mm height. The specimens are

made of aluminium ($\sigma = 150$ MPa and Young's modulus is E = 72 GPa), and steel ($\sigma = 320$ MPa and Young's modulus is E = 210 GPa), specimens with $D_1 = \phi 10$ mm, shown in Fig 7.2.

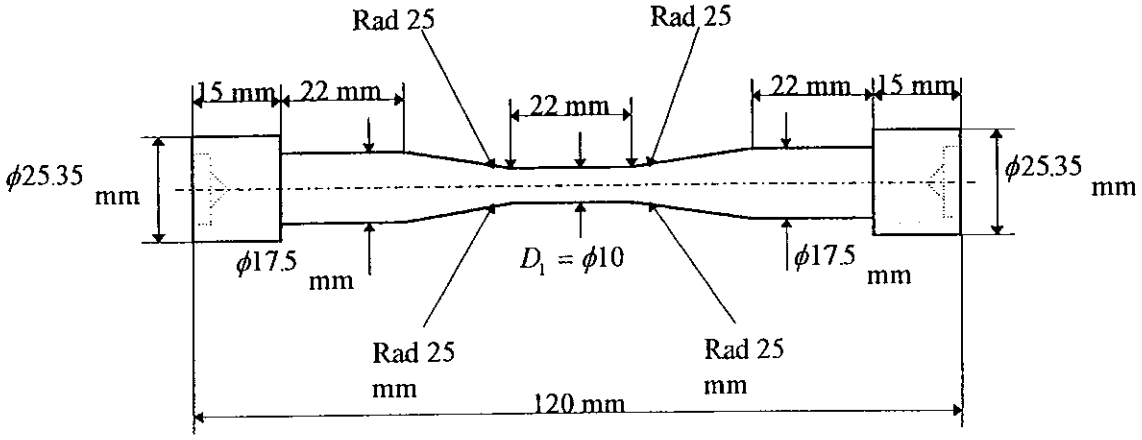

Fig. 7.2: The aluminium and steel specimen with $\phi 10$ mm.

The collets made installation easy, by providing complete support to the specimens, and preventing the slip of the plates and the specimens, therefore it made possible to have predetermined fixed gauge length. Contact between the plates and the specimens is made by three M3 screws, for this reason, three M3 tap are located on the neck of the top and bottom plates, as shown in Fig. 7.3.

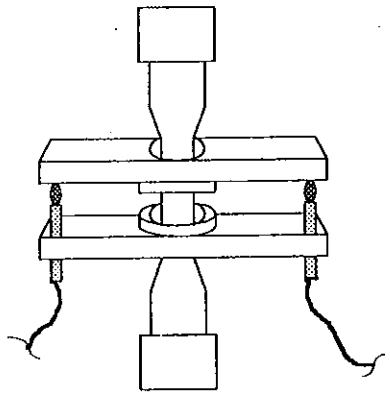

Fig .7.3: The test specimen and extensiometer

All together, there are 6 M3 taps located as 120^0 from each other on the neck of the top and bottom plates, to provide good contact between the specimens and the plates. The structure of the extensometery is rather simple and it is designed for only room temperature. Alignment and bonding of the strain gauge require a high degree of skill and the process of installing a gauge is time consuming. After fixing the extensometer on the specimens, the whole construction was loaded to the ESH materials testing machine under MCS load control, as shown in Fig. 7.4.

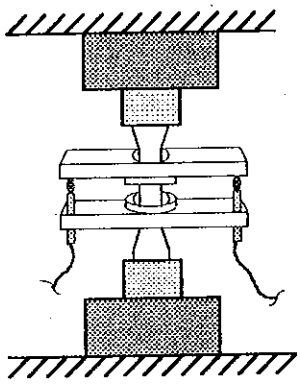

Fig. 7.4: Test specimen under MCS load control

7.3.3 - Implementation of the MCS Control

The MCS control was implemented in two degrees of freedom form, there was no control action in the second degree (strain) of the controller. In fact, this implementation is only for controlling the load signal. The strain signal is not controlled. Therefore it can be treated as SISO MCS. While the specimen is controlled under MCS load control the strain signal is read and logged by the controller. Thus, the second degree of the control used as measurement channel of the strain signal.

Controller hardware consisted of a 486 PC machine equipped with 12-bit D/A and A/D converters. In the case of the aluminium alloy specimens with $D_1 = \phi 10$ mm, the reference r was chosen as a sine wave of frequency 0.4 Hz, and amplitude 2 V. This amplitude corresponds to the elastic region ($\sigma_y = 150$ MPa) for the aluminium specimens. The desired settling time was $t_s = 0.2$ s, a reasonable choice of Δ was $\Delta = 10$ ms. The adaptive rates are chosen empirically, the values are $\alpha = 0.1$ and $\beta = 0.01$. The stiffness diagram for the aluminium specimens in elastic region is shown in Fig. 7.5a, where k is the

stiffness of the specimen. The control input and MCS gains are shown in Figs. 7.5b and c. In the elastic region, the modulus of elasticity of the specimens can be computed from Hooke's Law ($\sigma = E\varepsilon$). The corresponding, the elasticity modulus and the strain signals are shown in Figs. 7.5d and e respectively. In the case of perfectly plastic region the amplitude of the reference signal was 2.7 V (13.5 kN). The stiffness of the aluminium alloy specimens in plastic region is shown in Fig. 7.6a, together with control signal, gains and strain signal in Figs. 7.6b, c and d respectively. Following the stiffness signal, the steel specimens with $D_2 = \phi 7$ mm produced in elastic region as shown in Fig. 7.7a. In this case, the reference signal was a sine wave of amplitude 2.5 V and frequency 0.4 Hz. The desired settling time was $t_s = 0.4$ s, a suitable choice of Δ was $\Delta = 20$ ms. The adaptive rates were $\alpha = 0.01$ and $\beta = 0.001$. Corresponding control signal, MCS gains, the modulus of elasticity and strain signals are shown in Figs. 7.7b, c, d and e. The stiffness of the steel specimens in elastic-plastic region is shown in Fig. 7.8a, together with the control input, MCS gains, and strain signals are shown in Fig 7.8b, c, and d. In this case the amplitude of the reference signal was 3.4 V. The standard yielding point for the aluminium alloy given as $\sigma_y = 120 - 200$ MPa. The corresponding yielding point measured by MCS is $\sigma_y = 150$ MPa (see in Fig. 7.6a). In the case of the steel specimens the standard yielding point is given as $\sigma_y = 300 - 670$ MPa. Following the yielding point, MCS produced, $\sigma_y = 320$ MPa as shown in Fig. 7.8a. The results produced by the MCS control are in the range of the actual values, indicating that the MCS control can be used in strain and stiffness measurement very effectively. The results confirmed that the robustness of the MCS control in the presence of unmodelled dynamics as proven in Chapter 4.

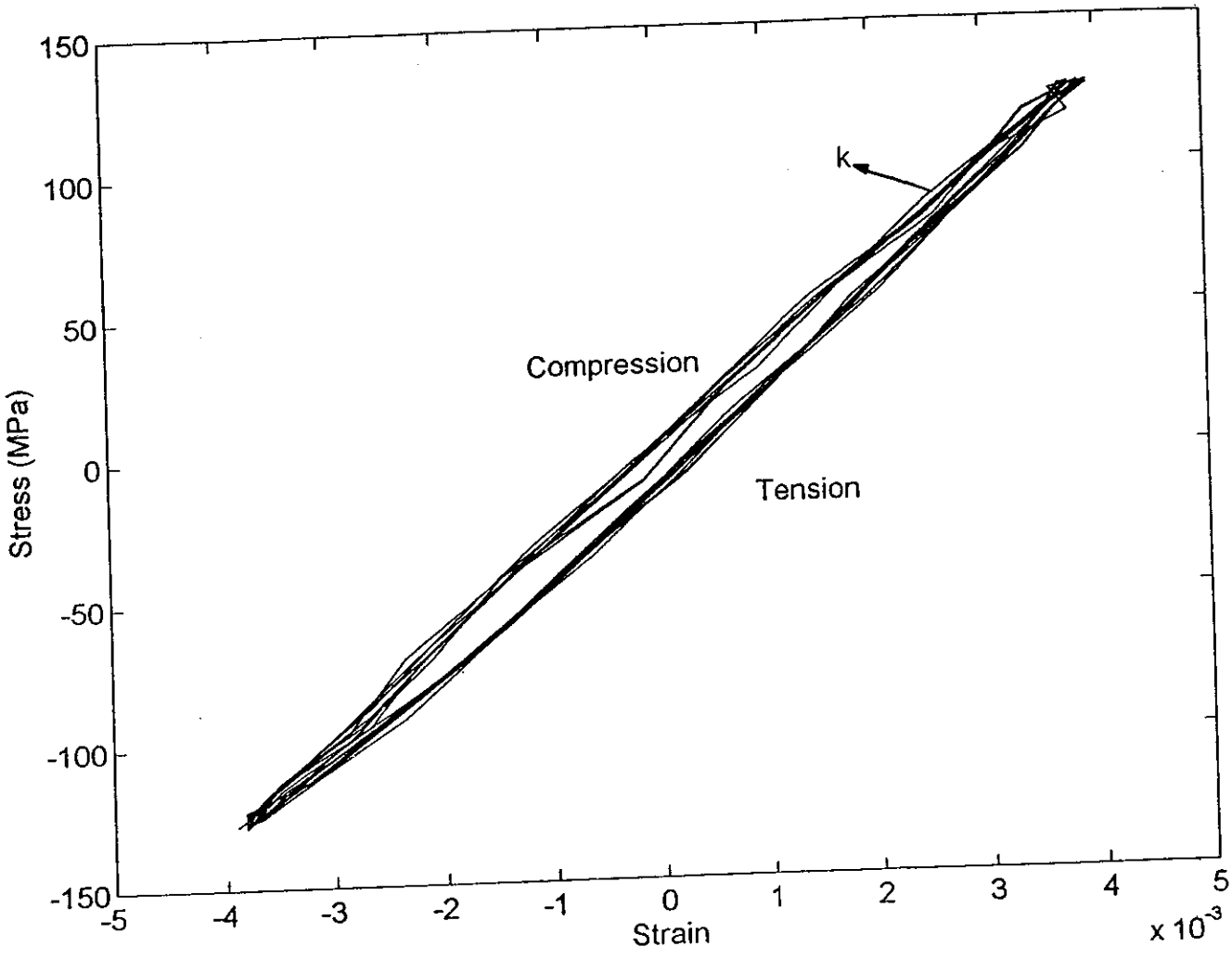

(a) The stiffness of the aluminium alloy specimens with $\phi 10$ mm

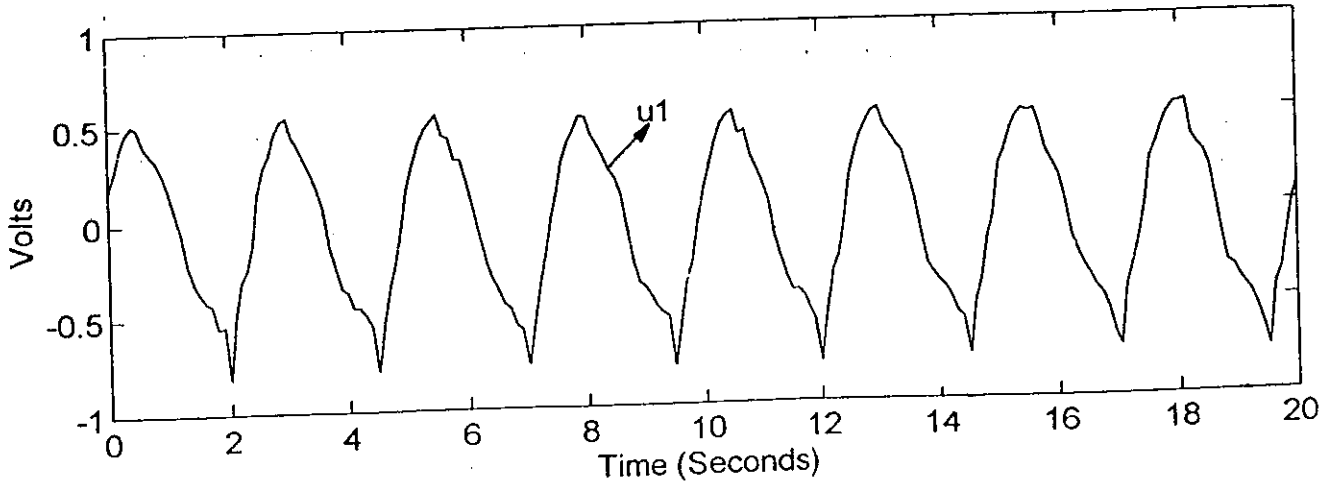

(b) Control signal

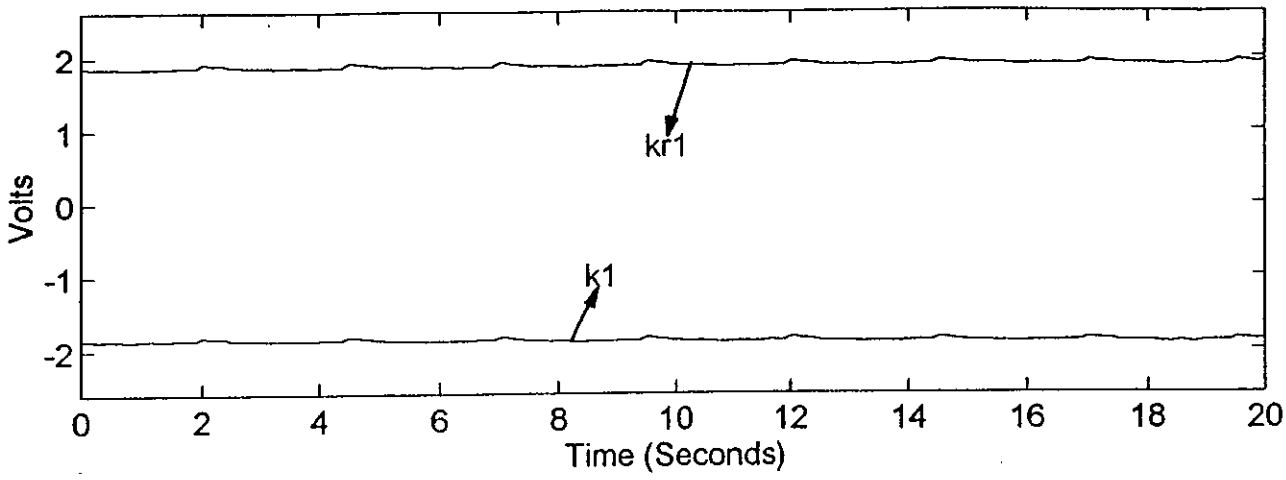

(c) MCS gains

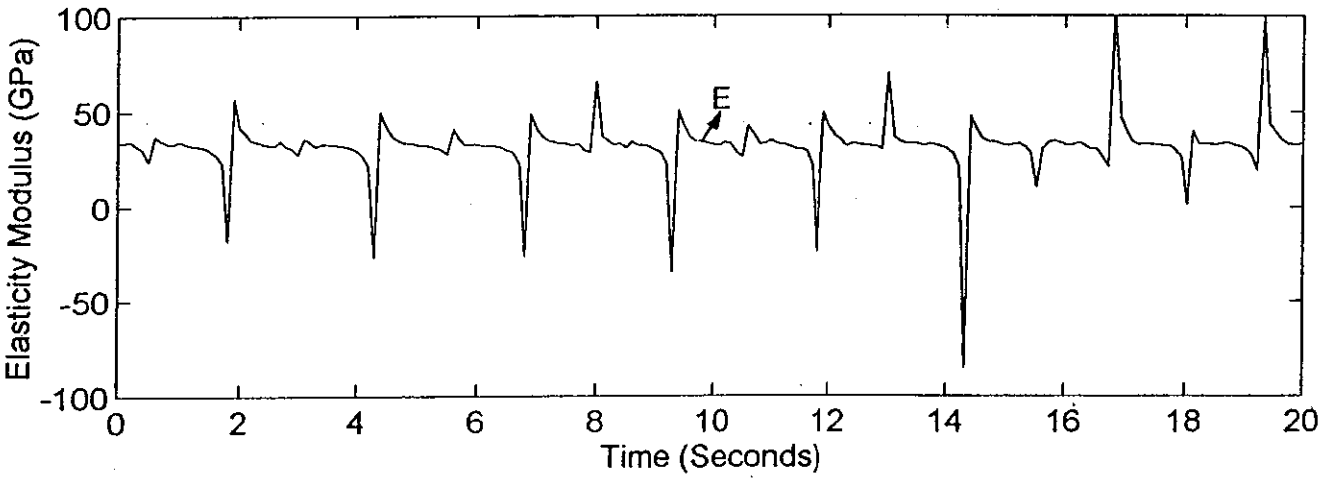

(d) The elasticity modulus

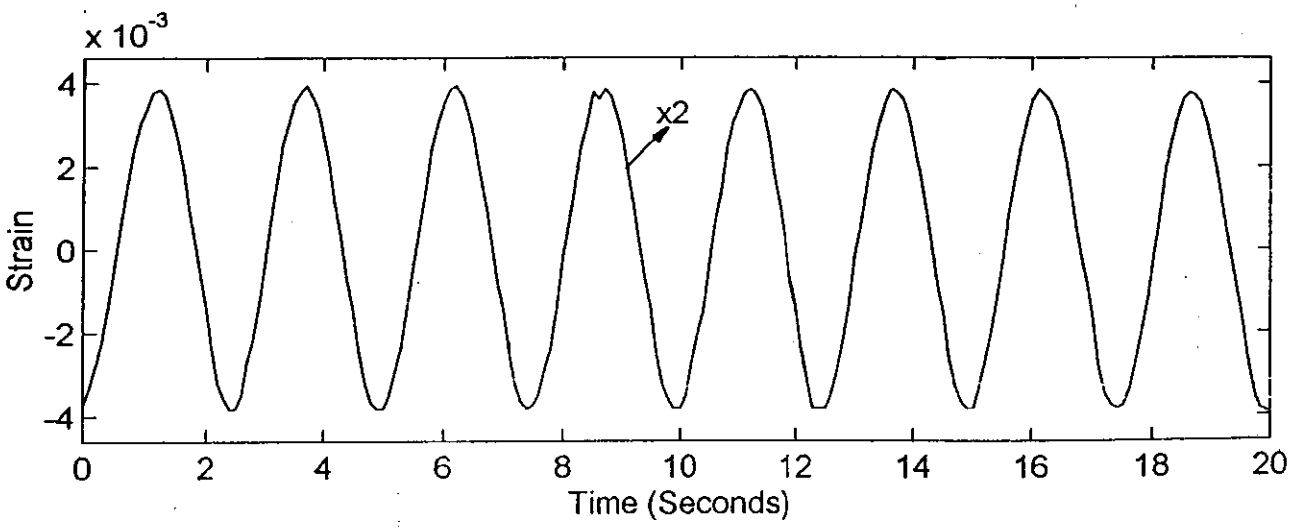

(e) Strain signal

Fig. 7.5: The aluminium specimens with $\phi 10$ mm, in elastic region

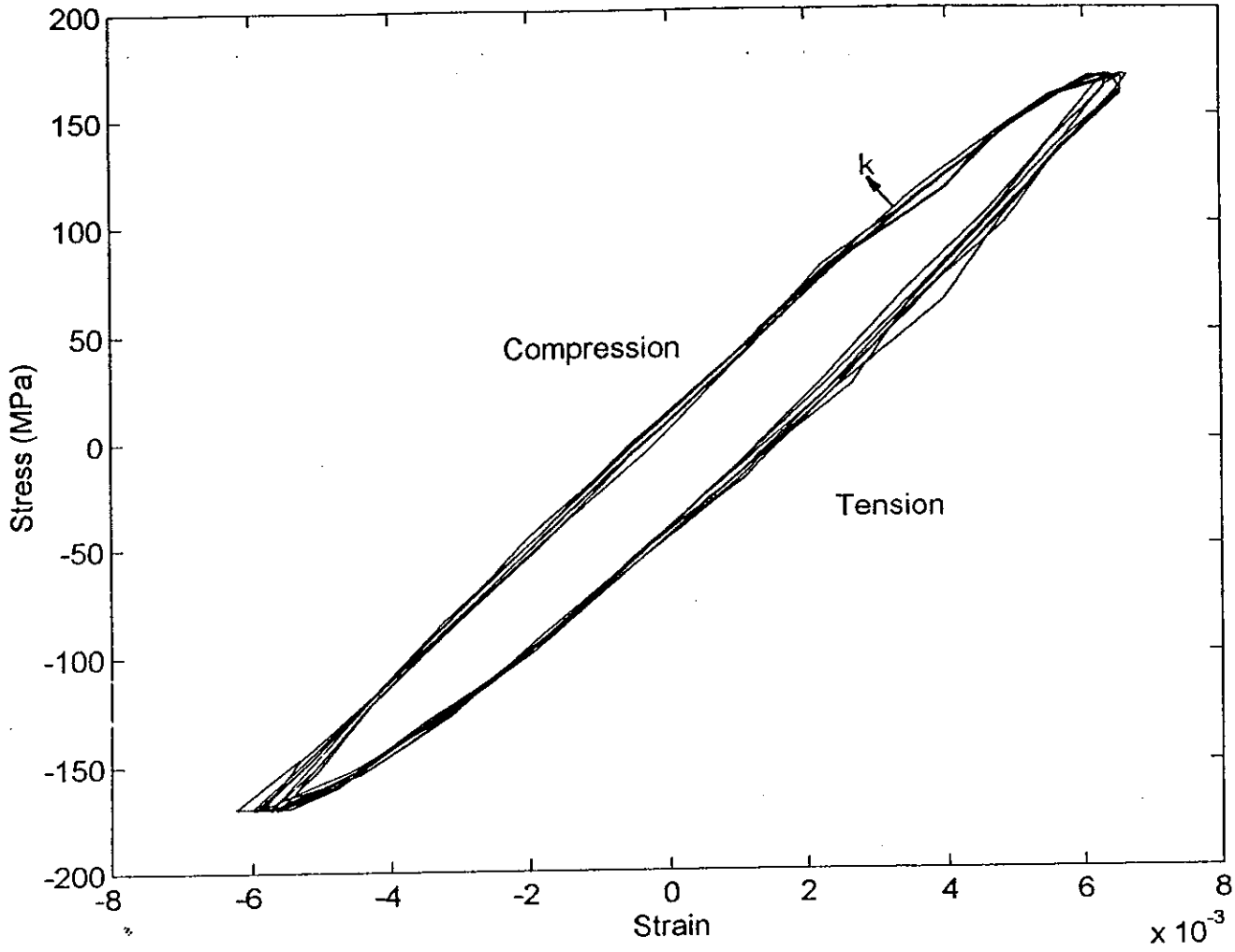

(a) The stiffness of the aluminium alloy specimens with $\phi 10$ mm

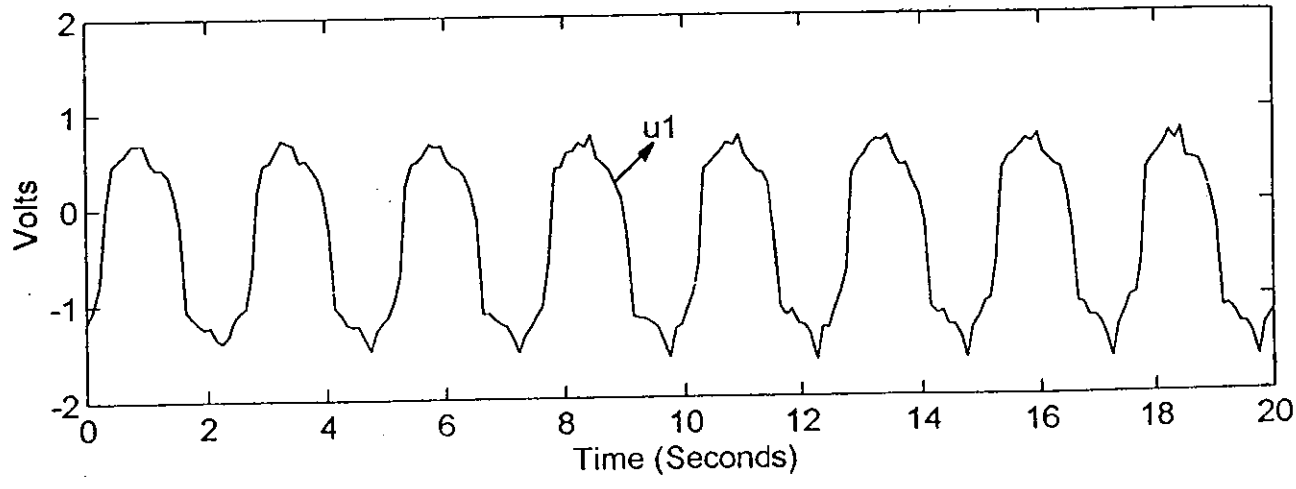

(b) Control signal

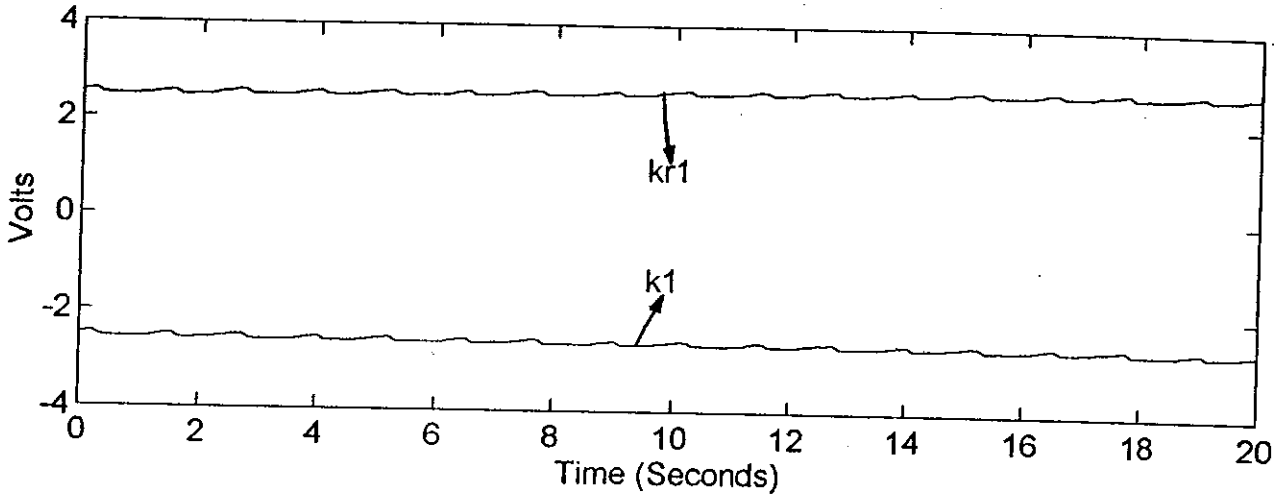

(c) MCS gains

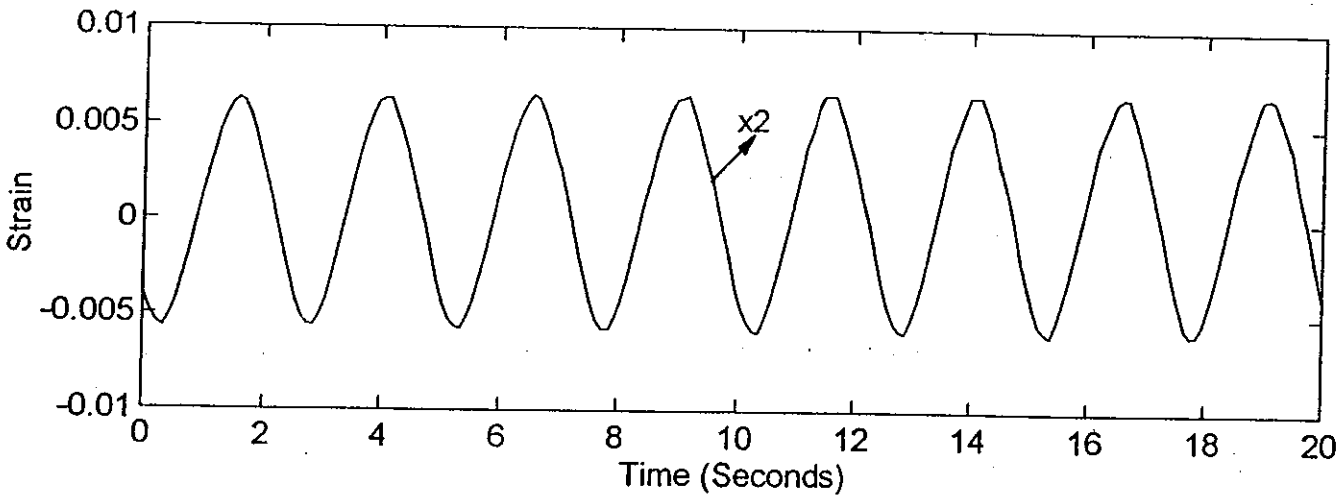

(d) Strain signal

Fig. 7.6: The aluminium specimens with $\phi 10$ mm, in elastic-plastic region

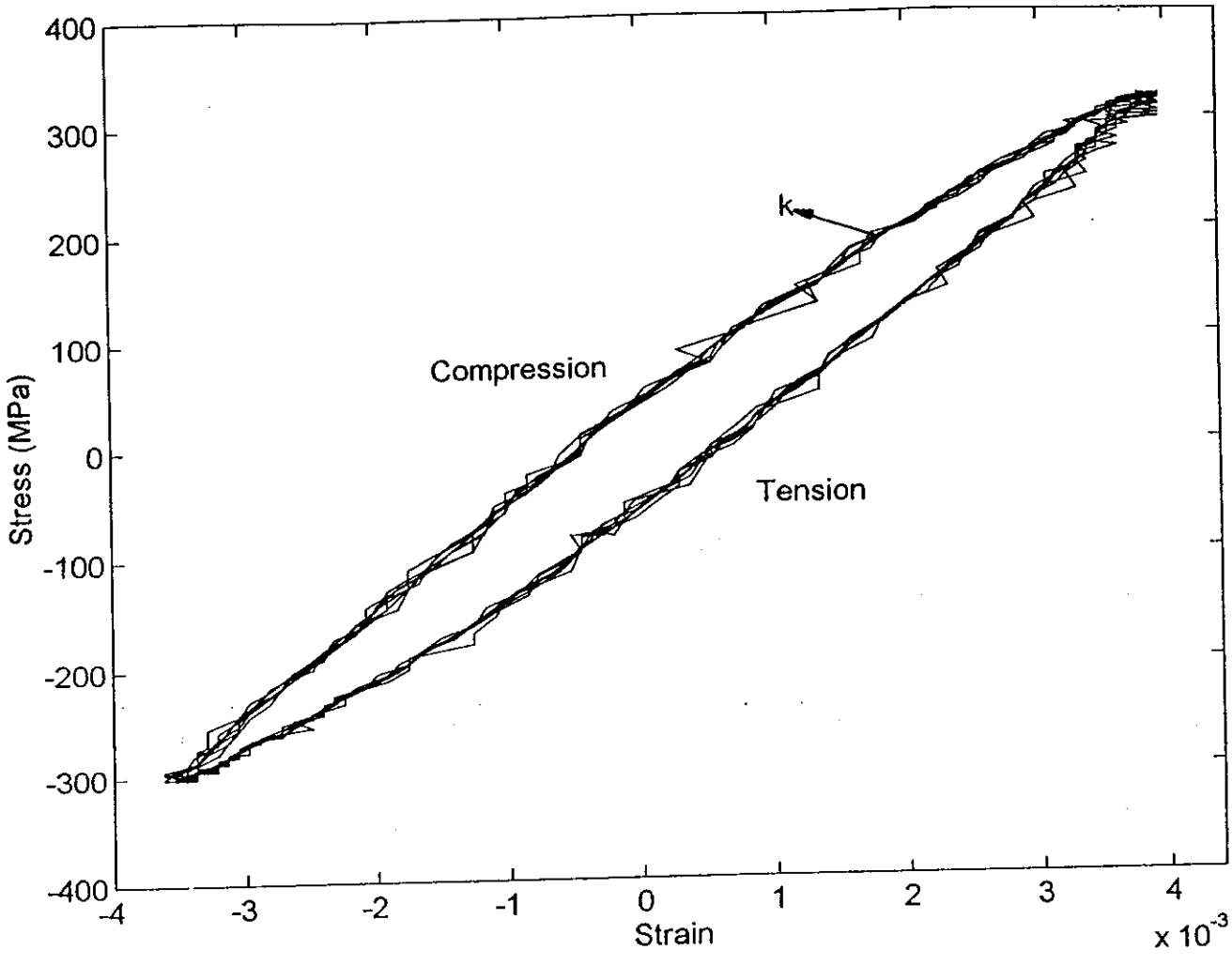

(a) The stiffness of the steel specimens with $\phi 7$ mm

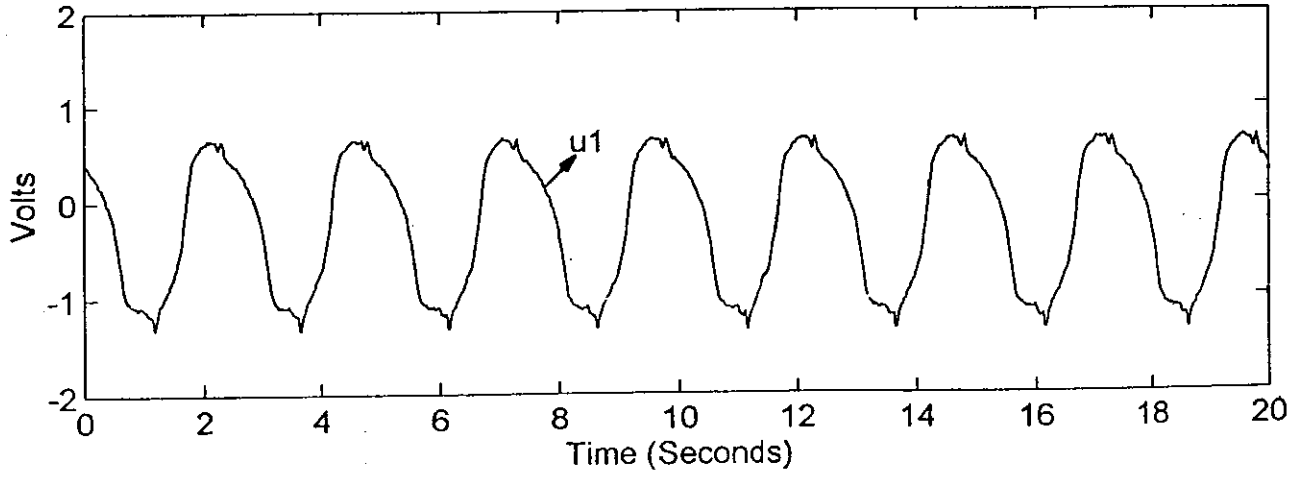

(b) Control signal

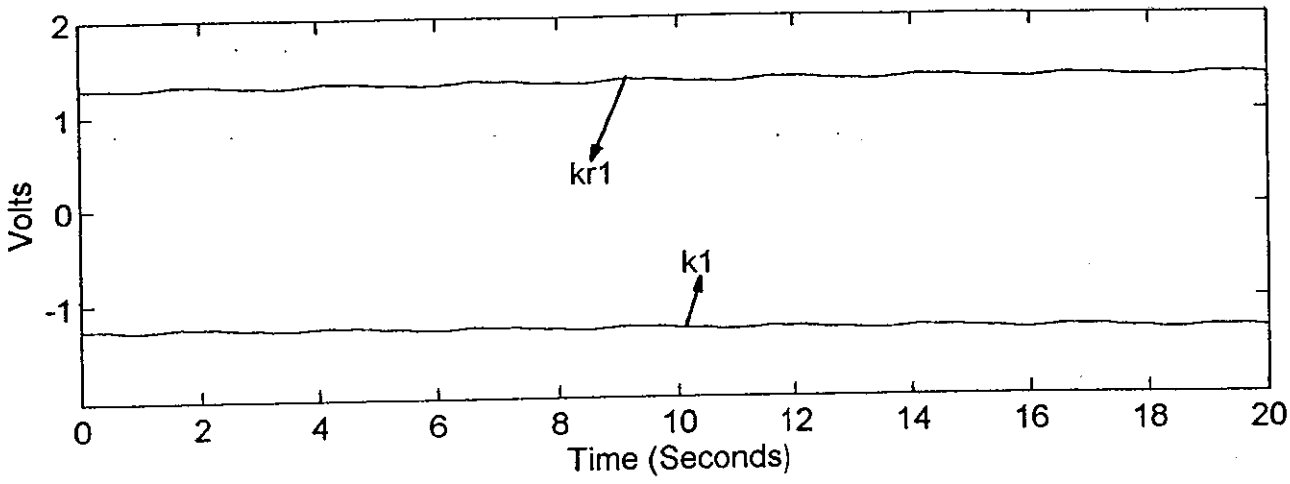

(c) MCS gains

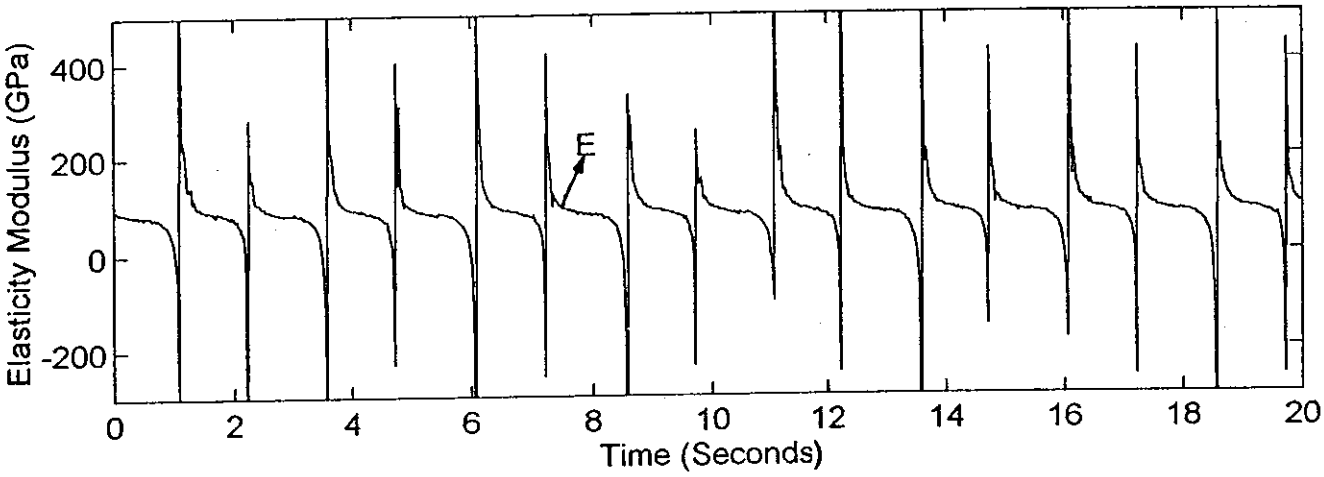

(d) The elasticity modulus

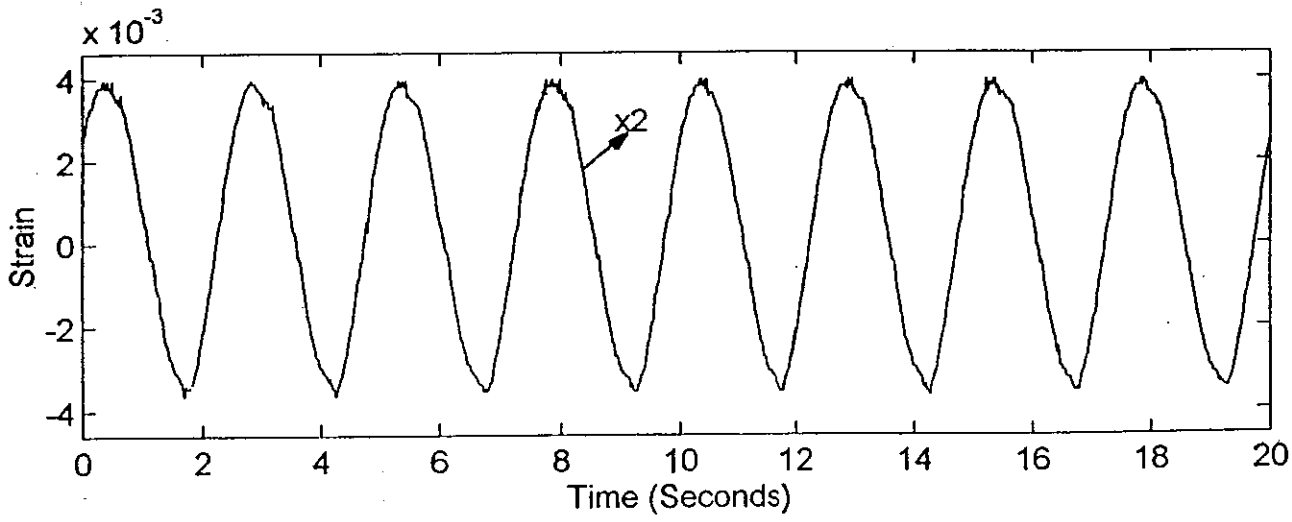

(e) Strain signal

Fig. 7.7: The steel specimens with $\phi 7$ mm, in elastic region

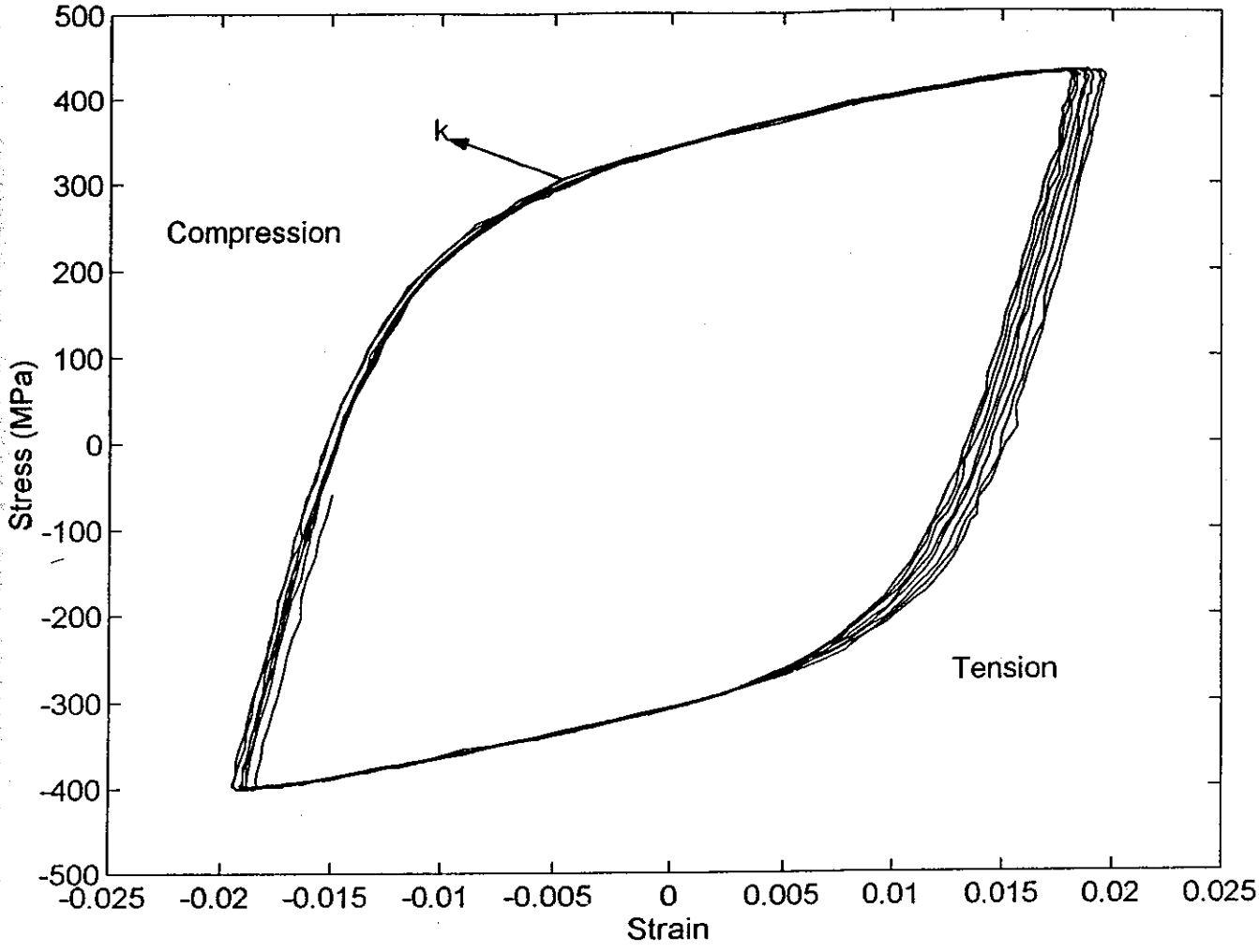

(a) The stiffness of the steel specimens with $\phi 7$ mm

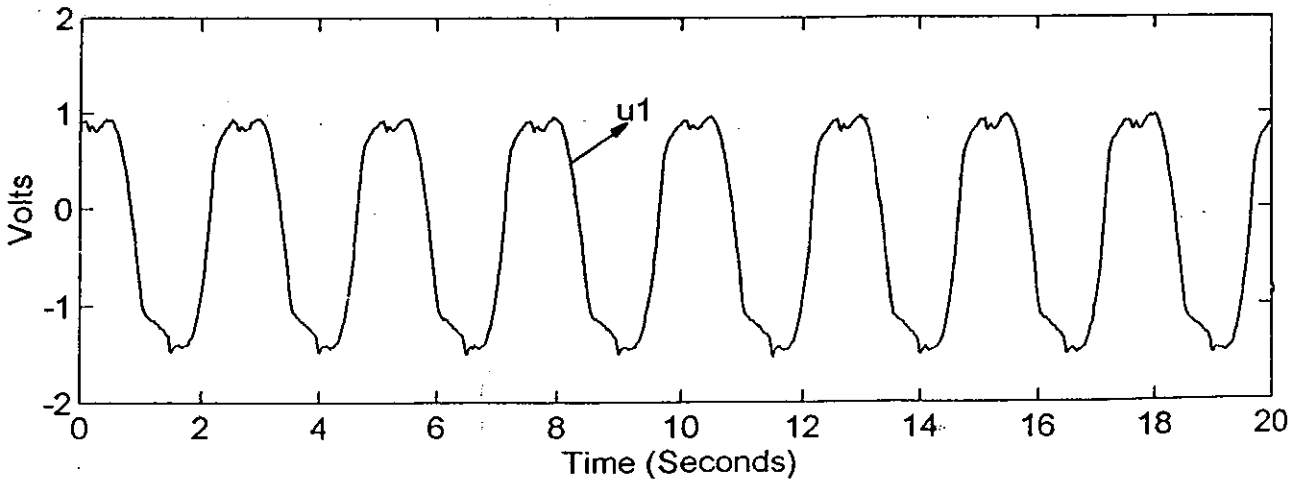

(b) Control signal

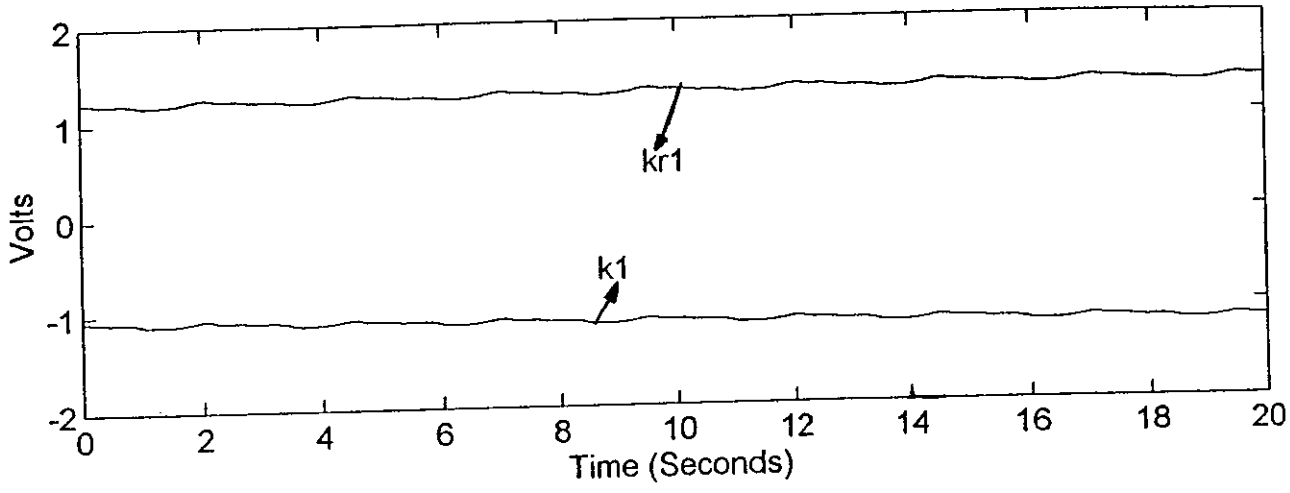

(c) MCS gains

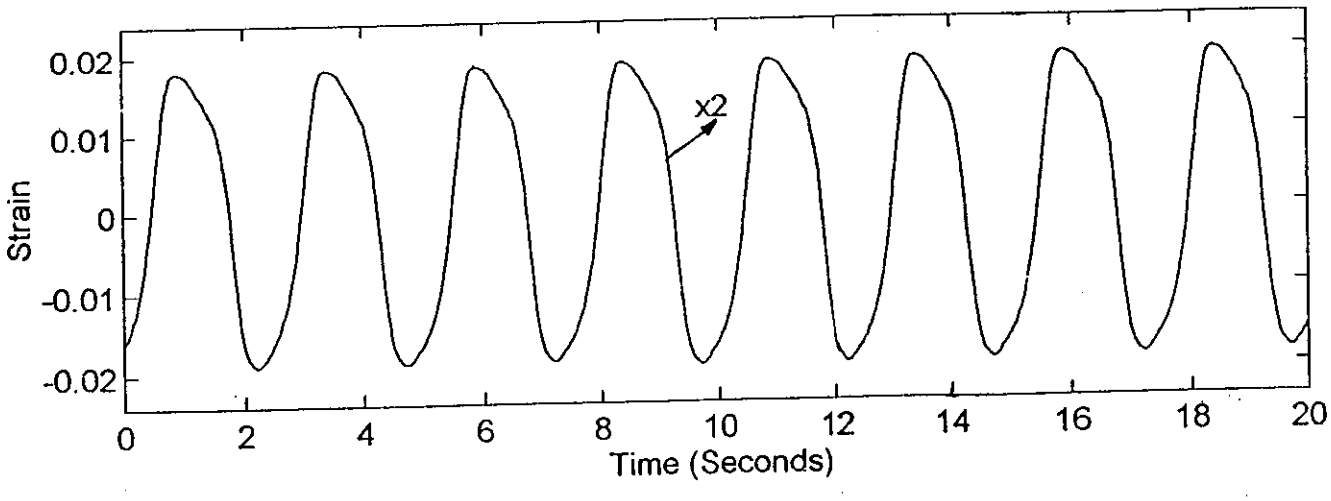

(e) Strain signal

Fig. 7.8: The steel specimens with $\phi 7$ mm, in elastic-plastic region

7.4 - COMPARATIVE ROBUSTNESS TESTS

Both P+I and MCS control have been implemented on the ESH material testing machine in Chapter 6. In this case, the aluminium specimens with ϕ 10 mm taken as the standard tests specimens, then both P+I and the MCS controllers implemented for the standard test condition under load control.

7.4.1 - Tests Specimens

The specimens which are used in comparative elastic and elastic-plastic step response tests shown in Figs. 7.9-7.10.

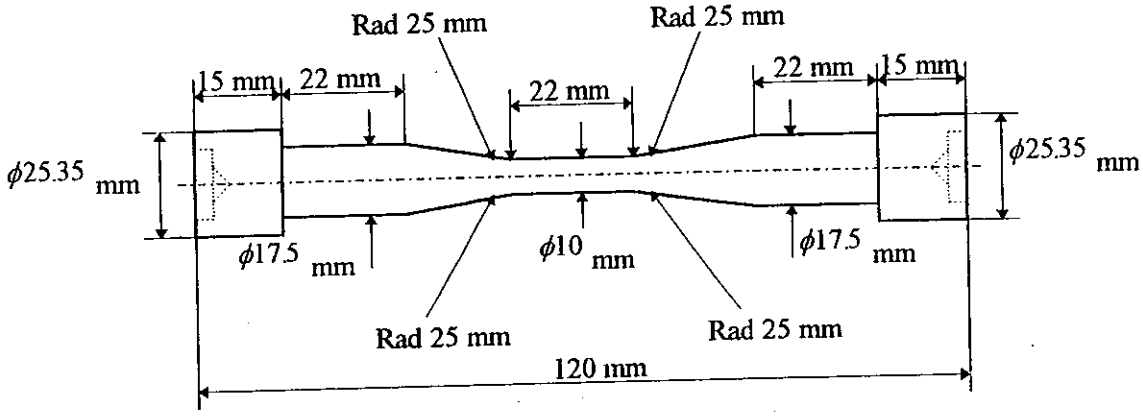

Fig. 7.9: The aluminium and steel specimens with ϕ10 mm.

All together four different specimens used in this set of tests which are given as below:

1 - Aluminium specimens

1.1 - The specimens with $D_1 = \phi 10$ mm

1.2 - The specimens with $D_2 = \phi 7$ mm

2 - Steel specimens

2.1 - The specimens with $D_1 = \phi 10$ mm

2.2 - The specimens with $D_2 = \phi 7$ mm

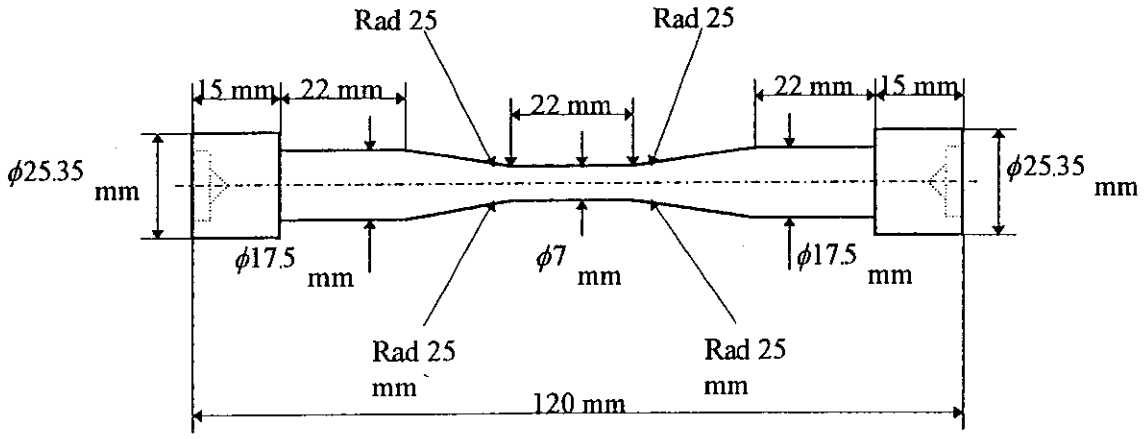

Fig 7.10: The steel and aluminium specimen with $\phi 7$ mm.

7.4.2 - Stiffness of Specimens

In the case of axially loaded test specimen the stiffness is defined in the same manner as axially loaded bar (in Fig. 6.3), that is, the stiffness k is the force required to produce a unit elongation. The elongation of the axially loaded specimen can written as:

$$\delta = \frac{PL}{EA_P} \tag{7.3}$$

where P is the axial force, L is the unloaded length of the specimen, E is the elasticity modulus and A_p is the cross-sectional area of the specimen, which is given as:

$$A_P = \frac{\pi D^2}{4} \tag{7.4}$$

where D is diameter of the specimen. The stiffness of the specimen can be written as below:

$$k = \frac{EA_P}{L}$$

or from Equation (7.4)

$$k = \frac{E\pi D^2}{4L} \tag{7.5}$$

In table 7.1 E_{al} is the modulus of elasticity of the aluminium alloy specimens, E_{st} is the modulus of elasticity of the steel specimens, k_{a10} is the stiffness of aluminium specimens with $D_1 = \phi 10$ mm, k_{a7} is the stiffness of aluminium specimens with $D_2 = \phi 7$ mm, k_{s10} is

the stiffness of steel specimens with $D_1 = \phi 10$ mm and k_{s7} is the stiffness of steel specimens with $D_2 = \phi 7$ mm. From table 7.1, four different specimens stiffness differences were computed in terms of percentage, which are shown below:

k_{a10} is % 65.713 less than k_{s10},

k_{a10} is % 30.0291 less than k_{s7},

k_{a10} is % 51 bigger than k_{a7}.

	The Specimens with $\phi 10$ mm	**The Specimens with $\phi 7$ mm**
Aluminium Alloy	$k_{a10} = \frac{E_{al}\pi D_1^2}{4L}$ $k_{a10} = 47124$ N/mm	$k_{a7} = \frac{E_{al}\pi D_2^2}{4L}$ $k_{a7} = 23091$ N/mm
EN24T (Steel)	$k_{s10} = \frac{E_{st}\pi D_1^2}{4L}$ $k_{s10} = 137440$ N/mm	$k_{s7} = \frac{E_{st}\pi D_2^2}{4L}$ $k_{s7} = 67348$ N/mm

Table 7.1: Stiffness of specimens

7.4.3 - The First Set of Tests (Elastic Region)

In the case of first set of tests (elastic step response tests), both the MCS and P+I controllers performed in the elastic region. The first set of tests consisted of square wave reference signal, of frequency 0.25 Hz and amplitude equivalent to 0.9 V, which was correspond to 4.5 kN (applied load on specimens). This amplitude corresponds to dynamics in elastic region for all specimens, therefore first set of the tests can be called as elastic step response tests. It was required that the P+I and MCS controllers yield critically damped closed-loop responses which settled in 0.35 s. In all cases supply pressure kept on 13.8 MPa during the tests.

For the first set of tests, the steel and aluminium specimens with a cylindrical test section is used and the test specimens deformation restricted to the elastic region.

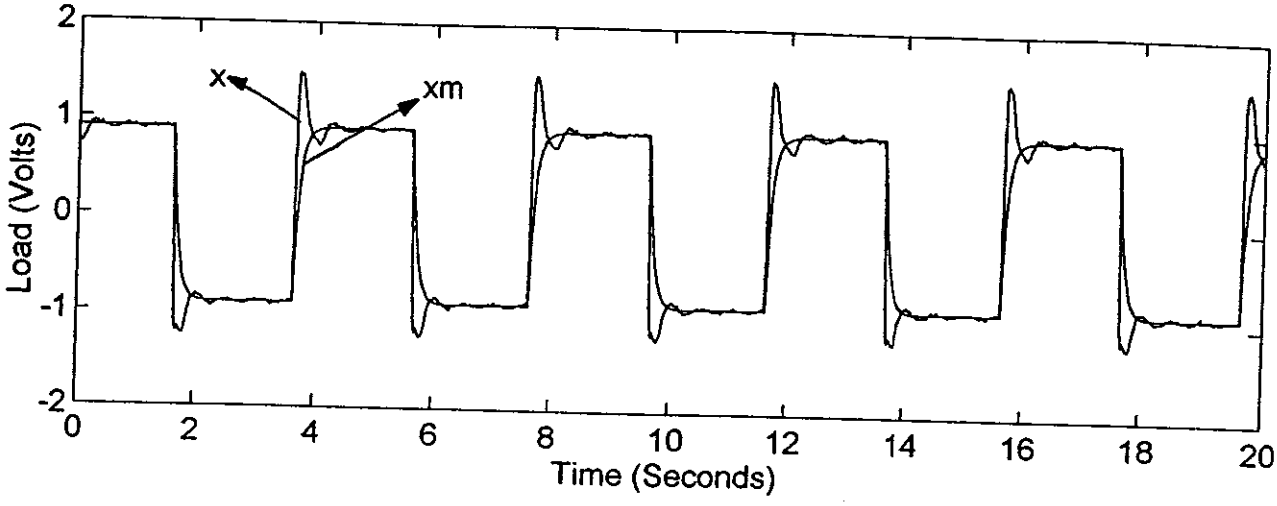

(a) Reference model and plant output signal

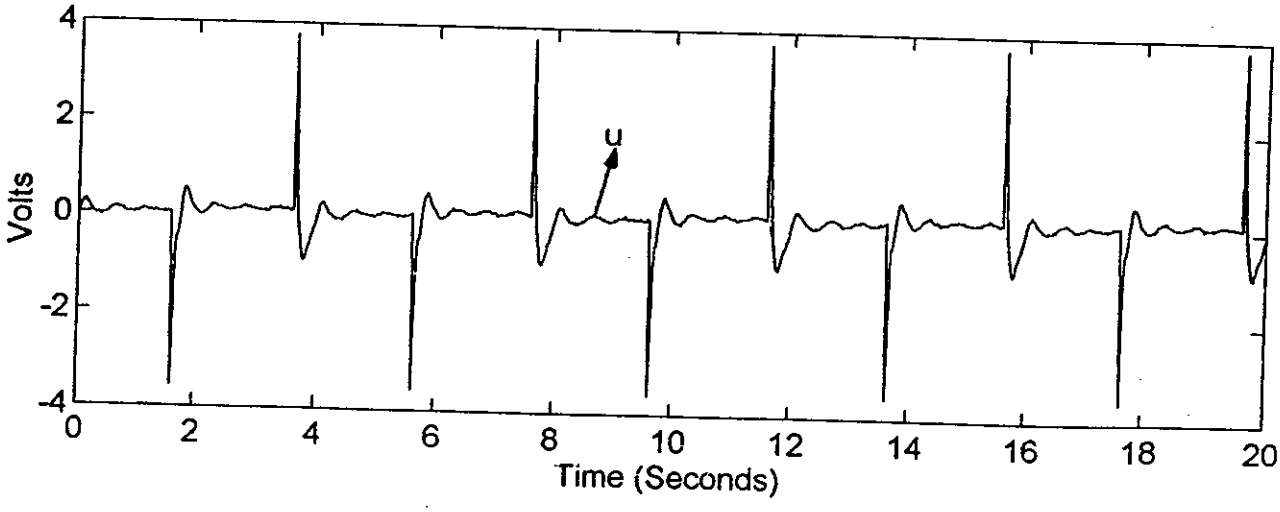

(b) Control signal

Fig. 7.11: P+I control step response, the aluminium specimens with $\phi 10$ mm

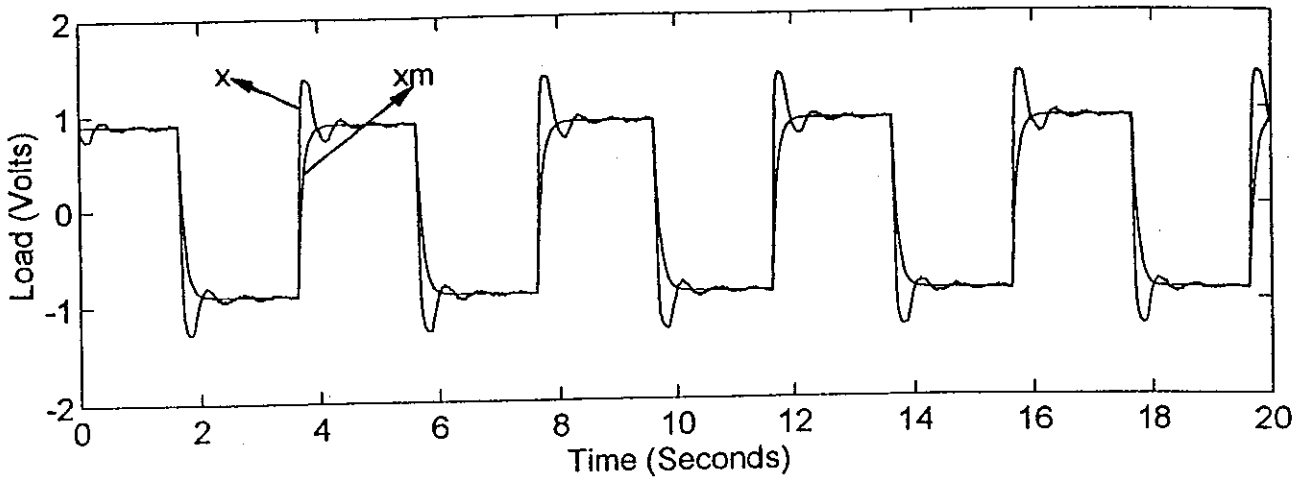

(a) Plant and reference model output signals

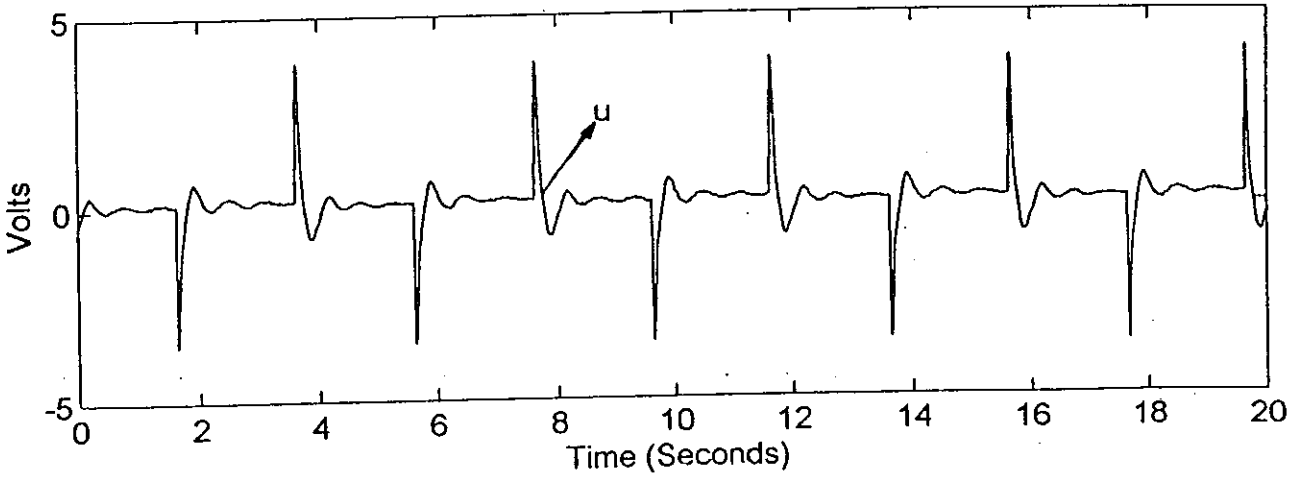

(b) Control signal

Fig. 7.12: P+I control step response, the aluminium specimens with $\phi 7$ mm

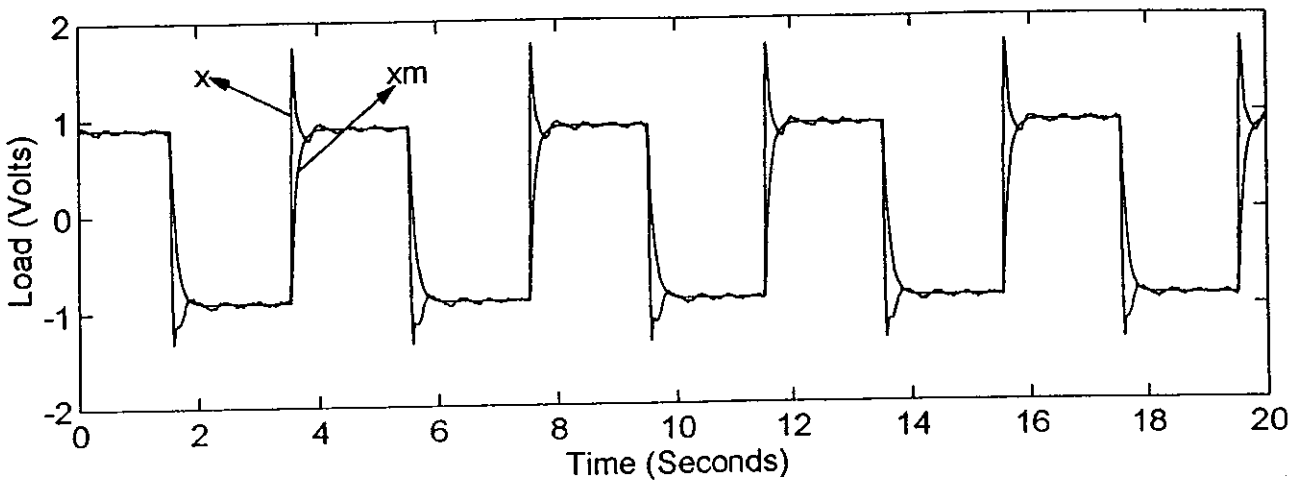

(a) Plant and reference model output signals

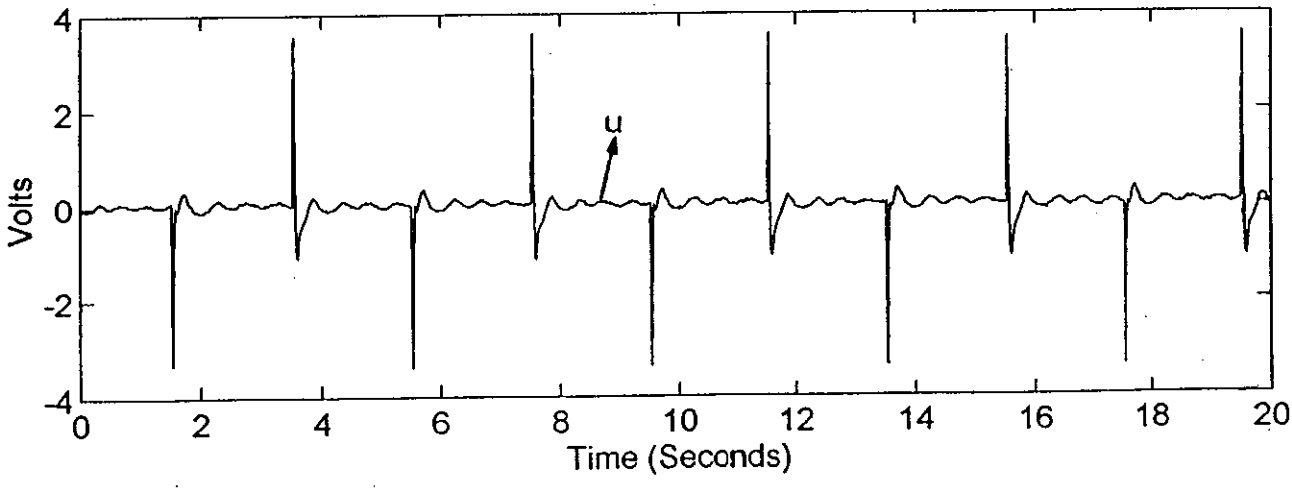

(b) Control signal

Fig. 7.13: P+I control step response, the steel specimens with $\phi 10$ mm

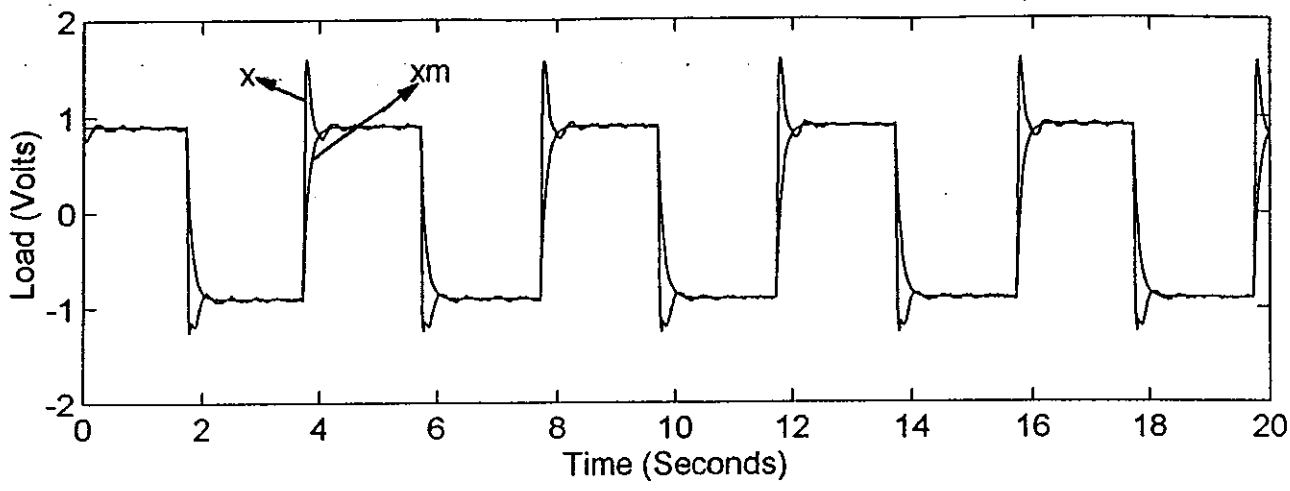

(a) Reference model and plant output signals

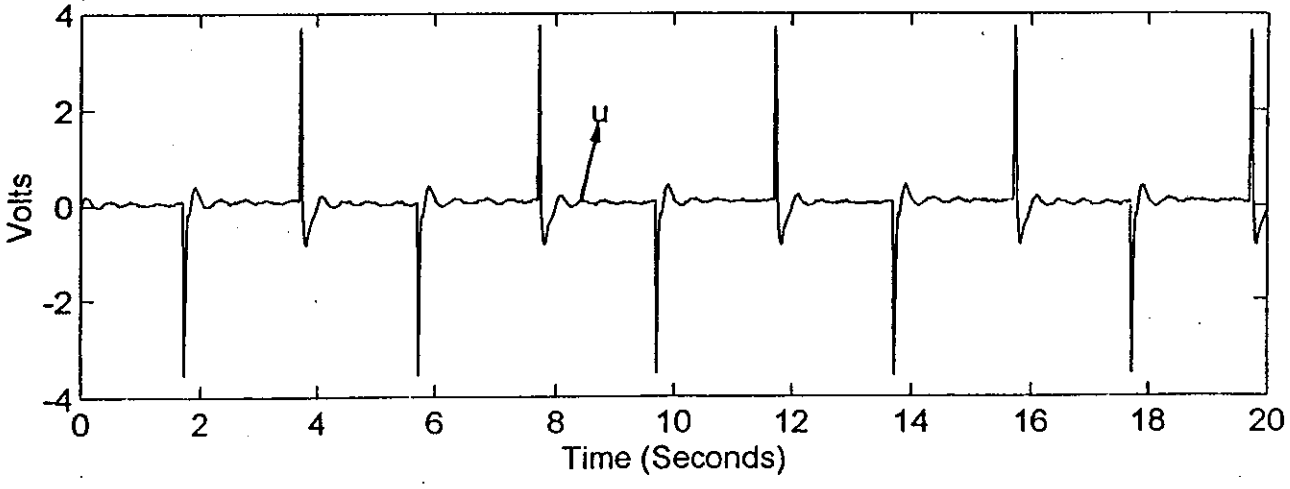

(b) Control signal

Fig. 7.14: P+I control step response, the steel specimens with $\phi 7$ mm

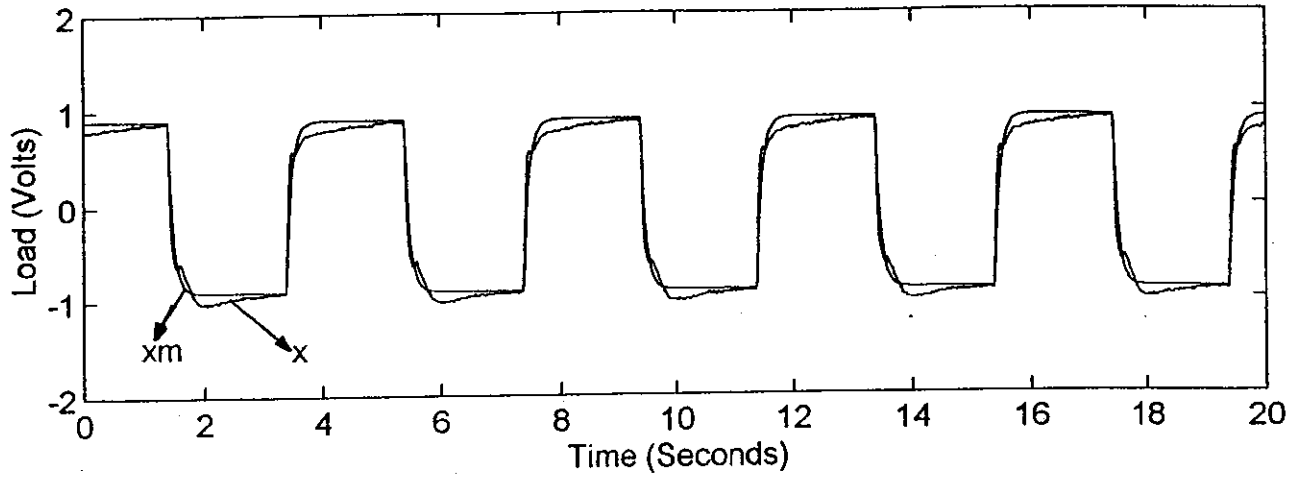

(a) MCS control step response, reference and output signals

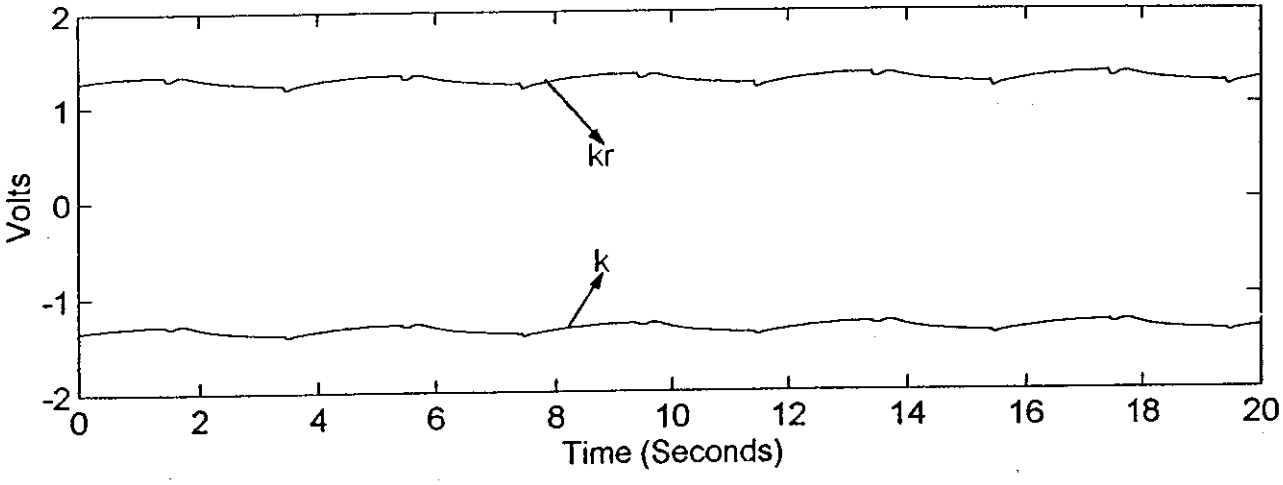

(b) MCS gains

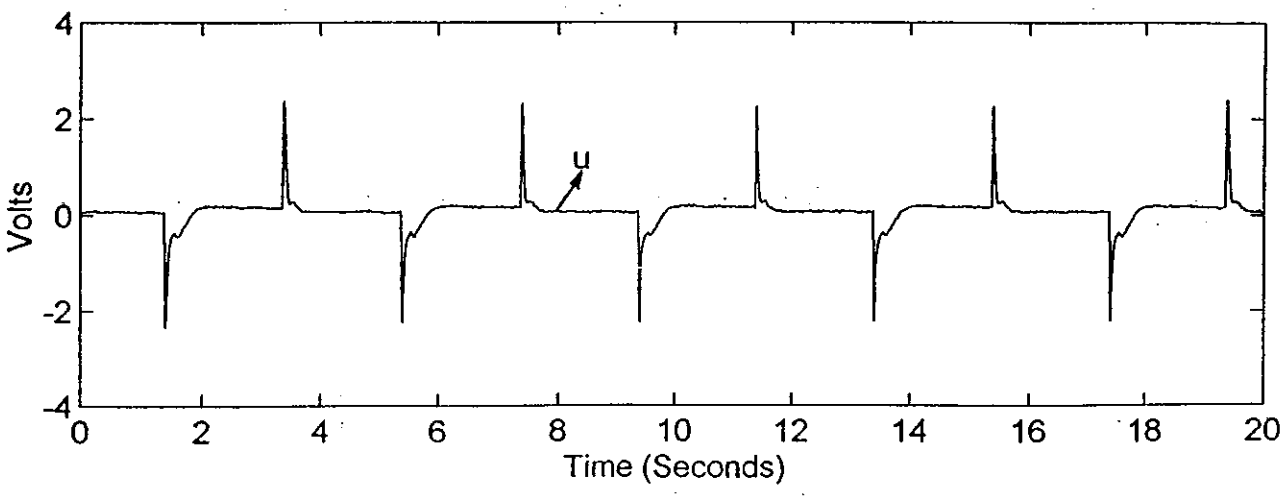

(c) Control signal

Fig. 7.15: The responses of the MCS control, the aluminium specimens with ϕ10 mm

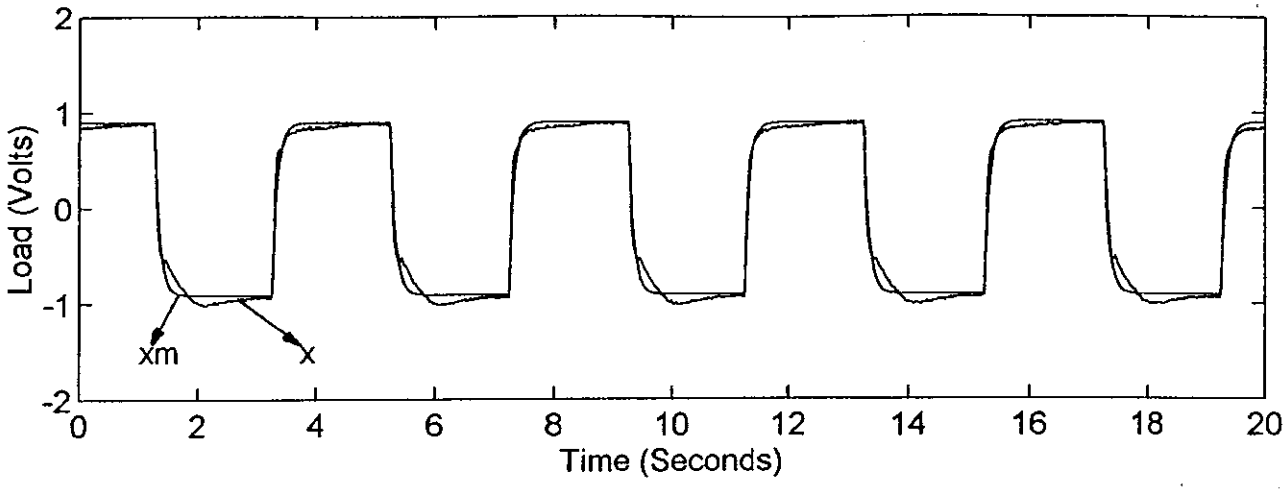

(a) MCS control step response, reference and output signals

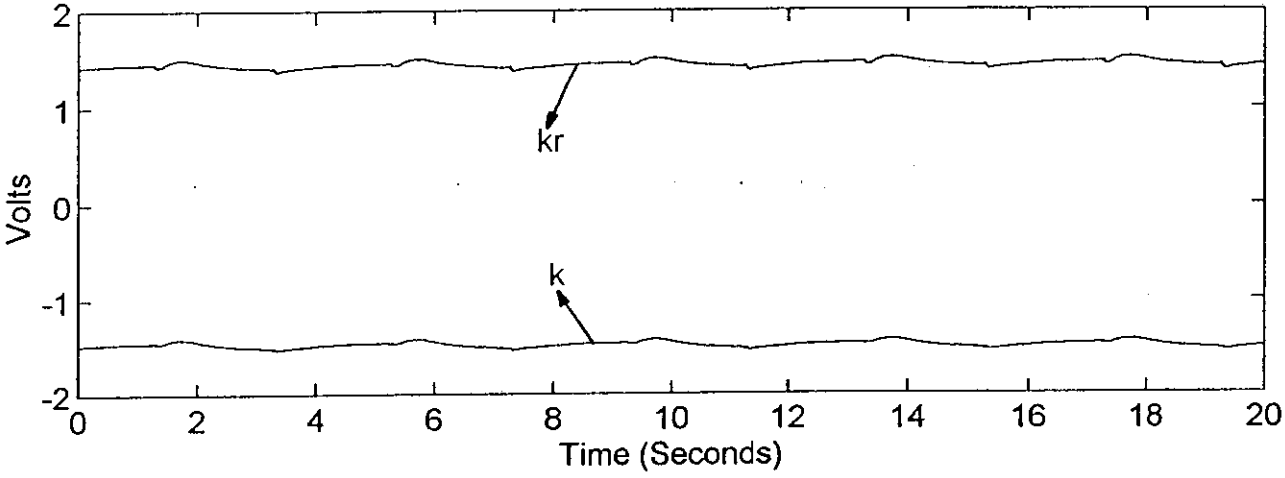

(b) MCS gains

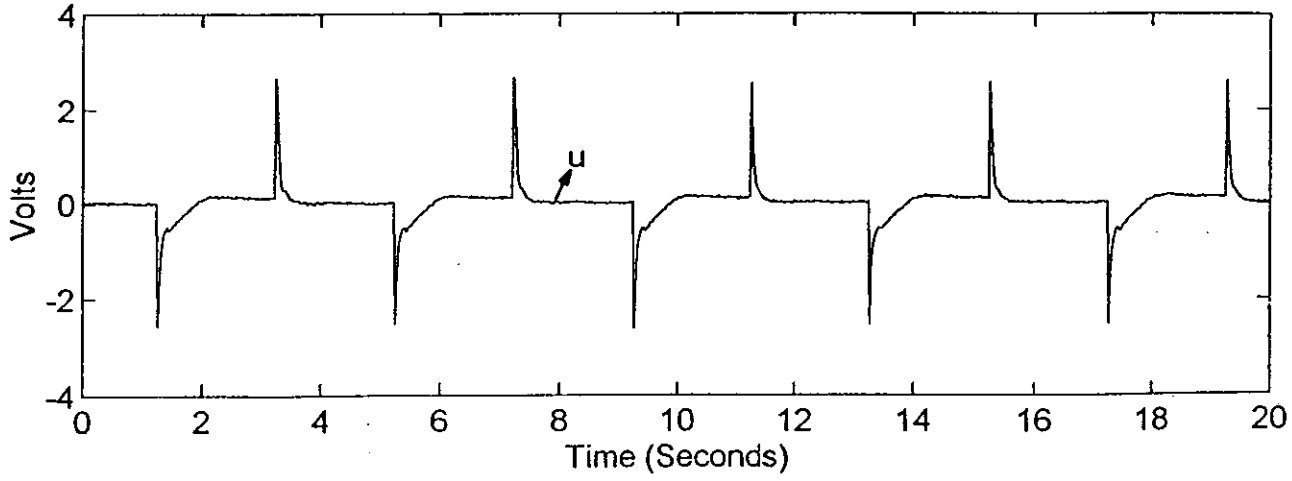

(c) Control signal

Fig. 7.16: The responses of the MCS control, the aluminium specimens with $\phi 7$ mm

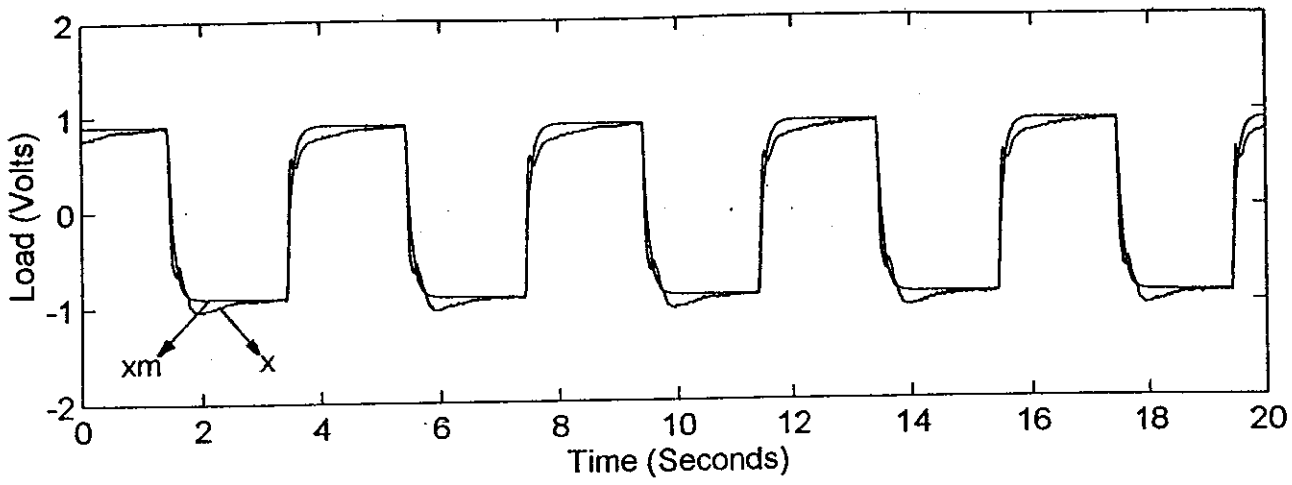

(a) MCS control step response, reference and output signals

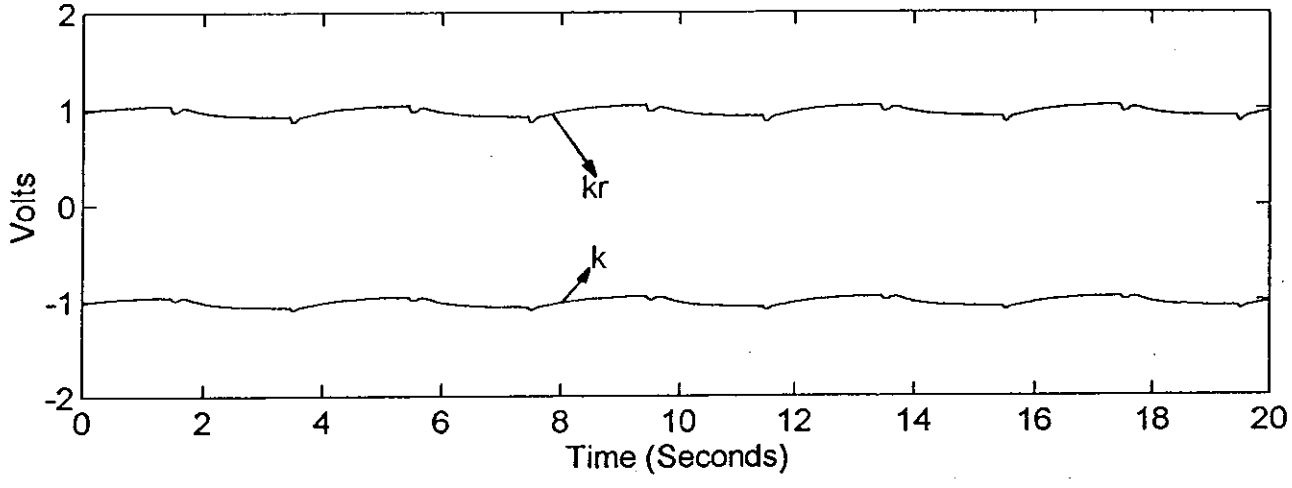

(b) MCS gains

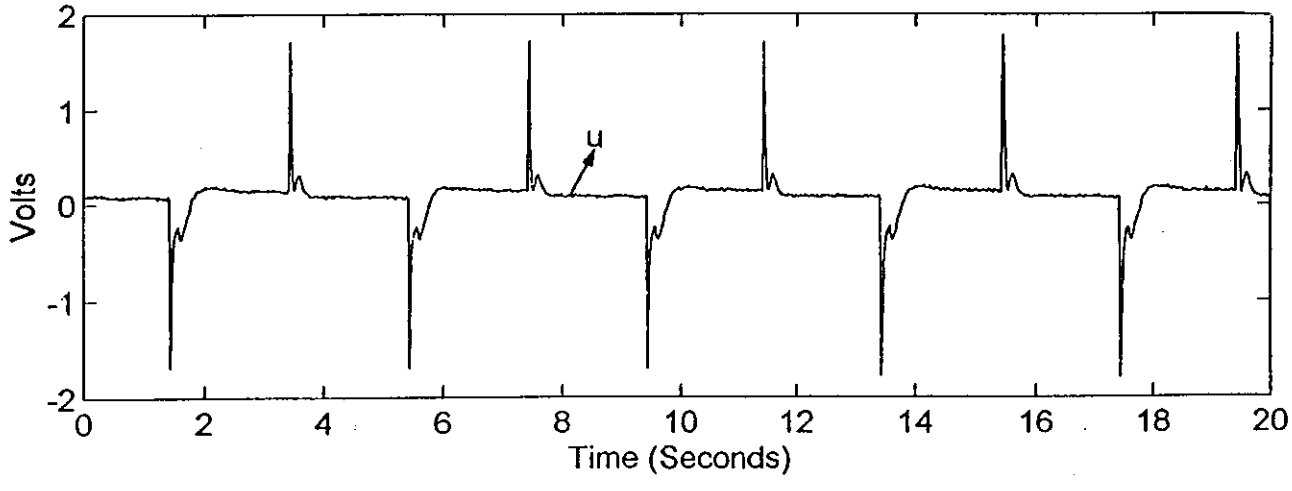

(c) Control signal

Fig. 7.17: The responses of the MCS control, the steel specimens with $\phi 10$ mm

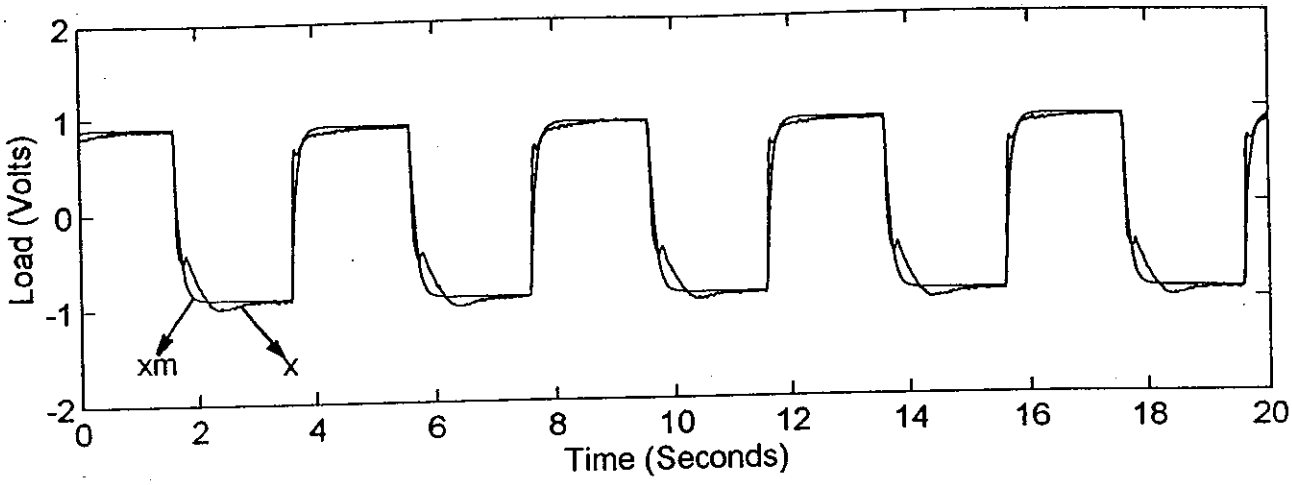

(a) MCS control step response, reference and output signals

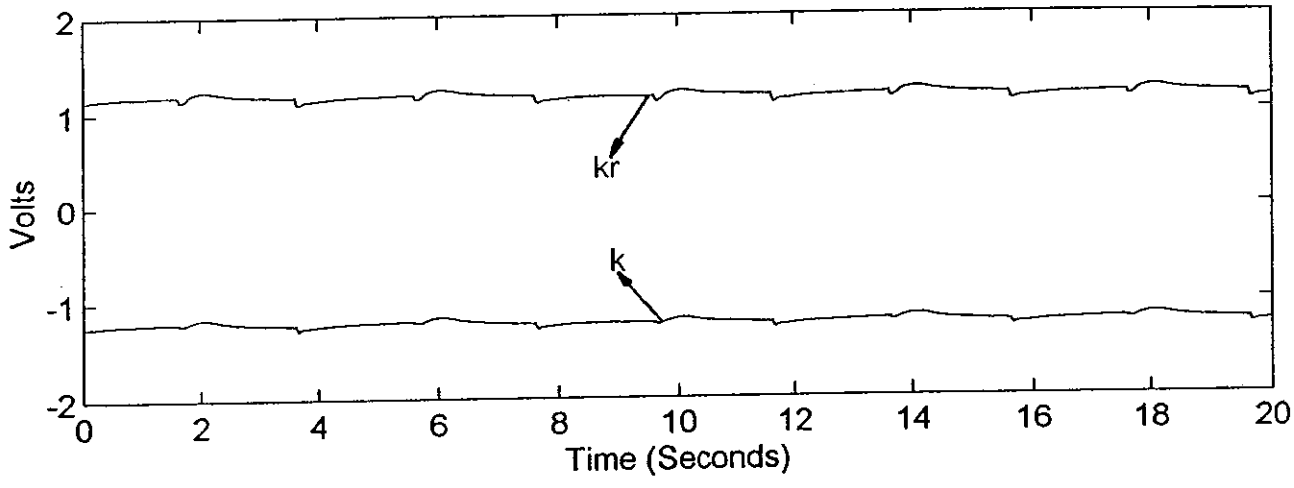

(b) MCS gains

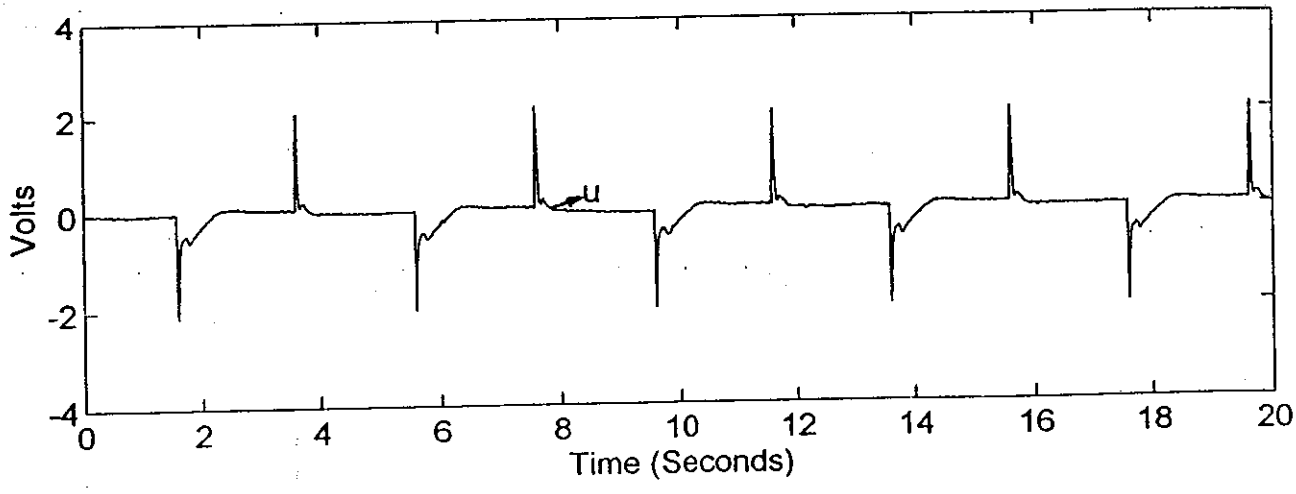

(c) Control signal

Fig. 7.18: The responses of the MCS control, the steel specimens with $\phi 7$ mm

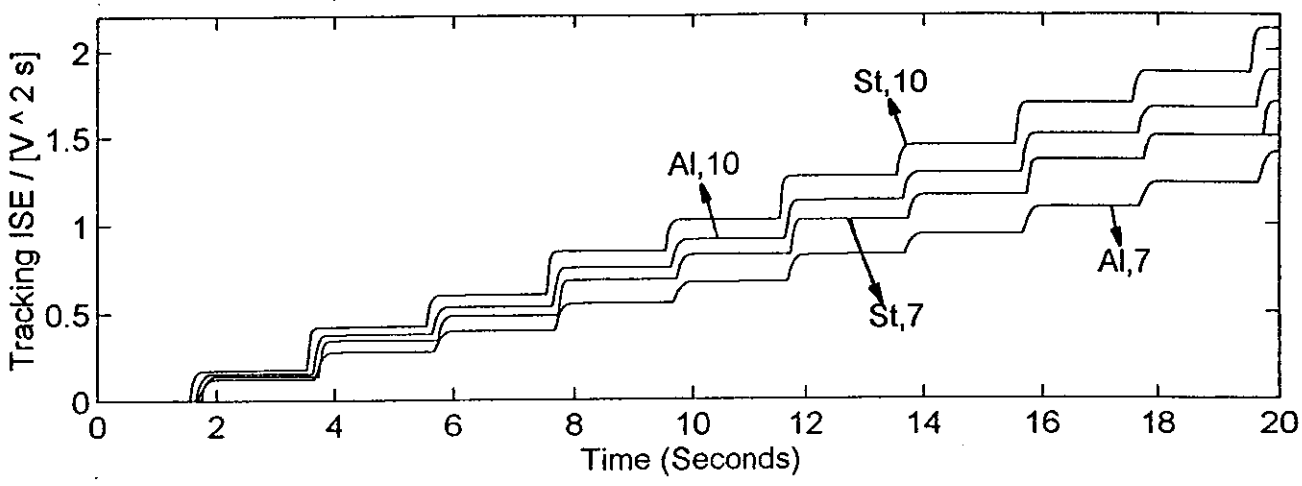

Fig. 7.19: ISE criteria P+I responses, supply pressure 13.8 MPa, elastic region.

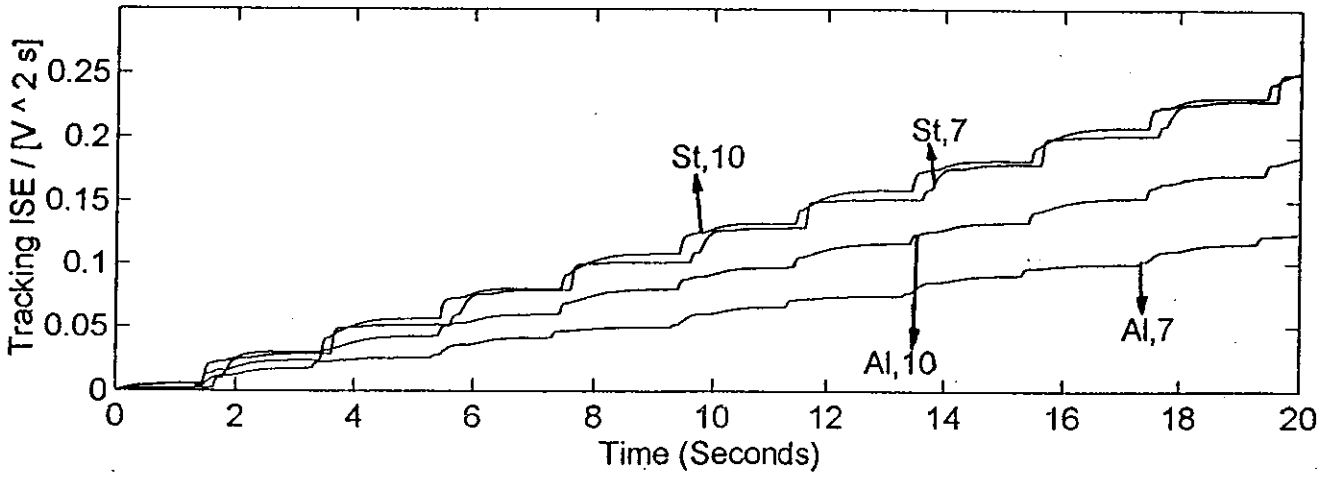

Fig. 7.20: ISE criteria MCS responses, supply pressure 13.8 MPa, elastic region.

7.4.3.1 - The Results and Discussions of the First Set of Tests

The MCS and P+I controller are implemented in Chapter 6 by using an aluminium specimens with 10 mm diameter. The relevant designs are shown in Table 7.3 and Table 7.4. Under the nominal condition (the aluminium specimens with ϕ10 mm) P+I load control responses are shown in Fig. 7.11a, together with control signal shown in Fig. 7.11b. The plant responded rather roughly to the changes in the amplitude of the input signal. There is a good correspondence between desired and actual responses, apart from small overshoots and undershoots beginning of each period due to the nonlinear relationship between the flow and the position in the servovalve and the sudden changes in the amplitude of the input signal. This indicates that the second order model and also P+I synthesis are well designed. The responses of the MCS control in the nominal case is shown in Fig. 7.15a, there is a small spikes in comparison with P+I control at the begining of each step changes. The responses were satisfactory. The MCS gains are shown in Fig. 7.15b, they are steady and do not vary much which is good indication of the stability of the controller.

Except the aluminium specimens with ϕ10 mm, other specimens with different diameters or different materials are considered away than the nominal condition. Same controller gains and input signals are used for all specimens. In elastic region all specimens are tested under 4.5 kN force. The MCS control in the case of steel specimens with ϕ10 mm, ϕ7 mm are shown in Fig. 7.17 and 7.18 respectively. The error is slightly bigger due to changes in the specimens characteristics. The MCS control result in the case of the aluminium specimens with ϕ7 mm is shown in Fig. 7.16. The error is smaller than the nominal case. The corresponding P+I controller responses in the case of aluminium specimens with ϕ7 mm, steel specimens with ϕ10 mm and ϕ7 mm are shown in Fig. 7.12, 7.13 and 7.14 respectively. In general, the steady-state error in the case of the MCS control is smaller than the P+I control, indicating that the MCS control can adapt itself to the changes in the specimens stiffness in elastic region better than the P+I controller.

In the elastic region the slow part of the plant is dominant, due to using small amplitude (comparatively small load). In the case of MCS the steady-state error can be

made zero using higher adaptive gains or increasing the controller amplitudes. The integral square error criterion is used to quantify the tracking performance of each of the controller strategies which were applied to the aluminium and steel specimens with different stiffness and yielding stress. In elastic region, the MCS controller performed significantly better than a conventional, P+I control, in the case of both the aluminium and steel specimens, the fact most noticeably demonstrated by the ISE plots in Figs. 7.19 and 7.20.

Away from nominal operation, the linear plant model parameters changed. Therefore, the effects of nonlinearity and noise due to unmodelled dynamics which appeared in the plant dynamics, hence in the plant responses. In Figs 7.19 and 7.20, the MCS control produced a smaller tracking ISE in both the nominal condition and away than the nominal operating condition (in the case of the steel specimens with $\phi 7-10$ mm and the aluminium specimens with $\phi 7$ mm). Another important point was that tracking ISE of the steel specimens was larger than those in the aluminium specimens in the case of both controllers, due to significant changes in the plant parameters.

7.4.4 - The Second Set of Tests (Elastic-Plastic Region)

The second set of tests is called as elastic-plastic step response tests. In this set of tests specimens were tested in elastic-plastic region. Firstly, it is necessary to know the yielding stress of the EN24T and aluminium alloy specimens, then to figure out the loads which can be applied on each specimen in plastic region.

For the steel specimens, beyond proportional point, the proportionality between stress and strain no longer exists. Beyond the proportional limit, the strain begins to increase more rapidly, for each increment in the stress until yielding point, beginning at this point, the steel starts to yield. After the proportional limit, the steel behaves perfectly plastic. Therefore, for second set of the tests in the case of steel specimens it is crucial that the test is being conducted beyond the proportional limit, ideally in the perfectly plastic region.

The steel specimens are made of EN24T, a high quality alloy steel that can provide in the hardened and tempered condition to a tensile range of 87-102 kg/mm^2. Content of the material is: % 0.36 - 0.44 carbon, % 0.1 - 0.35 silicon, % 0.45 - 0.7

manganese, % 1.3 - 1.70 nickel, %1 - 1.40 chromium, % 0.2 - 0.35 molybdenum. The steel exhibits good ductility and shock resisting properties combined with resistance to wear. A stress- strain tests was carried out using steel specimens with $\phi 7$ mm under the MCS control. From a stress-strain test, it was observed that the proportional limit of the specimens is ≈ 300 MPa and yielding stress is $\sigma_y \approx 320$ MPa shown in Fig. 7.8a. In this diagram k is the stiffness of the specimens. This test consisted of sine wave reference signal of frequency 0.4 Hz, and amplitude equivalent to 3.4 V. The settling time was t_s = 0.4 s, and reasonable choice of Δ was $\Delta = 20$ ms. Empirically chosen adaptive rates are $\alpha = 0.01$ and $\beta = 0.001$. The elasticity modulus of the specimens is E = 210 GPa. Therefore, 2.2 V (11 kN) and 5.2 V (26 kN) of amplitudes corresponds to loads in the plastic region for steel specimens with $\phi 7$ mm and $\phi 10$ mm respectively.

The aluminium test specimens are made of an aluminium alloy which has the yielding stress of $\sigma_y = 140 - 150$ MPa and Young's modulus of E = 72 GPa. Many aluminium alloys do not have clearly definable yielding point, a typical stress-strain diagram is shown in Fig. 6.4. In this diagram, a line drawn on the stress-strain diagram parallel to the initial linear part of the curve (Hooke's law holds and material is elastic in this region) but offset by some standard amount of strain curve. The intersection of the offset line and the stress-strain curve gives the yield stress. For aluminium the offset yield stress is slightly above the proportional limit.

Under a MCS stress-strain test, it was found that the offset yielding stress of aluminium specimens with $\phi 10$ mm is $\sigma_y = 140 - 150$ MPa shown in Fig. 7.6a. In this test, the demand signal was sine wave of amplitude 2.5 V (12.5 kN) and frequency 0.4 Hz. Reasonable choice of settling time was t_s = 0.2 s and sampling interval $\Delta = 10$ ms. The adaptive rates are chosen empirically; values found to be suitable in this case are α = 0.1 and $\beta = 0.01$. In this diagram k is the stiffness of the specimens. In the second set of tests, 1.2 V (6 kN) and 2.2 V (11 kN) amplitudes are applied on the aluminium specimens with $\phi 7$ mm and $\phi 10$ mm respectively, which were beyond the proportional limit. Therefore, the tests were conducted in the perfectly plastic region.

	The Specimens with ϕ10 mm	The specimens with ϕ7 mm
Aluminium Alloy	$\sigma_{y_{al}} \approx 150$ MPa $P_L = 11$ kN $P_L = 2.2$ V	$\sigma_{y_{al}} \approx 150$ MPa $P_L = 6$ kN $P_L = 1.2$ V
EN24T (Steel)	$\sigma_{y_{st}} \approx 320$ MPa $P_L = 26$ kN $P_L = 5.2$ V	$\sigma_{y_{st}} \approx 320$ MPa $P_L = 12$ kN $P_L = 2.4$ V

Table 7.2: Applied load on specimens in elastic-plastic region

Reference model signal in all cases were equivalent to critically damped response to a square wave of frequency 0.4 Hz. The settling time of the reference model, following a constant demand, was $t_s = 0.35$ s with zero error in steady state. The controller gains of each controller strategy were kept same as in the first set of tests, which were $\alpha = 0.01$ and $\beta = 0.001$ in the case of MCS. Similarly, $k_p = 2$ and $k_i = 24$ for P+I control. This was the standard test signal applied to all cases. In the case of the first set of tests amplitude of controller kept constant at 0.9 V (4.5 kN) in the case of four specimens.

Each specimen needs different load to reach its plastic region. Therefore, in the second set of tests amplitude of the controller was varied due to use of two different materials which have different yielding stresses and stiffness. Clearly, mechanical and chemical properties of aluminium alloy and EN24T steel are considerably different from each other. In addition, using the same material two different specimens made by changing cross-sectional area which were $A_p = 78.5398$ mm^2 and $A_p = 38.4845$ mm^2. Overall, four different specimens in terms of materials and diameters; therefore, four different amplitudes which correspond to applied load on specimens are used in this set of tests. These amplitudes are as follows: 1.2 V for the aluminium specimens with ϕ7 mm, 2.2 V for the aluminium specimens with ϕ10 mm, 2.4 V for the steel specimens with ϕ7 mm, and 5.2 V for the steel specimens with ϕ10 mm. Applied load for each specimen together with yielding stress of materials is shown in Table 7.2 .

	The Steel Specimens with ϕ10 mm	**The Steel Specimens with ϕ7 mm**	**The Aluminium Specimens with ϕ10 mm**	**The Aluminium Specimens with ϕ7 mm**
Elastic Region	$k_p = 2$, $k_i = 24$, amp = 0.9 V, frq = 0.4 Hz, t_s = 0.35 s, Δ = 20 ms	$k_p = 2$, $k_i = 24$, amp = 0.9 V, frq = 0.4 Hz, t_s = 0.35 s, Δ = 20 ms	$k_p = 2$, $k_i = 24$, amp = 0.9 V, frq = 0.4 Hz, t_s = 0.35 s, Δ = 20 ms	$k_p = 2$, $k_i = 24$, amp = 0.9 V, frq = 0.4 Hz, t_s = 0.35 s, Δ = 20 ms
Elastic-Plastic Region	$k_p = 2$, $k_i = 24$, amp = 5.2 V, frq = 0.4 Hz, t_s = 0.35 s, Δ = 20 ms	$k_p = 2$, $k_i = 24$, amp = 2.4 V, frq = 0.4 Hz, t_s = 0.35 s, Δ = 20 ms	$k_p = 2$, $k_i = 24$, amp = 2.2 V, frq = 0.4 Hz, t_s = 0.35 s, Δ = 20 ms	$k_p = 2$, $k_i = 24$, amp = 1.2 V, frq = 0.4 Hz, t_s = 0.35 s, Δ = 20 ms

Table 7.3: P+I controller gains and reference signal variables.

	Steel Specimens with ϕ10 mm	**Steel Specimens with ϕ7 mm**	**Aluminium Specimens with ϕ10 mm**	**Aluminium Specimens with ϕ7 mm**
Elastic Region	$\alpha = 0.01$, $\beta = 0.001$, amp = 0.9 V, frq = 0.4 Hz, t_s = 0.35 s, Δ = 20 ms	$\alpha = 0.01$, $\beta = 0.001$, amp = 0.9 V, frq = 0.4 Hz, t_s = 0.35 s, Δ = 20 ms	$\alpha = 0.01$, $\beta = 0.001$, amp = 0.9 V, frq = 0.4 Hz, t_s = 0.35 s, Δ = 20 ms	$\alpha = 0.01$, $\beta = 0.001$, amp = 0.9 V, frq = 0.4 Hz, t_s = 0.35 s, Δ = 20 ms
Elastic-Plastic Region	$\alpha = 0.01$, $\beta = 0.001$, amp = 5.2 V, frq = 0.4 Hz, t_s = 0.35 s, Δ = 20 ms	$\alpha = 0.01$, $\beta = 0.001$, amp = 2.4 V, frq = 0.4 Hz, t_s = 0.35 s, Δ = 20 ms	$\alpha = 0.01$, $\beta = 0.001$, amp = 2.2 V, frq = 0.4 Hz, t_s = 0.35 s, Δ = 20 ms	$\alpha = 0.01$, $\beta = 0.001$, amp = 1.2 V, frq = 0.4 Hz, t_s = 0.35 s, Δ = 20 ms

Table 7.4: MCS control gains and reference signal variables.

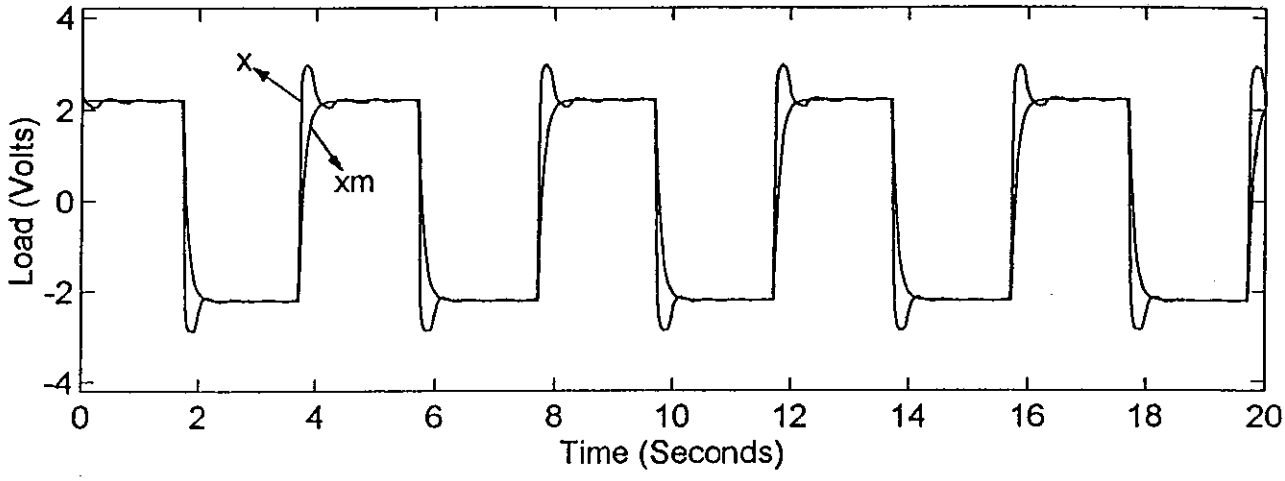

(a) Reference and output signals

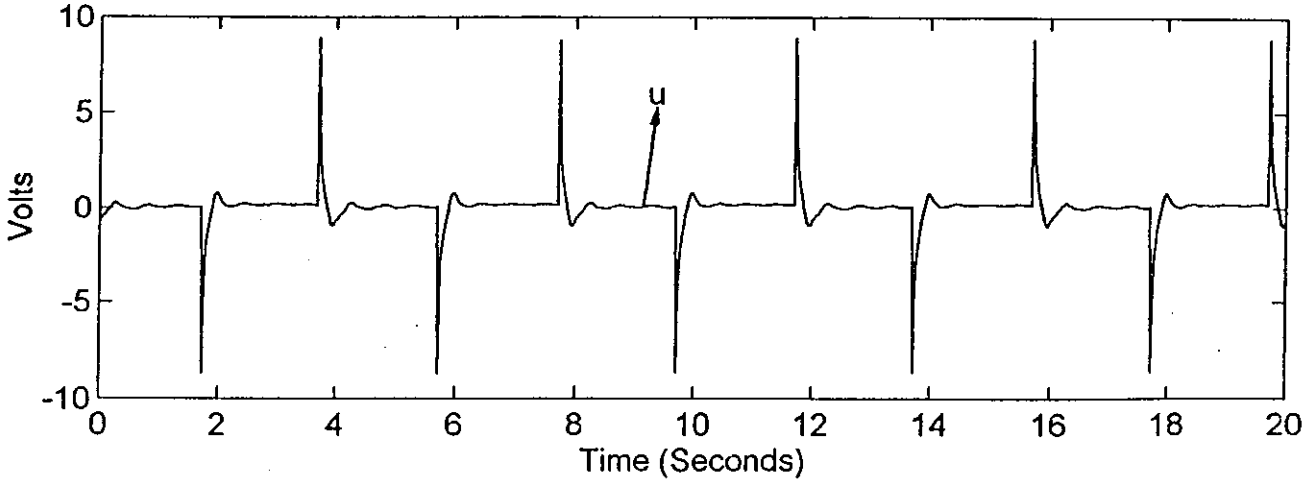

(b) Control signal

Fig. 7.21: The responses of P+I control, the aluminium specimens with $\phi 10$ mm

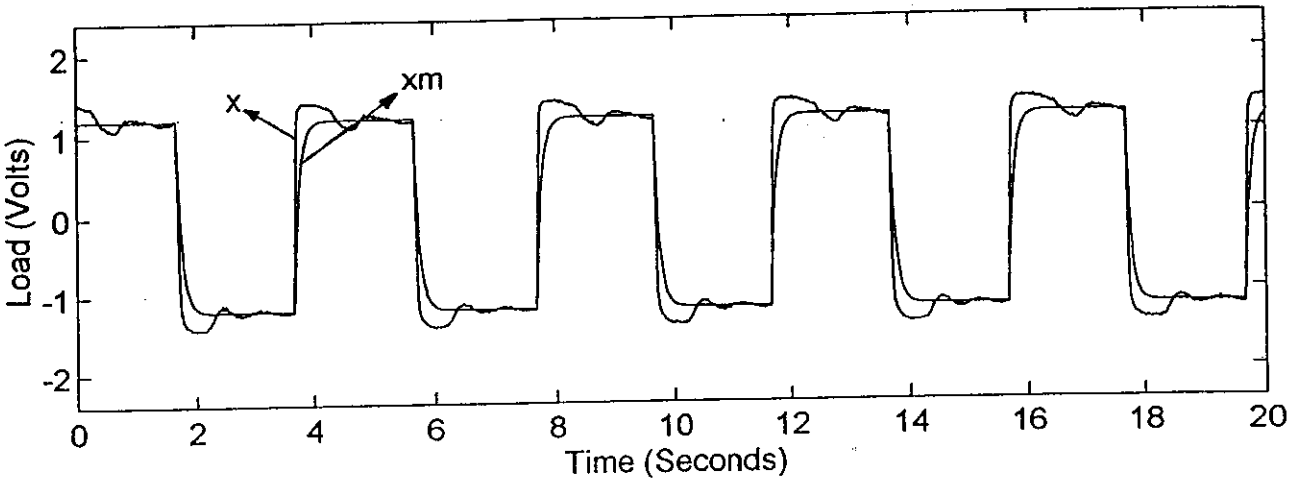

(a) Reference and output signals

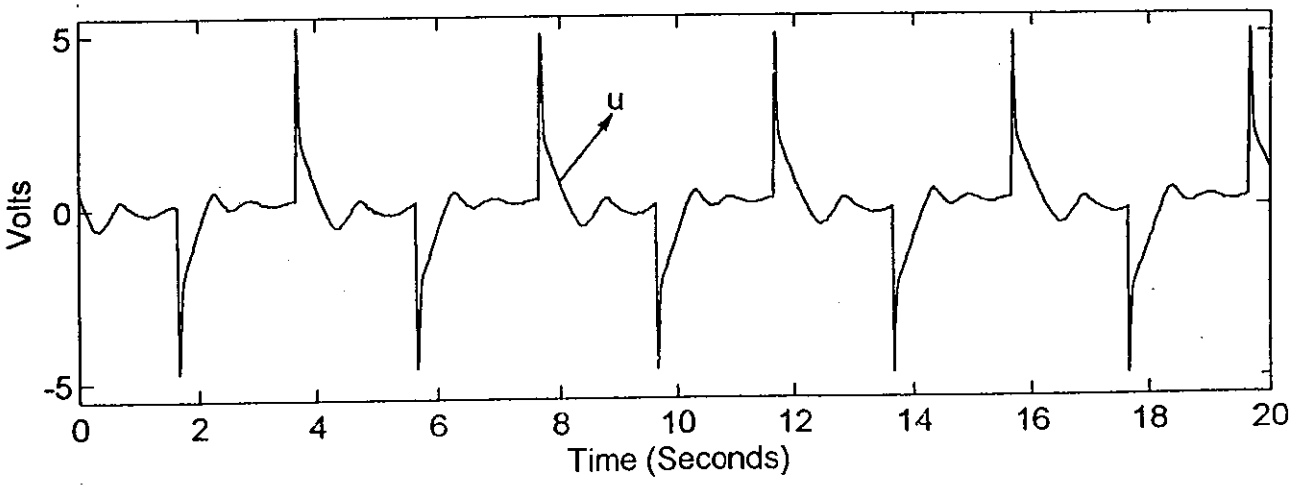

(b) Control signal

Fig. 7.22: The responses of P+I control, the aluminium specimens with $\phi 7$ mm

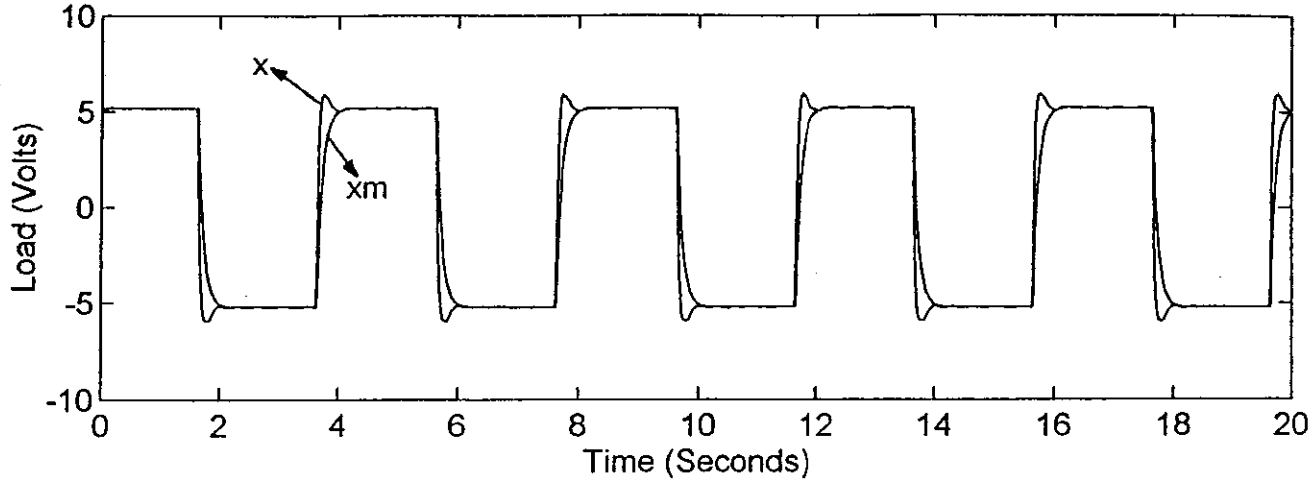

(a) Reference and output signals

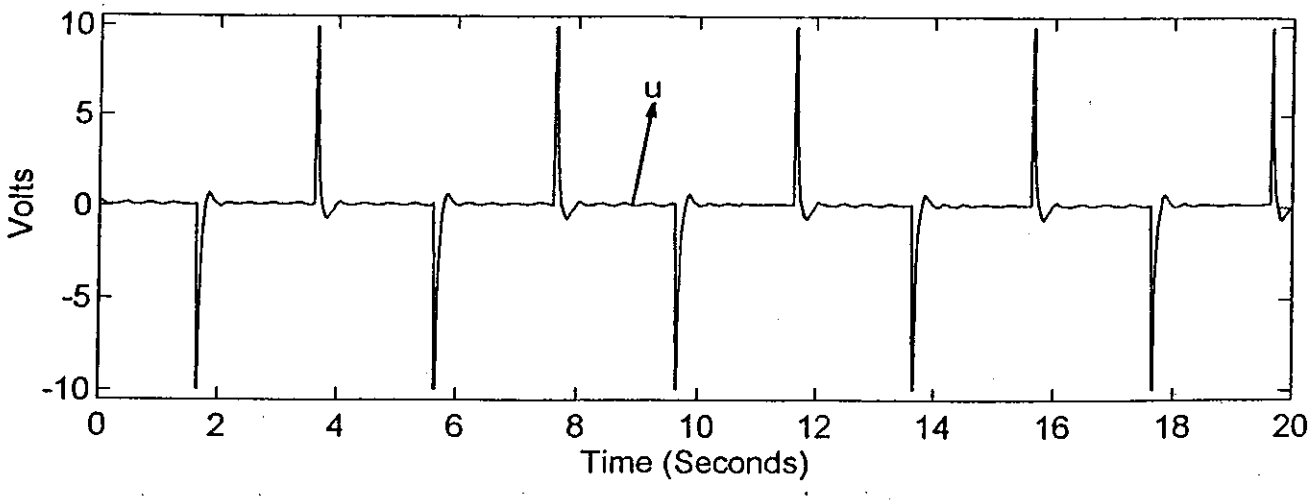

(b) Control signal

Fig 7.23: The responses of P+I control, the steel specimen with $\phi 10$ mm

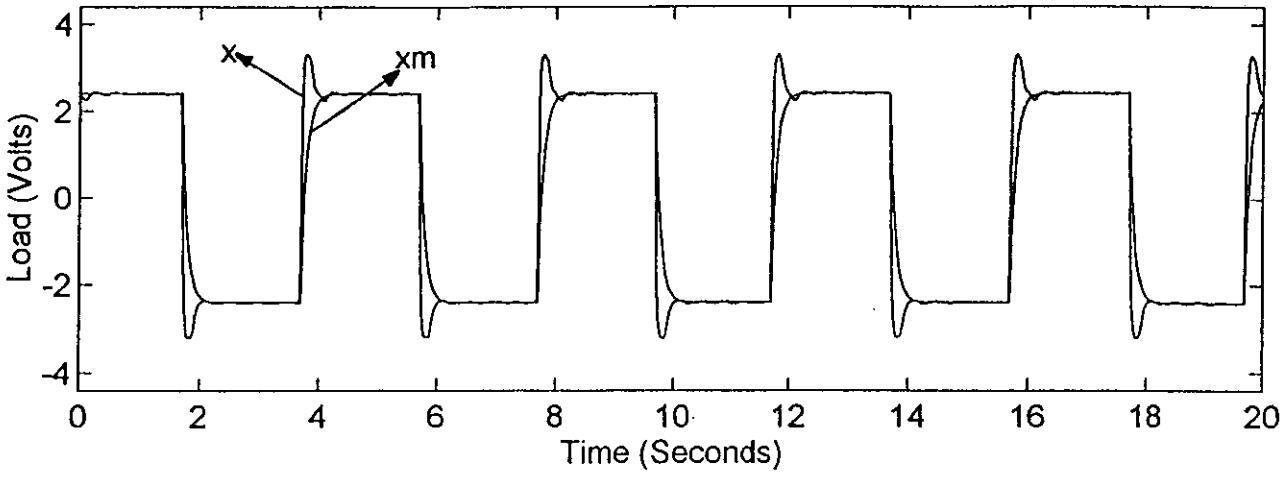

(a) Reference and output signals

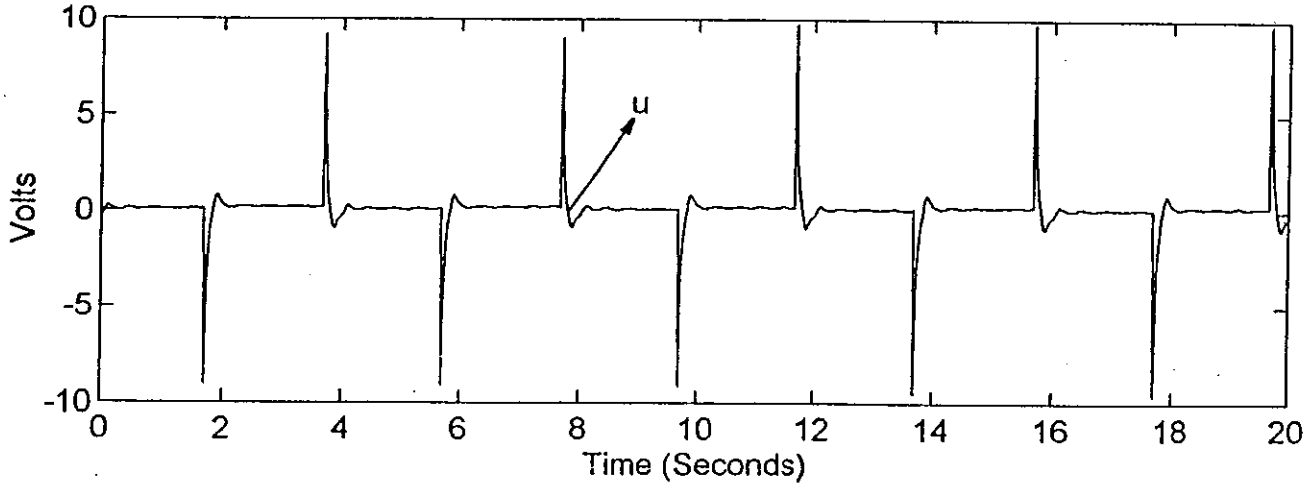

(b) Control signal

Fig. 7.24: The responses of P+I control, the steel specimens with $\phi 7$ mm

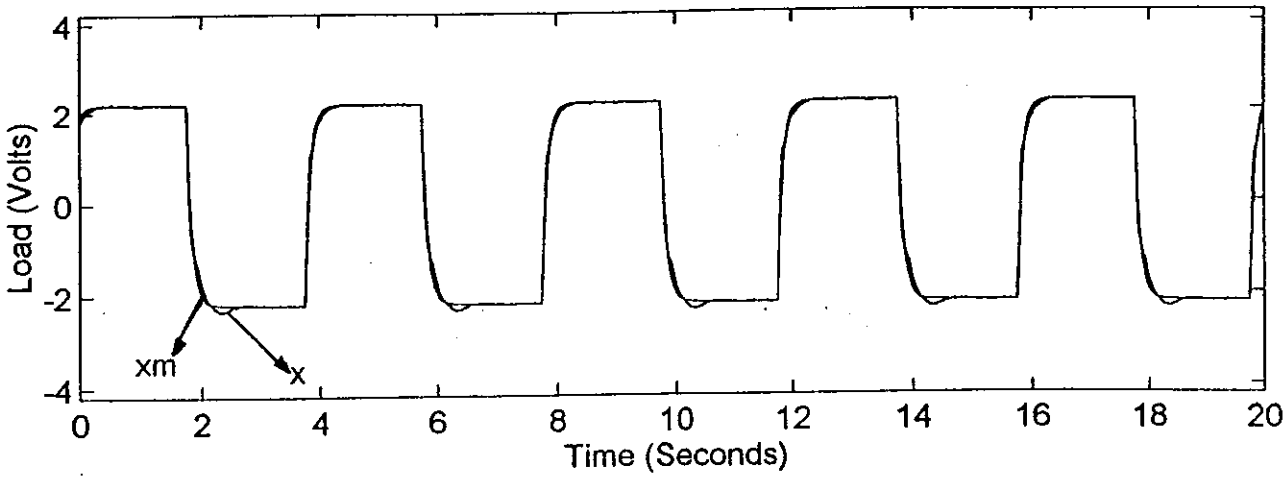

(a) MCS control step response, reference and output signals

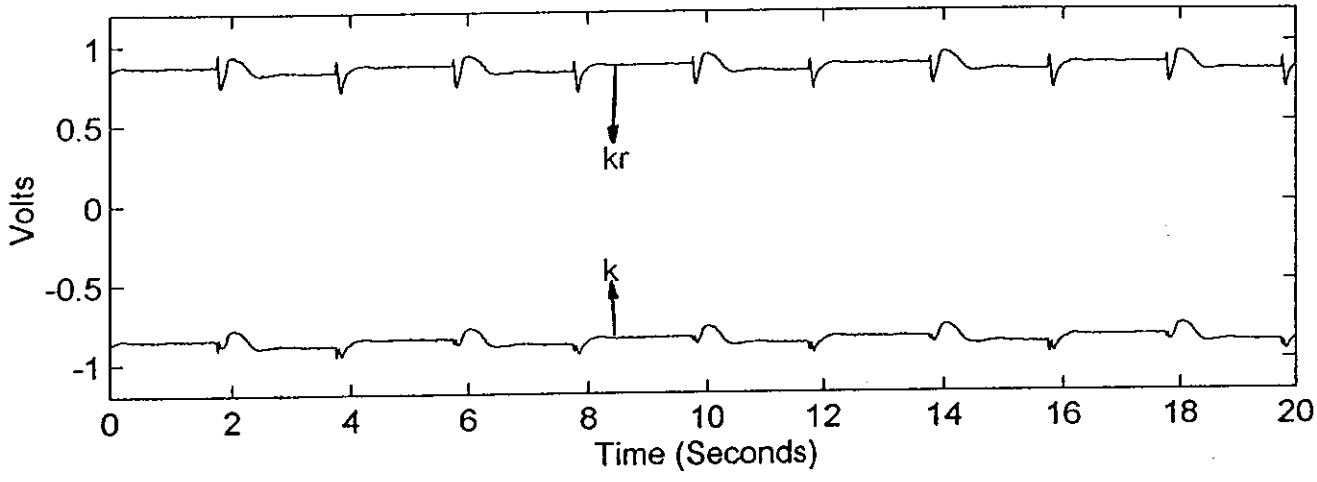

(b) MCS gains

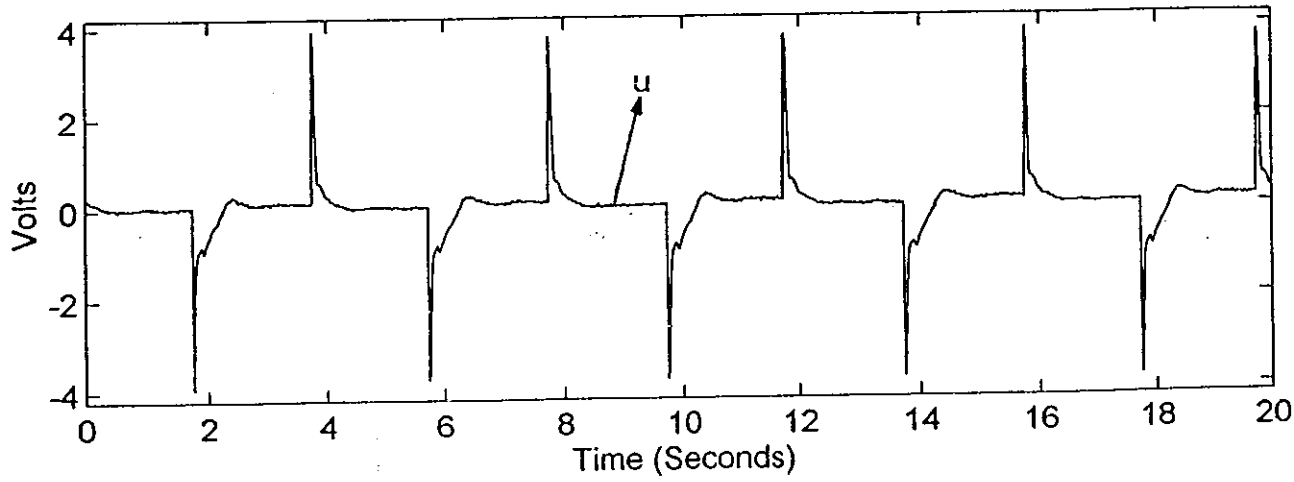

(b) Control signal

Fig. 7.25: The responses of the MCS control, the aluminium specimens with $\phi 10$ mm

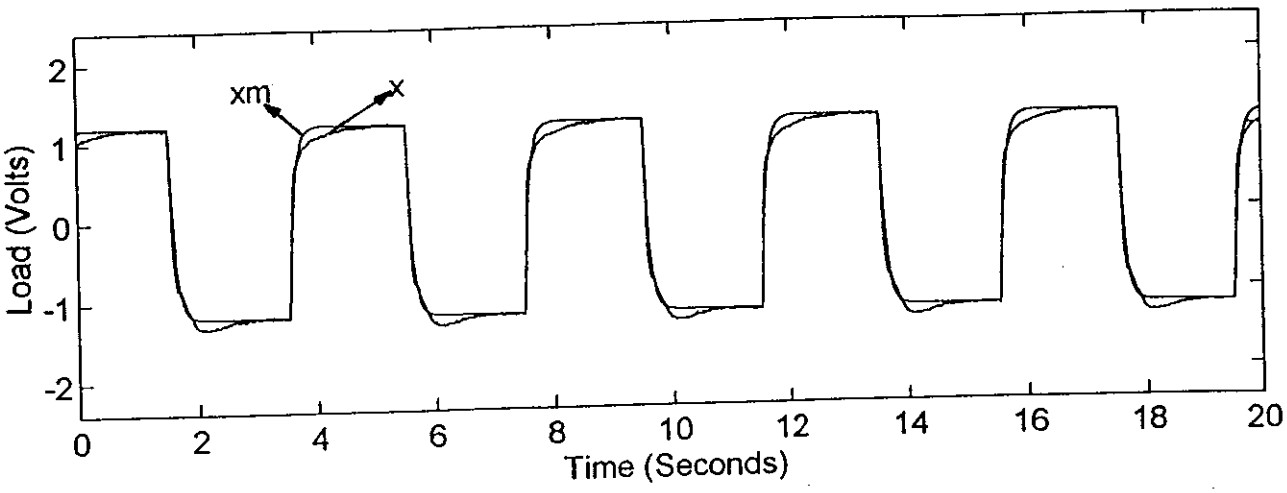

(a) MCS control step response, reference and output signals

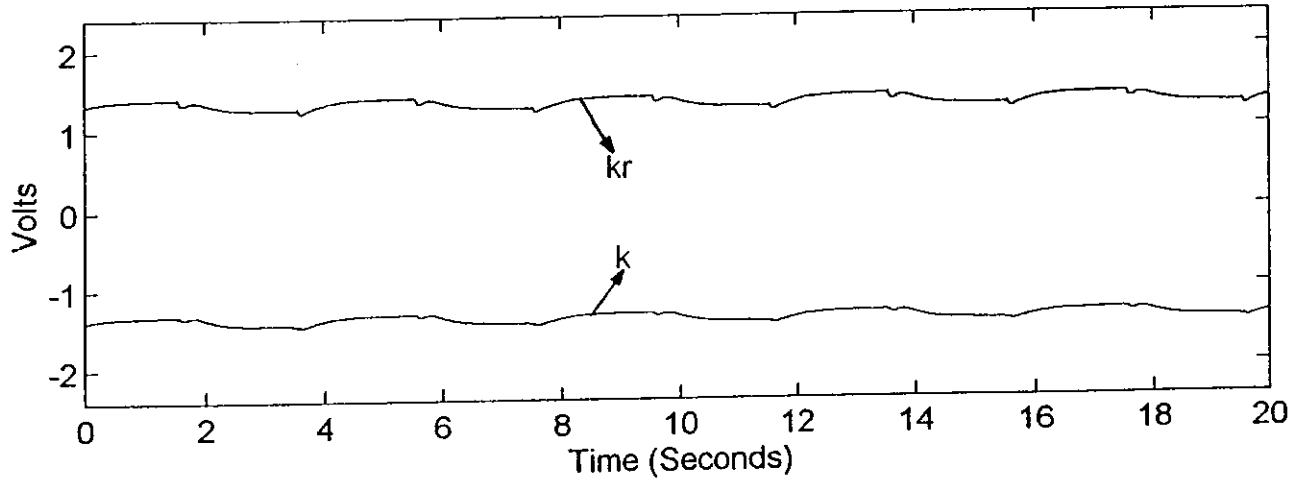

(b) MCS gains

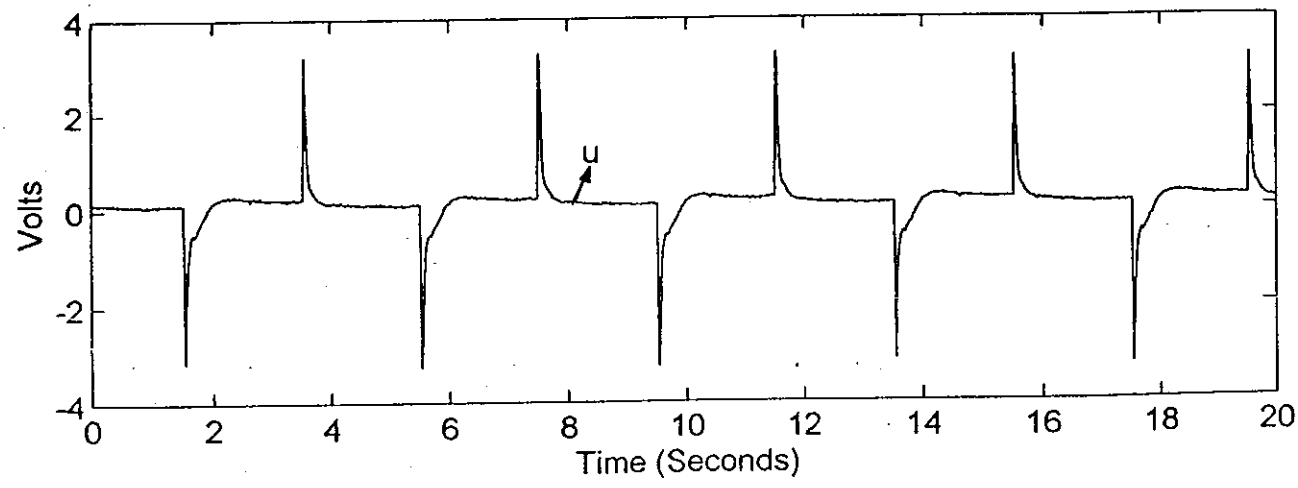

(c) Control signal

Fig. 7.26: The responses of the MCS control, the aluminium specimens with $\phi 7$ mm

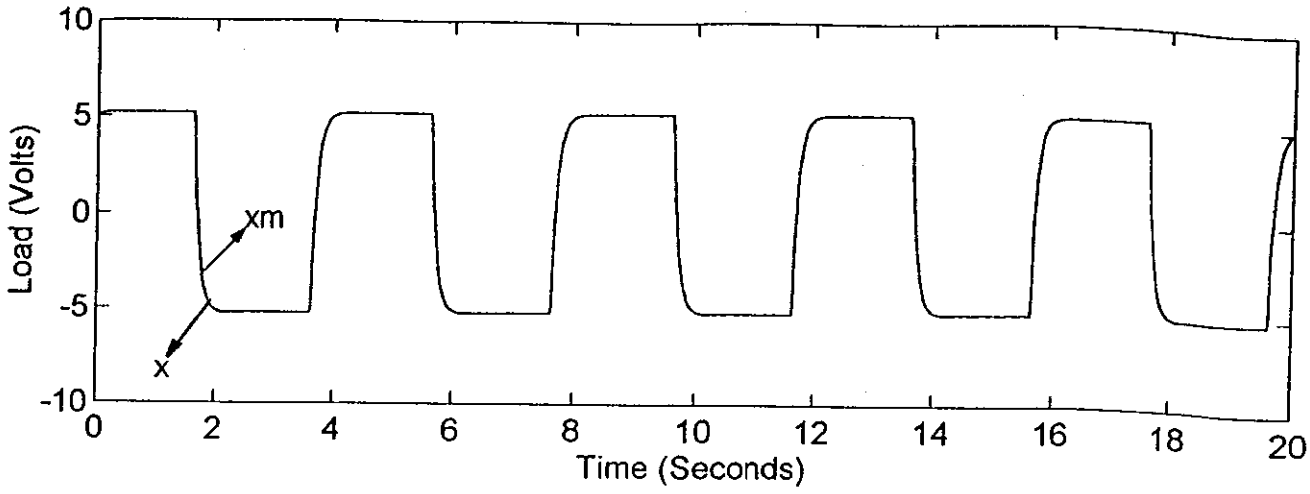

(a) MCS control step response, reference and output signals

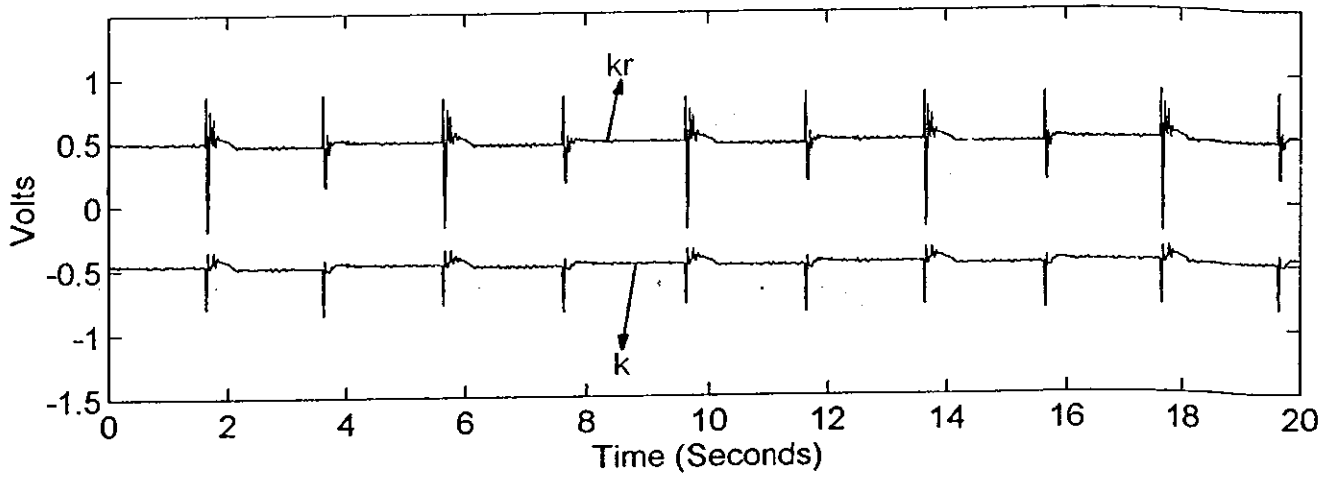

(b) MCS gains

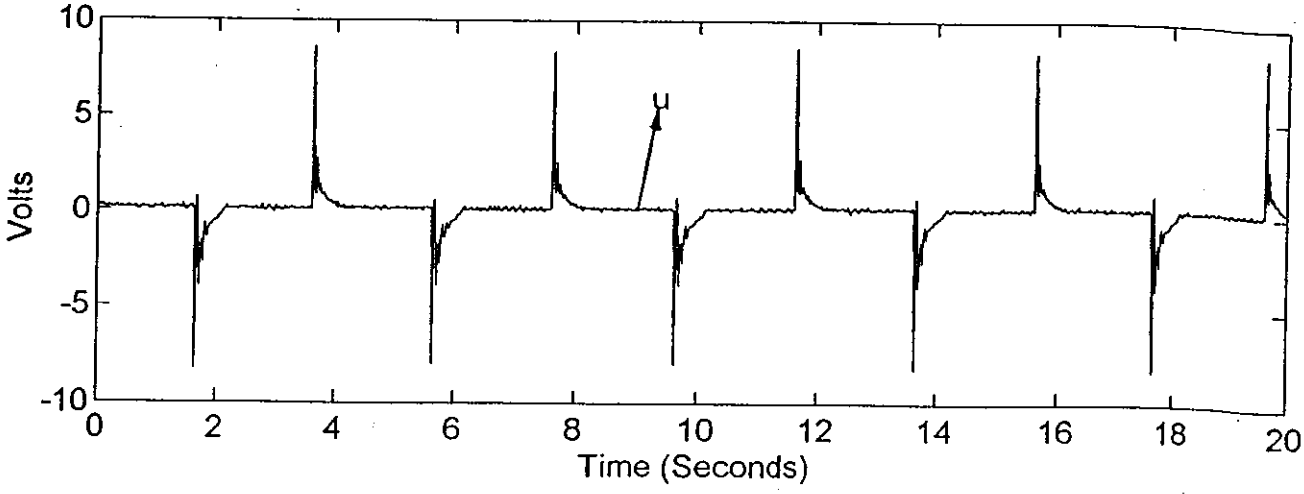

(c) Control signal

Fig. 7.27: The responses of the MCS control, the steel specimens with $\phi 10$ mm

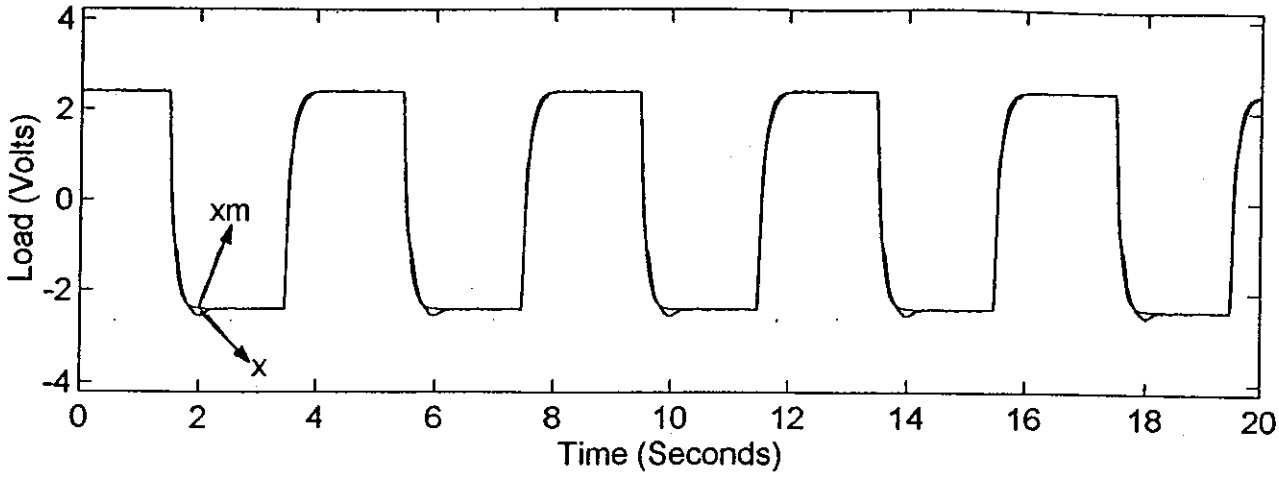

(a) MCS control step response, reference and output signals

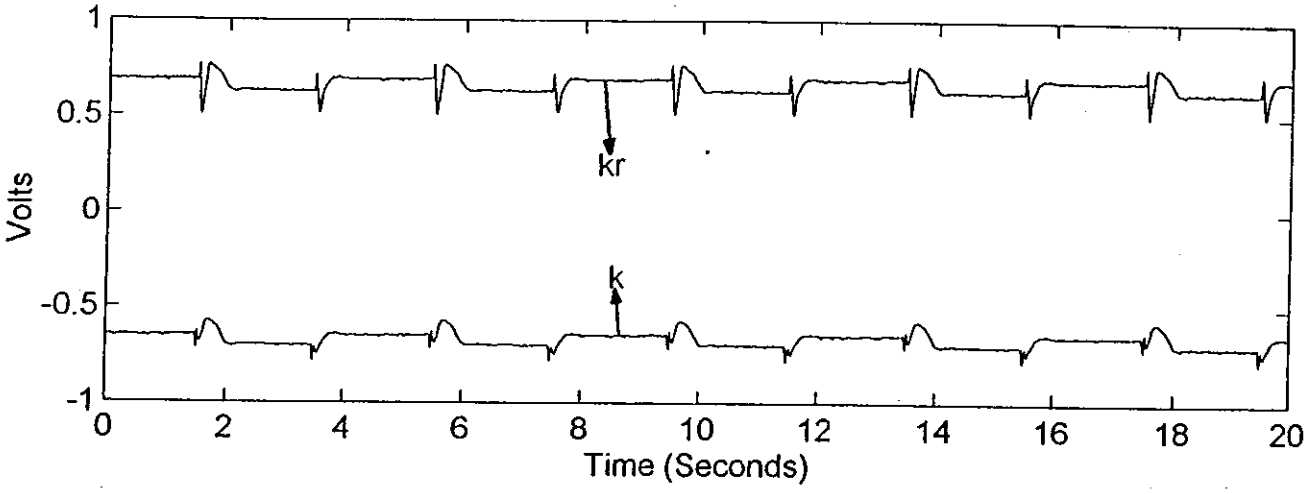

(b) MCS gains

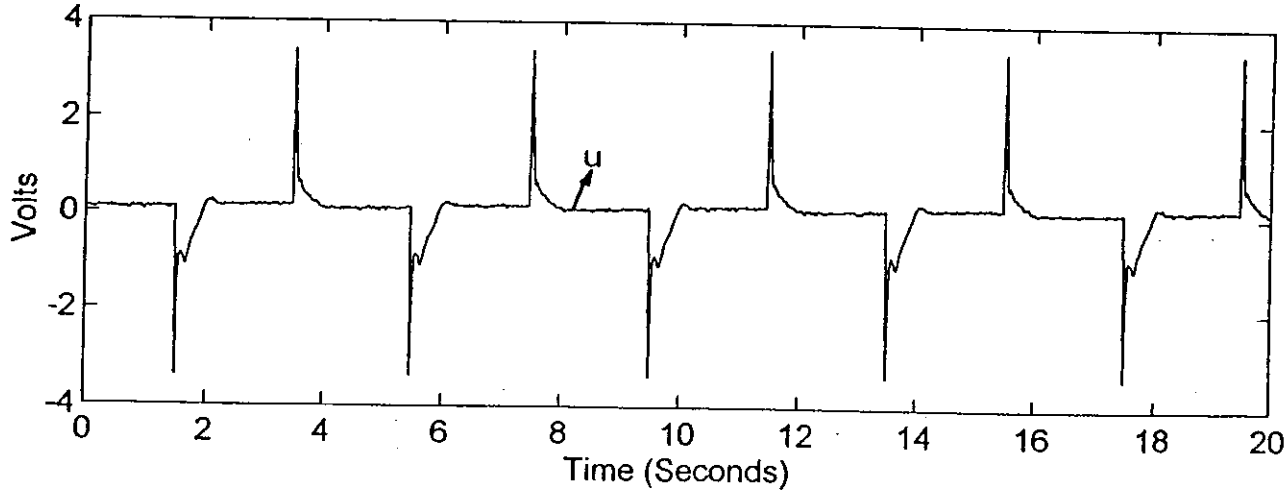

(c) Control signal

Fig. 7.28: The responses of the MCS control, the steel specimens with $\phi 7$ mm

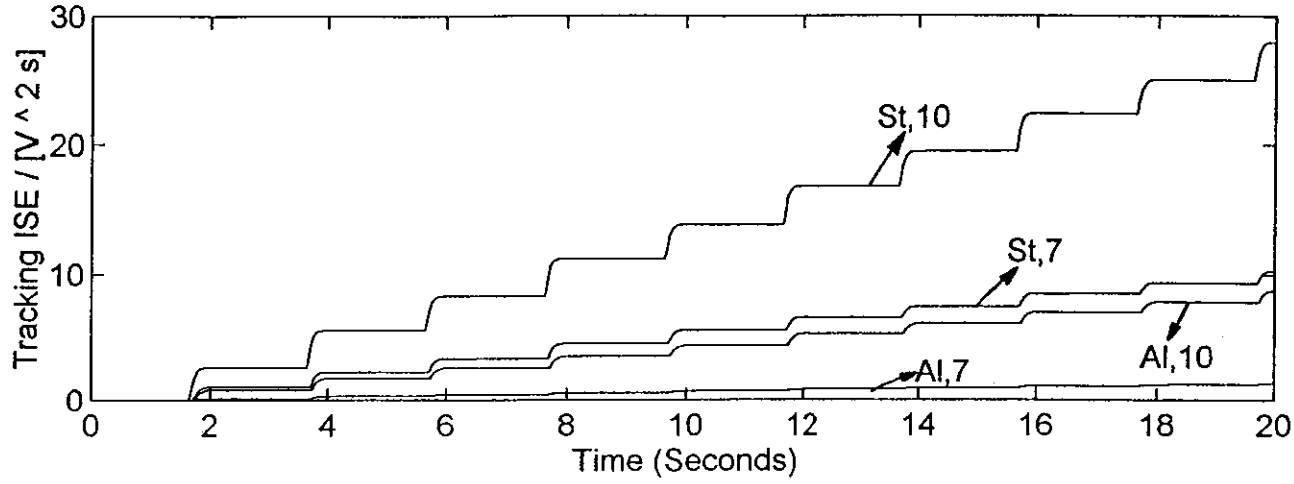

Fig. 7.29: ISE criteria responses of P+I controller, supply pressure 13.8 MPa, elastic-plastic region.

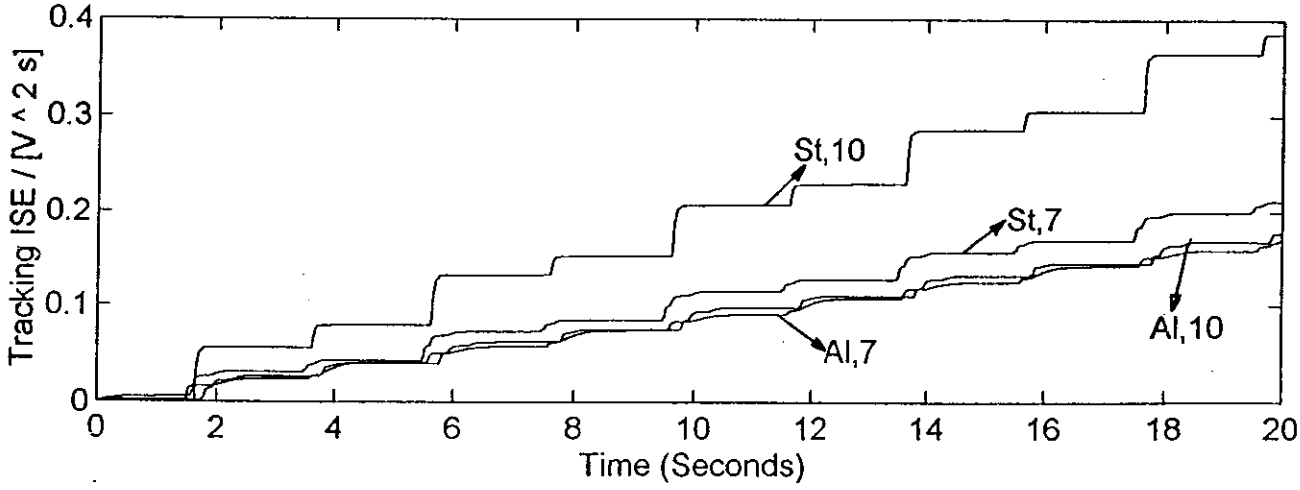

Fig. 7.30: ISE criteria responses of the MCS control, supply pressure 13.8 MPa, elastic-plastic region

7.4.4.1 - The Results and Discussions of the Second Set of Tests

In the first set of tests the amplitude of the tests was limited as 0.9 V (4.5 kN) for all specimens, therefore the changes in the plant parameters was limited as well. In the case of second set of tests, the changes in the plant parameters are more significant due to the fact that each specimen was tested beyond its proportional limits (plastic region), therefore the dynamics of the specimens had more effect in the plant dynamics.

Following the step reference signals a P+I controller produced the set of results in the case of aluminium specimens with $\phi 10$ and $\phi 7$ mm and steel specimens with $\phi 10$ mm and $\phi 7$ mm are shown in Figs. 7.21, 7.22, 7.23 and 7.24 respectively. The results showed that manual tuning of controller gains, k_p and k_i are crucial in the case of P+I control in order to get noise free, zero steady-state plant output. In all cases the P+I control give stable responses. The steady-state errors and spikes are bigger than the MCS control for all specimens, otherwise the controller is stable.

The results presented here show that effective control in material testing can be achieved using the MCS control. The plant responses are virtually indistinguishable from the reference model outputs. Therefore, the responses are very satisfactory, shown in Figs 7.25, 7.26, 7.27 and 7. 28 in the case of aluminium specimens with $\phi 10$ mm, $\phi 7$ mm and steel specimens with $\phi 10$ mm, $\phi 7$ mm. respectively, together with MCS control gains. The gains are very rapid, subsequently they settle to new levels that are appropriate for the new applied load on specimens. It is shown that the transient terms are rapid and noise is not a problem. The corresponding control signals are shown in Figs. 7.25c-7.28c: compared with P+I controller response in Figs. 7.21b-7.24b. The steady-state errors in the case steel specimens is bigger than the aluminium specimens due the fact that great plant parameters variations occurs due to use of different materials. In general the MCS control adapts itself very smoothly to the changes in the plant parameters. The steady-state error was very small, there was a very small spike at the bottom of the each step. The actuator is in retract position at the bottom of the each step and the load force pushes the specimen down beyond the demand signal. The bottom grip is not firmly fixed as the top grip due to the fact that it is attached to the actuator piston therefore, every little movement and the

nonlinearities in the actuator causes disturbances in the output signal when the amplitude of the input signal is negative.

It is shown that, in the case of the steel specimens control signals are comparatively more noisy than the aluminium specimens, due to relatively large variations in stiffness. It is observed that control signals were large and noisy in P+I control when compared with those produced by MCS.

In the elastic-plastic region the MCS control has outperformed the P+I controller, the fact is most clearly demonstrated in the ISE plots, Figs 7.29 and 7.30. As it is shown the ISE error in the case of the MCS control is far less than the P+I controller for all four specimens.

7.5 - CONCLUSIONS

This chapter is concerned with comparative implementation studies of the Minimal Controller Synthesis (MCS) algorithm applied to a material load control problem. Certainly the MCS responses were superior to those resulting from the implementation of a conventional proportional plus integral (P+I) fixed gain, linear, controller.

In considering robustness of the MCS control and P+I controller, when comparing their effectiveness in elastic and elastic-plastic region, it was observed that since tests are consistent (same controller gains, amplitude, frequency, sampling interval, settling time) in their nature, the MCS control is more effective at both conditions than P+I control. Additionally, the MCS control was robust in the presence of parameter changes in specimens (for example crack growths and modulus of elasticity variation) and in the test machine itself.

Parameter changes were introduced due to use of specimens with different diameters and materials in these tests. It was observed that MCS responses were virtually unaffected, and yet the P+I responses were significantly effected. A fact was more clearly demonstrated by the ISE plots in Figs. 7.19 and 7.20 for elastic region and in Figs. 7.29 and 7.30 for elastic-plastic region. In addition, the dynamics of the servovalve and load inertial and frictional effects have been ignored in all the control systems designs (including MCS, since the dimension of the reference model state is only 1). Additionally, control

signal was large and noisy in elastic-plastic region than in elastic region, due to large and rapid plant parameter variations.

In order to design structures and components using modern engineering materials, it is essential to have a good understanding of the materials stress and strain characteristics. Since strain is directly related to a dimensional change, it can be measured on small specimen. In this case, the accuracy of the measuring device is crucial. It was shown that the MCS algorithm can be used in strain and stiffness measurements very effectively.

Furthermore, the MCS control offers the potential of improving the effectiveness of control. Due to adaptation mechanism the MCS control feedback and feedforward gains change continuously according to plant parameters change and nonlinearities in the plant. Similarly, reasonable control is achieved by P+I control. However, the latter requires manual tuning of proportional gain k_p and integral gain k_i. It was observed that control signal was larger and more noisy in the case of P+I control than MCS.

However, the servovalve stiction has had an effect on the MCS and P+I responses in elastic region. In the second set of tests the steady-state error is bigger than the first set of tests due to the larger variations of the specimens characteristics, unmodelled dynamics and nonlinearieties in the system. The steady-state error is insignificant in the case of the MCS control, but it was significant in the case of P+I control. Indicating that MCS is a robust controller in the presence of plant parameter changes, nonlinearities and external disturbances. Therefore, it is suitable for systems which are working under different operating conditions.

The MCS algorithm was implemented in a simplified reduced first order form. The nominal plant was of a second order. The fact that the MCS was of lower order than the plant. Indicating, that MCS appears to be robust and quite insensitive to such mismatches.

Since electrohydraulic servomechanisms are widely used for a great variety of closed loop material testing application, many applications can benefit from MCS control performance. In particular in all closed loop electrohydraulic load, strain and temperature cycle tests, the nonlinear aspect of servovalve are significant in high frequency and it can be handled effectively by the MCS control.

REFERENCES

[1] - **DYSON, B. F., M. S. LOVEDAY & M. G. GEE**, *Materials Metrology and Standards for Structral Performance*, Chapman & Hall, First Edition, 1995.

CHAPTER 8

CONCLUSIONS AND FUTURE WORK

8.1 - INTRODUCTION

Adaptive control has been researched for number of decades. In recent years, however, consistent levels of system performance have resulted in greater attention being devoted to it. In this thesis the application of the MCS control in the electrohydraulic field is presented together with stability analysis.

The main purpose of this chapter is to make final conclusions about the application of the MCS control in the electrohydraulic field together with robustness analysis which are explained in detail in previous chapters. Later in this chapter, the possible improvements and applications of the MCS control including the reduced order MCS control in the case of electrohydraulic systems will be discussed.

The importance of modelling and simulation of the hydraulic systems is emphasised in Chapter 2. In this chapter, some modelling methods which are being used in this field are also discussed. Modelling and simulation of hydraulic systems has many advantages and it has been successfully used in this field.

The conventional model reduction methods are discussed together with adaptive model reduction methods in Chapter 3. Various model reduction methods are explained in this chapter. Subsequently, the servohydraulic actuator plant and the ESH materials testing machine transfer functions are reduced by using conventional model reduction methods. Some of the model reduction methods produced very accurate reduced order models which are in very close agreement with the response of the nominal plant models. Although the MCS control does not need plant parameters, these parameters are still needed in the case of comparative studies.

The robustness of the MCS control in the presence unmodelled dynamics is proven by either Popov's hyperstability or Lyapunov's function depending on the nature of the disturbances due to the unmodelled dynamics in Chapter 4. Later in this chapter, the stability of the electrohydraulic actuator plant and ESH material testing machine in the presence of unmodelled dynamics are proven using both methods.

The MCS control is implemented in a reduced order form in the case of position control of the electrohydraulic actuator plant in Chapter 5. The plant had a nominal third order model and the MCS control is implemented in reduced second order form. The MCS control is implemented one degree lower than the nominal plant model. Very satisfactory results are generated. The results of the MCS control responses are compared with those produced using P+DFB control.

Another application of the reduced order MCS control in the servohydraulic field was on the ESH material testing machine in this thesis (Chapter 6). In this case, the plant had a second order nominal plant model and the MCS control is implemented in first order form. Again, the MCS control produced very satisfactory results compared with results which are generated from P+I control. It is shown that the MCS is robust in the presence of plant parameters changes, nonlinearities, external disturbances and changes in the specimens.

The MCS control is used in the case of strain measurement and satisfactory results are derived in Chapter 7. Both aluminium alloys and EN24 steel specimens are used and specimens are controlled under cyclic MCS load control. These test results were very useful to find the yielding point of each material. Although each material has a known yielding point which is given by the manufacturing company but those numbers are not accurate enough, their values being higher than those obtained during testing. The exact yielding point is important, especially during the second set of tests where the elastic boundary is found to ensure that the tests are carried out in elastic-plastic region.

8.2 - ADAPTIVE CONTROL

Important theoretical results on stability and structure of the adaptive controller have been established. Much theoretical work still remains to be done. Laboratory

experiments and industrial applications have contributed to a better understanding of the practical aspects of adaptive control. In some cases, an arbitrary small disturbance can destabilise an adaptive system which is otherwise proved to be bounded-input bounded-state (BIBS) stable (Exponential stability or global asymptotic stability). Exponentially stable systems can tolerate a certain amount of disturbance. First, it is worth pointing out that the nominal adaptive system (assuming there are no disturbances and unmodelled dynamics) is exponentially stable. The robustness of the MCS control is investigated both analytically and empirically on the electrohydraulic actuator rig. Additionally, the robustness of the reduced order MCS controller is proven in the case of both the electrohydraulic actuator plant and the ESH material testing machine in Chapter 4. The practical concept of robustness is that stability should be preserved in the presence of actual disturbances present in the system. The main difference from classical linear control system robustness margins is that robustness depends not only on the plant and control system but also on the reference input. The reference input should guarantee persistent excitation of the nominal adaptive system. The exponential stability of the adaptive system is guaranteed by a persistency excitation (PE) condition. This will lead to a robustness margin, that is, bounds on disturbances and unmodelled dynamics which will not destroy the stability of the adaptive system.

8.3 - HYDRAULIC SYSTEMS

The field of hydraulics is wide and it has been very effectively used in the industrial machines. There has been a considerable amount of improvement in system performance utilising hydraulics. One such application is an electrohydraulic robotics system. Electric motors are found unsatisfactory due to their poor power and heavy weight. Some features of the hydraulic system include low friction (since the hydraulic oil being used in most cases act as lubricant), high capacity to take up heavy loads with little amount of energy consumption (the hydraulic cranes), the portability and flexibility to transfer power from applications near by (if two robots with similar moments are needed the piping can be arranged such that the fluid power can be divided to both robots).

8.4 - MODELLING AND SIMULATION OF HYDRAULIC SYSTEMS

Modelling and simulation of hydraulic systems are extensively used as a design tool. In order to investigate larger and more complex systems within an economic time frame. Simulation of hydraulic systems is crucial, as it may indicate whether or not the designed system will be stable. In addition, it may be helpful in choosing a suitable configuration for a given application. Also, it may help in choosing suitable controller parameters satisfying stable closed-loop system response. Many different modelling methods and software packages have been used to model and analyse the hydraulic systems. Some of those methods are presented in Chapter 2. In this chapter the electrohydraulic actuator plant is modelled and simulated by Simulink. Simulink is a software package for analysing and simulating dynamic systems. It is shown that there is a good correspondence between the simulated and the actual system responses, indicating that the mathematical model of the system which is analysed and modelled by Simulink is accurate.

8.5 - APPLICATIONS OF ADAPTIVE CONTROL IN ELECTROHYDRAULIC SERVO FIELD

Adaptive control has been applied to electrohydraulic systems (position control of hydraulic system, material testing machine) using both direct (Model Reference Adaptive control) and indirect (Self-tuning regulator) methods. In the case of the direct method (MRAC) the controller parameters are estimated directly from input-output data, and not calculated from the plant model. By contrast, in indirect adaptive control (or self-tuning regulator) the parameters are derived from the estimated model. If the estimated model is far from the real plant, then the controller will not perform accurately. Generally, plant models always contain some nonlinearities and unmodelled dynamics, and therefore Model Reference Adaptive control is more accurate than Self-tuning regulators and it is easy to implement. The hydraulic system equations are nonlinear and parameters of hydraulic systems vary greatly. Hydraulic systems exhibit significant nonlinearities. Using linear control theory in the case of the position control of hydraulic actuator does not produce satisfactory performance. The adaptive control can adapt itself the sudden changes in the

plant and good performance can be obtained despite the presence of many nonlinear characteristics.

8.6 - ROBUSTNESS OF ADAPTIVE CONTROL IN THE CASE OF UNMODELLED DYNAMICS

Adaptive control method ensures the stability of the plant with unmodelled dynamics. It has been shown that if the reference input is persistently exciting, then adaptive control possesses convergence properties which are strong enough to ensure that disturbances can be tolerated to some extent.

Adaptive control with unmodelled dynamics can be unstable without any disturbances. Two main instability mechanisms occur due to the unmodelled dynamics. In the first one, instability occurs due to increments in the adaptive gains while the second one is less obvious; it occurs when the reference input had too much energy in the frequency range of the unmodelled dynamics. For those reasons, choosing a suitable reference model is crucial in the case of adaptive control with unmodelled dynamics. The dynamics of the whole structure are slowed down by the unmodelled part of the plant, hence the controller gains should not excite the high frequency modes of the system. This is important to preserve the stability of the system.

8.7 - THE MCS CONTROL

8.7.1 - Application of the MCS Control in Servohydraulic Field

It has been shown that MCS works very effectively in servohydraulic applications. The MCS control can adapt to changes in pressure and temperature, and therefore it performs better than a linear controller strategy. The MCS control can be used very effectively in the case of hydraulic positioning systems. These type of systems are gain sensitive, in other words the set points may change greatly for a variety of reasons. The changes are even bigger in the case of hydraulic positioning systems with single rod actuator. In addition, in the case of material testing field the MCS control can adapt to

changes in the specimens as well as in the system itself. This was very clearly demonstrated in Chapter 7.

8.7. 2 - Applications of the MCS Control in Materials Testing Applications

The MCS control has been used in the materials testing field. The MCS control was first implemented in the materials testing machine in [1] and very satisfactory result were generated. In Chapter 6, the MCS controller is implemented on the ESH materials testing machine under load control. The derived results are better than the conventional P+DFB controller despite the fact that MCS does not need plant parameters for implementation, and it can still adapt to plant parameter variations due to the changes in pressures, temperatures and in the specimens. This fact is very clearly demonstrated in Chapter 7. In this chapter, specimens having different diameters and materials have been used and performance of the MCS control is compared with the P+DFB control. The second set of tests was very useful to show the robustness of the MCS control in the presence of unmodelled dynamics and parameter variations in the plant. The two controllers are implemented in the case of the aluminium specimens with $\phi 10$ mm. It is shown that the MCS control performed better than a well tuned P+DFB control in both elastic and plastic regions. The fact is shown very clearly by ISE plots. This indicates that the MCS can adapt to changes in the plant parameters.

The MCS control is used in the case of strain measurement as well in Chapter 7. These strain measurements is used to obtain the proportional limits of the specimens. After the proportional limit, the material behave plastically. In Chapter 7, the second set of tests are planned to be carried out in the elastic-plastic region, therefore it was important to know for each type of specimens when the specimens start to behave plastically.

8.7.3 - Application of the MCS Control On the Electrohydraulic Actuator Plant

The MCS can overcome the difficulties related to the strong nonlinear characteristic of the electrohydraulic systems. In the case of a hydraulic positioning system, the MCS control achieved zero steady-state error in the face of load disturbances. Most importantly, it showed a high degree of robustness and good performance in the presence of nonlinearities, unmodelled dynamics and parameter variations in the plant. Position control of a single-rod actuator systems are gain sensitive. This type of system always gives position errors when operating with a load force. The MCS control is implemented on the electrohydraulic single-rod actuator plant in Chapter 5. It is shown that the MCS can overcome the nonlinearities in the plant. The results of the MCS position control is compared with those produced by P+DFB in the Chapter. Under the nominal operating condition, the two controllers produced very similar responses despite the fact that the MCS does not require plant dynamic parameters. Away from normal operating condition (accumulators switched on and supply pressure is 110 bar), the MCS control performed better than a well tuned P+DFB controller.

8.8 - THE REDUCED ORDER ADAPTIVE CONTROLLER

Implementing the MCS controller in a reduced order form has many advantages. Firstly, the structure of the closed-loop system will be simplified. In many cases, although the transfer function of the plant is derived from the system identification test, there are always some nonlinearities, disturbances and unmodelled dynamics in plants. In some other cases, the plants may be over-parameterised. Additionally, even if the plants have higher order dynamics, if they are not working in the high frequency range then the higher order dynamics will not be activated and the plant will behave rather like a lower order one. Hence, using a reduced order controller in the low frequency range can avoid complication of the controller structure. Therefore, depending on the systems working conditions, the reduced order controller will make the whole controller structure simple and more efficient.

Two points are important in this case. The first is choosing suitable values for the adaptive weights. Secondly, choosing a reasonable value for the settling time. Both values should be chosen to not excite the high frequency modes of the plant which are found in the unmodelled part of the plant, and will be discussed in the following sections (sections 8.9.1, 8.9.2).

8.9 - THE REDUCED ORDER MCS CONTROL

The reduced order MCS controller is a form of the standard MCS controller, in which the controlled plant contains some unmodelled dynamics term inside the controller structure. The order of the controller reference model is therefore less than the nominal transfer function of the system. Generally the slower parts of the plant, which are more dominant than the fast part of the system, can be matched by the reduced order MCS control. The fast parts of the plant unmodelled (neglected) and included into the disturbance term. Then, the whole structure is represented in state space form. It is assumed that fast part of the plant does not contribute much to the plant output response if the system is working in low or mid frequency range. The robustness of the reduced order MCS controller is proven by Popov's and Lyapunov's method depending on the nature of the disturbance term in Chapter 4.

8.9.1 - Applications of the Reduced Order MCS Control

In the case ESH material testing machine, the first order SISO MCS control is implemented. Under the load control the plant is described by a second order nominal plant transfer function. It has been shown that the MCS control can cope with the unmodelled dynamics, parameter changes in the plant parameter due to the changes in the pressures, temperatures and the changes in the specimens. Similarly, the electrohydraulic actuator plant is modelled in Simulink by a 5^{th} order transfer function. Subsequently, the system identification made it clear that no model matched the fifth order models. The fifth order models are over parameterised. The third order model was relevant for the nominal

operating condition (accumulators on-line, supply pressure is 110 bar). Hence, the electrohydraulic actuator plant is controlled under the second order SISO MCS control. In both cases the MCS was lower order than the plants. The results were very satisfactory, as is shown in Chapter 5, 6, 7.

8.9.2 - Stability of the Reduced Order MCS Control (Lyapunov and Popov's theory)

Lyapunov's direct method is a powerful tool to prove the stability of the reduced order MCS control. In general, unmodelled dynamics always exist in the plant model. It has been assumed that if the disturbance term due to the unmodelled dynamics, plant nonlinearities and parameter variations is small then Popov's method is suitable to prove the stability of the reduced order MCS system. If the disturbance term is large and rapidly varying then the Lyapunov's method is more suitable to guarantee the stability of the whole system. The stability of the reduced order MCS control is proven in Chapter 4, in the case of both SISO and MIMO systems. It has been shown that the MCS control is stable in the presence of unmodelled dynamics provided that the input signal is persistently exciting and the controller parameters are chosen to not excite the high frequency modes which are taking place in the unmodelled part of the plant. In this chapter the stability of the reduced order MCS control is proven using both Popov's and Lyapunov's methods.

8.9.3 - Choosing Suitable Settling-time in the Case of Reduced Order MCS Control

Choosing a suitable settling time of the MCS control in the case of a plant with unmodelled dynamics is crucial. When the unmodelled dynamics are introduced into the system, it is assumed that some parts of the plant have negligible effects on plant output result. Therefore, the slower part of the plant dynamics has been used. Compared to the nominal plant the reduced order plant has slower dynamics. The reduced order MCS control can produce very good response if the system is operated in low or mid frequency

range. Hence, it is necessary to use a larger value for the settling time compared to the nominal case assuming that the closed loop system is slower.

8.9.4 - Choosing Suitable Values for Adaptive Weights α and β in the Case of the Reduced Order MCS Control

The speed of the adaptation can be increased by increasing the value of the integral gain coefficient α. The higher values of α will therefore excite the high frequency modes of the plant which are assumed to take place in the unmodelled part of the plant. In this case smaller values of integral gain are used compare to the plant without any unmodelled dynamics (the nominal plant transfer function).

The influence of the proportional gain coefficients β is to reduce the magnitude of the ultimate region of convergence of the error, x_e as β is increased. Hence, the increment in the proportional gain will decrease the output error. For slow and medium plants, increasing the proportional gain will decrease the output error. However in the case of the plants which are subjected to the rapidly varying external disturbances, unmodelled dynamics, or the plant which is working in the high frequency range, large values of β can lead to large output errors even instability. Very large adaptive gains (α, β) can cause instability. Therefore, they should not increased beyond a certain point.

8.10 - FUTURE WORK

8.10.1 - Application of the MCS Control on MIMO Electrohydraulic Systems

The stability of the MCS control in MIMO servohydraulic systems may be investigated. The MCS control can be implemented on a large hydraulic system (e.g. electrohydraulic multi arm manipulators, earthquake rig, widely distributed electrohydraulic systems, etc.). The MCS can be very efficient in the case of multivariable servohydraulic systems, which are known to suffer from plant order changes under

different operating conditions. The MCS control can be implemented in centralised or decentralised form.

8.10.2 - Implementation of the Reduced Order MCS Control on MIMO Servohydraulic System

One of the future investigations of the reduced order MCS control could be implementation of the MCS control in MIMO servo-hydraulic fields. The reduced order MIMO MCS control will simplify the dynamics of the electrohydraulic system, due to the fact that it will ignore the high frequency modes of the system. The reduced order MCS control will simplify the structure of the MIMO servohydraulic system and it will make it possible to control the large or widely distributed servohydraulic systems in a stable manner.

Another possibility is using the reduced order MIMO MCS control in the case of large interconnected non-servohydraulic systems. The reduced order MIMO MCS controller can be implemented in either centralised or decentralised form.

8.10.3 - Temperature Cycle

In general, during the temperature cyclic loading materials behave nonlinearly with high temperature. At high temperature the strength of most materials falls, due to the increasing mobility of dislocations, coupled with a general reduction in the strength of interatomic bonds and therefore of the rigidity of the lattice.

At high temperature, a small amount of internal intergranular cracking can occur over extended time periods. Nonlinear material oscillations are encountered during thermal cycling. Other nonlinearities include:

(1) - Temperature is not well distributed along the length of gauges.

(2) - Temperature changes during tests

According to [2], a thermal cycle could lead to unexpected early failure. This indicates the possibility that a temperature cycle promotes more rapid failure than an isothermal test. Adaptive control will preserve the stability of the system in the presence of the

nonlinearities due to the peaks of oscillations and other sudden changes in the specimen. Further, using the MCS control in the case of temperature cycling will bring many advantages, such as rapid adaptation to the changes in the specimens as well as in the systems.

8.10.3.1 - Thermal Strain Control

Thermal strain is a special class of elastic strain that results from expansion with increasing temperature or contraction with decreasing temperature. Increased temperature causes the atoms in a solid to vibrate by a larger amount. Thermal effects are generally greater at higher temperatures. The coefficient of thermal expansion increases with temperature.

The most direct method of using strain gauges is bonding to the material surface, but this method can not be used at high temperature; and the cyclic life of strain gauges is limited when operating at high strains. Again, the MCS control can be a good option in the case of thermal strain control.

8.10.3.2 - Thermal Fatigue Testing

Changing the temperature usually affects the fatigue crack growth rate, with higher temperature often causing faster growth. If a material is tested in a temperature range where creep occurs, creep strains will contribute to the inelastic deformation in the test. Fracture toughness generally increases with temperature. The coefficient of thermal expansion will decrease rapidly when the temperature is increased. Physical properties of the material vary with temperature. Moreover, greater creep strain occurs if the speed of the test is slower, as a slower test provided more time for the creep strain to accumulate. Using the MCS control in the case of thermal fatigue testing can be very helpful to overcome the nonlinearities and parameter variations in the plant and specimens.

8.11 - THE MCS STRAIN CONTROL (UNDER ROOM TEMPERATURE)

The interpretation of strain becomes extremely important when a strain controlled test is undertaken in an axially loaded machine. In the case of fatigue test, if the material cyclically hardens or softens, the ratio of elastic to plastic strains cannot be held constant by this method of displacement control. To overcome this problem, the instantaneous load signal may be fed to a microprocessor that determines the elastic displacement from knowledge of load and Young's modulus. Another further implementation of the MCS control in the material testing field can be strain control in room temperature. Under plastic strain control, the materials behaves nonlinearly, therefore using the MCS control in this case has many advantages because it can adapt itself to sudden changes in the both plant and the specimens.

8.12 - FATIGUE TESTING UNDER THE MCS CONTROL (ROOM TEMPERATURE)

Under fatigue testing, materials are subjected to repeated loading. In general, one or more tiny cracks start in the material, and these grow until complete failure occurs. Prevention of fatigue fracture is a vital aspect of design for machines, vehicles and structures that are subjected to repeated loading or vibration. In fatigue, materials are tested under a cyclic load which is lower than the proportional limit of the material. The test therefore take place completely in the elastic region. After thousands or millions of repeated loads the structure of the material changes. Using the MCS control or the reduced order MCS control in fatigue testing may bring advantages due to the adaptability of the MCS control to changes inside the specimens.

8.13 - THE MIMO MCS CONTROL IN MATERIALS TESTING FIELD

For servohydraulic materials testing machine the MIMO MCS algorithm can be a very good option. In this case, the MCS could be implemented in both centralised and decentralised form. The decentralised MCS algorithm uses only local information of each

subsystem. Therefore, the synthesis of each MCS control input is simplified. Additionally, this property helps to extent the controller structure when it is needed, e.g. when the additional parts are added into the interconnected systems. In certain circumstances it is important to control two variables at the same time. In the case of material testing field the MIMO MCS control can be used to control two variables such as, stress-temperature, strain-temperature at the same time.

REFERENCES

[1] - **STOTEN, D. P.** , "Implementation of Minimal Control Synthesis on a Servo-Hydraulic Testing Machine", *Proc. Instn. Mech. Engrs.*, Vol. 206, pp. 189-194.

[2] - **BEAUCHAMP, D. J.**, "*Thermal-mechanical strain cycling at elevated temperature*", PhD Thesis, Faculty of Engineering, University of Bristol, U. K., 1982.

APPENDIX 1

POPOV'S HYPERSTABILITY THEORY

The hyperstability theory was developed by Popov as a generalisation of the absolute stability problem [1]. It was shown in this work that the absolute stability of feedback systems that can be represented by the standard form, consisting of two blocks, a linear system in the feedforward block and a nonlinear system in the feedback block as shown in Fig. 1.

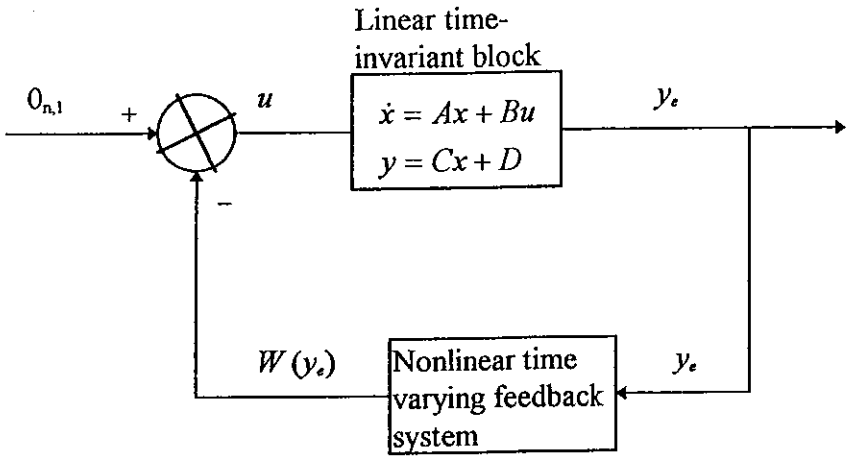

Fig.1: Standard Nonlinear Time-Varying Feedback System

The feedback block is assumed to varying an input-output relation of the form

$$W(y_e)y_e \geq 0$$
$$W(y_e) = 0 \qquad \text{(A1.1)}$$

where y_e and $W(y_e)$ are scalar and are respectively the input and the output of the nonlinear time-varying block. It was observed that the feedback system shown in Fig.1 is absolutely stable if it is asymptotically stable for all the feedback blocks satisfying the condition (A1.1).

The hyperstability theory is a generalisation of the absolute stability problem where the feedback block in Fig. 1 is assumed to satisfy a more general input-output relation, i.e.:

$$\int_{t_0}^{t_1} y_e^T W dt \geq -c_0^2 \qquad \text{(A1.2)}$$

where c_0^2 is a positive constant independent of t_1. The stability properties of the feedback system (in Fig. 1) are entirely dependent on the feedforward block characteristics if the feedback block satisfies inequality (A1.2).

Definition 1:

The linear completely controllable and observable system is given as

$$\dot{x} = Ax - BW$$
$$y_e = Cx - DW \qquad \text{(A1.3)}$$

where the dimensions of x, W and y_e are respectively n, m and m, is hyperstable for all feedback blocks satisfying (A1.2) if there exist two constant $\delta(\delta > 0)$ and $\gamma(\gamma \geq 0)$ so that the solution of (A1.3) satisfies the following inequality:

$$\|x(t)\| < \delta\left(\|x(0)\| + \gamma\right) \qquad \text{for all } t,\ t \geq 0 \qquad \text{(A1.4)}$$

Definition 2:

The linear system (A1.3) is asymptotically hyperstable if it is hyperstable and if:

$$\lim_{t\to\infty} x(t) = 0 \qquad \text{(A1.5)}$$

Definition 3:

The linear system (A1.3) is hyperstable if there exist two constants β_0 and β_1 so that the following inequality :

$$\int_{t_0}^{t_1} -W^T(\tau) y_e(\tau) dt + \beta_0 \|x(t_0)\|^2 \geq \beta_1 \|x(t_1)\|^2 \qquad \text{(A1.6)}$$

is satisfied for all $t_1 \geq t_0$ and for all functions W and y_e that satisfy inequality (A1.2).

If we interpret quantity $\frac{1}{2}x^T(t_1)x(t_1)$ as the stored energy at instant t_1, then by setting $\beta_1 = \beta_2 = \frac{1}{2}$, we observe that the hyperstability condition (A1.6) corresponds to a *passivity* condition, where the stored energy at instant t_1 must be less or equal to the initial energy $\left(\frac{1}{2}x^T(t_0)x(t_{01})\right)$ plus the added energy between t_0 and t_1.

Moreover, it is well known that a linear passive network is characterised by a positive real transfer function matrix, see [2]. We therefore obtain an equivalent definition to the hyperstability condition (A1.6).

Theorem 1:

The linear system (A1.3) is hyperstable for all the feedback blocks verifying inequality (A1.2) if the transfer function matrix $G_p(s) = C[SI - A]^{-1}B + D$ is positive real.

Theorem 2:

The linear system (A1.3) is asymptotically hyperstable for all the feedback systems satisfying inequality (A1.2) if the transfer function matrix $G_p(s) = C[SI - A]^{-1}B + D$ is strictly positive real.

REFERENCES

[1] - **POPOV, V. M.**, *Hyperstability of Control systems*, Springer Verlag, Berlin, 1973.

[2] - **ANDERSON, B. D. O. & S. VONGPANITLERD**, Network Analysis and Synthesis, Prentice Hall, 1973.

APPENDIX 2

POSITIVE REAL TRANSFER FUNCTIONS

Definition 1

A rational function $G_p(s)$ of the complex variable $s = \sigma + j\omega$ is positive real (PR) [1] if the following conditions are satisfied:

1 - $G_p(s)$ is real for real s.

2 - $G_p(s)$ has no poles in the open right half plane, Re(s) > 0.

3 - The poles of $G_p(s)$ on the axis Re(s) = 0 are distinct, and the associated residues are real and positive (or null).

4 - For all real ω for which $s = j\omega$ is not a pole of $G_p(s)$, we have

$$\mathrm{Re}\left[G_p(s)\right] \geq 0$$

Definition 2

A rational function $G_p(s)$ of the complex variable $s = \sigma + j\omega$ is strictly positive real if the following conditions are satisfied:

1 - $G_p(s)$ is real for real s.

2 - $G_p(s)$ has no poles in the closed right half plane Re(s) = 0.

3 - Re[($G_p(s)$)] > 0 for all ω.

Property 1

If $G_p(s) = \dfrac{n(s)}{d(s)}$ is a positive real function, then we have:

1 - $n(s)$ and $d(s)$ have real coefficients.

2 - $1/G_p(s)$ is also positive real function.

3 - $n(s)$ and $d(s)$ are Hurwitz polynomials.

4 - The order of $n(s)$ does not differ from the order of $d(s)$ by more than ± 1.

Property 2

If $G_{p1}(s)$ and $G_{p2}(s)$ are positive real functions, then we have:

1 - $\alpha_1 G_{p1}(s) + \alpha_2 G_{p2}(s)$ is positive real (provided that α_1 and $\alpha_2 \in \mathbb{R}^+ > 0$).

2 - $\dfrac{1}{1 + G_{p1}(s) G_{p2}(s)}$ is positive real.

Definition 3

An nxn matrix $G_p(s)$ of real functions is positive real if the following conditions are satisfied:

1 - All elements of $G_p(s)$ do not have poles in the open right half plane, Re(s) > 0.

2 - The poles of any element of $G_p(s)$ on the axis Re(s) = 0 are distinct, and the associated residue matrix is a positive semidefinite Hermitian.

3 - The matrix $G_p(j\omega) + G_p^T(-j\omega)$ is a positive semidefinite Hermitian for all real values of ω which are not a pole of any element of $G_p(s)$.

Definition 4

An nxn matrix $G_p(s)$ of real rational functions is strictly positive real if the following conditions are satisfied:

1 - All elements of $G_p(s)$ are analytic in the closed right half plane $\mathrm{Re}(s) \geq 0$.

2 - The matrix $G_p(j\omega) + G_p^T(-j\omega)$ is a positive definite Hermitian for all real ω.

Kalman-Yacubovitch Lemma

1 - Consider the linear system:

$$\dot{x} = Ax + Bu$$
$$y = Cx$$

The transfer function matrix $C(sI - A)^{-1}B$ is a positive real matrix if, and only if, there exists a symmetric positive definite matrix P and a symmetric positive semidefinite matrix Q such that:

$$PA + A^T P = -Q$$
$$C = B^T P$$

2 - The transfer function matrix $C(sI - A)^{-1}B$ is a strictly positive real matrix if, and only if, there exists a symmetric positive definite matrix P and a symmetric positive definite matrix Q such that:

$$PA + A^T P = -Q$$
$$C = B^T P$$

3 - Consider the linear time varying system:

$$\dot{x} = A(t)x + B(t)u$$
$$y = C(t)x$$

The transfer function matrix $C(t)[sI - A(t)]^{-1}B(t)$ is a positive real matrix if and only if there exists a symmetric positive definite matrix $P(t)$ and a symmetric positive semidefinite matrix $Q(t)$ such that:

$$P(t)A(t) + A(t)^T P(t) + \dot{P}(t) = -Q(t)$$
$$C(t) = B(t)^T P(t)$$

For the strictly positive realness condition, the matrix $Q(t)$ must be positive definite.

REFERENCES

[1] - **SLOTINE, J.-J. E. & W. LI**, *Applied Nonlinear Control*, Prentice-Hall International, London, 1991.

APPENDIX 3

LYAPUNOV'S STABILITY THEORY

Consider the free system described by the following differential equation:

$$\dot{x} = f(x,t) \tag{A3.1}$$

where $x \in \mathbb{R}^n$. It is assumed that the function $f(x,t)$ is sufficiently smooth so that the equation has a unique solution starting at any initial state x_0 at any time t_0. We further assume that there exists a unique vector solution $\Phi(t, x_0, t_0)$, differentiable in t, such that, for any fixed x_0 and t_0:

$$\Phi(t_0, x_0, t_0) = x_0$$

$$\frac{d}{dt}\Phi(t, x_0, t_0) = f\left(\Phi(t, x_0, t_0), t\right)$$

Definition 1

An equilibrium state x_e of the free dynamic system (A3.1) is stable if for every real number $\varepsilon > 0$ there exists a real number $\delta(\varepsilon, t_0) > 0$ such that the condition $\|x_0 - x_e\| \le \delta$ implies $\|\Phi(t, x_0, t_0) - x_e\| \le \varepsilon$ for all $t \ge t_0$.

Definition 2

An equilibrium state x_e of the free dynamics system (A3.1) is asymptotically stable if:

1 - it is stable

2 - every motion starting sufficiently near x_e converges to x_e as t tends to infinity.

Definition 3

An equilibrium state x_e of the free dynamic system (A3.1) is globally asymptotically stable if

1 - it is stable

2 - every motion converges to x_e uniformly in x_0 for $\|x_0\| \leq r$ is fixed but arbitrarly large.

Definition 4

An equilibrium state x_e of the free dynamic system (A3.1) is uniformly asymptotically stable if:

1 - it is stable

2 - every motion starting sufficiently starting near x_e converges to x_e uniformly in t_0, i.e. the term δ does not depend on t_0.

Theorem (Lyapunov)

Consider the free dynamical system

$$\dot{x} = f(x,t) \tag{A3.2}$$

where $f(0,t) = 0$ for all t. Suppose there exists a scalar function $V(x,t)$ [1] and [2] with continuous first partial derivatives with resspect to x and t such that $V(0,t) = 0$ and

1 - $V(x,t)$ is positive definite, i.e. there exists a continuous, nondecreasing scalar function α such that $\alpha(0) = 0$ and all t and all $x \neq 0$

$$0 < \alpha(\|x\|) \leq V(x,t)$$

2 - There exists a continuous scalar function γ such that $\gamma(0) = 0$ so that the derivative $\dot{V}$ of V along the motion starting at t, x satisfies, for all t and $x \neq 0$:

$$\dot{V}(x,t) = \frac{d}{dt}V(x,t) \leq -\gamma(\|x\|) < 0$$

3 - $\alpha(\|x\|) \to \infty$ as $\|x\| \to \infty$.

then the equilibrium state $x_e = 0$ is globally asymptotically stable and $V(x,t)$ is called a Lyapunov function of the sysstem (A3.2).

For the uniform asymptotic stability of the equilibrium state $x_e = 0$, condition **(3)** is replaced by the following condition:

- there exists a continuous, nondecreasing scalar function β such that $\beta(0) = 0$, and all t, we have:

$$V(x,t) \leq \beta(\|x\|)$$

REFERENCES

[1] - **KALMAN, R. E. & J. E. BERTRAM,** "Control Systems Analysis and Design via the Second Method of Lyapunov", *ASME Journal of Basic Engineering*, pp. 371-393, June 1960.

[2] - **LA SALLE, J. & S. LEFSCHETZ,** *Stability by Lyapunov's Direct Method, with Applications*, Academic Press, 1961.

Application of the MCS Algorithm to the Control of an Electrohydraulic System

D P Stoten, S Bulut

Department of Mechanical Engineering, University of Bristol, Bristol, BS8 1TR, UK
Phone ++44 (0)272 288208

Abstract - **This paper describes the application of the direct adaptive minimal control synthesis (MCS) algorithm to a specific problem in electrohydraulic control. In particular, comparative implementation studies are presented of a typical servohydraulic positioning system, as used in aerospace applications. It is shown that MCS outperforms a well-designed conventional controller, especially when the plant is subjected to gross internal parameter changes.**

Introduction

The adaptive MCS algorithm was first proposed in 1990 [1] as a form of direct adaptive control for multivariable plant subject to unknown (but bounded) plant parameter changes and external disturbances. In addition, closed-loop stability and robustness proofs were presented for the large class of (electromechanical) plant with Lagrangian dynamics - despite the fact that no *a priori* knowledge was required concerning the nominal values of the plant parameters. The implemented form of MCS therefore required a minimal amount of information on the plant, and since no on-line plant estimation procedure was required, only a minimal amount of control code (*cf* a PID controller) was necessary. These attributes of minimal design input and coding requirements led to the coining of the controller's name. Since 1990, significant extensions to the basic MCS algorithm have been presented (including a decentralised version), together with sets of implementation studies. An overview of the algorithm, its extensions, together with implementation case studies, is presented in [2]. In all the cases described in [2], the predicted performance characteristics of MCS were matched in practice.

Of particular relevance to this paper is a study briefly described in [2], and in more detail in [3], concerning the MCS control of a servohydraulically actuated materials testing machine. The problem investigated in [3] was the load (force) control of a fatigue test specimen subjected to varying degrees of crack propagation. Although [3] indicated that MCS held much promise for application to the field of servohydraulic control, the test rig used was of a rather specific nature, and atypical of a wide range of practice. Hence, one of the main objectives of this paper is to present the application of MCS to the control of a typical servohydraulic positioning system as used, for example, within aerospace systems for actuation of flight control surfaces.

The remainder of this paper is structured as follows: in the next section, the test rig is described, together with the dynamic modelling and system identification results. Then, the linear fixed gain and MCS control system designs are presented, followed by the comparative test results. Finally, the main conclusions to the paper are presented together with further implications for MCS control within this general field.

Plant Dynamics And System Identification Tests

The plant consists of Moog E760 torque motor/flapper operated four-way double-acting servovalve, hydraulically connected to a cylinder/actuator arm. The actuator cylinder has a diameter of 32mm, the actuator arm has a stroke of approximately 100mm, and the end of the arm is connected to an inertial load representing an aircraft control surface. See Fig 1. In this arrangement there is no representation of the effect of aerodynamic forces (which would normally produce a restoring force on the actuator arm in flight). However, the rig is in all other respects quite representative of servohydraulic systems used in aerospace (and other) systems. The input to the plant is the control voltage, u, applied to the torque motor current amplifier, and the output, y, is an LVDT measure of the actuator arm displacement, x_1.

Switchable accumulators are situated either side of the actuator arm piston; in normal use these devices would generate a source of energy to smooth out hydraulic pressure fluctuations and/or make provision for short-term increases in load. In the context of the tests described in this paper, the switching of the accumulators is a method for changing the plant parameters - thus providing a mechanism for gauging closed-loop system robustness. Another method of plant parameter variation used in the tests is to lower the supply pressure - from 11.0MPa to 1.4MPa (*ie* 1600psi to 200psi).

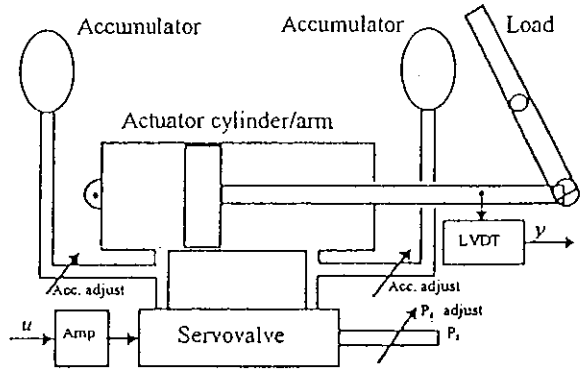

Fig 1 Servohydraulic test rig

The dynamics of systems as depicted in Fig 1 are known to contain significant non-linear elements, *eg* see [4], [5]. However, a linearised representation of the input/output relationship is used in the design of a conventional fixed-gain controller for the comparative tests. A typical transfer function model is then given by [4], [5], [6]:

$$G_p(s) = y(s) / u(s) = G_1(s)G_2(s)G_3(s)$$

where $G_1(s)$ represents the amplifier/torque motor transfer function, $G_2(s)$ is the servovalve transfer function and $G_3(s)$ is the actuator arm transfer function. Each of these terms is typically modelled as follows:

$$G_1(s) = \frac{K_1}{1+\tau_1 s}$$

$$G_2(s) = \frac{K_2}{\frac{s^2}{\omega_{n2}^2} + \frac{2\zeta_2 s}{\omega_{n2}} + 1}$$

$$G_3(s) = \frac{K_3}{s(1+\tau_3 s)}$$

Consequently, the nominal linearised model is of 5th-order, including a free integrator. However, various further simplifications can be justifiably made. For example, the pole of $G_1(s)$ is typically much faster than those of $G_2(s)$ and $G_3(s)$, so that the plant can be adequately modelled by a 4th-order transfer function. Similarly, the relative locations of the servovalve and actuator arm poles can lead to 3rd- and 2nd-order models (all including the free integrator).

A series of system identification tests were conducted on the open-loop plant, which yielded a number of transfer function models for different operating conditions (as discussed above, and summarised in row 1 of Table 1). The test results were generated from a swept sinusoid input signal, with data analysed by the Matlab System Identification Toolbox macro *oe* (output-error method). Consistent 5th-order models were not generated by the method, leading to the conclusion that such models were over-parameterised, and that the torque motor pole was indeed much faster than all the others. Hence, Table 1 shows the resulting 4th-, 3rd- and 2nd-order transfer function numerators and denominator roots, under the different operating conditions [A]-[C].

Order	Condition [A]: 11.0MPa; Accum. on	Condition [B]: 11.0MPa; Accum. off	Condition [C]: 1.4MPa; Accum. on
4	num = 9.11×10^4 den roots: 0; -15.5; $-7.51\pm j22.9$	num = 7.08×10^4 den roots: 0; -4.32; $-35.8\pm j23.1$	num = 22.1×10^4 den roots: 0; -30.1; $-33.5\pm j27.6$
3	num = 2.83×10^3 den roots: $0; -8.80\pm j16.0$	num = 17.9×10^3 den roots: $0; -40.9\pm j20.3$	num = 4.60×10^3 den roots: $0; -27.8\pm j20.4$
2	num = 62.4 den roots: 0; -4.58	num = 108 den roots: 0; -10.3	num = 47.2 den roots: 0; -9.19

Table 1 Identified plant transfer function data

Several points are worth noting from this table:

(i) For Condition [A], the 4th-order model poles are dominated by the conjugate pair at $s = -7.51 \pm j22.9$, so that the actuator arm pole at $s = -15.5$ may (as an approximation) be ignored. This justifies the use of the given 3rd-order model for Condition [A] - *ie* the normal operation case.

(ii) For Condition [B], the above situation is reversed, for now the pole associated with the actuator arm provides the dominant component of the dynamics. Hence, the given 2nd-order model is a justifiable approximation of Condition [B] dynamics.

(iii) For Condition [C], the servovalve and actuator arm poles are equally significant, and the given 4th-order model is the most justifiable approximation in this case.

(iv) The conventional controller will be designed for the nominal operation of the plant, *ie* Condition [A], with the third order model for $G_p(s)$ being used.

(v) Changes in the plant supply pressure and/or accumulator settings have significant effects on the plant parameters and plant dominant dynamics.

Controller Designs

Conventional Fixed Gain Control

Bode plots for the nominal (Condition [A]) third order plant transfer function are shown in Fig 2 (labelled 'Gp'), indicating that there is sufficient low frequency gain (due to the free integrator), but a requirement to increase the margins (from 2.1dB and 55°) and the closed-loop bandwidth (from 10 rad/s). A proportional-plus-derivative feedback (P+DFB) controller was proposed with a proportional gain $k_p = 1.0$ and a derivative feedback gain $k_d = 0.1$. The resulting open-loop transfer function plots are also shown in Fig 2 (labelled 'GH'), which yield margins of ∞ dB and 61°, plus a bandwidth of 18.2 rad/s. The closed-loop step response settling time was therefore predicted to be $t_s \approx 4/(0.61\times18.2) \approx 0.4$s, with an oscillatory component containing approximately two overshoots - this was deemed to be an acceptable performance. In discrete-time, the implemented form of the controller was:

$$u(k) = k_p e(k) - k_p k_d [y(k) - y(k-1)] / \Delta \qquad (1)$$

where $u(k)$ was the current control signal, $e(k)$ the current tracking error, $y(k)$ the current measured actuator arm position and Δ the sampling interval.

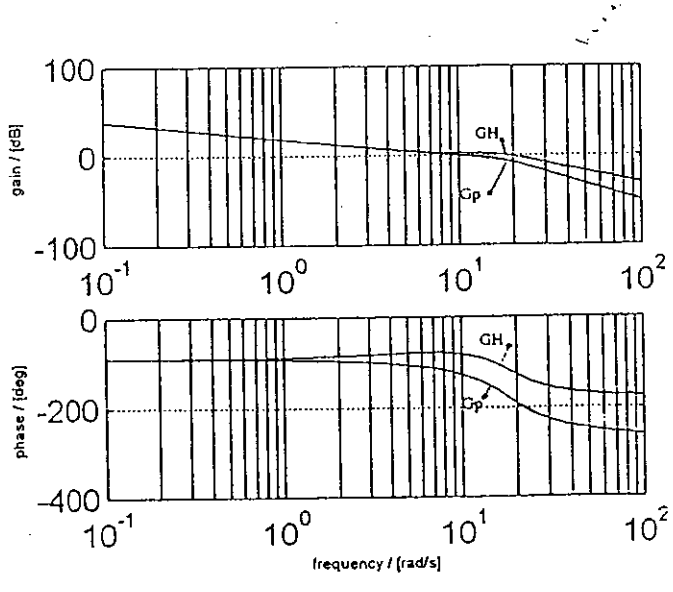

Fig 2 Plant and plant/controller Bode plots

MCS Control

Details of the MCS structure have been presented elsewhere (*eg* [1]-[3]). Often, an *a priori* estimate is made of the nominal plant order, and the order of the MCS algorithm matches this figure - hence, for the given nominal plant, one would normally expect to implement a 3rd-order algorithm. However, it has been observed, *eg* [3], that MCS possesses a degree of robustness to mismatches in orders. In particular relatively low order MCS controllers can be very effective in the control of higher order plants.

Therefore, one objective of this work is to provide further experimental evidence of this form of robustness via implementation of the *2nd-order MCS equations* (i = 1,2) which are summarised below, in discrete-time scalar form:

$$u(k) = k_r(k)r(k) + k_1(k)x_1(k) + k_2(k)x_2(k) \quad (2)$$

$$k_r(k) = k_r(k-1) + \beta y_e(k)r(k) - \sigma y_e(k-1)r(k-1) \quad (3)$$

$$k_i(k) = k_i(k-1) + \beta y_e(k)x_i(k) - \sigma y_e(k-1)x_i(k-1) \quad (4)$$

$$y_e(k) = (16/t_s^2)x_{e1}(k) + (4/t_s)x_{e2}(k) \quad (5)$$

$$x_{ei}(k) = x_{mi}(k) - x_i(k) \quad (6)$$

$$x_{m1}(k) = x_{m1}(k-1) + \Delta x_{m2}(k-1) \quad (7)$$

$$x_{m2}(k) = (-16\Delta/t_s^2)x_{m1}(k-1) + (1-8\Delta/t_s)x_{m2}(k-1) + (16\Delta/t_s^2)r(k-1) \quad (8)$$

Here, $\sigma = \beta - \alpha\Delta$, where $\{\alpha, \beta\}$ are the adaptive weights, with a typical ratio of $\alpha/\beta = 10$ and $\alpha > 0$. During the tests presented in the next section, the values of the adaptive weights were fixed at 0.001 and 0.0001, these values having been deduced experimentally as providing a good compromise between the speed of adaption and noise propagation. Also, $\{k_r \; k_1 \; k_2\}$ are the adaptive forward, positional and velocity gains, r is the reference signal, x_1 (= y) is the measured actuator arm position, x_2 is the measured velocity, y_e is the output error (which ensures positive realness of the forward loop error dynamics, [1]), x_{mi} are the reference model states and t_s (= 0.25s in the following tests) is the step response settling time of the reference model. Thus, (2) is a standard state feedback control equation with adaptive gains given by (3), (4). Coefficients in the output error equation (5) ensure positive realness of the forward error dynamics by satisfying, in turn, an associated Lyapunov equation [1]. The coefficients in the reference model equations (7), (8) ensure, to a first approximation, that the ideal step response is critically damped, with a settling time of t_s and zero steady state error. It may be noted that (2)-(8) contain no explicit (or implicit) reference to any plant parameter values.

Comparative Implementation Tests

Step response tests; Condition [A]; Supply pressure 11.0MPa; Accumulators on-line.

The conventional P+DFB response with the rig in the nominal configuration, *viz* a supply pressure of 11.0MPa and the accumulators on-line, is shown in Fig 3. In this case, the demand was a square wave of amplitude 1.0V and frequency 0.25Hz. (All controllers were implemented via *WinCtrl* [7], on a 486 PC, with Δ = 5.0ms). The desired response - as specified by t_s = 0.25s - is shown in Fig 3 as 'xm1', together with the actual response 'x1'. There is good correspondence between the desired and actual responses (apart from small steady-state errors due to spool valve stiction), indicating that the third order plant model and P+DFB synthesis are well-founded.

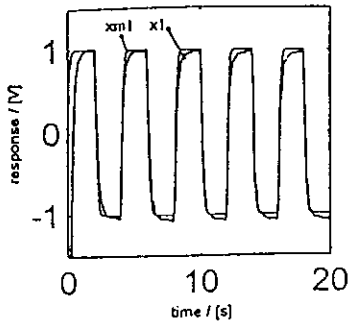

Fig 3 P+DFB step response for the nominal case

With the initial conditions on the adaptive gains set to zero, the MCS yielded the steady state response (*ie* when the gains were in a quasi-static state) shown in Fig 4a, together with the gains themselves in Fig 4b. There is no significant difference in response from the P+DFB case, and so MCS matches the performance of this well-tuned conventional controller - however, without the necessity for system identification and controller synthesis. The initial adaptive stage of the MCS controller is shown in Fig 5.

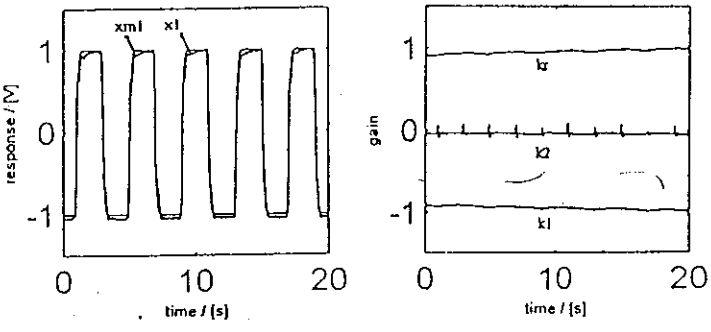

Fig 4a Responses Fig 4b Gains

Fig 4 MCS step response for the nominal case: steady-state

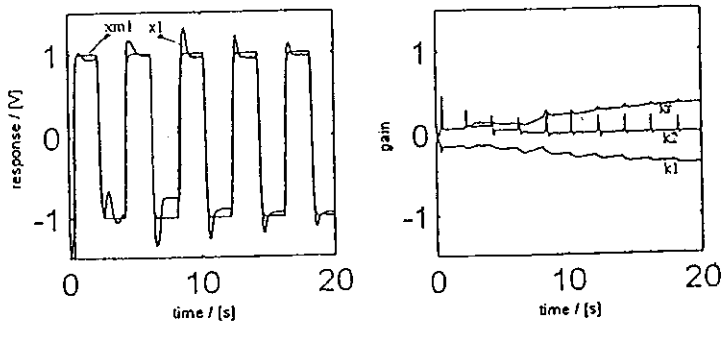

Fig 5a Responses Fig 5b Gains

Fig 5 MCS step response for the nominal case: initial adaption

Sinusoidal tests; Condition [A]-[B]; Supply pressure 11.0MPa; Accumulators switched.

Switching the accumulators suddenly off-line, and then on-line again, produces significant changes in the plant dynamics. The purpose of this set of tests is to compare the efficacy of MCS in the face of such changes, when compared with the P+DFB controller. The demand signal in this case was a sinusoid of amplitude 2.0V and frequency 3.0Hz - sufficient to test the closed-loop systems near to the expected bandwidth of the nominal plant.

The resulting tracking error ('xm1-x1') for P+DFB control is shown in Fig 6a, whilst that of MCS is in Fig 6b. Comparing these figures, it is evident that the MCS controller has out-performed P+DFB. A comparison of the corresponding controls in Fig 7 reveals that MCS produces a signal with a greater amplitude and (in this case) with more effect. The difference in performance is most evident in Fig 8, plots of the corresponding integral-square-error (ISE) criterion for each closed-loop response. Of particular note is the slope of the ISE plot during each section of the test - the slope for MCS remains less than that for P+DFB, whether the accumulators are on-line or off-line.

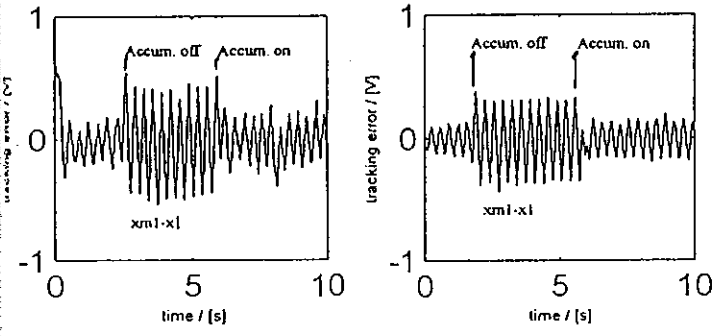

Fig 6a P+DFB Fig 6b MCS

Fig 6 Tracking error; supply 11.0MPa; accumulators switched

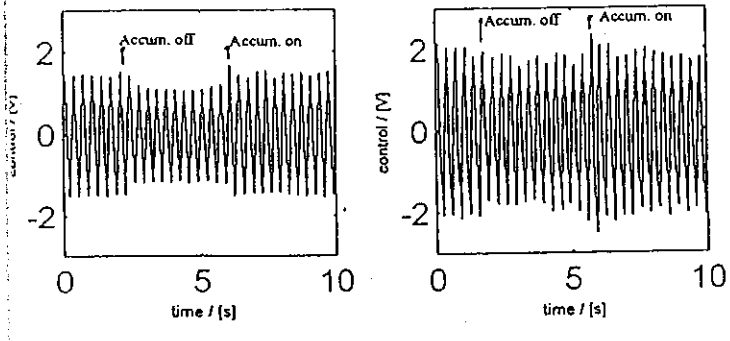

Fig 7a P+DFB Fig 7b MCS

Fig 7 Control signals; supply 11.0MPa; accumulators switched

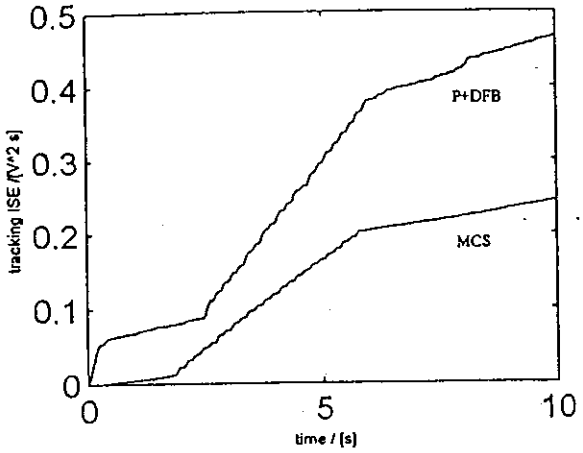

Fig 8 ISE criteria; supply 11.0MPa; accumulators switched

Sinusoidal tests; Condition [A]-[C]; Supply pressure varied; Accumulators on-line

In order to investigate the robustness of MCS in the face of supply changes, the sinusoidal tests were repeated with the accumulators on-line, but with a decrease in the pressure. This decrease was from the nominal 11.0MPa to 1.4MPa (*ie* to approximately 13% of the normal operating pressure) over a period of about 6s. The significance of this test, over and above it being another demonstration of MCS robustness in the face of plant parameter variations, is that in practice a coupled servohydraulic system can be subjected to a decrease in supply pressure, following increased demands from other services. In such circumstances, the affected system should be able to perform the given task with minimum disturbance.

Fig 9a presents the P+DFB tracking error under the stated test conditions, with the corresponding MCS results being shown in Fig 9b. Again, comparison of the figures shows that MCS has out-performed P+DFB. Plots of the corresponding control signals in Fig 10 clearly show the greater contribution of MCS as the pressure is decreased - the control signal reaches the servovalve solenoid amplifier saturation limits of ±2.5V on each cycle. During periods of saturation, an anti-windup strategy is vital; in this case the adaptive gains are locked at their current values, and then released when $|u| < 2.5$. The excellence of MCS performance is further amplified by the ISE plots in Fig 11, whereby the rate of increase of the MCS ISE is always less than that of P+DFB. Exact parity of the transients in the pressure supply was not achievable, and so only the steady state (*ie* 'straight-line') sections of the plots are of significance.

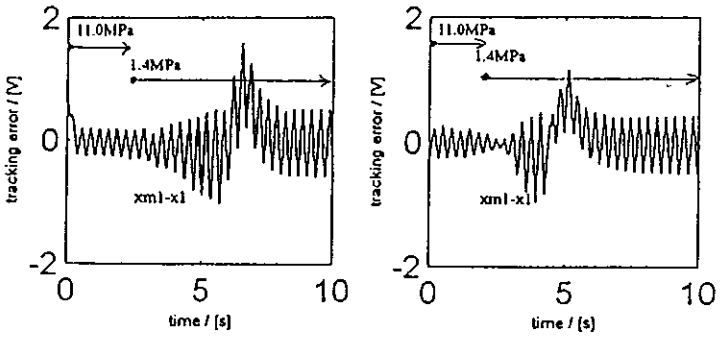

Fig 9a P+DFB Fig 9b MCS

Fig 9 Tracking error; supply decreased; accumulators on-line

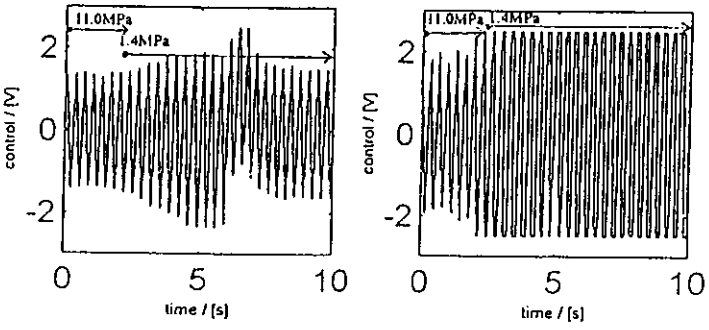

Fig 10a P+DFB Fig 10b MCS

Fig 10 Control signals; supply decreased; accumulators on-line

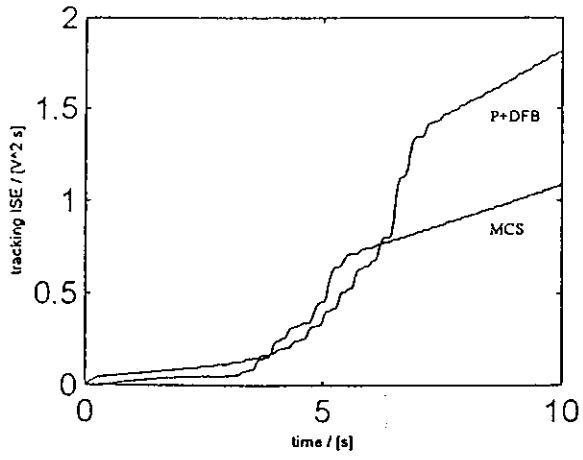

Fig 11 ISE criteria; supply decreased; accumulators on-line

Conclusions

The main conclusions to be drawn from this paper are as follows:

- Linear models of a typical servohydraulic system have been derived under a number of operating conditions. For nominal operations, a 3rd-order transfer function model was seen to be an appropriate choice, and this particular model was used to design a fixed gain proportional-plus-derivative feedback (P+DFB) controller for the plant. The closed-loop performance of the P+DFB controller matched the design expectations when the plant was operated under nominal conditions.
- Away from nominal operations, the linear plant model changed in order and in parameter values. Under these circumstances, it was seen that the P+DFB performance deteriorated significantly.
- The direct adaptive minimal control synthesis (MCS) algorithm was implemented on the servohydraulic plant, and the closed-loop results compared with those produced by P+DFB. Under nominal operating conditions, the two controllers produced very similar responses, despite the fact that MCS required neither prior, nor on-line, estimates of the plant dynamic parameters.
- When the plant was operated away from the nominal condition, the MCS algorithm significantly outperformed P+DFB - a fact most noticeably demonstrated by the ISE plots in Figs 8 and 11.
- The robustness of MCS to plant parameter variations has been proven in, for example, [1]. However, this paper has demonstrated, for a specific case, that MCS also possesses a degree of robustness to plant order changes. In particular, a 2nd-order MCS algorithm produced excellent closed-loop responses under the nominal operating condition (when the plant was approximately 3rd-order), and under other operating conditions (when the plant was approximately 2nd- or 4th-order).
- Robustness issues of MCS to changes in plant order will be the subject of a formal analysis in future work on this topic. In particular, this feature of MCS will be applied to multivariable servohydraulic systems powered by a single supply - a common design feature of (aerospace) servohydraulic systems, which are known to suffer from plant order changes under different operating conditions.

Acknowledgements

The authors wish to thank Mr P R Brinson, of the Avionics Laboratory, University of Bristol, UK, for the use of his servohydraulic test rig. Also, we wish to thank Cumhuriyet University, Sivas, Turkey, for their continued support for (SB).

References

[1] D P Stoten and H Benchoubane, "Robustness of a Minimal Controller Synthesis Algorithm", *International Journal of Control*, 51, No.4, pp 851 - 861, 1990.

[2] D P Stoten, "An Overview of the MCS Algorithm", Inst. Mech. Eng International Conf. on *Aerospace Hydraulics and Systems*, Ref. C474-033, London, 1993.

[3] D P Stoten, "Implementation of MCS on a Servohydraulic Testing Machine", *Proc I Mech E - Part I, Journ. Sys Cont Eng*, 206, No I3, pp 189 - 194, 1992.

[4] D McLean, *Automatic Flight Control Systems*. London: Prentice Hall Int., 1990.

[5] C M Bingham, *Application of Variable Structure Control Methods to Actuator Nonlinearities in Aerospace Systems*. PhD Thesis, SEES, RMCS Shrivenham (UK), 1994.

[6] W J Thayer, "Transfer Functions for Moog Servovalves", Moog Inc. Technical Bulletin 103, 1965.

[7] M G Dye and D P Stoten, *WinCtrl - Implementation of Real Time Controllers in Windows 3.1*, Department of Mechanical Engineering, University of Bristol, Bristol, BS8 1TR, UK, 1993.